Université Catholique de Louvain
Institute of Neuroscience
Laboratory of Neural Differentiation

Roles of Onecut factors in spinal dorsal interneuron and in sensory neuron development

Thesis submitted for the degree of Doctor of Philosophy in Biomedical and Pharmaceutical Sciences

Gauhar Masgutova

Promoter – Pr. Frédéric Clotman
President – Pr. Pascal Kienlen-Campard
Pr. Françoise Gofflot
Pr. Yves Jossin
Pr. Joriene De Nooij
Pr. Alexandre Pattyn

…and that's the end and that's the start of it
that's the whole and that's the part of it
that's the high and that's the heart of it
that's the long and that's the short of it
that's the best and that's the test in it
that's the doubt, the doubt, the trust in it
that's the sight and that's the sound of it
that's the gift and that's the trick in it

you're the truth, not I

Pour pouvoir citer et remercier toutes les personnes qui ont contribué à l'aboutissement de ce travail, il me faudrait rédiger un second manuscrit de 200 pages à part entière. Néanmoins, je tiens à mettre en avant certaines de ces personnes, qui se sont retrouvées, pour le meilleur et pour le pire, impliquées dans cette aventure.

Je remercie les Fonds de la Recherche Scientifique, l'Université Catholique de Louvain et l'ONEM, des institutions qui m'ont permis, grâce à une allocation de recherches ou de chômage, de me consacrer sereinement (ou presque) à l'élaboration de ma thèse de doctorat.

Ce travail n'aurait pas été possible sans le soutien de mon jury de thèse composé de mon promoteur, le Pr. ***Frédéric Clotman****, mes deux président.e.s successifs, la Pre.* ***Ilse Dewachter*** *et le Pr.* ***Pascal Kienlen-Campard****, ainsi que mes deux membres de jury internes, la Pre.* ***Françoise Gofflot*** *et le Pr.* ***Yves Jossin****. Je remercie également mes deux membres de jury externe, la Pre.* ***Joriene De Nooij****, pour son intérêt, sa lecture attentive de ce manuscrit et ses commentaires précieux sur ce dernier, et le Pr.* ***Alexandre Pattyn****, pour l'agréable discussion autour des travaux de recherche lors de la défense privée.*

Je tiens à remercier très chaleureusement ***Youri Adolfs*** *pour son investissement dans mon projet, plus précisément les nombreuses heures passées à m'apprendre la technique de transparisation & d'immunofluorescence sur embryons entiers (3DISCO), mais également pour la confiance totale qu'il a eu concernant mon utilisation de l'Ultramicroscope, parfois à des heures très nocturnes ou trop matinales, dépendant du point de vue pris. De même, je suis très reconnaissante au Pr.* ***Jean-Marie Vanderwinden****, pour sa bienveillance et l'accessibilité très flexible de la plateforme LiMif.*

C'est grâce à une équipe NEDI des plus incroyables que le périple de la thèse a été une aventure parsemée d'éclats de rire, de délires, de confidences, de complicité, de soutien, mais aussi de jolies soirées qui se sont prolongées jusqu'aux petites heures. Les moments partagés avec les membres de cette équipe forte et soudée resteront des souvenirs doux. J'ai poussé la porte de ce labo en saluant des collègues, je pars serrer dans mes bras de précieuses amitiés. J'aimerai ouvrir ces remerciements par ***Audrey****. Mille merci de m'avoir prise sous ton aile alors que tu étais toi-même jeune doctorante avec déjà assez de monde à encadrer. Du début à la fin de cette thèse, j'ai adoré faire partie de la team AH-GM, autrement dit « à la hâte et dans la grosse misère », d'avoir pu partager les rires et les peines du projet chkoumoune Pou2f2 (la galère des paillettes de sperme venues tout droit d'Australie, le prolapsus de la femelle fondatrice, les embryons complètement déformés, et on peut dire … vive le microarray et ses résultats presque annotés), sans parler de la pire activité du monde – l'analyse de distribution. Merci d'avoir été le Pipo de mon Mario, d'avoir ris jusqu'aux larmes dans cette animalerie alors que les souris avaient vraiment trop de peau, de m'avoir épaulée et soutenue grâce à ta présence, ton écoute, tes encouragements, ta patience pour mon impatience (jusque dans les toilettes). Un immense merci d'avoir mis tellement de croquant dans cette thèse & de raviver les cœurs les plus tristes avec ton accent marseillais pur produit du terroir.* ***Steph****, tu es celle qui réussit à mener 4 vies en même temps tout en restant à 100% dans chacune d'elles sans jamais perdre le sourire. Je tiens à te remercier d'avoir rempli cette thèse de ton rire, de tes petits applaudissements mignons, de ta démarche rapide que j'ai toujours fait semblant de suivre mais je t'avoue, c'était avec difficulté ! Et je tiens à rappeler que j'ai adoré apprendre les secrets de la mafia Debrulle qui possède tout Villers-la-Ville/Tilly (le système de jardin communicants est très bien pensé). Merci pour ton franc-parler qui reste toujours bienveillant. Merci pour toutes les fois où j'ai pu*

venir dans votre bureau, à Audrey & toi, pour chuchoter, rire et même pleurer. Merci à ***Mathilde*** *dont j'ai eu l'immense chance et plaisir de partager le périple thèse dans son entièreté. Toutes ces belles années à nous connaître et se rendre compte, assez rapidement, de nos points en commun. Comme tu le dis si bien, c'est vraiment un « vis ma vie » en 6 tomes. Je tiens à te remercier pour les moments de partage, de soutien, de rire, de larmes, de confidences et de complicité. Je pense que parler en emoji, on est maintenant passées expertes, et on peut même publier ces conversations sous le nom de : les petits cercueils aux biceps bien musclés, aussi connu sous le nom de « recueil des malheurs en thèse ». J'ai hâte de boire encore mille et un Kisskiss avec toi, de finir par danser sur des tables, d'apprendre à des bébés coincés à Berlin à boire des shots de Tequila, de réaliser des petits et grands voyages (M comme Maroc ?) mais surtout, de pouvoir goûter encore plus de tes créations douces & sucrées, assise à une jolie table pendant que la chef pâtissière s'installe en face de moi. Merci à* ***Vince****, le seul mec de la bande de nanas ! Merci d'avoir été un coéquipier de rigolades déjà depuis les débuts à Sitges (la balade Martini ou Bacardi, je me souviens même plus de son nom, on n'a vraiment rien écouté) puis un voisin de bureau toujours à l'écoute et attentif à mon bien-être mental, mais aussi de bon conseil à plein de niveaux, dont les voitures et leur lot de problèmes. Merci à* ***Aléxia*** *pour les rigolades, l'adversité franco-belge de la Coupe du Monde, et les vipères-time ! Merci à* ***Karolina*** *d'avoir initié le projet dont j'ai repris le flambeau. Merci à* ***Maria*** *et* ***Barbara*** *pour leur expertise. Merci à* ***Romélia****, la fée de l'animalerie sans qui rien ne tournerait plus.*

Merci à toutes les personnes chaleureuses de l'équipe ***CARD*** *pour les moments de rire partagés sur un temps de midi, entre deux expériences, à un TGIF, lors du week-end NEDI&CARD ou bien, pour certains, à des soirées perdues entre le 6ème et 7 ème shot de Pisco Sour pour finir par se retrouver, par un choix binaire, chez Ginette ou au Corbeau.*

Je tiens à remercier les merveilleuses amitiés qui peuplent ma vie, toutes ces étoiles qui font que mon ciel est moins noir. Sans vous, je ne serai pas moi. Sans vous, je ne serai pas arrivée si loin. Je remercie tout d'abord ***Morgane****, l'amie précieuse dont les épreuves de la vie n'ont fait que renforcer notre amitié. Je ne me lasserai jamais de nos délires parfois drôles parfois fous mais parfois, complètement bizarres. Les histoires qu'on a vécues sont trop nombreuses pour être décrites succinctement mais elles sont précieusement gardées dans mon cœur. Merci d'être la personne qui lit si bien en moi que même mes micro-expressions sont décryptées en un temps plus court que la vitesse de transmission d'un influx nerveux. Merci de toujours me pousser à aller de l'avant, à faire de mon mieux et de m'encourager, à distance ou quand tu me serres fort dans tes bras. Merci de me faire sentir comme à la maison où que je sois quand tu es avec moi. Une maison chaleureuse, douce et reposante. Promis, maintenant que cet enfer est fini, je viendrai enfin investiguer les thermes & spa allemands. Et tu connais mon excès de zèle, on le fera plus d'une fois ! Comme dirait Mérédith à Christina et Christina à Mérédith, you are my person. You will always be my person. Merci à* ***Carole****, ce bout de femme indépendante que j'admire et dont je suis fière ! Merci pour toutes les fois où j'ai pu changer d'apparence, enfiler un costume tout en sachant que parmi la foule de visages masqués, j'en ai toujours un familier auprès de moi. Je suis si chanceuse de pouvoir compter sur toi pour partager mes peines & mes joies, mes peurs & mes envies mais aussi des moments intenses devant un film, entre deux voyages préparés à l'arrache, et plein d'autres aventures gravées dans ma mémoire. Je te remercie aussi de toujours rigoler à mes blagues pourries. Merci à* ***Benoit****, une amitié qui s'est faite si rapidement, et qu'on a cimenté depuis. Tu as été la plus agréable des compagnies matinales sur le chemin du labo. Voilà pourquoi j'ai toujours essayé de te réveiller malgré la difficulté de cette mission ! Merci pour ton écoute et ton soutien peu importe la situation ou le contexte.*

Rappelle-toi, de nos débuts, on est arrivés pas mal loin dans nos vies, et on continuera à se donner la main pour aider l'autre à avancer avec moins de peine. Merci à ***Simon****, depuis tant d'années qu'on se connait et tu n'as jamais cessé de croire en moi. Je suis si chanceuse d'avoir un bff avec qui je peux partager les pires selfies, manger les meilleures pizza peppéroni à Milan ou m'empiffrer de sushis. Enfin, il est loin le temps de Ninja House et Anata. Merci d'avoir été le designer de l'Homme-Poubelle dont la compagnie a égayé mes journées au labo toutes ces années. Merci d'avoir rendu la fin de cette thèse plus simple, sans toi, ce manuscrit ne serait jamais arrivé à temps. Mais surtout, merci pour ton aide et ta confiance depuis toujours.* ***Xavier****, mon grand ami d'1m98, dont la bienveillance, l'écoute, la compréhension, et les mains kinésithérapeutico-magiques ont permis à mon esprit et mon corps, meurtris par la fatigue et les blessures, à aller mieux. Vivement plus de petites soirées devant un film, à manger des ramens à Bailli ou au bout du monde. Copenhague c'est bien, mais vient on repart ? Merci à* ***Guillaume*** *pour les nombreux thés (ou infusions au gingembre que j'ai toujours réussi à éviter), les blagues Mer du Nord & autres pitreries dont tu as le secret, les histoires trépidantes et variées de ta vie qui me font rire même si je roule souvent des yeux. C'est grâce à toutes ces palettes de couleur qui font ta personnalité que j'ai pu oublier les soucis que cette thèse m'a infligée. Et bonne nouvelle, maintenant, on mangera plus souvent ailleurs qu'au Lucullus. J'aimerai aussi remercier* ***Adriano****, l'ami à l'esprit si drôle, dont l'éloquence et la repartie me font très souvent rêver ou pleurer de rire. Merci d'avoir senti les moments où j'avais besoin de partir dans des délires interminables qui commençaient à un point de départ sans qu'on puisse en deviner l'arrivée. Merci d'avoir mis tant de confettis et de paillettes dans ma vie grâce à la Fête avec un grand F. Même si j'ai souvent eu l'impression de traverser l'enfer, avec comme seul accessoire, une couverture anti-flammes trouée à 90%, je savais que je pouvais compter sur soit le Sgt. TKilla pour oublier cette*

traversée ou que tu arrives avec un camion rempli d'extincteurs de malheur, ou autrement connu comme étant des blagues hardcores ou une tasse de thé réconfortante dans ton joli jardin. Merci aussi aux ***Bios*** *de vendre du rêve depuis toutes ces années :* ***Timur, Pierre, Cédric, Timothée, Guillaume, Thomas, Quentin, Kathleen & Delphine*** *avec qui le cœur est toujours en fête, autour d'un verre, au détour d'un lac ou bien à une fête locale à Monceau-Momignies, sans parler de nos autres voyages, parfois très spirituels. Je tiens aussi à remercier* ***Loic****, le plus gentil des Minions. On se connait depuis les bancs de l'Université, et je ne regretterai jamais ce moment où je suis venue te parler après le TP de Chimie infernal qu'on venait d'avoir. Merci d'avoir été présent tout au long de cette épreuve, d'être venu de si loin (Fleurus, une petite ville pittoresque proche de Charleroi) pour passer des journées à flâner dans Bruxelles avec moi. Les oiseaux chantent souvent fort, parfois un peu moins mais ils continueront toujours le chant de notre amitié.* ***Gilles****, l'ami avec qui je peux parler de tellement de choses, parfois même très difficiles à aborder mais dont la bienveillance est telle que rien n'est effrayant à dévoiler. Merci aussi pour toutes ces discussions autour de la photo et de jolies modèles, des questions autour du féminisme et de la société et de partager ces réflexions avec moi ! Merci à tous les autres pour les grands et petits moments de joie dont* ***Antoine*** *pour nos discussions sur les galères de la thèse, les explications très justes sur les rouages enraillés de la CAPAC mais aussi toutes ces fois où on a dansé jusqu'aux petites heures,* ***Fabrice*** *pour tes blagues pourries mais aussi pour ton déhanché légendaire qui rendrait Beyoncé verte de jalousie, sans oublier nos réflexions sur des questions délicates mais colorées. Un dernier merci aux autres drôles de personnages qui de près ou de loin, ont rendu ces 5 années merveilleuses.*

*Mes remerciements vont aussi à **ma famille** qui a toujours cru en moi, écouté mes plaintes chargées en émotions concernant les problèmes récurrents au labo sans forcément comprendre tous les tenants et aboutissants des tensions d'authorship, de financements de congrès et de thèse, etc. Je suis profondément reconnaissante pour leur soutien sans faille, surtout cette dernière année, qui a été la plus difficile à tout point de vue. Merci **Maman** pour ton oreille attentive, ton soutien et toutes les images drôles envoyées sur Whatsapp. Merci d'avoir su comprendre mon absentéisme aux moments de famille, et de m'avoir laissé le temps pour terminer ce travail. Merci **Papa**. Merci de m'avoir rappelé à chaque fois que la thèse n'est pas une fin en soi, mais un moment, bon comme mauvais, à passer, le tout avec tes petits plats préparés alors que je passais en coup de vent. Merci à **Boubou**. Merci d'avoir insisté pour parfois m'emmener au cinéma, me faire réfléchir à certaines questions très importantes, mais surtout, merci d'avoir été d'un soutien discret mais toujours présent. Je vous aime et je vous chéri, ma famille.*

I've been watching you for some time
Can't stop staring at those ocean eyes

I've never fallen from quite this high
Falling into your ocean eyes
Those ocean eyes

*Merci à **Nikolay** pour le soutien infaillible depuis toutes ces années, la patience surhumaine pour mes longs monologues interminables sur les bonnes comme les mauvaises expériences vécues au cours de cette thèse, les mille émotions que je ressentais à chaque événement, souvent mineur, qui m'arrivait au labo mais que tu canalisais en deux phrases et trois câlins. Merci pour les petits plats préparés en urgence alors que je rentrais fatiguée et de mauvaise humeur (le couscous minute, devenu un plat qui me rappelle l'enfance), les Kinder Surprise qui m'a remise à flot après chaque coup de mou, et malgré toutes les épreuves, tu es un pilier que rien ne fait trembler. Merci de me rappeler par cette phrase courte mais très efficace : « tu t'en fou !! » qui, à ta façon, veut dire qu'il faut relativiser par rapport à toutes les choses difficiles auxquelles j'ai dû faire face car demain sera une nouvelle et belle journée. Merci d'avoir essuyé mes larmes, partagés mes rires, serré ma main, enlacé mon cœur pour contrer le malheur ou embrassé ma tête lourde d'angoisses. Merci d'être venu tellement de fois me tenir compagnie pour rendre les couloirs effrayants du labo moins sombres. Merci d'être venu jusqu'en bas de la tour pour que je marche en toute tranquillité les quelques mètres qui séparent le labo du parking. Merci d'avoir réanimé à maintes reprises mes disques durs, le tout très souvent la veille ou le jour d'une deadline critique. Merci pour ces voyages qui m'ont insufflé du courage et de l'énergie. Merci de toujours croire en moi, d'être fier de ce que j'accomplis malgré parfois la pudeur de tes sentiments. Merci infiniment de continuer à m'écouter, à me soutenir, à rester cette belle âme qui m'accompagne à travers vents et marées, en pensées, en actes et parfois avec les crêpes les plus délicieuses du monde. Merci pour ton amour. Je te sens toujours près de moi. Любовь моя.*

Гуся,

Твоя гордая птица

*Merci à **Baptiste** sans qui cette dernière année de thèse n'aurait pas été la même. Merci pour tous ces moments passés à rire, à parler de Jean-Guy, les petits bonhommes, les poutous, les aventures éclectiques et hétéroclites, sans oublier le jeu du cercle. Merci aussi d'avoir géré les courses et préparé les petits plats qui m'ont permis de terminer ce marathon de très longue haleine, ainsi que d'être resté éveillé malgré la fatigue pour me soutenir jusqu'au bout. Je te remercie aussi d'avoir été un soutien enthousiaste, doux et tendre depuis le début de la fin et surtout ces derniers jours. Merci pour cette chaleur qui m'a préservée de la froideur de ma déprime. Merci pour les belles phrases et les textes doux qui font sourire mon cœur. Merci de partager mes peines et mes joies, d'avoir ressenti et compris mes angoisses qui se sont parfois transformées en détresses. Tu as su les effacer très rapidement à l'aide d'une blague ou d'un personnage (Jason ou Gulk ? Je ne saurai choisir, je les veux tous !). La fin d'une thèse n'est pas une tâche facile, même plutôt une épreuve à laquelle tu as su faire face, à ta jolie façon, pour me faire tenir. Merci d'avoir été celui qui contrait les actes vils de Jean-Guy, de m'avoir encouragée et poussée à chercher dans mes derniers retranchements la force de terminer cette thèse et d'avoir cru et de continuer à croire en moi. Merci de rendre ma vie plus simple, plus gaie et plus drôle. L'amour que tu me portes m'enveloppe à chaque fois pour me protéger de toutes les peines. Je t'aime.*

Abbreviation list

2polyPro	Two polyproline
3polyGly	Three polyglycine
Ascl1	Achaete-scute complex homolog 1
Atoh1	Atonal homolog 1
Barhl	BarH like homeobox
Bax	BCL2-associated X protein
BDNF	Brain-derived neurotrophic factor
bHLH	Basic helix loop helix
BMP	Bone morphogenic protein
BP	Brachial plexus
Brn	Brain-specific homeobox
CBP	CREB-binding protein
CD	Cut domain
CGRP	Calcitonin gene-related peptide
Chip-seq	Chromatin immunoprecipitation/sequencing
CNS	Central nervous system
CP	Cervical plexus
CPG	Central pattern generator(s)
DCC	deleted in colorectal carcinoma
DF	Dorsal funiculus
dIN	Dorsal interneuron(s)
Dmrt	Doublesex- and mab-3-related transcription factor
dP	Dorsal progenitor(s)
DREZ	Dorsal root entry zone
DRG	Dorsal root ganglion/ganglia
Drg11	Dorsal root ganglia homeobox protein 11
DV	Dorso-ventral
E	Embryonic stage
EMSA	Electrophoretic mobility shift assay
Eph	Erythropoietin-producing hepatocellular carcinoma cell receptor
Er81	ETS-related protein 81
Fox	Forkhead Box Protein
FP	Floor plate
Gsx	GS homeobox
HC	Horizontal cell(s)

HD	Homeodomain
HMC	Hypaxial motor column
HNF	Hepatocyte nuclear factor
Isl1	ISL LIM Homeobox 1
IN	Interneuron(s)
Krox20	Early Growth Response 2
Lbx	Ladybird Homeobox
LC	Locus coeruleus
Lhx	LIM Homeobox
LMC	Lateral motor column
LMCl	Lateral division of the lateral motor column
LMCm	Medial division of the lateral motor column
Lmx	LIM Homeobox Transcription Factor
LTMR	Low threshold mechanoreceptor(s)
Md	Mandibular
Met	Tyrosine-Protein Kinase Met
ML	Medio-lateral
MMC	Medial motor column
MN	Motor neuron(s)
MTN	Mesencephalic trigeminal nucleus
Mx	Maxillary
NCC	Neural crest cells
Neurog	Neurogenin
NGF	Nerve growth factor
NMJ	Neuromuscular junction
Npn	Neuropilin
NT	Neurotrophin
OC	Onecut
Op	Ophthalmic
Olig	Oligodendrocyte transcription factor
P	Postnatal day
Pax	Paired box
pCAF	P300/CBP-associated factor
PGC	Preganglionic motor column
Phox	Paired mesoderm homeobox protein
Plxn	Plexin
PNS	Peripheral nervous system
polyHis	Polyhistidine

polyGly	Polyglycine
polySer	Polyserine
Pou2f2	POU class 2 homeobox 2
Ptf1a	Pancreas transcription factor 1 subunit alpha
RC	Renshaw cells
Ret	Ret proto-oncogene
RGC	Retinal ganglion cells
ROBO	Roundabout receptor
RP	Roof plate
Sema	Semaphorin
Shh	Sonic hedgehog
SLIT	Slit glycoprotein
Sox	SRY-related HMG-box
STM	Septum transversum mesenchyme
TF	Transcription factor
TG	Trigeminal ganglion
Tlx	T-cell leukemia homeobox
Trk	Neurotrophic receptor tyrosine kinase
Ttr	Transthyretin
VLF	Ventral lateral funiculus
vIN	Ventral interneuron
Wnt	Wingless-type MMTV integration site family member
Wt1	Wilms Tumor Protein
UNC5	Unc-5 Netrin Receptor

Summary

Sensory experience is encoded by specific neurons located both in the peripheral and in the central nervous systems to integrate and elicit adequate responses. Sensory neurons, the cell bodies of which reside in dorsal root ganglia (DRG), relay input such as pain, temperature, itch, touch and limb and muscle length. This information is largely integrated and relayed in the spinal cord. During development, distinct neuronal types, including sensory neurons and dorsal interneurons (dIN), differentiate from progenitors into neurons characterized by distinct molecular identities, localizations and connectivity. However, the molecular mechanisms that control those processes remain incompletely characterized. Previous data obtained in our laboratory have shown that the Onecut (OC) transcription factors are present in sensory neurons and in several spinal dIN populations. This suggests that these factors could contribute to the regulation of the sensory neuron and spinal dIN development. My thesis goal is to study OC roles during these processes and to elucidate the underlying molecular mechanisms in the spinal cord. In this work, I provide evidence that the OC factors are necessary for proper diversification of dI5 interneurons and migration of early-born dIN populations. Moreover, I highlight that the OC factors control the expression of spinal *Pou2f2.* Using gain- or loss-of-function experiments, we show that Pou2f2 contributes to the regulation of dIN distribution. Also, I show that OC factors regulate early differentiation and segregation of distinct sensory subsets. Furthermore, OC are required for proper positioning and for normal projections of sensory neurons into the spinal cord or towards their peripheral targets. Thus, we uncover mechanisms of action of OC proteins in the regulation of spinal dIN development and OC involvement in sensory neuron differentiation, positioning and axonal projections during embryonic development.

Table of contents

1 General introduction

The vertebrate somatosensory system is critical for the perception and the transmission of external as well internal sensory information. The latter includes stimuli as pain, temperature, itch, touch, and limb and body positions conveyed from the periphery to the central nervous system (CNS) where an integrated response leads to an adaptive outcome (Lai et al., 2016). Although the general structure of the somatosensory system has been known for more than a century, the identification of molecular determinants that regulate neuronal development and subsequent circuit formation is only beginning to be uncovered. This thesis focuses on the molecular mechanisms underlying different steps of neuronal development, ranging from neurogenesis to axonal growth, that are involved in the development of dorsal interneurons (dIN) of the spinal cord and of sensory neurons of the dorsal root ganglia (DRG).

1.1 Spinal cord development

Gradients of diffusible signals, known as morphogens, provide positional information that leads to the organization of gene expression and cellular differentiation of the vertebrate neural tube. They establish a homeodomain (HD) and basic helix-loop-helix (bHLH) transcription factor (TF) code that progressively defines discrete and ordered progenitor domains along the dorso-ventral axis of the neural tube (Briscoe et al., 2000; Jessell, 2000; Helms and Johnson, 2003; Alaynick et al., 2011). The expression pattern of genes encoding those TF is progressively achieved in response to opposing morphogen gradients of bone morphogenetic proteins (BMP) and wingless-related mouse mammary tumor

virus integration site proteins (WNT) from the roof plate (RP) and Sonic hedgehog (Shh) from the floor plate (FP) of the neural tube (Briscoe and Small, 2015; Andrews et al., 2019). Thirteen transcriptionally distinct post-mitotic populations are generated in the neural tube between embryonic days (e) 9.5 and e13.5 from eleven non-overlapping progenitor domains along the dorso-ventral axis (Le Dréau and Martí, 2012; Lai et al., 2016; Hernandez-Miranda et al., 2017). Between e10 and e12.5, six of these are found in the ventricular zone of the dorsal neural tube, namely dorsal progenitors (dP) dP1-dP6, and give rise to six early dI1-dI6 dIN populations. In the ventral spinal cord, five progenitor domains p0-p3 and pMN produce four major ventral interneuron populations V0-V3 and the motor neurons (MN). In addition, between e11 and e13.5, two late-born dIL^{A} and dIL^{B} dorsal populations differentiate from a single broad dPIL in a salt and pepper pattern (Figure 1) (Wildner et al., 2006; Alaynick et al., 2011).

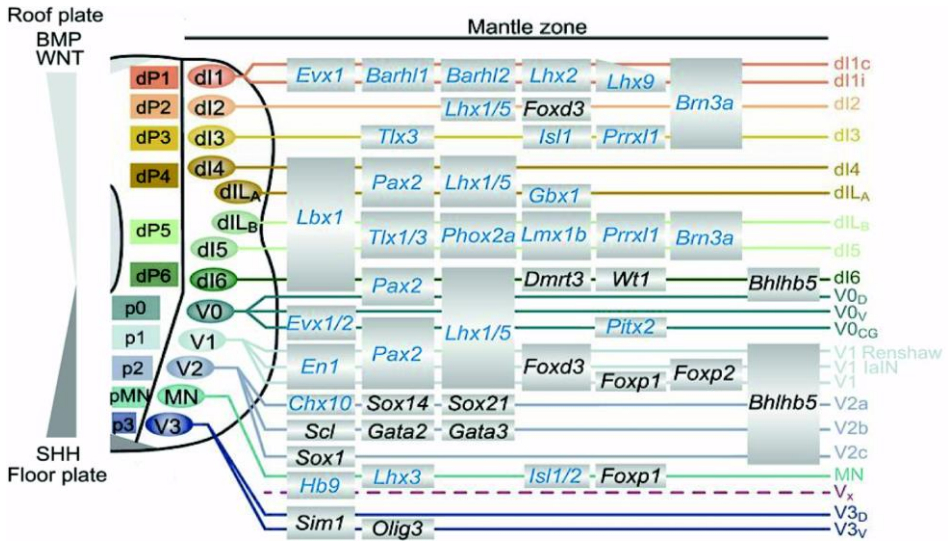

Figure 1. Summary of the TF that establish spinal cord neuronal diversity (adapted from Lai et al., 2016). In the developing spinal cord, eleven progenitor domains (dP1-dP6, p0-p3 and pMN) produce, in two neurogenic waves, distinct neuronal populations (dI1-6, dIL$^{A/B}$, V0-3 and MN) and their subsets. The key TF that define cardinal neuronal populations are shown.

Opposing morphogens released from the RP (BMP, WNT) and the FP (Shh) set up signaling gradients that impact the spatial expression of TF in the developing neural tube. The initial regional identities specified by these TF have fuzzy borders leading to broad and overlapping domains. Nevertheless, the pattern subsequently sharpens due to mutual repression of pairs of transcription factors to form discrete progenitor domains. Thus, specification of distinct classes of neurons depends both on the proper induction of cell-type specific genes and the cross-regulation between genetic networks. In the dorsal half of the spinal cord, the resulting pattern determines dI1-3 (class A) neurons that are induced by BMP and WNT signaling, while dI4-6 (class B) neurons remain independently generated (Dennis et al., 2019; Sagner and Briscoe, 2019). In various dP domains, cross-repression occurs between bHLH factors encoded by *Atonal homolog 1 (Atoh1)*, *Neurogenin 1 (Neurog1)* and *Achaete-scute complex homolog 1 (Ascl1)* (Gowan et al., 2001). Atoh1 and Neurog1 share a cross-inhibitory relationship demonstrated by the dorsal expansion of *Neurog1* expression domain in *Atoh1*$^{-/-}$ embryos. Conversely, *Atoh1* expands ventrally to the dorsal border of *Ascl1* domain in *Neurog1/2*$^{-/-}$ embryos (Gowan et al., 2001). Similarly, Neurog1 is able to repress *Ascl1* expression as shown after *Neurog1* overexpression in chicken embryonic spinal cord (Kriks, 2005). In contrast to the cross-inhibition between Atoh1, Neurog1 and Ascl1, Neurog2 co-localizes with Ascl1 in some cells of the ventricular zone. This bHLH factor is required to restrict Ascl1 activity in dI3 and dI5 interneurons leading to generation of proper numbers of these cells (Helms, 2005). Taken together, opposite morphogen gradients and cross-repression between domain-specific TF subdivides the dorsal spinal cord into discrete dP domains that generate distinct dIN populations along the dorsoventral axis (Caspary and Anderson, 2003; Helms and Johnson, 2003; Alaynick et al., 2011; Sagner and Briscoe, 2019).

1.1.1 Class A or roof-plate dependent dorsal populations

Class A progenitors are the dorsal-most precursors in the spinal cord, namely dP1-dP3, mainly identified by the expression of the bHLH factor *Oligodendrocyte transcription factor (Olig) 3* that starts from e9 under the control of BMP and WNT signals (Zechner et al., 2007). Olig3 plays an essential role in the maintenance of *Atoh1*, *Ngn1* and *Ngn2* expression in the developing spinal cord. The presence of Olig3 is essential for correct specification of dIN from dP1-dP3 cells (Takebayashi et al., 2002; Müller et al., 2005). Furthermore, specific and non-overlapping proneural bHLH TF expression defines restricted dP1 to dP3 domains (Helms and Johnson, 2003). The dI1 progenitors are characterized by the presence of Atoh1 (Lee et al., 1998; Bermingham et al., 2001) while both Neurog1 and Neurog2 define dI2 progenitors (Gowan et al., 2001). The progenitors of dI3 interneurons are comprised in the most dorsal part of a broad *Ascl1* expression domain (Nakada et al., 2004). *Olig3* deletion leads to a reduced dI1 population due to the reduction of *Atoh1* expression domain in the dP1. In addition, dI2 and dI3 populations are incorrectly specified to a class B fate in *Olig3* mutant mice (Müller et al., 2005). Furthermore, Olig3 suppresses the production of Ladybird homeobox (Lbx) 1^{+} class B interneurons, preventing the expansion of class B identity neurons into the class A domain (Müller et al., 2002, 2005). In the developing spinal cord, proneural bHLH factors promote neuronal differentiation as demonstrated after overexpression of *Atoh1*, *Neurog1/2* and *Ascl1* by *in ovo* electroporation in chicken spinal cords (Dubreuil et al., 2002; Nakada et al., 2004). Furthermore, Atoh1 is required for the development of dI1 interneurons. Indeed, its absence results in the loss of dI1 interneurons (Bermingham et al., 2001) while *Atoh1* ectopic expression results in dI1 increase (Gowan et al., 2001; Nakada et al., 2004). *Atoh1* mutant spinal cords display expansion into the dP1 of roof plate

markers dorsally and of *Neurog1/2* expression ventrally (Bermingham et al., 2001; Gowan et al., 2001). Neurog1/2 is necessary for the formation of dI2 interneurons as demonstrated by their complete loss in *Neurog1* and *Neurog2* compound mutant (Gowan et al., 2001). In addition to its function in the specification of all class A neurons, Olig3 instructs the generation of dI3 in cooperation with Ascl1. In chick spinal cords, *Olig3* misexpression along with *Ascl1* induces dI3 interneurons while *Olig3* deletion results in unspecified dI3 interneurons. Furthermore, *Ascl1* mutant mice produce less dI3 neurons (Müller et al., 2005). In addition to bHLH TF, Genetic-screened homeobox (Gsx) 2, a HD TF, acts sequentially with Ascl1 to promote dI3 differentiation by suppressing *Neurog1* and *Neurog2* expression (Kriks, 2005). Each generated dIN population is characterized by specific function, migration pattern and connectivity.

1.1.1.1 dI1 interneurons

The excitatory dI1 interneurons, born between e10.0 and e12.5 from the most dP domain dP1, are characterized by the expression of *Lim homeobox (Lhx) 2/9*, *BarH like homeobox (Barhl) 1/2* and *Brain-specific homeobox (Brn) 3a.* The dI1 population is heterogeneous with at least two subclasses: $dI1_i$ interneurons that express $Lhx2^{high}$ and $Lhx9^{low}$, whereas $dI1_c$ interneurons express *Lhx9* (Helms and Johnson, 1998; Lee et al., 1998; Bermingham et al., 2001; Gowan et al., 2001; Ding et al., 2012). The dI1 interneurons migrate deeply into the dorsal horn and the intermediate gray where they integrate the spinocerebellar tract. These neurons project anteriorly, in an ipsi- or contralateral manner, through the spinocerebellar tract that relays proprioceptive information from spinal levels to the cerebellum (Figure 2) (Bermingham et al., 2001; Yuengert et al., 2015).

1.1.1.2 dI2 interneurons

Between e10.0 and e12.5, the dP2 generates excitatory dI2 interneurons that express *Lhx1/5*, *Forkhead box (Fox) d3* and *Brn3a.* The dI2 population settles in the intermediate layers VI, VIII and in the ventral horn of the spinal cord (Bermingham et al., 2001; Gowan et al., 2001; Gross et al., 2002). Based on their location, intermediate dI2 interneurons might convey sensory information to the thalamus via the spinothalamic tract, while ventral dI2 project ascending commissural axons (Figure 2) (Brown, 1981; Gross et al., 2002).

1.1.1.3 dI3 interneurons

Excitatory dI3 interneurons, generated from e10.0 and/to e12.5 by dP3 cells, express *Brn3a, T cell leukemia homeobox (Tlx) 3*, *Islet1 (Isl1)* and *Dorsal root ganglia homeobox (Drg11)* (Chen et al., 2001; Gross et al., 2002; Qian et al., 2002; Cheng et al., 2004; Müller et al., 2005). The dI3 interneurons migrate to the intermediate and deep dorsal horn of the spinal cord, wherein they receive monosynaptic inputs from cutaneous and proprioceptive sensory neurons (Bui et al., 2013). In turn, dI3 directly convey this information to MN for forelimb grasping control (Stepien et al., 2010; Bui et al., 2013, 2016; Goetz et al., 2015). Rostrally, the dI3 send ipsilateral axonal projections that segregate in two longitudinal fascicles: a dorsal fascicle that enters the dorsal funiculus (DF) and a ventral fascicle entering the ventral lateral funiculus as studied in chick embryos (Figure 2) (Avraham et al., 2010).

1.1.2 Class B or roof-plate independent dorsal populations

The dP4-dP6 cells, known as class B progenitors, are generated independently from RP signals. In contrast to class A progenitors defined by Olig3, class B progenitors are characterized by several TF (Hernandez-Miranda et al., 2017). High levels of Paired box (Pax) 7^{high} combined with Ascl1 define dI4 and dI5 progenitors, followed by Ptf1a requirement for dI4 (and dIL^{A}) further specification, while $Pax7^{high}$ without Ascl1 marks dI6 progenitor domain (Gross et al., 2002; Müller et al., 2002; Glasgow et al., 2005). Neuronal derivatives of dP4-dP6 present a shared expression of *Lbx1* that acts as a determinant of dI4-dI6 cell types (Gross et al., 2002; Müller et al., 2002). Indeed, *Lbx1* mutant presents a broad switch of dI4 and dI5 interneurons into dI2 and dI3, respectively. Furthermore, even if dI6 neurons continue to express their characteristic *Pax2* marker, their migratory behavior follows a radial trajectory like that of dI4 neurons. Complementary to loss-of-function studies, misexpression of *Lbx1* suppresses Brn3a in dI2 and Isl1 in dI3 neurons, while inducing ectopic *Pax2* expression (Figure 2) (Gross et al., 2002; Müller et al., 2002).

1.1.2.1 dI4 interneurons

At early developmental stages, between e10.5 and e11.0, the dP4 produces inhibitory dI4 interneurons expressing *Lbx1*, *Pax2* and *Lhx1/5* (Gross et al., 2002; Müller et al., 2002; Glasgow et al., 2005; Helms, 2005). The dI4 interneurons migrate into the lateral deep dorsal horn where they project ipsilaterally to the superficial layers of the spinal cord (Gross et al., 2002; Müller et al., 2002; Pillai et al., 2007). Recent studies uncovered a gating role of dI4 interneurons in sensory modalities as pain, itch and touch (Figure 2) (Bourane et al., 2015a, 2015b; Watanabe et al., 2017).

1.1.2.2 dI5 interneurons

Also arising between e10.5 and e11.0, but from the dP5, excitatory dI5 interneurons express *Lbx1*, *Brn3a*, *Tlx1/3* and *Lim homeobox TF (Lmx) 1b* (Gross et al., 2002; Müller et al., 2002; Qian et al., 2002; Ding et al., 2004; Glasgow et al., 2005). A subset of dI5 interneurons is identified by *Paired like homeobox (Phox) 2a* expression (Ding et al., 2004). As dI4 interneurons, they function in pain, itch and touch sensory signal relay (Figure 2) (Bourane et al., 2015a, 2015b; Watanabe et al., 2017).

1.1.2.3 dI6 interneurons

The most ventrally located dorsal progenitors, namely the dP6, produces the inhibitory dI6 interneurons around e10.5-e11.0, characterized by the expression of *Lbx1*, *Lhx1/5* and *Pax2* (Gross et al., 2002; Müller et al., 2002; Ding et al., 2004; Glasgow et al., 2005; Pillai et al., 2007). The dI6 population subdivides in *Doublesex and mab-3 related TF (Dmrt) 3* and *Wilms tumor suppressor gene (Wt1)* expressing subtypes (Goulding, 2009; Andersson et al., 2012). The dI6 $Dmrt3^{+}$ subset is involved in the left/right coordination resulting in an altered gait when mutated whereas the dI6 $Wt1^{+}$ cells participate in the fore-/hindlimb coordination (Figure 2) (Andersson et al., 2012; Vallstedt and Kullander, 2013; Schnerwitzki et al., 2018).

1.1.2.4 $dIL^{A/B}$ interneurons

During the second wave of neurogenesis, between e11.5 and e13.5, a single dPIL generates late born dIL^{A} and dIL^{B} interneurons. Similar TF are expressed in early and late dorsal progenitors: *Gsx1/2*, *Ascl1* and *Pancreas associated transcription factor (Ptf) 1a* (Gowan et al., 2001; Glasgow et al., 2005; Kriks, 2005). Again, Gsx1/2 and Ascl1 domains overlap whereas Ptf1a is distributed in a mosaic

fashion among dIL progenitors (Mizuguchi et al., 2006). Contrary to their action during the initial wave of neurogenesis (Kriks, 2005), *Gsx1/2* and *Ascl1* act separately from a common bipotential progenitor pool to generate dIL^A or dIL^B neurons in a "salt-and-pepper" pattern. In fact, Ascl1 regulates *Ptf1a* expression cell-autonomously and Notch signaling in a non-cell autonomous manner to direct *Gsx1/2* progenitors to a dIL^A fate instead of their normally biased dIL^B fate (Mizuguchi et al., 2006). Loss of *Ptf1a* leads dIL^A to trans-fate to the dIL^B identity (Glasgow et al., 2005). The dIL^A are inhibitory association interneurons identified by *Lbx1*, *Pax2,* and *Lhx1/5* expression that settle in the superficial layers I – III of the spinal cord where they gate somatosensory information (Gross et al., 2000; Pillai et al., 2007). The excitatory dIL^B association interneurons express *Lbx1*, *Brn3a, Tlx3* and *Lmx1b* (Gross et al., 2000; Müller et al., 2002; Borromeo et al., 2014a) and migrate to layers I-V of the dorsal horn, wherein they receive temperature, mechanosensory and nociceptive input from the skin (Figure 2) (Xu et al., 2013; Szabo et al., 2015).

Thus, the dIN populations diversify and settle in very defined positions on the dorso-ventral, the medio-lateral and the antero-posterior axis of the spinal cord. Some recent studies highlighted that the settling position of interneuron populations is critical for their connectivity (Borowska et al., 2013, 2015; Bikoff et al., 2016; Hilde et al., 2016; Sweeney et al., 2018). This suggests that they integrate specific local neuronal networks governing somatosensation and locomotion, namely the central pattern generator (CPG). However, the molecular and cellular mechanisms involved in the regulation of dIN diversification and migration remain until now elusive.

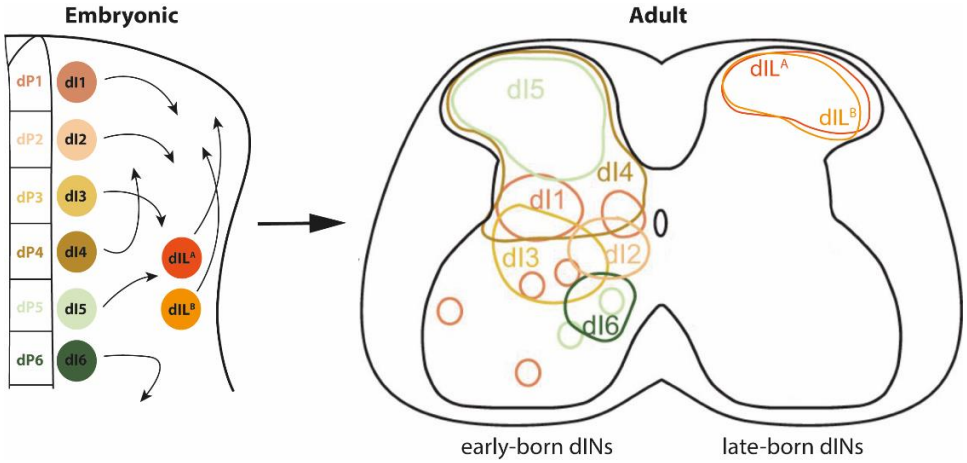

Figure 2. Schematic representation of dorsal interneuron migration during spinal cord development (adapted from Lai et al., 2016). Early during embryogenesis, each dorsal population migrates extensively from their birth location to their settling position. Dorsal neurons reach their target positions just before birth where they remain throughout adulthood. Among early-born dIN, class A dI1 – dI3 cells will populate the deep dorsal horn whereas class B dI4 – dI6 interneurons migrate either dorsally to more superficial layers of the dorsal horn or ventrally to the deep dorsal horn and the ventral spinal cord. The late born dIL^{A} and dIL^{B} cells travel dorsally and laterally to the most superficial layers of the dorsal horn.

1.2 Dorsal root ganglia development

In the vertebrate peripheral nervous system (PNS), cell bodies of somatic and visceral sensory neurons are clustered in the DRG, spherical structures distributed on both sides of the spinal cord. Different types of DRG sensory neurons specialize in distinct perceptual modalities such as small-diameter lightly myelinated Að-fibers, or unmyelinated C-fibers that perceive pain (nociceptors), temperature (thermoceptors), itch (pruriceptors), and gentle touch (C-fiber low-threshold mechanoreceptors (LTMR)). Larger-diameter myelinated Aß-fibers (also include Aα- and Að-fibers) convey mechanical stimuli (LTMR) and large-diameter thickly myelinated Aα-fibers (also include Aß- and Að-fibers) sense limb and muscle position. During development, immature sensory neurons progressively diversify into the many types of DRG sensory neurons that discriminate between various types of sensation (Marmigère and Ernfors, 2007; Lallemend and Ernfors, 2012).

1.2.1 Sensory neuron neurogenesis

Although sensory neurons are characterized by a great diversity regarding their types and functions, all these neurons arise from the same transient population of multipotent stem cells, the neural crest cells (NCC). Between e8.5 and e10, under strictly controlled signals from the neural tube, part of the NCC delaminate from the dorsal neural tube and migrate ventrally to coalesce into DRG between the somite and the neural tube in three successive but overlapping neurogenic waves in a ventral to dorsal chronology (Marmigère and Ernfors, 2007). During the first wave of neurogenesis, which contributes to an estimated 4% of DRG neurons, migrating NCC mostly generate neurotrophic tyrosine receptor kinase (Trk) B^+ large-diameter mechanoreceptive, $TrkC^+$ proprioceptive and early RET proto-oncogene (Ret) $^+$ mechanoreceptive neurons but also a minor proportion of $TrkA^+$

large-diameter nociceptors (Frank and Sanes, 1991; Ma et al., 1999; Bachy et al., 2011). In coalescent DRG, the second neurogenic wave produces ±91% of the sensory neurons, predominantly small TrkA$^+$ nociceptors and to a lesser extent large TrkB$^+$ and/or TrkC$^+$ mechanoreceptors and proprioceptors (Ma et al., 1999). A last wave generates approximately 5% of small-size nociceptors from NCC derivatives located at the dorsal root entry zone (DREZ), the boundary cap cells, a transient reservoir of multipotent progenitors (Figure 3) (Maro et al., 2004; Hjerling-Leffler et al., 2005).

Before NCC delamination from the dorsal neural tube and during their ventral migration, sensory neuron precursors express *Sry-box (Sox) 10* and *Pax3* transcription factors (Goulding et al., 1991; Kim et al., 2003; Nakazaki et al., 2008). Sox10 maintains NCC multipotency, whereas Pax3 promotes NCC ventral migration (Kim et al., 2003). Under the influence of morphogens, the DRG precursors begin to express Neurog2 and Neurog1, which are the earliest sensory precursor markers (Ma et al., 1999). From e9.5 to e11.5, *Neurog2* expression in

Figure 3. Neurogenic waves in the sensory neuron lineage (adapted from (Marmigère and Ernfors, 2007). (A) Three waves of neurogenesis generate DRG neurons. Large-diameter TrkB$^+$ and/or TrkC$^+$ mechanoreceptive and proprioceptive neurons arise at early stages of NCC delamination and migration from the first wave (± 3.1 neurons per NCC). The second wave produces all types of sensory neurons (± 35.9 neurons per NCC) throughout NCC migration. These two waves of neurogenesis contribute to an estimated 4% (first wave) and 91% (second wave) of the DRG neuronal population. From boundary cap cells, the third wave mainly produces small-diameter TrkA$^+$ nociceptors that contribute to ~5% of adult mouse DRG neurons. (B) During the first wave, multipotent NCC migrate with limited cell division and contribute to mechanoreceptive and to proprioceptive neurons in the DRG. (C) Later, the second wave generates all sensory neuron subtypes from postmigratory and highly proliferative NCC. (D) At e10.5, the neural crest-derived multipotent boundary cap cells are located at the DREZ of the spinal cord. (E) From late e10.5, boundary cap cells proliferate and generate mainly small TrkA$^+$ neurons.

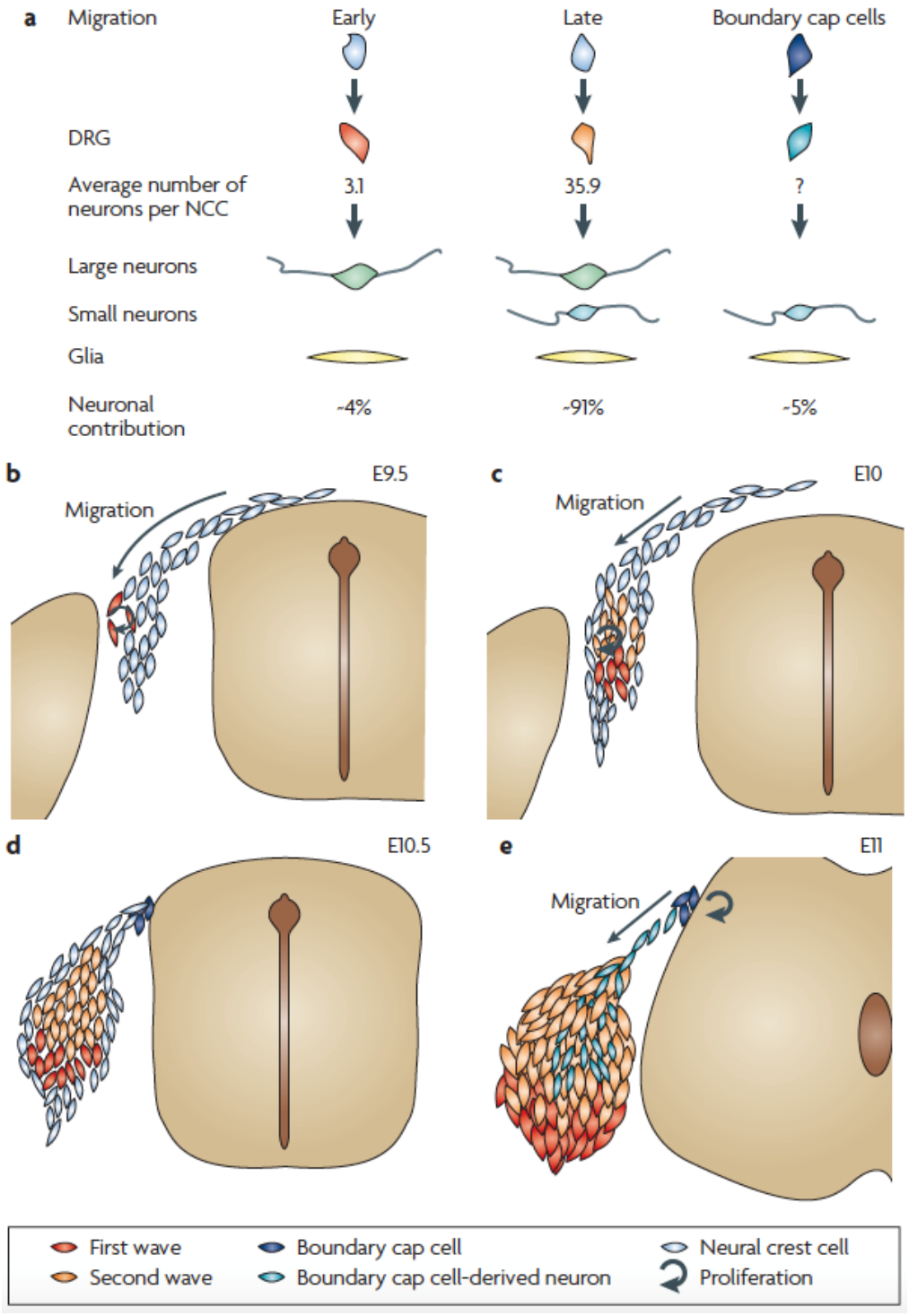
a
Migration
Early
Late
Boundary cap cells
DRG
Average number of neurons per NCC
3.1
35.9
?
Large neurons
Small neurons
Glia
Neuronal contribution
~4%
~91%
~5%
b
E9.5
Migration
c
E10
Migration
d
E10.5
e
E11
Migration
First wave
Second wave
Boundary cap cell
Boundary cap cell-derived neuron
Neural crest cell
Proliferation

migrating NCC defines the first wave of neurogenesis and biases Sox10^{+} cells towards a sensory fate (Ma et al., 1999; Zirlinger et al., 2002). As NCC condense into ganglion primordia, *Neurog2* transient expression is extinguished. In parallel, between e10.5 and e13.5, *Neurog1* expression triggers a second wave of neurogenesis amid remaining Sox10^{+} multipotent cells within the DRG (Southard-Smith et al., 1998; Ma et al., 1999). As mentioned above, Neurog2 regulates the first wave, as demonstrated by the analysis of *Neurog2*$^{-/-}$ mutant embryos. Although initial *TrkC* and *TrkB* sequential expression was delayed, TrkC^{+} and TrkB^{+} neurons developed normally at later stages. At later developmental stages, Neurog1 compensates the initial *Neurog2* requirement as demonstrated by a complete DRG loss in *Neurog1/2*$^{-/-}$ mutants, while at e13 and later, DRG were normally formed in *Neurog2*$^{-/-}$ embryos (Ma et al., 1999). Neurog2-Cre lineage-tracing analysis demonstrated that a significant number of TrkA^{+} neurons is generated during the first wave from NCC expressing low *Neurog2* levels (Bachy et al., 2011). During the second neurogenic wave, mutant mice analysis revealed that most of the TrkA^{+} neurons are Neurog1-dependent as they are lost in *Neurog1* mutant embryos. In contrast, Neurog1 depletion resulted in TrkB^{+} and TrkC^{+} neuron reduction (Ma et al., 1999). Besides their roles during different waves of neurogenesis, both Neurog1 and Neurog2 specify NCC to the sensory fate as *Neurog1/2* double-mutant embryos completely lack DRG. Even if the fate of sensory subtypes is strongly related to the timing of neurogenic waves, it remains unclear if Neurog1/2 promote specific sensory subtypes (Ma et al., 1999; Zirlinger et al., 2002; Marmigère and Ernfors, 2007). Expression of neuron-specific TF Foxs1, Brn3a, and Isl1 marks the transition of neuronal progenitors into postmitotic sensory neurons (McEvilly et al., 1996; Montelius et al., 2007; Sun et al., 2008). Coincident with cell cycle exit, sensory neurons upregulate *Brn3a* and *Isl1*,and downregulate *Sox10*, from e10.5 onward (Fedtsova and Turner, 1995; Sun

et al., 2008; Dykes et al., 2011). Both Brn3a and Isl1 directly repress *Neurog1/2* and their downstream targets to route sensory neurons towards specification (Lanier et al., 2007; Raisa Eng et al., 2007; Sun et al., 2008). Together, Brn3a and Isl1 regulate the expression of essential sensory-specific gene expression in developing sensory neurons including *TrkA, TrkC, Runt-related TF (Runx) 1* and *Runx3* (Chen et al., 2006b; Kramer et al., 2006; Marmigère et al., 2006; Dykes et al., 2011). *Brn3a* mutation leads to aberrant $TrkB^+$, $TrkC^+$, $TrkA^+/B^+$ sensory neurons development and a strong *Runx1* downregulation (Zou et al., 2012). In *Isl1* conditional knockout embryos, $TrkA^+$ and $TrkC^+$ neurons diverge normally, whereas $TrkB^+$ population decreases. Also, TrkA and Runx1 nociceptive markers decrease dramatically and *TrkC* expression is delayed (Sun et al., 2008). Although sensory neurons are produced in *Brn3a/Isl1* double mutant mice, only generic neural markers are maintained but fail to differentiate into functional subtypes. Furthermore, DRG neurons exhibit defective ventral migration and peripheral axonogenesis (Dykes et al., 2011). Brn3a and Isl1 function in parallel as *Brn3a* expression is unaffected in $Isl1^{-/-}$ mutant DRG, and vice versa (Eng et al., 2004; Raisa Eng et al., 2007; Sun et al., 2008).

1.2.2 Sensory neuron specification

Sensory neuron diversification requires transcriptional programs to promote and maintain the expression of *TrkA, TrkB, TrkC, MET proto-oncogene (Met)*, and *Ret* that partly discriminate between sensory types. In addition, several studies of knockout mice for neurotrophin (NT) or their receptor uncovered their requirement in neuronal survival but also specification. Briefly, Nerve growth factor (NGF) binds to TrkA, Brain-derived neurotrophic factor (BDNF) and NT-4 interact with TrkB, and NT-3 with TrkC but also activates less efficiently TrkA and TrkB (Fariñas et al., 1998). *NGF*$^{-/-}$ or *TrkA*$^{-/-}$ mice are mainly devoid of unmyelinated and small myelinated nociceptors, whereas *NT3*$^{-/-}$ or *TrkC*$^{-/-}$ mice lose large myelinated proprioceptors (Crowley et al., 1994; Ernfors et al., 1994; Smeyne et al., 1994; Snider and Wright, 1996). Besides survival, NT have instructive roles during neuronal specification as demonstrated for NGF by apoptosis elimination within neurotrophic factor-dependent neurons using mice deficient in both proapoptotic *BCL2-associated X protein (Bax)* gene and *NGF* or *TrkA* (Patel et al., 2000, 2003b). At early stages, TrkA, TrkB and TrkC are among the earliest markers for sensory subtypes and exhibit broader and partially overlapping expression patterns in different sensory types than at later stages (Ernfors et al., 1992; Snider and Wright, 1996; Kramer et al., 2006; Bourane et al., 2009; Luo et al., 2009; Bachy et al., 2011). Therefore, the timely repression of Trk appears another important mechanism in the generation of distinct sensory subtypes (Lallemend and Ernfors, 2012). *Runx1* and *Runx3* differential and non-redundant expression profiles play critical roles in sensory neuron diversification (Levanon et al., 2001, 2002; Inoue et al., 2002, 2003; Chen et al., 2006a, 2006b; Kramer et al., 2006; Marmigère et al., 2006). *Runx* expression correlates with functional sensory types as first-born cells, the putative TrkB^{+} mechanoreceptors and TrkC^{+} proprioceptors

express high levels of *Runx3* from e10.5 while *Runx1* expression is restricted to $TrkA^+$ nociceptors (Levanon et al., 2001, 2002).

Runx1 expression is very dynamic during embryogenesis of $TrkA^+$ sensory neurons (Levanon et al., 2001; Chen et al., 2006b; Kramer et al., 2006; Marmigère et al., 2006). At early developmental stages, almost all $TrkA^+$ nociceptors express *Runx1*, but it is not required during early embryogenesis as *Runx1* conditional inactivation using $Runx1^{flox/flox}$; Wnt1-Cre mice, to avoid embryonic lethality, had no effects on $TrkA^+$ sensory neuron production (Chen et al., 2006b). However, during late embryonic and early postnatal periods, *Runx1* inactivation resulted in impaired $TrkA^+$ peptidergic and $TrkA^-$ non-peptidergic neuron segregation, the latter typically switching to *Ret* expression around birth (Molliver et al., 1997; Chen et al., 2006b). Indeed, in *Runx1* mutant mice, $TrkA^+$ neurons were present in higher numbers, while Ret^+ cells decreased. Typically, Runx1 suppresses *TrkA* and promotes *Ret* expression necessary to $TrkA^+$ to $TrkA^-/Ret^+$ transition at postnatal stages. Additionally, Runx1 acts as a repressor of peptidergic-related genes while it activates transcription of genes related to the non-peptidergic phenotype (Chen et al., 2006b). All functions above are supported by findings using $Runx1^{-/-}$ mice in which specific *Runx1* expression rescue takes place in liver hematopoietic cells to avoid early embryonic lethality (Yoshikawa et al., 2007). As will be introduced later in this manuscript, *Runx1* depletion affects spinal targeting of $TrkA^+$ nociceptive axons (Chen et al., 2006b; Kramer et al., 2006). Complementary, *Runx1* overexpression in all DRG neurons suppresses the emergence of Calcitonin gene-related peptide (CGRP), a peptidergic marker normally excluded from $Runx1^+$ DRG neurons (Kramer et al., 2006). Furthermore, it appears that Runx1 acts with Tlx3 to control the molecular identity of Ret^+ non-peptidergic neurons. Nevertheless, Runx1 regulation of TrkA lineage segregation occurs both by Tlx3-dependent and independent pathways (Lopes et al., 2012).

Several studies demonstrate Runx3 involvement in the diversification of the initial TrkC$^+$ neurons into several subtypes (Inoue et al., 2002, 2003; Levanon et al., 2002; Kramer et al., 2006). In mice, DRG neurons start to express *TrkC* ahead of other *Trk* or *Ret.* At e11.5, *TrkB* and *Ret* expressions are established in two transient and distinct populations: TrkB$^+$/TrkC$^+$ and TrkB$^+$/Ret$^+$ neurons (Kramer et al., 2006; Marmigère and Ernfors, 2007). Then, *TrkB* expression among TrkC$^+$ neurons drops between e11.5 and e12.5 before reaching almost a complete divergence of TrkB$^+$ and TrkC$^+$ neurons by e14.5 (Scott et al., 2011). Divergence of early hybrid TrkB$^+$/TrkC$^+$ neurons leads to the generation of two mature TrkB$^+$ cell

Figure 4. Neurogenesis and sensory neuron specification genetic control (adapted from Marmigère and Ernfors, 2007). During the first wave of neurogenesis, Sox10$^+$ cells start to express *Neurog2* that biases them towards a sensory fate as they migrate into ventral territories. High Neurog2 levels commit cells to a sensory neuronal fate as defined by *Foxs1* expression during migration. Cells with low or absent Neurog2 remain multipotent (hatched arrow and horizontal arrow to Sox10$^+$ migrating cells). After migration, *Brn3a* expression starts in cells that form large proprioceptive and mechanoreceptive neurons, both Runx3- and TrkC-positive at early developmental stages. The second neurogenic wave consists of cells with continuous expression of *Sox10* throughout migration and after coalescence in DRG. After dividing at a high rate, these cells start to express *Foxs1, Brn3a* and *Neurog1* in the DRG before expressing either *Runx1* or *Runx3*, in presumptive TrkA$^+$ and TrkC$^+$ neurons, respectively. The third wave of neurogenesis starts from boundary cap cells expressing *Sox10* and *Zinc finger protein Krox* (*Krox) 20* that mainly produce Runx1$^+$/TrkA$^+$ neurons and glial cells. The genetic cascade that regulates this wave remains unknown. Runx protein level participates in the diversification of sensory neurons into different cell types, as shown at the bottom of the figure. Cells from the first wave that maintain *Runx3* expression specify into TrkC$^+$ proprioceptors, whereas those that decrease or lose *Runx3* expression become TrkB$^+$/TrkC$^+$, TrkB$^+$ alone, Ret$^+$ alone or Ret$^+$/TrkB$^+$ mechanoreceptors. Small neurons that maintain *Runx1* expression generate TrkA$^-$ non-peptidergic neurons, whereas reduction of *Runx1* directs to TrkA$^+$ peptidergic neurons. The vertical axis represents the dorsoventral position and migratory status of the cells during development. The thickness of curved arrows indicates different rates of proliferation. E embryonic day; P, postnatal day.

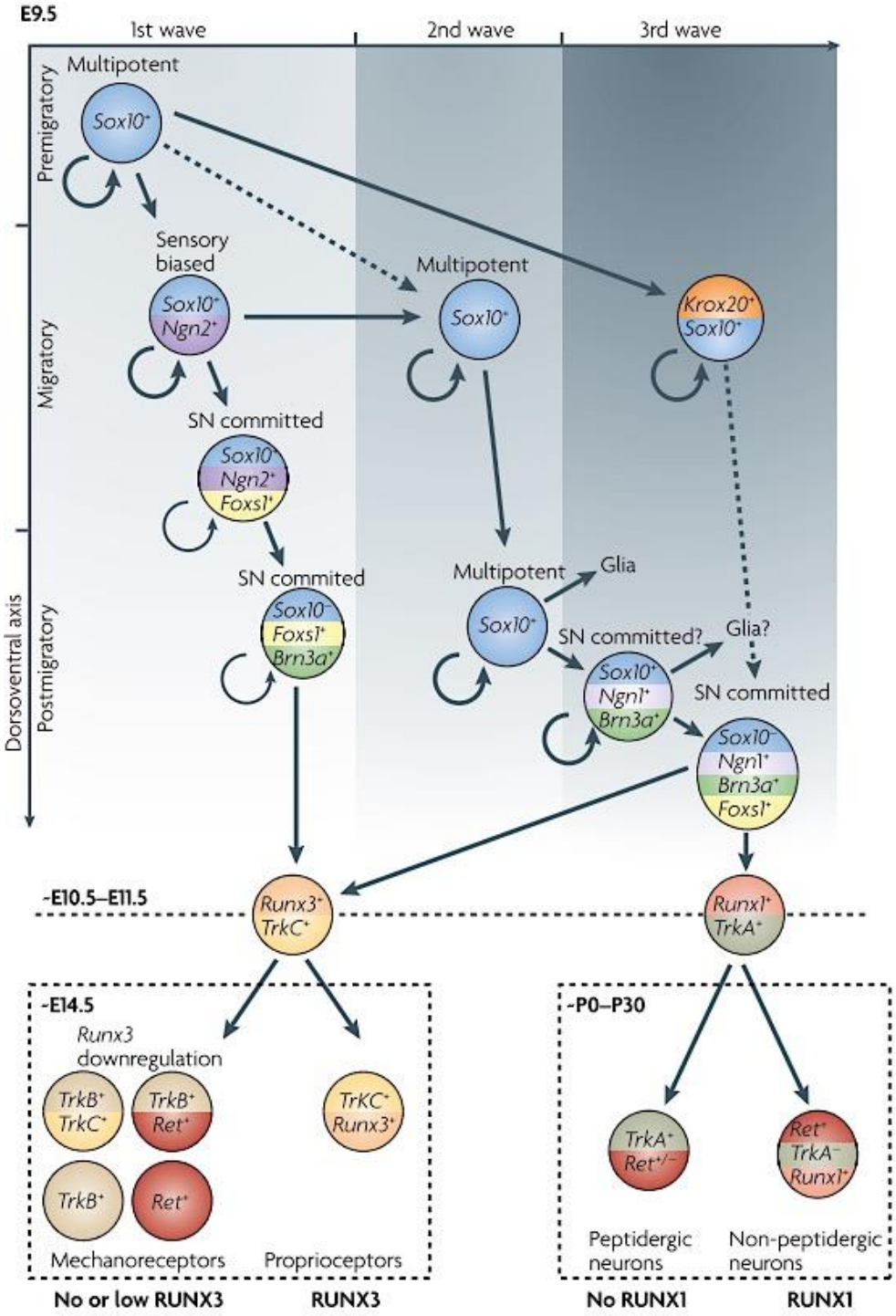
E9.5
1st wave
2nd wave
3rd wave
Premigratory
Migratory
Postmigratory
Dorsoventral axis
Multipotent
Sox10+
Sensory biased
Sox10+ Ngn2+
Multipotent
Sox10+
Krox20+ Sox10+
SN committed
Sox10+ Ngn2+ Foxs1+
SN commited
Sox10+ Foxs1+ Brn3a+
Multipotent
Glia
Sox10+
SN committed?
Glia?
Sox10+ Ngn1+ Brn3a+
SN committed
Sox10+ Ngn1+ Brn3a+ Foxs1+
~E10.5–E11.5
Runx3+ TrkC+
Runx1+ TrkA+
~E14.5
Runx3 downregulation
TrkB+ TrkC+
TrkB+ Ret+
TrkC+ Runx3+
TrkB+
Ret+
Mechanoreceptors
Proprioceptors
No or low RUNX3
RUNX3
~P0–P30
TrkA+ Ret+/−
Ret+ TrkA− Runx1+
Peptidergic neurons
Non-peptidergic neurons
No RUNX1
RUNX1

types, $TrkB^{high}$ Aδ LTMR and $TrkB^{low}$ Aß rapidly-adapting LTMR in which *TrkC* expression is extinguished, and a $TrkC^+$ Aß slowly-adapting LTMR from those maintaining *TrkC* but extinguishing *TrkB* expression (Kramer et al., 2006; Bourane et al., 2009; Lallemend and Ernfors, 2012). In contrast to the touch sensitive types, $TrkC^+$ proprioceptors express *Runx3* that contributes to the segregation of $TrkC^+$ presumptive proprioceptors from $TrkB^+$ future mechanoreceptors (Levanon et al., 2002; Kramer et al., 2006; Abdo et al., 2011; Scott et al., 2011). *Runx3* overexpression in all DRG neurons resulted in a mild increase in $TrkC^+$ neurons while it eliminates *TrkB* expression in $TrkC^+$ and Ret^+ neurons. Therefore, Runx3 functions to repress *TrkB* in neurons directed towards $TrkC^+$ identity (Kramer et al., 2006; Inoue et al., 2007). Moreover, Runx3 hinders *TrkB* transcriptional activation in differentiating proprioceptors by repressing *Shox2.* Oppositely, Shox2 is necessary for *TrkB* expression in $TrkB^+$ presumptive mechanoreceptors (Abdo et al., 2011). Consequently, $TrkC^+$ proprioceptors are lost, whereas $TrkB^+$ neurons are increased in *Runx3* mutant mice. Therefore, *Runx3* expression is necessary to consolidate $TrkC^+$ neuron identity while its decrease might be required for $TrkB^+/TrkC^+$ mechanoreceptor subtype diversification (Figure 4) (Kramer et al., 2006; Inoue et al., 2007). As for Runx1 instructive role in axon projection, Runx3 requirement for $TrkC^+$ afferent growth will be detailed later.

1.2.3 Sensory neuron projections

Transduction of specific signals from the periphery to central structures requires the establishment of modality-specific contacts between primary sensory neuron axons and the spinal cord throughout embryogenesis and postnatal stages. Briefly, adult nociceptive and thermoceptive C- and Aϑ-fibers target superficial dorsal laminae I and II, cutaneous Aϑ- and Aß-fibers invade more ventral dorsal laminae II-V, both innervating skin, whereas proprioceptive Aß- and Aα-fibers from muscle spindles and Golgi tendon organs reach intermediate and ventral spinal cord regions as laminae V-VII and IX (Todd, 2010; Lai et al., 2016) Laminar-specific segregation of afferents is regulated by extrinsic cues and intrinsic factors to achieve a stereotypical termination pattern (Figure 5) (Ozaki and Snider, 1997; Marmigère and Ernfors, 2007).

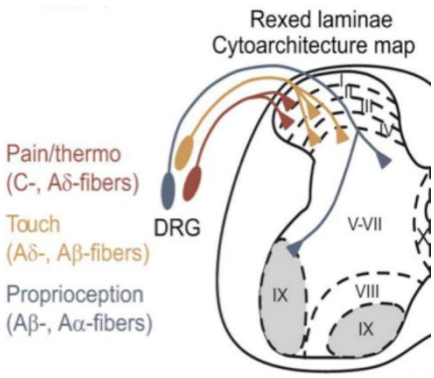

Figure 5. Central laminar termination of afferents from different sensory neuron subtypes (adapted from Lai et al., 2016). Central axons of main C- and Aϑ-fiber subclasses, transmitting nociceptive and thermoceptive inputs, innervate the superficial dorsal lamniae I – II. Cutaneous Aϑ- and Aß-fibers terminate in deep dorsal horn lamniae III – V. Proprioceptive Aß- and Aα-fibers target lamniae VII and IX of the ventral horn.

During embryogenesis, DRG neurons undergo a morphological transition from bipolar, extending one axon each centrally and peripherally, to the canonical pseudo-unipolar structure. One branch, the distal process, projects to deep peripheral or cutaneous tissues, while the other, namely the proximal process, invades the dorsal horn of the spinal cord (Matsuda et al., 2000). Around e10.5, early born DRG sensory neurons extend central afferents into the dorsal root and

reach the DREZ, then bifurcate to extend rostrocaudally along the dorsolateral margin of the spinal cord. At e11.5, with more axons reaching the dorsolateral margin of the spinal cord, sensory afferents form a DF primordium. After a waiting period, at e12.5, a flatter and thicker DF primordium containing more stem axons sends first interstitial collaterals into the gray matter. A day later, DF and DREZ shift dorsomedially compared to their position at e12.5 with axon collaterals projecting from the dorsal spinal cord towards intermediate regions, wherein they ramify to contact with adequate target neurons during terminal branching (Figure 6) (Brown, 1981; Ozaki and Snider, 1997; Dumoulin et al., 2018).

The molecular mechanisms underlying the early organization of peripheral sensory projections into tight fascicles, and subsequent sorting into target-specific bundles are crucial to their pathfinding success but are still poorly understood. During development, DRG sensory axons and MN axons exit the DRG and the

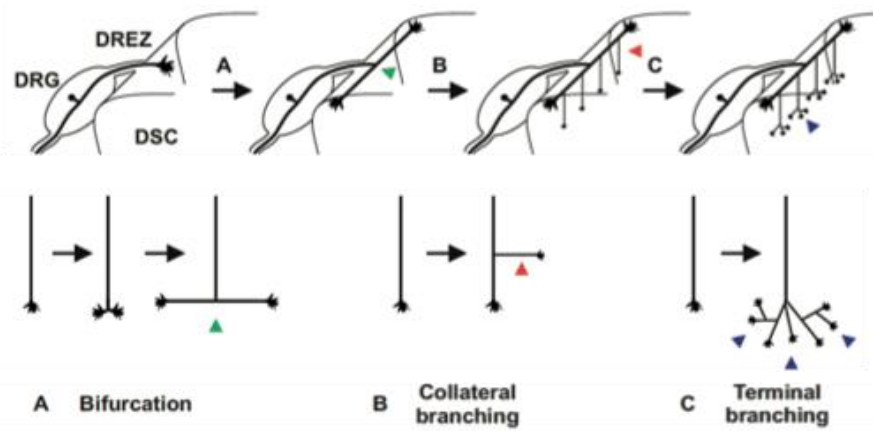

Figure 6. Extension and branching of sensory axons in the spinal cord (adapted from Dumoulin et al., 2018). (A) DRG sensory axons enter the DSC at the DREZ and then bifurcate (green arrowhead) to send stem axons rostrocaudally. (B) Collaterals from stem axons (red arrowhead) invade the grey matter of the spinal cord. (C) Last, collaterals establish terminal branches in the target layers (blue arrowhead). DREZ, dorsal root entry zone; DRG, dorsal root ganglia; DSC, dorsal spinal cord.

spinal cord, respectively, to converge in the plexus regions. Sensory-motor axon fascicles are sorted into bundles that extend over long distances to reach their respective peripheral targets (Landmesser and Honig, 1986; Wang and Scott, 1999; Huettl et al., 2011). Recent findings determine that sensory axon trajectory depends on minimal motor fiber scaffolds. Interestingly, the guidance receptor neuropilin (Npn) 1 contributes to sensory-motor axon trajectories to the limbs. *Npn-1* sensory-specific ablation resulted in severe defasciculation before, in and beyond plexus regions both regarding sensory and motor projections to fore- and hindlimbs. Surprisingly, *Npn-1*$^{-/-}$ sensory fibers lead motor fibers in their trajectories (Huettl et al., 2011). However, despite some progress, the genetic programs governing peripheral sensory projections remain unclear.

Already from embryonic stages, functionally distinct populations of sensory neurons exhibit specific projection fields in the spinal cord. TrkA^{+} nociceptive and thermoceptive projections are in the distal half of the DF where they invade the dorsal-most laminae of the spinal cord. In contrast, TrkC^{+} axons are positioned more medially in the DF where they navigate toward the intermediate and ventral spinal cord to synapse on MN (Brown, 1981; Yoshida et al., 2006). Along with specification, sensory neurons establish connections with their termination fields. Although several guidance cues and surface receptors regulate the targeting of sensory axons (Yoshida et al., 2006), a growing body of elegant studies have demonstrated involvement of the same genetic programs, that control specification, in axon connectivity (Arber et al., 2000; Raisa Eng et al., 2001; Inoue et al., 2002; Levanon et al., 2002; Zhong et al., 2006; Dykes et al., 2011; Zou et al., 2012). Indeed, Brn3a regulates central projections as *Brn3a*$^{-/-}$ mutant mice exhibit a loss in TrkA^{+} and TrkC^{+} axon segregation at the DF, probably as a consequence of improper segregation of Trk in the DRG. Also, most TrkA^{+} afferents remain at the edge of the dorsal horn and TrkC^{+} afferent fibers fail to reach the ventral horn

(Zou et al., 2012). Although Brn3a shares similar function to Isl1 (Dykes et al., 2011), in *Isl1* mutant mice, consequently to TrkA$^+$ cell loss, the innervation of superficial laminae is hindered. Oppositely, TrkC$^+$ fibers project correctly even if *TrkC* expression is initially delayed (Sun et al., 2008). In addition, *Brn3a*$^{-/-}$, *Isl1*$^{-/-}$, and *Brn3a*/*Isl1*$^{-/-}$ peripheral axon growth defects increase in severity, respectively. Depletion of both *Brn3a* and *Isl1* led to heavily impaired cervical (CP) and brachial (BP) plexuses formation (Figure 7) (Dykes et al., 2011).

Axon spinal targeting also requires Runx1 and Runx3, already known in fate specification, for cutaneous and proprioceptive sensory neuron innervation, respectively (Chen et al., 2006b; Kramer et al., 2006; Marmigère et al., 2006). *Runx1* loss-of-function switches the targeting of Ret$^+$ fibers from lamina II$_i$ to superficial laminae I/II$_o$ (Chen et al., 2006b). A complementary *Runx1* gain-of-function strategy drives TrkA$^+$ axons into the deep dorsal horn (Kramer et al.,

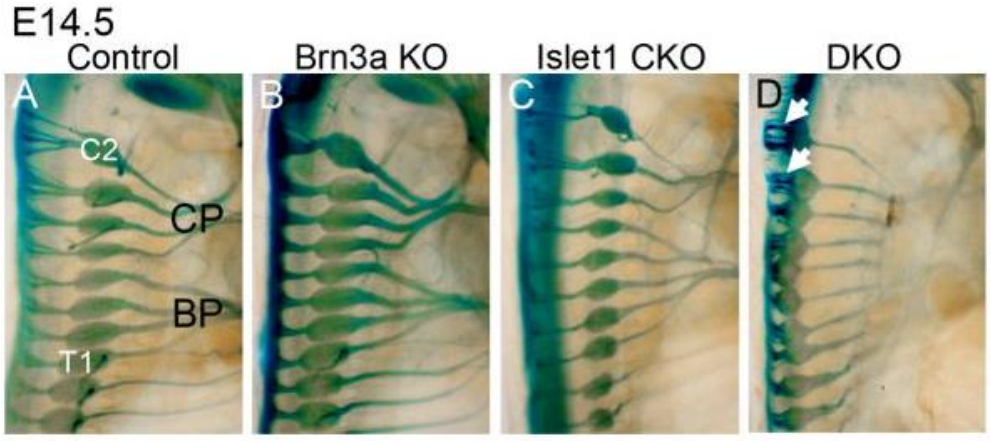

Figure 7. Peripheral innervation phenotype at mid-gestation in single or double Brn3a/Isl1 mutant embryos (adapted from Dykes et al., 2011). (A-D) DRG sensory neuron peripheral growth is increasingly disturbed in *Brn3a*$^{-/-}$, *Isl1*$^{-/-}$ and *Brn3a*/*Isl1*$^{-/-}$ mutant embryos at e14.5, respectively. Cervical DRG contribute to cervical (CP; C2-C4) and brachial (BP; C5-T1) plexuses that innervate the occiput, neck, and upper limbs. The initial segments of spinal nerves are present but do not reach the CP or BP in *Brn3a*/*Isl1*$^{-/-}$ mutant mice.

2006). In *Runx3* mutant mice, TrkC$^+$ axons fail to terminate into the intermediate zone and the ventral horn (Inoue et al., 2002; Levanon et al., 2002). In chick embryos, ectopic *Runx3* expression switched dorsal horn entrance of TrkA$^+$ central trajectories from lateral to medial. Furthermore, TrkA$^+$ axons were redirected from dorsal to intermediate or even ventral horn regions. In contrast, *Runx3* knock-down in TrkC$^+$ neurons redirects their axons to dorsal or intermediate regions of the spinal cord (Chen et al., 2006a).

Other transcription factors were demonstrated to participate in the control of axonal growth. Proper ventral termination of proprioceptive axons requires ETS-related protein (Er) 81, as *Er81* inactivation causes TrkC$^+$ axons to terminate in ectopic dorsal position within the intermediate cord (Arber et al., 2000). Drg11, a HD TF expressed in both DRG and dorsal spinal cord neurons contributes to nociceptive connectivity. Although TrkA$^+$ afferences enter properly to the dorsal spinal cord, the delayed fiber ingrowth is rerouted to the medial region of the dorsal horn in *Drg11*$^{-/-}$ mice (Chen et al., 2001).

1.3 The Onecut transcription factors

The Onecut (OC) transcription factor family is composed of three members in mammals: OC-1, OC-2 and OC-3 (Lemaigre et al., 1996; Samadani and Costa, 1996b; Jacquemin et al., 1999; Vanhorenbeeck et al., 2002). OC-1, also known as Hepatocyte nuclear factor-6 (HNF-6), was identified in the rat liver as an activator of the 6-phosphofructo-2-kinase gene promoter (Lemaigre et al., 1996; Samadani and Costa, 1996b). Alternative splicing generates two OC-1 isoforms. A predominant OC-1α isoform and a ß isoform that differs by an 26 amino acid insert located between the cut and the HD (Lannoy et al., 1998). Its two paralogs *Oc2* and *Oc3* were identified based on computational identification of *Oc1* homologous sequences from a fetal human retina cDNA library and a screening of the human genome data bank, respectively (Jacquemin et al., 1999; Vanhorenbeeck et al., 2002). During embryogenesis, OC factors are expressed in the liver, the pancreas, the stomach, the duodenum, and in the nervous system (Figure 8). Generally, OC proteins are either transiently or continuously expressed in a characteristic spatial OC-1 > OC-2 > OC-3 hierarchy. Also, highly homologous OC-2 and OC-3 frequently overlap with OC-1 suggesting similar and even redundant functions during development.

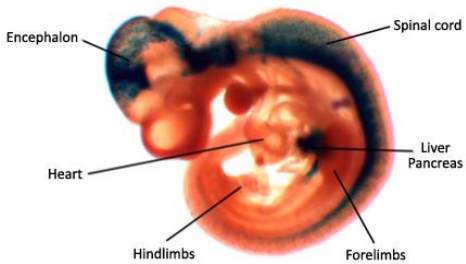

Figure 8: Expression pattern of *Oc2* in a mouse embryo (courtesy of Pr. P. Jacquemin). Whole-mount β-galactosidase staining for expression of Oc2-lacZ on wild-type embryo at e9.5 revealed *Oc2* expression in the developing liver, pancreas, and duodenum and in the nervous system. X-gal staining recapitulates the expression pattern of all three OC factors.

1.3.1 Onecut transcription factor structure

OC proteins harbor a single cut domain (CD) and an atypical HD, which constitutes the bipartite DNA-binding domain linked by a short 27 amino acid sequence (Lemaigre et al., 1996). The unique CD is organized in five α helices (helices 1 – 3 and 5 – 6) and a 3_{10} helix (helix 4) with the third helix acting as the recognition helix that binds to the target DNA (Iyaguchi et al., 2007). Moreover, a conserved LXXLL motif located in the third helix interacts with co-activators (Lannoy et al., 2000). The divergent HD consists of three α helices (helices 7 – 9) with the ninth helix functioning as the DNA recognition helix. Phenylalanine at position 48 and methionine at position 50, in helix 9, form the distinctive F48M50 dyad of OC particular HD (Lemaigre et al., 1996; Lannoy et al., 1998). Besides these conserved domains, several other highly conserved regions are found in OC sequences. A 24 amino acid serine, threonine, and proline enriched region, namely the TP box, is present in all OC proteins albeit the OC-3 TP box is devoid of serine residues. A C-terminal polyserine (polySer) 19 amino acid sequence and a polyhistidine (polyHis) tract downstream of the TP box were identified in OC-1 and OC-2. Although these tracts were absent in OC-3, it shares a polyglycine (polyGly) tract upstream of the TP box with OC-2 (Jacquemin et al., 1999; Vanhorenbeeck et al., 2002). Finally, OC-3 is distinct from OC-1 and OC-2 by its C-terminal 5 threonine residues, two polyproline (2polyPro) and three polyglycine (3polyGly) tracts (Figure 9) (Vanhorenbeeck et al., 2002).

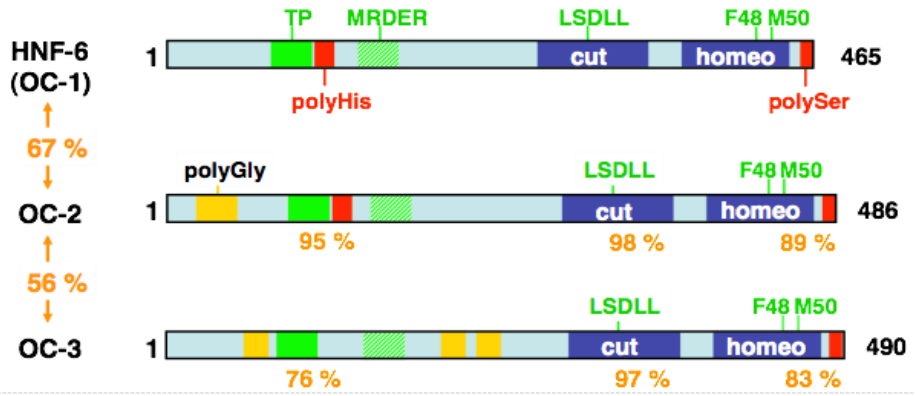

Figure 9. Schematic structure of conserved regions of OC transcription factors. The OC CD and HD, the two DNA-binding domains, are displayed in blue. The CD displays an LXXLL motif. The HD contains an F48M50 dyad. Residues or regions that stimulate OC factor transcriptional activity are in green. Inhibitory residues or regions are depicted in red. Conserved residues or regions with uncharacterized activity are shown in orange. Identity percentages between conserved regions compared to OC-1 and between the three OC proteins are identified in light blue.

1.3.2 Onecut transcriptional activity

In mammals, all three OC proteins act as transcriptional activators with CD and HD binding target DNA regions. A dual-mode of DNA binding and transcription activation is used by OC factors depending on the target genes, illustrated by the OC-1 regulatory mechanism on *transthyretin* (*ttr*) or *Hnf-3ß* representative genes. Electrophoretic mobility shift assay (EMSA) experiments demonstrated that the *ttr* promoter requires both CD and HD DNA binding, whereas only the CD binds the *Hnf-3ß* promoter (Lannoy et al., 1998). The CD is indispensable for DNA binding to all target genes while the HD binds only to a subset of these sequences. The HD is either required for DNA-binding or transcriptional stimulation (Lannoy et al., 1998, 2000). As mentioned earlier, OC proteins can interact with co-activators. On the one hand, CREB-binding protein (CBP) and p300/CBP-associated factor (p300) interact with the CD LXXLL motif and the HD F48M50 dyad to

stimulate OC transcriptional activity when both domains bind target DNA. On the other hand, p300 is recruited in an LXXLL-independent manner when only the CD is utilized for DNA-binding (Lannoy et al., 2000).

Several conserved residues contribute to the transcriptional stimulation ensured by OC proteins as demonstrated by co-transfection of mutant *Oc1* expression vectors and luciferase reporter constructs harboring regulatory sequences bound by OC-1. The CD LXXLL motif and the HD characteristic F48M50 dyad stimulate OC transcriptional activity along with the TP box. In contrast, transcription activity is inhibited by polySer and polyHis tracts (Lannoy et al., 2000). EMSA experiments based on the consensus sequence 5' (A/T/G)-(A/T)-(A/G)-T-C-(A/C)-A-T-N-(A/T/G) 3' found in *ttr* and *Hnf-3ß* regulatory regions resulted in the identification of several sequences that bind all OC proteins, except for *Hnf4* which does not bind OC-2. Five out of six target sequences contain the conserved TCAAT core in the recognition sequence of OC target sequences (Table 1) (Lannoy et al., 1998; Jacquemin et al., 1999, 2001; Vanhorenbeeck et al., 2002).

Target gene	Recognition sequences	OC1	OC2	OC3
Hnf3ß	GAAAAAA**AAATCAATAT**CGGGCCT	+++	++	+++
transthyretin	GTCTGCT**AAGTCAATAA**TCAGAAT	+++	+	+
Hnf4	AGGATAG**AAGTCAATGA**TCTGGGA	+	-	++
glucokinase	GGGAAAG**TGATCAATCG**TGTCAAG	+++	++	+
mitf	AAAAATA**AAATCAACAT**TTAA	+++	++	+
pdx1	AGGCATG**TAATCAATAA**ATAACAT	++	++	+
mutated *pdx1*	AGGCATG**TAACAAATAA**ATAACAT	-	-	-

Table 1. OC recognition sequences on different target genes (adapted from Vanhorenbeeck et al., 2002). The first column refers to the target gene names. The target gene recognition sequences are represented in bold with the core TCAAT sequence highlighted in red in the second column. For each recognition sequence, the affinity of each OC factor is represented by plus (+) and minus (–).

1.3.3 Onecut factors expression and functions in development

1.3.3.1 OC expression and roles in endoderm derivatives

OC factors are expressed in the endoderm and its derivatives: the liver, the pancreas, the gut and the stomach, the two latter organs do not express OC-1 (Landry et al., 1997; Vanhorenbeeck et al., 2002; Pierreux et al., 2004). In the liver OC-1 and OC-2 are present in hepatoblasts, in hepatocytes, and in the biliary cells (Jacquemin et al., 2003b). In the pancreas, OC are initially present in pancreatic progenitors, and then become restricted to ductal cells (Jacquemin et al., 2003b; Pierreux et al., 2006).

During liver development, OC-1 and OC-2 redundantly regulate hepatoblast differentiation into hepatocytes or biliary epithelial cells. Also, OC-1 is required for biliary tract differentiation and morphogenesis (Clotman et al., 2002, 2005). Moreover, OC-1 and OC-2 control hepatoblast migration into the septum transversum mesenchyme (STM). In *Oc1/Oc2*$^{-/-}$ mutants, the basal lamina surrounding the liver bud is reduced, hepatoblast delamination and STM invasion decreases (Margagliotti et al., 2007). In the pancreas, OC-1 and OC-2 are crucial for pancreas specification, pancreatic endocrine differentiation and duct morphogenesis (Jacquemin et al., 2000, 2003a; Pierreux et al., 2006). Even if expressed in enteroendocrine cells of the stomach and intestine, OC-2 and OC-3 are dispensable for enteroendocrine differentiation (Vanhorenbeeck et al., 2007).

1.3.3.2 OC expression and roles in the nervous system

During the characterization of OC factors in endoderm-derived tissues, they were detected both in murine developing CNS and PNS (Block et al., 1996; Landry et al., 1997; Jacquemin et al., 1999, 2003b; Vanhorenbeeck et al., 2002; Hodge et al., 2007). During CNS neurogenesis, OC factors are present in several post-mitotic neuronal populations (Francius and Clotman, 2010; Espana and Clotman, 2012b; Wu et al., 2012; Audouard et al., 2013; Francius et al., 2013; Kabayiza et al., 2017). In the developing PNS, only OC-1 and OC-2 are detected in the trigeminal ganglia and the DRG (Landry et al., 1997; Hodge et al., 2007).

1.3.3.2.1 OC expression and roles in the CNS

Extensively described in the embryonic spinal cord, OC factors expression begins within the newly born MN. Until e11.5, OC protein spatial distribution is partially overlapping with an OC-1 > OC-2 > OC-3 hierarchy. Then, OC-2 predominates in medial (MMC) and hypaxial motor column (HMC) neurons, whereas OC-1 and OC-2 presence declines. In preganglionic motor column (PGC) neurons, OC-1 is the main OC protein as OC-2 and OC-3 presence is transiently detected at e12.5. At limb levels, OC proteins are enriched in the medial columnar subdivision of the lateral motor column (LMC_m) as compared to its lateral division (LMC_l). Moreover, OC factors exhibit a dynamic temporal profile in each MN subtype (Francius and Clotman, 2010). Compound *Oc1/Oc2* deletion demonstrated OC factor requirement in MN proper diversification. At *Oc1/Oc2*$^{-/-}$ mice limb levels, the LMC_m is converted into neurons of the LMC_l as total LMC neuronal numbers are not affected. LMC neuron identity conversion resulted in redirected LMC ventral axonal projections to dorsal territories. At thoracic level, OC factors regulate the ratio between visceral and somatic MN, contained in PGC or MMC and HMC respectively (Figure 10) (Roy et al., 2012).

Additionally to MN, the ventral spinal cord is enriched in OC factors in ventral interneuron (vIN) populations (Francius and Clotman, 2010; Francius et al., 2013). The OC were differentially detected in several vIN subpopulations and their

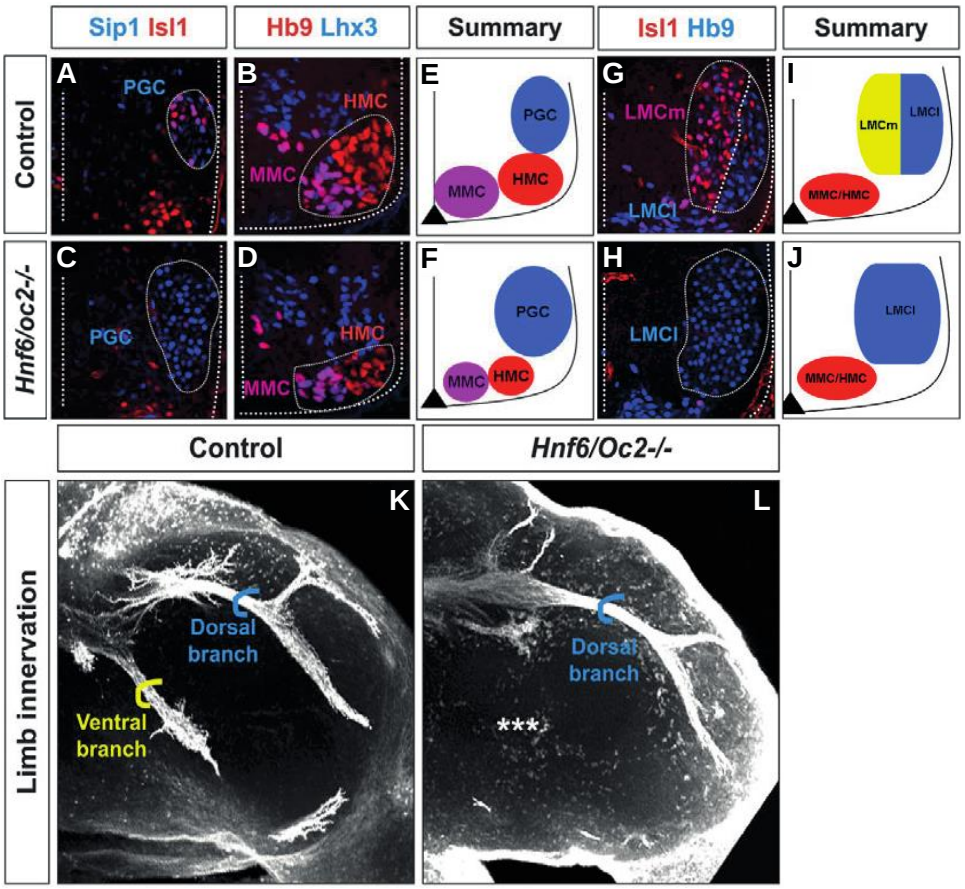

Figure 10: The OC factors control the diversification of MN (adapted from Roy et al., 2012). (A-F) At thoracic level, OC factors control the differentiation ratio between the somatic (HMC and MMC) and visceral (PGC) MN. In the absence of OC factors, the visceral MN are produced in excess at the expense of somatic MN. (G-J) At limb levels, OC factors promote the diversification of the LMC_m neurons and control the LMC_m/LMC_l ratio. In the absence of OC factors, the LMC_m neurons are converted into LMC_l neurons, while the total number of the LMC neurons is not affected. (K-L) This molecular identity switch is accompanied by a redirection of the LMCm axons towards the dorsal mesenchyme of the limbs.

subsets: $V0_V$, $V0_{CG}$, V1 Renshaw cells (RC), V2a to V2c and $V3_D$ neurons (Stam et al., 2012; Francius et al., 2013; Harris et al., 2019). Among V1 neurons, OC-2 and then OC-1 are the first factors to be activated in RC, the first produced V1 subtype (Stam et al., 2012). All three OC factors are present in multiple V2 IN subsets (Francius et al., 2013; Harris et al., 2019).

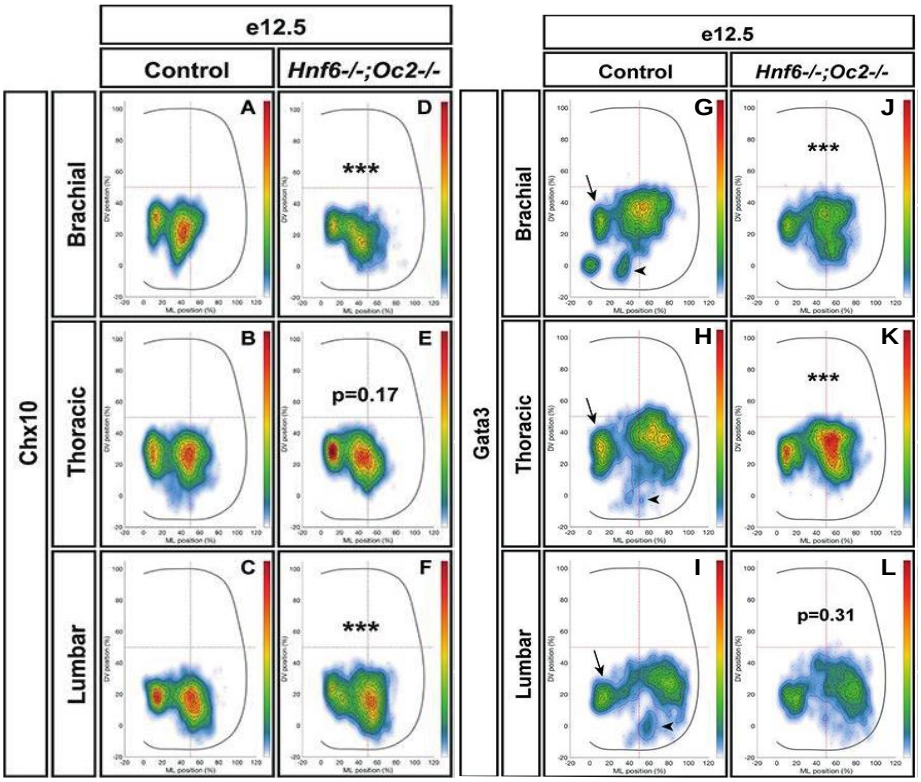

Figure 11: OC factors regulate the distribution of V2a and V2b interneurons (adapted from Harris et al., 2019). (A-C) At e12.5, control V2a interneurons distribute in a major central group and a minor medial group, at each level of the spinal cord. (D-F) In mutant embryos, the relative cell distribution seems altered, with relatively fewer central cells at the brachial level and less medial cells at the lumbar level. (G-I) V2b cells are distributed in a major central (brachial level) or lateral (thoracic and lumbar levels) cluster with minor subsets located more medially (arrows) or ventrally (arrowheads). (J-L) In OC mutant embryos at e12.5, the major population remains more compact, more centrally located and slightly more ventral. In addition, the ventral V2b subset is significantly depleted.

In vIN development, OC factors are required for V1 RC identity maintenance, while in V2 they regulate diversification of V2a MafA^{+} and cMAf^{+} subsets and differentiation of V2c neurons. Finally, OC regulate V2a and V2b distribution along the dorso-ventral (DV) axis of the spinal cord through a genetic pathway involving Pou2f2 (Figure 11) (Harris et al., 2019).

As in the developing spinal cord, OC factors are detected in several populations of the mouse encephalon wherein they exert various roles. First, in the A13 nucleus dopaminergic population, OC factors are dynamically and differentially expressed throughout the two phases of A13 development. In the first phase, OC protein distribution follows a partially overlapping OC-1 > OC-2 > OC-3 spatial hierarchy. Later, OC-2 presence is progressively decreased resulting in only OC-1 and OC-3 maintenance during the second phase. During the latter, OC proteins regulate A13 population displacement from the pial surface towards their final location, namely the vicinity of the third ventricle, and the maintenance of their specific identity. Indeed, *Oc* depletion leads to a scattered A13 dopaminergic nucleus that eventually no longer conserves its dopaminergic phenotype (Espana and Clotman, 2012b). Second, OC factors are detected in developing sensory neurons of the rhombencephalic part of the mesencephalic trigeminal nucleus (rMTN) and are required for their production. Being transiently present in developing noradrenergic Locus coeruleus (LC) neurons, a nucleus close to the rMTN, OC regulate the migration and maintenance of this nucleus probably in a non-cell autonomous manner (Espana and Clotman, 2012a). Third, OC factors are detected in retinal progenitor cells and persist in developing retinal ganglion cells (RGC) and horizontal cells (HC) (Wu et al., 2012). OC-1 and OC-2 promote RGC and HC as inactivation of both *Oc1* and *Oc2* led to complete HC depletion, while cones and RGC were modestly reduced (Sapkota et al., 2014). Lastly, *Oc1* is detected from birth until P7 in Purkinje cells. After birth, Purkinje cells undergo reorganization

from a multilayered to a mature single-layered population, a process affected in *Oc1* mutants. Indeed, Purkinje cells form an irregular cell layer with absent, superposed, or even mislocated cells in some *Oc1*$^{-/-}$ cerebellum regions (Audouard et al., 2013).

Moreover, OC-1 regulates the postnatal formation of hindlimb neuromuscular junctions (NMJ), the synapses between MN and muscle fibers. Morphological alteration and delayed formation of hindlimb NMJ in *Oc1*$^{-/-}$ mice resulted in hindlimb muscle weakness, accompanied by tibialis anterior and gastrocnemius hypotrophy, and abnormal hindlimb positioning during locomotion (Audouard et al., 2012). In addition, *Oc1* mutant mice also had poor balance and coordination defects likely due to Purkinje cells disorganization (Audouard et al., 2013).

1.3.3.2.2 OC expression and roles in the PNS

In the developing PNS, both *Oc1* and *Oc2* are expressed in the trigeminal ganglion (TG). Initially, *Oc2* is expressed homogeneously in TG neurons. Then, strong *Oc2* expression is restricted to the ventral half of the maxillary (Mx) and the majority of mandibular (Md) neurons. Nevertheless, the dorsal half of the Mx and the ophthalmic (Op) regions continue to produce weak *Oc2* levels. *Oc1* expression is limited to Md neurons and a narrow ventral stripe of the Mx neurons. In the TG, OC-2 alone contributes to proper central projections of sensory neurons. Indeed, *Oc2*$^{-/-}$ TG sensory neurons form defective central projections into the brainstem. Also, the somatotopic maps of whiskers contained misaligned large barrelettes while small barrelettes formed blurred individual boundaries (Figure 12) (Hodge et al., 2007).

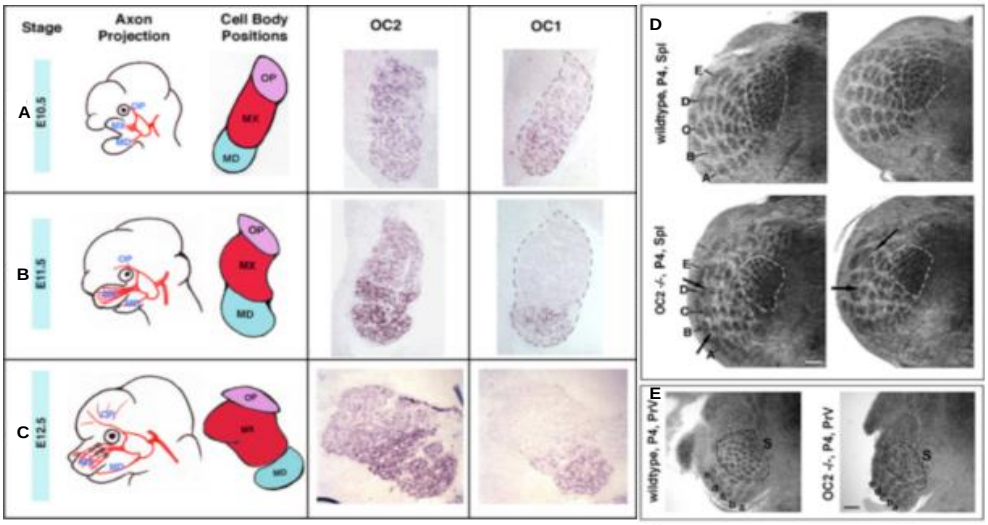

Figure 12. OC-2 control the proper central projection of TG sensory neurons (adapted from Hodge et al., 2007). (A–C) Schematic drawing represents the mouse head with TG location, the initial outgrowth of TG axons, and the developing craniofacial structures. In situ hybridization of genes encoding Oc1 and Oc2 within the e10.5 (A), e11.5 (B), and e12.5 (C) TG. (D–E) Cytochrome oxidase staining in the pars interpolaris nucleus (D) and the principal trigeminal nucleus (E) at P4 in wildtype or $Oc2^{-/-}$ mutant mice. Barrelettes are variably misaligned and fused while small barrelettes are poorly formed with blurred boundaries between individual small barrelettes. Arrows point to misaligned and fused barrelettes in $Oc2^{-/-}$ mice. Dotted lines delineate small barrelettes that map small maxillary whiskers on the upper lip. The five rows designated as A-E represent large whiskers. Dotted line circles designated as S delimitate the small whiskers designated as S.

To summarize, extensive studies of OC roles in the developing nervous system demonstrated their involvement in production, diversification, maintenance, settling position, and connectivity of specific neuronal populations (Table 2). By controlling these processes, OC factors probably contribute to the integration of neuronal populations into networks that form functional circuits. Interestingly, OC are also detected in the dorsal spinal cord where they might participate in the diversification and/or migration of dIN. The two processes are essential for proper

integration into functional circuits as observed in several vIN subsets and populations (Harris et al., 2019).

Function	OC	Neuron type	Targets	Mechanism	Reference
Production	All	mdDA neurons	N.D.	N.D.	(Chakrabarty et al., 2012)
	All	MTN neurons	N.D.	N.D.	(Espana and Clotman, 2012a)
Diversification	All	MN	*Isl1*	Direct binding	(Roy et al., 2012)
Maintenance	All	RC	N.D.	N.D.	(Stam et al., 2012)
	All	LC neurons	N.D.	Possibly non-cell autonomous	(Espana and Clotman, 2012a)
Neuronal connectivity	OC-2	TG neurons	N.D.	N.D.	(Hodge et al., 2007)
	OC-1	NMJ	*Agrin, TGFbRII* & *Neuregulin-2*	Direct/indirect binding	(Audouard et al., 2012)
Migration	OC-1	Purkinje cells	N.D.	N.D.	(Audouard et al., 2013)
	All	A13 neurons	N.D.	N.D.	(Espana and Clotman, 2012b)
	All	vIN	Pou2f2	N.D.	(Harris et al., 2019)

Table 2: Summary of OC various roles during the nervous system development.

Although their mechanisms of actions are partially understood in the developing liver and pancreas, they remain elusive in the nervous system. In fact, OC directly target the expression of genes essential for proper liver and pancreas development, namely *Hnf1ß, Hnf3α/ß, Hnf4α*, *Pdx1, neurogenin-3, PFK2, PEPCK, glucokinase,* or control TGFß/activin signaling (Samadani and Costa, 1996b; Rausa et al., 1997; Landry et al., 1997; Jacquemin et al., 1999, 2000, 2003a; Gannon et al., 2000; Clotman et al., 2002, 2005; Vanhorenbeeck et al., 2002, 2007; Pierreux et al., 2004, 2006; Margagliotti et al., 2007; Zhang et al., 2009). Although *Hnf1ß*, *neurogenin-3* and *Pdx1* are also expressed during CNS development, OC factors do not seem to act upstream as observed in the endoderm derivatives. Nevertheless,

some OC targets were identified in developing MN. First, OC factors stimulate *Isl1* expression by direct binding on one of the *Isl1* regulatory elements, namely the CREST2 enhancer (Uemura et al., 2005; Roy et al., 2012; Toch and Clotman, 2019). Second, OC absence resulted in PGC *Isl1* and *Foxp1* downregulation, the two TF being required for PGC differentiation (Thaler et al., 2004; Rousso et al., 2008; Roy et al., 2012). Lastly, OC-1 acts on NMJ development via a genetic program including several factors such as *agrin*, *neuregulin-2*, and *TßRII* as demonstrated by their downregulation in lumbar MN lacking *Oc1* (Audouard et al., 2013).

2 Objectives and strategies

The great variety of sensory information, such as nociceptive, thermal, mechanical or proprioceptive stimuli, is conveyed from the periphery to the spinal cord by dedicated sensory neurons, which cell bodies reside in the DRG. Although progress has been made in elucidating the establishment of sensory neuron and dorsal interneuron diversity in the DRG and the spinal cord, respectively, the mechanisms that regulate early differentiation of each specific neuronal population are only partly understood. Previously detected in both neuronal types (Landry et al., 1997; Francius and Clotman, 2010), OC distribution profile and function in the development of these neurons remain elusive. Thus, the aim of my thesis was to determine the roles of OC TF in the development of spinal dIN and of DRG sensory neurons. The main research questions of my thesis and the corresponding goals were:

What kind of function do the OC factors have in the development of dorsal interneurons?

1. Identification of OC^+ dIN populations and characterization of OC distribution profile.
2. Characterization of OC roles during dIN diversification and distribution using *Oc1/Oc2*$^{-/-}$ mice embryos.

First, our strategy was to determine the distribution of OC-1, OC-2 and OC-3 in combination with specific markers of each dIN population. Second, using transgenic mouse line deficient for *Oc1* and *Oc2* (Jacquemin et al., 2000; Clotman et al., 2005), wherein *Oc3* expression is lost in the central nervous system (Roy et al., 2012), we determined OC roles in dIN diversification and distribution. On the

one hand, the diversification study of the *Oc1/Oc2*$^{-/-}$ mutant embryos consisted in quantifying cell numbers of each distinct population and subpopulation of dIN in control or *Oc1/Oc2*$^{-/-}$ embryos. On the other hand, the distribution of dIN population was evaluated using a quantitative method initially developed for MN distribution analysis, which we adapted for analysing the distribution of any spinal population in control or *Oc1/Oc2*$^{-/-}$ spinal cords.

By which mechanism of action do they regulate dorsal interneuron development?

1. Unraveling OC molecular and cellular mechanisms in the regulation of dIN diversification and distribution.
2. Elucidation of the selected candidate roles, downstream of OC, during dIN population development.

First, we identified *Pou2f2* as a candidate gene downstream of OC factors from transcriptome comparison of control or *Oc1/Oc2*$^{-/-}$ neural tubes (Harris et al., 2019). *Pou2f2* differential expression in *Oc1/Oc2*$^{-/-}$ mutants indicated its potential involvement in the control of dIN development by the OC factors. After determining *Pou2f2* expression profile and its protein distribution in the dorsal spinal cord of control or *Oc1/Oc2*$^{-/-}$ mutant embryos, our goal was to investigate putative involvement of Pou2f2 in dIN differentiation and/or distribution by loss- or gain-of-function approaches (Corcoran et al., 1993; Harris et al., 2019).

What role do OC-1 and OC-2 play in DRG sensory neuron development?

1. Identification of OC-1^{+} and OC-2^{+} sensory neurons and characterization of OC distribution profile.
2. Characterization of OC-1 and OC-2 roles during SN development using *Oc1/Oc2*$^{-/-}$ mice embryos.

In parallel, we started by describing OC-1 and OC-2 distribution, wherein OC-3 is absent, in TrkA$^+$, TrkB$^+$ or TrkC$^+$ neurons. Then, using the same transgenic mouse line deficient for *Oc1* and *Oc2,* we determined their roles in sensory neuron differentiation and extension of central or peripheral projections (Jacquemin et al., 2000; Clotman et al., 2005). On the one hand, differentiation studies of the *Oc1/Oc2*$^{-/-}$ mutant embryos consisted in quantifying cell numbers of each distinct sensory neuron subtype in control or *Oc1/Oc2*$^{-/-}$ embryos. On the other hand, projections were evaluated using two approaches: either TrkA$^+$, TrkB$^+$ and TrkC$^+$ central afferents were analyzed on transversal sections of control or *Oc1/Oc2*$^{-/-}$ embryos or using whole-mount immunolabelings of TrkA combined to volume imaging of whole cleared control or *Oc1/Oc2*$^{-/-}$ embryos with cutting-edge lightsheet microscopy (Renier et al., 2014).

So far, most studies on the Onecut factors have focused on their role in the development of neuronal populations involved in the motor functions of the organism (Audouard et al., 2012, 2013; Roy et al., 2012; Harris et al., 2019). In this study, we tried to shift the focus on the sensory part of the nervous system by studying spinal dIN and sensory neurons of the DRG. On the one hand, the results of this thesis dissertation unveil the involvement of OC factors in the development of spinal dorsal interneurons and new molecular insights into the mechanism by which OC proteins control the distribution of these cells. On the other hand, this work establishes a new role of OC transcription factors in the development of sensory neurons of the DRG.

3 Results

3.1 The Onecut transcription factors regulate differentiation and distribution of dorsal interneurons during spinal cord development

3.1.1 Foreword

The dorsal neuronal populations of the spinal cord, generated from dP domains, progressively subdivide in neuronal subsets (Lu et al., 2015; Bikoff et al., 2016) and migrate along stereotyped pathways to eventually settle at target locations in the developing spinal cord. The acquisition of adequate neuronal position is crucial for microcircuit organization. For example, dIN position along the mediolateral axis in lamina V determines their connectivity with sensory afferents (Ladle et al., 2007; Tripodi et al., 2011; Hilde et al., 2016). Also, positional distinction among Lbx1-derived premotor interneurons constrains patterns of input from sensory neurons (Goetz et al., 2015). Although dIN migrate according to highly specific and distinct directions and patterns, and display various final settling positions ranging from ventral to the dorsal most regions of the spinal cord (Lai et al., 2016), the molecular mechanisms that regulate their distribution remain unknown.

In this study, we elucidate the role of OC during dIN differentiation and distribution. In order to study the consequences of the absence of OC factors on dIN distribution, we adapted a quantitative analysis method of cell distribution within the developing spinal cord.

This work was published in **Frontiers in Molecular Neuroscience** the 26th of May 2017. I personally contribute to the characterization of the dI5 diversification and dI3, dI5 and dI6 distribution (Figures 4 – 6).

The Onecut transcription factors regulate differentiation and distribution of dorsal interneurons during spinal cord development

Karolina U. Kabayiza[1, 2†], **Gauhar Masgutova**[1†], Audrey Harris[1], Vincent Rucchin[1], Benvenuto Jacob[3] and Frédéric Clotman[1*]

[1]Université catholique de Louvain, Institute of Neuroscience, Laboratory of Neural Differentiation, Brussels, Belgium.

[2]Biology Department, School of Science, College of Science and Technology, University of Rwanda, Butare, Rwanda.

[3]Université catholique de Louvain, Institute of Neuroscience, System and Cognition Division, Brussels, Belgium.

[†]These authors have contributed equally to this work.

*** Correspondence:**

Corresponding author: Frédéric Clotman, Laboratory of Neural Differentiation, Institute of Neuroscience, Université catholique de Louvain
Avenue Hippocrate 55, box B1.55.11, B-1200, Brussels, Belgium
Phone: +32.2.764.55.71, Fax: +32.2.764.55.72,
Email: frederic.clotman@uclouvain.be

Keywords: onecut, transcription factors, spinal cord, dorsal interneurons, neural differentiation, neuronal migration, embryonic development

Abstract

During embryonic development, the dorsal spinal cord generates numerous interneuron populations eventually involved in motor circuits or in sensory networks that integrate and transmit sensory inputs from the periphery. The molecular mechanisms that regulate the specification of these multiple dorsal neuronal populations have been extensively characterized. In contrast, the factors that contribute to their diversification into smaller specialized subsets and those that control the specific distribution of each population in the developing spinal cord remain unknown. Here, we demonstrate that the Onecut transcription factors, namely Hepatocyte Nuclear Factor-6 (HNF-6) (or OC-1), OC-2 and OC-3, regulate the diversification and the distribution of spinal dorsal interneuron (dINs). Onecut proteins are dynamically and differentially distributed in spinal dINs during differentiation and migration. Analyses of mutant embryos devoid of Onecut factors in the developing spinal cord evidenced a requirement in Onecut proteins for proper production of a specific subset of dI5 interneurons. In addition, the distribution of dI3, dI5 and dI6 interneuron populations was altered. Hence, Onecut transcription factors control genetic programs that contribute to the regulation of spinal dIN diversification and distribution during embryonic development.

3.1.2 Introduction

During spinal cord development, numerous neuronal populations that progressively subdivide into smaller and discrete subsets are generated in a space- and time-regulated manner from a collection of distinct progenitor domains orderly distributed along the ventro-dorsal axis of the neural tube (Lewis, 2006; Lu et al., 2015). Each population (Grossmann et al., 2010), and each subset it generates (Bikoff et al., 2016), migrates along stereotyped pathways and settles at well-defined locations in the developing spinal cord. Several observations suggest that the position of spinal neurons is a critical determinant of microcircuit organization. Indeed, the clustering and dorsoventral settling position of motor neuron pools serve as a determinant of the pattern of sensory input specificity (Sürmeli et al., 2011). Similarly, position of dorsal interneuron (dINs) along the mediolateral axis in lamina V determines their connectivity with sensory afferents (Ladle et al., 2007; Tripodi et al., 2011; Hilde et al., 2016). Furthermore, positional distinctions among V1 interneuron subsets (Bikoff et al., 2016) or Lbx1-derived premotor interneurons (Goetz et al., 2015) constrain patterns of input from sensory and motor neurons. Finally, multiple interneuron subsets are differentially distributed along the antero-posterior axis of the spinal cord, consistent with their integration into specific but distinct local microcircuits (Francius et al., 2013). The genetic programs that support the generation and the diversification of spinal interneurons have been extensively investigated (Lu et al., 2015). However, in contrast to cortical interneurons whose migration mechanisms have been largely deciphered (Guo and Anton, 2014; Barber and Pierani, 2016), the molecular determinants that regulate the distribution of interneuron populations in the developing spinal cord remain elusive.

Spinal interneurons generated from dorsal progenitor domains of the neural tube integrate and relay proprioceptive, mechanosensory or nociceptive information to motor circuits or to higher brain centers (Windhorst, 2007; Todd, 2010; Abraira and Ginty, 2013; Bui et al., 2015; West et al., 2015; Lai et al., 2016). Dorso-ventral (DV) gradients of Bone morphogenic proteins (BMP) and wingless-type MMTV integration site family members (Wnt) signaling contribute to specify three dorsal progenitor domains (pdI1–3) according to their position along the DV axis (Wine-Lee, 2004; Timmer et al., 2005; Zechner et al., 2007; Tozer et al., 2013), whereas generation of the three more ventral domains (pdI4–6) occurs independently of these signals (Zhuang and Sockanathan, 2006; Le Dréau and Martí, 2012; Lai et al., 2016). Specific combinations of pro-neural factors and of bHLH or HD proteins direct the identity of the post-mitotic neuronal populations generated from these domains (Zhuang and Sockanathan, 2006; Lai et al., 2016). Subsequently, dorsal cells acquire an inhibitory or excitatory phenotype through a complex integrated network of factors (Cheng et al., 2004, 2005; Mizuguchi et al., 2006; Henke et al., 2009; Chang et al., 2013; Borromeo et al., 2014b; Hanotel et al., 2014). In contrast to spinal ventral interneurons, for which numerous subpopulations and subsets have been identified (Francius et al., 2013; Lu et al., 2015) and partly functionally characterized (Gosgnach et al., 2006; Zagoraiou et al., 2009; Borowska et al., 2013; Dougherty et al., 2013; Talpalar et al., 2013), the subdivision of dIN populations into more discrete subsets has only been sparsely investigated (Ding et al., 2004; Andersson et al., 2012; Dougherty et al., 2013; Bourane et al., 2015c; Hilde et al., 2016). In addition, although these cells migrate according to highly specific and distinct directions and patterns, and display various final settling positions ranging from ventral to the dorsal most regions of the spinal cord (Lai et al., 2016), the molecular mechanisms that regulate their distribution remain unknown.

Recent observations in our laboratory indicate that transcription factors of the Onecut (OC) family are present in numerous neuronal populations, including motor neurons and interneurons (Francius and Clotman, 2010; Roy et al., 2012; Francius et al., 2013) and regulate neuronal diversification and migration in the developing spinal cord (Francius and Clotman, 2014; Roy et al., 2012; unpublished data). Onecut factors, namely Hepatocyte Nuclear Factor-6 (HNF-6, or OC-1), OC-2 and OC-3, are transcriptional activators detected in liver, pancreas and CNS during embryonic development (Lemaigre et al., 1996; Landry et al., 1997; Jacquemin et al., 1999, 2003b; Vanhorenbeeck et al., 2002). In the CNS, they regulate the production (Espana and Clotman, 2012a), the diversification (Roy et al., 2012; Francius and Clotman, 2014), the distribution (Espana and Clotman, 2012a, 2012b; Audouard et al., 2013) and the maintenance (Espana and Clotman, 2012a, 2012b; Stam et al., 2012) of specific neuronal populations, as well as the formation of neuromuscular junctions (Audouard et al., 2012). In motor neurons, they are required to maintain levels of *Isl1* expression necessary to support the diversification of this population into distinct subsets (Roy et al., 2012). Their presence was also detected in the dorsal embryonic spinal cord (Francius and Clotman, 2010; Francius et al., 2013). However, their distribution in dINs and their possible functions in the development of these cell populations remain unknown. Here, we demonstrate that OC factors are produced in a temporally- and spatially defined manner in most early populations of spinal dINs. Furthermore, our analyses of mutant mice devoid of OC factors suggest that these proteins control genetic programs that contribute to the regulation of dIN diversification and distribution during embryonic development.

3.1.3 Results

OC factors are transiently detected in spinal dorsal interneurons during development

In the embryonic spinal cord, the OC transcription factors are present in motor neurons and in several populations of ventral interneurons at the onset of neuronal differentiation (Francius and Clotman, 2010; Stam et al., 2012; Francius et al., 2013). These proteins are also detected in more dorsal populations located in the mantle zone (Francius and Clotman, 2010), suggesting that they are present in differentiating dINs. To address this question, we analyzed the distribution of OC factors at thoracic levels in the dorsal embryonic spinal cord at early stages of dIN differentiation, namely e10.5 and e12.5. Dorsal populations were identified by immunofluorescence using combinations of specific markers, and the presence of HNF-6, OC-2 and OC-3 in each population was individually addressed and quantified. Immunolabelings are illustrated at thoracic levels of the spinal cord, similar observations were made at brachial and lumbar levels.

As previously reported in motor neurons and ventral interneurons (Francius and Clotman, 2010; Stam et al., 2012; Francius et al., 2013), the distribution of the three Onecut proteins in dINs was partially overlapping. Accordingly, subsets of cells in each dorsal population except dI1 interneurons (data not shown) contained either one, two or the three OC factors (Supplementary Figures S1, S2A,C). Newly-born dI2 cells express Lhx1 and Olig3 (Helms and Johnson, 2003; Müller et al., 2005), and HNF-6 was detected as early as e9–9.5 in a majority of these cells (Supplementary Figure S3). At later stages, dI2 interneurons are identified as Foxd3- and Brn3a-positive cells (Helms and Johnson, 2003) in dorsal and medial spinal cord. At e10.5, the three OC factors were detected in a limited number ofdI2 cells (Figures 1A–C,G), although corresponding to a significant

fraction of the differentiating dI2 interneurons (Figure 1H). However, the prevalence of dI2 containing OC factors quickly decreased and OC were completely absent from dI2 cells at e12.5 (Figures 1D–H).

The dI3 interneurons are defined by the presence of Isl1, Brn3a and Arx (Helms and Johnson, 2003; Poirier et al., 2004). The number of dI3 cells containing OC factors increased from e10.5 to e12.5 (Figures 1I–O), HNF-6 and OC-2 were present in a significant portion of these cells at e10.5 whereas this proportion remained below 10% at e12.5 and at both stages for OC-3 (Figure 1P). As strikingly evidenced at e12.5, most of those dI3 neurons containing OC proteins were located ventrally (Figures 1L–N).

The three OC factors were also present in dI4 interneurons, a dorsal population characterized by combined expression of Lbx1 and Lhx1/5, which is also found in more ventral dI6 cells (Helms and Johnson, 2003). Although OC were detected in a limited number of dI4 (Figures 1Q–V), these corresponded to a significant proportion of these interneurons at e10.5, which sharply decreased at e12.5 (Figure 1W).

The early-born dI5 interneurons and, from e11 onwards, late-born dILB neurons are identified by Lmx1b (Helms and Johnson, 2003; Ding et al., 2004). At e10.5, OC were present in a restricted number of dI5 interneurons (Figures 2A–C,G) corresponding to a large portion of this population for HNF-6, whereas the distribution of OC-2 and OC-3 was less extended (Figure 2H). As seen in the dI3 population, the number of dI5-containing OC factors rose from e10.5 to e12.5 (Figures 2D–G). However, due to intensive production of dI5 neurons in this time period, the proportion of OC-containing dI5 cells sharply decreased at e12.5 (Figure 2H). These observations suggested that OC factors might be present in a subpopulation of dI5 interneurons generated at early developmental stages. To

address this possibility, we investigated the distribution of OC factors in the dI5 subset characterized by the presence of Phox2a (Qian et al., 2002; Ding et al., 2004). At both stages, OC were detected in a number of Phox2a-positive neurons (Figures 2I–O) that corresponded to a majority of these cells at e10.5 and to a lower but significant proportion at e12.5 (Figure 2P). Thus, OC factors are present in dI5 interneurons and preferentially allocated to the Phox2a-positive dI5 subset generated at early developmental stages.

Finally, the dI6 population is defined by combined expression of Lbx1 and Lhx1/5 (Helms and Johnson, 2003) and includes Bhlhb5-expressing early-born dI6 subpopulation at e10.5 (Liu et al., 2007) and Dmrt3- and WT1-positive subsets at

Figure 1. Onecut (OC) factors are differentially and dynamically distributed in dI2 to dI4 populations. (A–F) Immunodetection of HNF-6, OC-2 or OC-3 (red) in Foxd3$^+$ (blue) Brn3a$^+$ (green) dI2 neurons on transverse sections of thoracic spinal cord at e10.5 (A–C) and e12.5 (D–F). HNF-6 (A–A"), OC-2 (B–B") and OC-3 (C–C") are visible in a few dI2 cells at e10.5 whereas they are not detected at e12.5 (D–F"). The number (G) and percentage (H) of OC-positive dI2 neurons per hemisection were quantified accordingly. (I–N) Immunodetection of HNF-6, OC-2 or OC-3 (red) in Isl1$^+$ (blue) Brn3a$^+$/Arx$^+$ (green) dI3 neurons on transverse sections of thoracic spinal cord at e10.5 (I–K) and e12.5 (L–N) demonstrates that OC factors are present in dI3 from e10.5 to e12.5 with a slight predominance of HNF-6 (I,L) compared to OC-2 (J,M) or OC-3 (K,N). Despite an increase in the number of OC$^+$ dI3 neurons from e10.5 to e12.5 (O), the percentage of dI3 neurons containing OC factors (P) is reduced at embryonic stage e12.5. (Q–V) Immunodetection of HNF-6, OC-2 or OC-3 (red) in Lbx1$^+$ (blue) Lhx1/5$^+$ (green) dI4 neurons on transverse sections of thoracic spinal cord at e10.5 (Q–S) and e12.5 (T–V) shows that OC factors are present in early dI4 neurons, HNF-6 (Q–Q") being the most represented. At e12.5, HNF-6 (T–T") and OC-2 (U–U") are still detected in a few dI4 neurons while OC3 (V–V") is barely detectable. Quantifications at embryonic stages e10.5 and e12.5 show that number (W) and percentage (X) of OC-positive dI4 neurons decrease from e10.5 to e12.5. The pictures show left hemisections as indicated to the left. Dashed lines delineate the spinal cord and the lumen of the ventricle. Insets are magnified views of boxed regions. Arrowheads point to double-labeled cells. Mean values ±SEM, n ≥ 3. Scale bars = 100 µm.

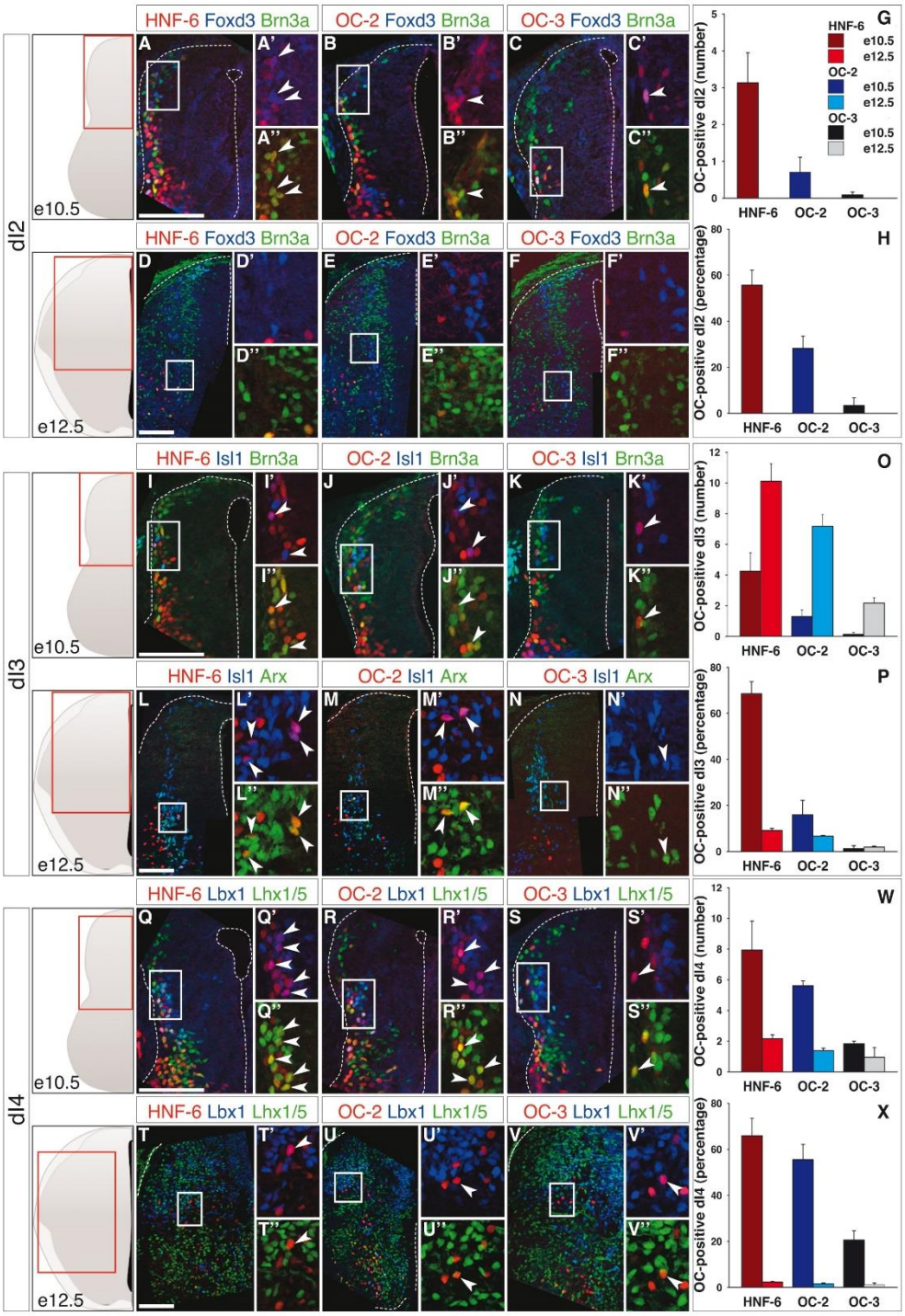
dI2
dI3
dI4
e10.5
e12.5
HNF-6 Foxd3 Brn3a
OC-2 Foxd3 Brn3a
OC-3 Foxd3 Brn3a
HNF-6 Isl1 Brn3a
OC-2 Isl1 Brn3a
OC-3 Isl1 Brn3a
HNF-6 Isl1 Arx
OC-2 Isl1 Arx
OC-3 Isl1 Arx
HNF-6 Lbx1 Lhx1/5
OC-2 Lbx1 Lhx1/5
OC-3 Lbx1 Lhx1/5
G
H
O
P
W
X
HNF-6
OC-2
OC-3
e10.5
e12.5
OC-positive dI2 (number)
OC-positive dI2 (percentage)
OC-positive dI3 (number)
OC-positive dI3 (percentage)
OC-positive dI4 (number)
OC-positive dI4 (percentage)

e12.5 (Goulding, 2009; Vallstedt and Kullander, 2013). At e10.5, OC factors were detected in a limited number of dI6 interneurons (Figures 3A–D), although corresponding to a significant portion of this population (Figure 3M). As observed for dI3 and dI5, the amount of OC-positive dI6 increased from e10.5 to e12.5 (Figures 3J–L,D) but the proportion of these cells in the global dI6 population significantly decreased (Figure 3M). In addition, OC were present in part of the Bhlhb5-positive dI6 neurons at e10.5 (Figures 3E–I) and in a fraction of the Dmrt3-positive subset at e12.5 (Figures 3N–Q), without any significant enrichment in any of these two subpopulations (compare Figure 3M with Figures 3I,Q, respectively).

Figure 2. OC factors are differentially and dynamically distributed in dI5 population and sub-population during development. (A–F) Immunodetection of HNF-6, OC-2 or OC-3 (red) in Lmx1b+ (green) dI5 population on transverse sections of thoracic spinal cord at e10.5 (A–C) and e12.5 (D–F). At e10.5, HNF-6 (A–A"), OC-2 (B–B") and OC-3 (C–C") are detected in a large number of dI5 neurons. At e12.5, the presence of HNF-6 (D–D"), OC-2 (E–E") and OC-3 (F–F") is still observed in a few Lmx1b+ dI5 neurons. (G–H) Quantifications of dI5 neurons containing HNF-6, OC-2 or OC-3 at embryonic stages e10.5 and e12.5 show that HNF-6 is broadly present in early Lmx1b+ dI5 neurons at e10.5 while OC-2 and OC-3 are less represented. Between e10.5 and e12.5, the number of dI5 neurons containing OC factors increases (G) but the ratio of those OC-positive neurons within Lmx1b+ dI5 population decreases (H). (I–N) Immunodetection of HNF-6, OC-2 or OC-3 (red) in Phox2a+ (blue) dI5 subpopulation on transverse sections of thoracic spinal cord at e10.5 (I–K) and e12.5 (L–N). At e10.5, HNF-6 (I–I"), OC-2 (J–J") and OC-3 (K–K") are detected in most of Phox2a+ dI5. At e12.5, HNF-6 (L–L"), OC-2 (M–M") and OC-3 (N–N") are still visible in a significant number of Phox2a+ interneurons. (O–P) Quantifications show an extended presence of OC factors in Phox2a subpopulation at e10.5 (P). As observed in Lmx1b+ dI5 population, the number of OC-positive cells increases between stages e10.5 and e12.5 (O), along with a moderate decrease in the ratio of Phox2a+ neurons containing OC factors (P). The pictures show left hemisections as indicated to the left. Dashed lines delineate the spinal cord and the lumen of the ventricle. Insets are magnified views of boxed regions. Arrowheads point to double-labeled cells. Mean values ±SEM, n ≥ 3; color code as for Figure 1. Scale bars = 100 μm.

OC factors were never detected in WT1-positive dI6 interneurons (Supplementary Figure S4).

Hence, OC factors were transiently detected in subsets of early-born dIN populations from dI2 to dI6 during the early steps of differentiation. Their distribution was generally broader and more persistent in more ventral dI populations as compared to dorsal cells, suggesting a possible repression of their expression by DV signaling gradients that contribute to dIN development. As previously observed in other neuronal populations (Francius and Clotman, 2010; Chakrabarty et al., 2012; Espana and Clotman, 2012b, 2012a; Roy et al., 2012;

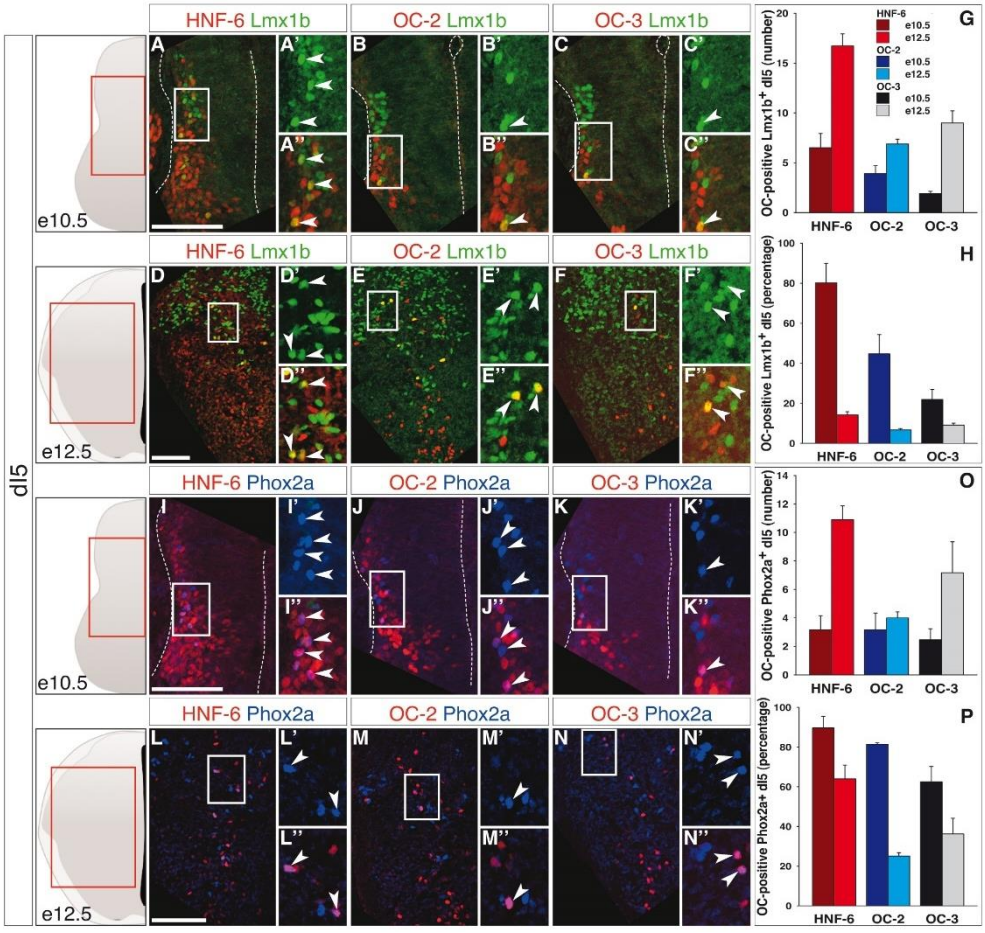

Stam et al., 2012), the three OC proteins displayed a partially overlapping distribution (Figures 1–3; Supplementary Figures S1, S2A,C). In addition, the hierarchy in their spatial extent (HNF-6 > OC-2 > OC-3) previously reported in other populations (Francius and Clotman, 2010; Espana and Clotman, 2012b) was also conserved, except for dI5 at e12.5 wherein OC-3 was more extended than OC-2. Thus, OC factors are dynamically and differentially distributed in early spinal dIN populations, suggesting that they may participate in some aspects of dIN development.

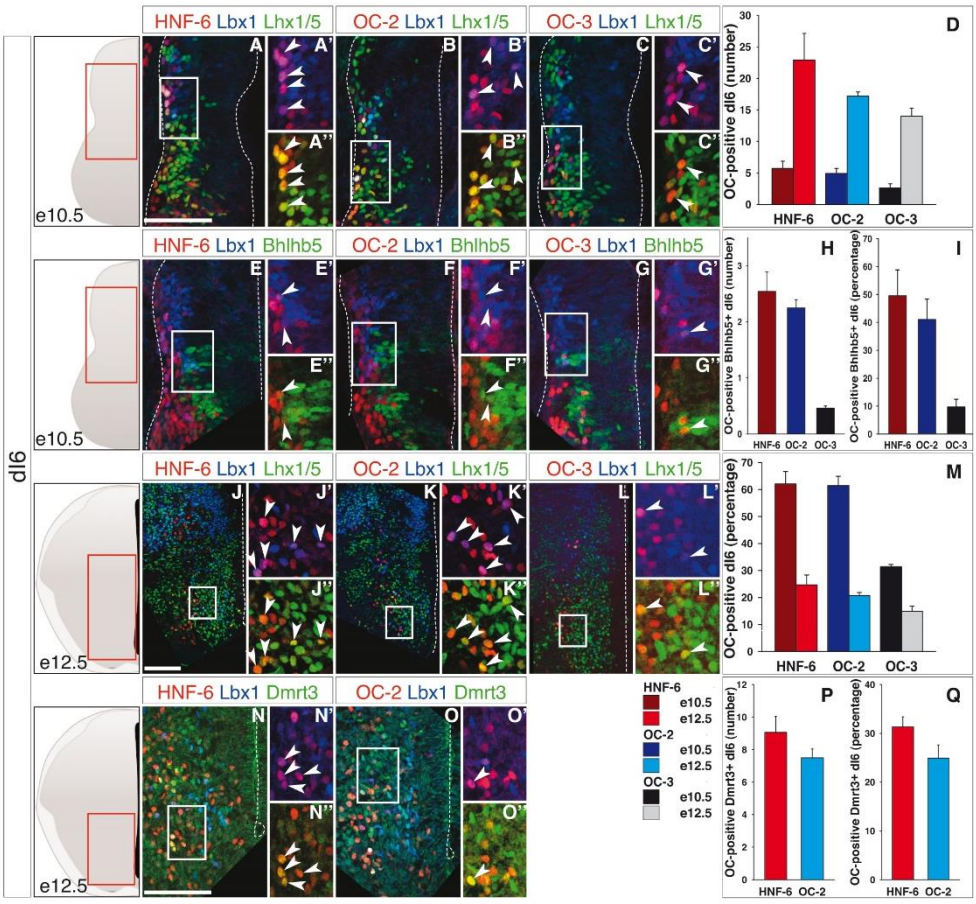

Onecut factors regulate the distribution of dI3 interneurons

To assess whether the OC proteins contribute to the development of dINs, we analyzed their phenotype in mouse embryos lacking OC factors, namely Hnf6/Oc2 double-mutant embryos. Indeed OC-3 is undetectable in the spinal cord of these mutants (Supplementary Figure S2; Roy et al., 2012), suggesting that HNF-6 and OC-2 cooperatively regulate Oc3 expression in the developing spinal cord. Considering possible differences at specific levels along the antero-posterior axis (Francius et al., 2013), analyses were performed at anterior limb (brachial region) and at thoracic levels. Since OC factors are barely detectable in the most dorsal dI1 and dI2 populations (Figures 1A–H and Supplementary Figure S3), we first addressed their potential role in dI3 development. Interestingly, dI3 is the single

Figure 3. OC factors are differentially and dynamically distributed in dI6 population and sub-populations during development. (A–I) Immunodetection of HNF-6, OC-2 or OC-3 (red) in double-labeled Lbx1+ (blue)-Lhx1/5+ (green, A–C) dI6 population or in Bhlhb5+ (green, E–G) dI6 subpopulation on transverse sections of thoracic spinal cord at e10.5. HNF-6 (A,E) and OC-2 (B,F) are present in a majority of Lbx1+Lhx1/5+ dI6 neurons and in a significant number of Bhlhb5+newly-born dI6 while OC-3 (C–G) is limited to a smaller number of cells. The number (D–H) and percentage (I–M) of OC-positive dI6 neurons per hemisection were quantified accordingly. (J–Q)Immunodetection of HNF-6, OC-2 or OC-3 (red) in double-labeled Lbx1+ (blue)-Lhx1/5+ (green, J–L) dI6 neurons or in Dmrt3+ (green, N,O) dI6 subpopulation on transverse sections of thoracic spinal cord at e12.5. HNF-6 (J,N) and OC-2 (K,O) are mainly detected in dI6 neurons located in ventral spinal cord. OC-3 (L) is also detected in Lbx1+Lhx1/5+ dI6 neurons. Its presence in Dmrt3+ dI6 could not be evaluated due to incompatibility between antibody species. (D,M) Quantifications of ventrally located dI6 neurons containing HNF-6, OC-2 or OC-3 at e12.5 show an important increase in the number of dI6 containing OC factors from stage e10.5 to e12.5 (D) but the percentage of dI6 containing OC decreases (M). (P,Q) The number of Dmrt3+ dI6 containing HNF-6 and OC-2 is small. The pictures show left hemisections as indicated to the left. Dashed lines delineate the spinal cord and the lumen of the ventricle. Insets are magnified views of boxed regions. Arrowheads point to double-labeled cells. Mean values ±SEM, n ≥ 3. Scale bars = 100 µm.

dIN population characterized by the presence of the LIM homeodomain protein Isl1, and OC factors are required in motor neurons to maintain proper Isl1 expression levels throughout differentiation (Roy et al., 2012). At e10.5 in control embryos, dI3 interneurons co-labeled for Isl1 and Tlx3 were located in a dorsal portion of the developing spinal cord, part of the population in register with the pdI3 progenitor domain while some cells did initiate ventral migration and extended to the Tlx3-single labeled dI5 domain (Figure 4A). In Hnf6/Oc2$^{-/-}$ mutant embryos, Tlx3 and Isl1 were co-detected in a dorsal population similarly distributed from the pdI3 DV position to the location of dI5 interneurons (Figure 4B), indicating that dI3 interneurons are produced in Oc mutant embryos and that OC factors are not required for Isl1 expression in these cells. The amount of dI3 cells was similar to that observed in control littermates, as confirmed by cell quantifications (Figure 4E). At e11.5, the number of control dI3 interneurons had increased and cells were distributed as a lateral stream extending from the pdI3 position to intermediate dorsoventral levels of the spinal cord (Figure 4C). In Hnf6/Oc2$^{-/-}$ embryos, dI3 interneurons similarly extended from dorsal regions to the middle of the spinal cord and their number was preserved (Figures 4D, 4F). At e12.5, to ascertain the identity of the cells that migrated in the ventral

Figure 4. OC factors control dI3 distribution. (A–M) Differentiation and distribution of dI3 interneurons in control or Hnf6/Oc2-/- embryos. At e10.5 (A,B) and e11.5 (C,D), dI3 interneurons containing Isl1 and Tlx3 in Hnf6/Oc2-/- embryos (B,D) are detected in numbers and distributions comparable to those observed in control embryos (A,C). Tlx3^{+}Isl1^{-} cells next to the ventricular zone in e11.5 control embryo are late-born dIL^{B} (C). (E–F) Quantitative analysis of control or Hnf6/Oc2-/-embryos at e10.5 (E, n = 4) and e11.5 (F, n = 4) shows no statistically significant difference in the number of dI3 cells. At e12.5, Isl1 combined with Tlx3, Brn3a or Arx identifies dI3 interneurons in the central intermediate spinal cord of control (H–J) or Hnf6/Oc2-/- (K–M) embryos. The number of dI3 cells is comparable in control and mutant embryos, and Tlx3, Brn3a and Arx are detected in the Isl1-positive cells (insets in H–M) indicating that the differentiation of dI3 interneurons is not affected by the absence of Onecut factors.

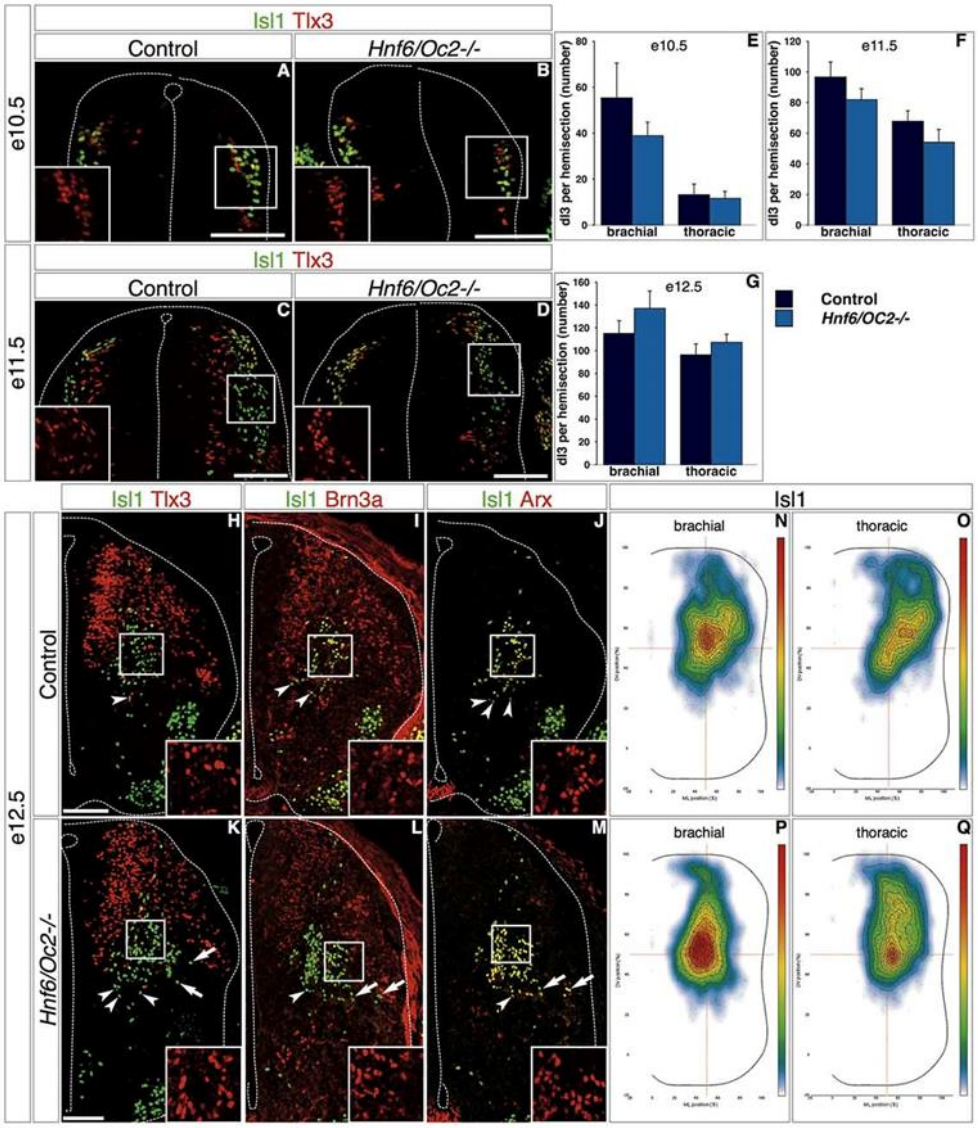

Quantitative analysis shows similar numbers of dI3 cells in control or mutant embryos (G, control n = 6, mutant n = 7). However, the distribution of these cells seems different in Hnf6/Oc2-/- embryos (arrows). (N–Q) Density plots of dI3 interneuron distribution at brachial (N,P) or thoracic (O,Q) levels in control (N,O) or Hnf6/Oc2-/- mutant (P,Q) spinal cord at e12.5 show an alteration in the localization of dI3 cells in mutant embryos. The dI3 interneurons migrate as a more compact population in a general dorso-medial to ventro-medial direction, with the densely packed cells closer to the migration front. Analysis was performed on at least

regions, dI3 interneurons were additionally labeled for Brn3a, which is detected in dI1/2/3/5/LB, and for Arx present in dI3 cells and V1 ventral interneurons (Francius et al., 2013). In control embryos, co-detection of these markers identified the dI3 population in the central intermediate region of the spinal cord, with a few dI3 cells migrating towards the floor plate (Figures 4H–J, insets show Tlx3, Brn3a and Arx labeling, respectively), consistent with their final location in the deep dorsal horn and in the intermediate laminae (Bui et al., 2015; Ding et al., 2005; Müller et al., 2005). In Hnf6/Oc2$^{-/-}$ embryos, dI3 interneurons were detected in similar regions of the spinal cord and the number of cells was comparable to that observed in controls (Figures 4K–M), as confirmed by quantifications (Figure 4G). Noticeably, the presence of the dI3 markers including Isl1 was not affected by the absence of OC proteins (Figures 4K–M, insets show Tlx3, Brn3a and Arx labeling, respectively), indicating that Isl1 maintenance in dI3 cells and proper differentiation of dI3 interneurons do not require OC factors. However, the distribution of these cells seemed different in the Hnf6/Oc2$^{-/-}$ embryos (Figures 4H–M).

Therefore, we decided to investigate the distribution of the whole dI3 population by adapting for interneurons a two-dimensional position analysis initially developed for motor neurons (Palmesino et al., 2010). Using this method, we observed that dI3 interneurons in control embryos migrated as a relatively loose population in an overall dorso-lateral to ventro-medial direction with highest density observed in the center of the distribution area (Figures 4N–O). In contrast,

three sections from five control and six mutant embryos ($n > 2600$ cells per condition; $p \leq 0.001$). The pictures show left hemisections. Dashed lines delineate the spinal cord and the lumen of the ventricle. Insets are magnified views of boxed regions and show Tlx3, Brn3a and Arx labeling, respectively. Arrowheads point to properly located dI3 neurons. Arrows indicate unproperly-located dI3 neurons in the Hnf6/Oc2-/- mutant embryos. Mean values ±SEM. Scale bars = 100µm.

the dI3 interneurons in Hnf6/Oc2$^{-/-}$ embryos migrated as a more compact population in a general dorso-medial to ventro-medial direction, with the densely-packed cells close to the migration front (Figures 4P–Q). Taken together, these observations indicate that OC factors are not required for proper differentiation of dI3 interneurons but regulate aspects of their distribution.

Onecut factors regulate diversification and distribution of dI5 subset and distribution of dI6 subpopulations

Due to the lack of specific markers and to perturbations in the distribution of several dI populations in Hnf6/Oc2$^{-/-}$ embryos (see above and below), the discrimination between early- and late-born populations of class B dINs was extremely difficult to rigorously achieve in mutant spinal cord. To circumvent this limitation, we restricted our analyses to dI5 and dI6 subsets wherein OC factors were detected (Figures 2, 3). In control embryos at e10.5, Lmx1b-positive interneurons were located in the ML region of the spinal cord, with the Phox2a dI5 subset corresponding to the most ventral cell complement (Figure 5A). In Hnf6/Oc2$^{-/-}$ embryos, Lmx1b-positive interneurons and the Phox2a subset were detected in a similar distribution (Figure 5B). Although the number of cells in each subpopulation seemed lower than in control littermates (Figure 5B), this difference was not statistically significant (Figures 5C–D). At e11.5 in control individuals, Lmx1b-positive interneurons devoid of Phox2a were migrating in a medio-ventral direction while the Phox2a subset remained in a ML position (Figure 5E). A similar situation was observed in mutant embryos, without any significant change in cell numbers (Figures 5F–H). At e12.5, Lmx1b-positive cells divided in lateral and medial cell clusters with some medial cells ventrally located. Phox2a-positive cells distributed equally between these different clusters (Figure 5I). In Hnf6/Oc2$^{-/-}$ embryos, the number of Lmx1b-positive interneurons and their location were unaffected (Figures 5J–K). However, the number of Phox2a-positive

dI5 cells decreased significantly at thoracic level of mutant embryo (Figure 5L; p = 0.011) and the relative distribution of these cells in the different clusters seemed different (Figure 5J). This was confirmed by distribution analysis, which showed that Phox2a-positive dI5 interneurons in the medial cluster were less densely-packed but instead spread along the DV axis of the spinal cord (Figures 5M–P).

Similarly, early dI6 interneurons in control embryos at e10.5 were initially located in a ML region of the spinal cord (Figure 6A, inset shows Lbx1). Their number and their location were comparable in Hnf6/Oc2$^{-/-}$ embryos (Figures 6B,C, inset shows Lbx1). At e11.5 in control embryos, these cells progressively migrated in a medio-

Figure 5. OC factors control the number and the distribution of Phox2a^{+} dI5 cells. (A–L) Identification of dI5 interneurons and Phox2a+ dI5 subset in control orHnf6/Oc2-/-embryos. At embryonic stage e10.5 (A,B), Lmx1b is present in dI5 interneurons and Phox2a is detected in a small subset of dI5 cells. (C,D) Quantitative analysis shows that number of Lmx1b+ and of Lmx1b+Phox2a+ dI5 neurons at brachial or thoracic levels are comparable in control or Hnf6/Oc2-/-mutant embryos (n= 4). At e11.5 (E,F) and e12.5 (I,J), most Lmx1b+ dI5 are located medio-laterally or migrating ventrally whereas Lmx1b+ late-born dILB extend dorsally along the ventricular zone. Phox2a labeling is still restricted to a medio-lateral (ML) subset of dI5 neurons at e11.5 but laterally and ventrally disperses (arrowheads) at e12.5. (G,H,K,L) Quantitative analysis shows similar numbers of Lmx1b+ and Lmx1b+Phox2a+ dI5 cells in control and in mutant embryos at embryonic stage e11.5 (n= 3) and e12.5 (n= 4 for control and n= 7 for mutant embryos) except for a significant decrease of Phox2a+ dI5 subset at thoracic level of e12.5 mutant embryo (p= 0.011). (M–P) Density plots of Phox2a+ dI5 interneuron distribution at brachial or thoracic levels of control or Hnf6/Oc2-/-mutant spinal cord at e12.5. Phox2a+ dI5 cells in the medial cluster are less densely-packed than in control spinal cord but instead spread along the dorso-ventral (DV) axis of the spinal cord. Analysis performed on at least three sections from five control and six mutant embryos (n> 250 cells analysed per condition; p≤ 0.001). The pictures show left hemisections as indicated to the left. Dashed lines delineate the spinal cord and the lumen of the ventricle. Arrowheads point to lateral and ventral groups of dI5 neurons. Arrows show the medial cluster of dI5 cells. Mean values ±SEM. Scale bars = 100 µm.

ventral direction and intimately intermingled with ventral interneurons characterized by the presence of Lhx1/5 without Lbx1 (Figure 6D, inset shows Lbx1). Hnf6/Oc2$^{-/-}$ dI6 interneurons seemed to migrate similarly and their number was not different from control littermates (Figures 6E,F, inset shows Lbx1). At e12.5 in control embryos, dI6 interneurons settled in the ventro-medial region of the spinal cord (Figure 6G). At that stage, two partially overlapping dI6 subsets characterized by the presence of Dmrt3 (Andersson et al., 2012; Vallstedt and

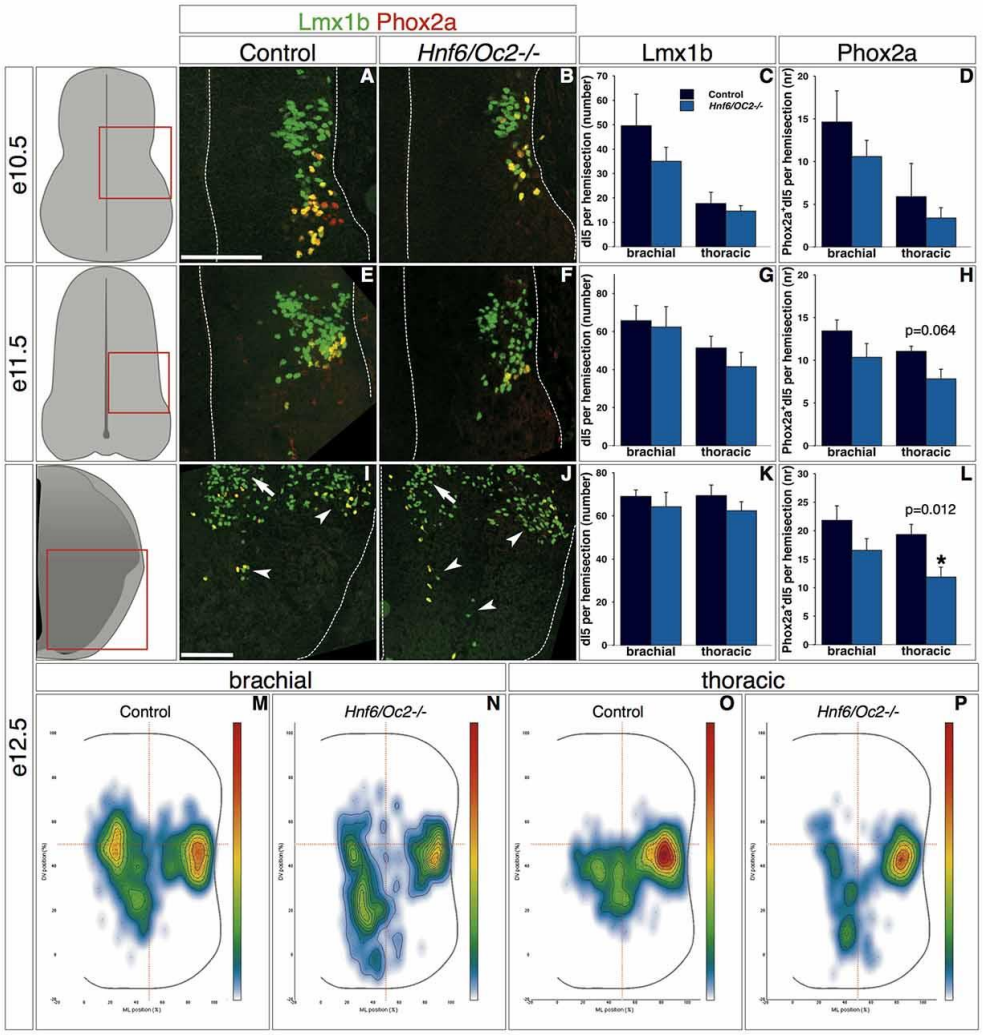

Kullander, 2013) or WT1 (Armstrong et al., 1993; Goulding, 2009) could be distinguished. Dmrt3-positive cells gathered in a medio-ventral position (Figure 6H) whereas WT1-positive cells were partly intermingled within and partly extended dorsally to Dmrt3 domain (Figure 6I). The cell number in the dI6 population and in each of these subsets was similar in the absence of OC factors Figures 6J–O). However, the distribution of each subset was modified. While Dmrt3-positive cells were slightly more densely packed in a more ventral location (Figures 6P–Q), the WT1 complement was also located more ventrally than in control littermates (Figures 6R–S). These observations indicate that the OC factors control some aspects of the diversification of dI5 interneurons and regulate the distribution of dI5 and dI6 subpopulations in the developing spinal cord.

Figure 6. OC factors control dI6 interneuron distribution. (A–O) Identification of dI6 interneuron population and subpopulations in control or Hnf6/Oc2-/- embryos. At the three embryonic stages, dI6 interneurons were identified as ventral Lbx1 + Lhx1/5+ cells. At e10.5, most dI6 interneurons are spread from ventricular zone to lateral deep dorsal spinal cord while fewer are visible in ventral horn (A,B; insets show Lbx1 labeling) with comparable amount of cells in control and mutant embryos (C, n = 4). At e11.5, more dI6 cells are present in lateral and ventral spinal cord of control and Hnf6/Oc2-/- embryos (D,E; insets show Lbx1 labeling) without any significant difference in their number (F, n = 3). At e12.5, Lbx1 + Lhx1/5+ dI6 interneurons are located in ventral regions in control and in mutant embryos (G,J). Two partially overlapping subsets of dI6 population are defined by Dmrt3 (H,K) and Wt1 (I,L) in the same area. Quantitative analysis of dI6 population or subsets shows comparable numbers of cells at brachial or and at thoracic levels in control or mutant embryos (M–O, n = 5). (P–S) Density plots of Dmrt3+ (P–Q) and of Wt1+ (R–S) dI6 interneurons at brachial level of control or mutant embryos at stage e12.5. Cells of these dI6 subsets are more densely packed in the ventral region of spinal cord in Hnf6/Oc2-/- embryos. Analysis was performed on at least three sections from four ($n > 760$ cells per condition; $p \leq 0.001$) or five embryos ($n > 350$ cells per condition; $p \leq 0.001$) for Dmrt3 and Wt1, respectively. The pictures show left hemisections as indicated to the left. Dashed lines delineate the spinal cord and the lumen of the ventricle. Insets are magnified views of boxed regions and show Lbx1 labeling. Mean values ±SEM. Scale bars = 100 µm.

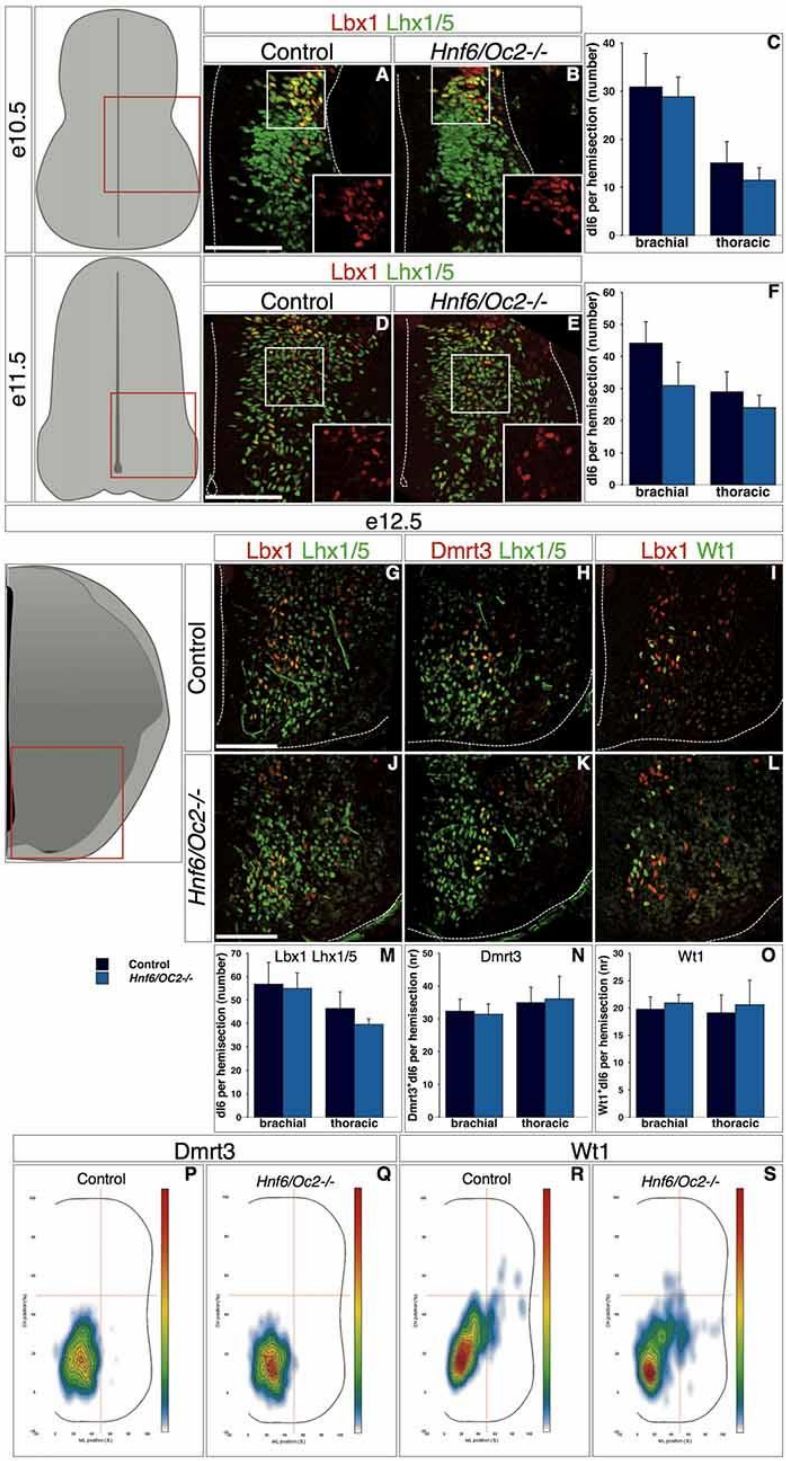
e10.5
Lbx1 Lhx1/5
Control
Hnf6/Oc2-/-
A
B
C
di6 per hemisection (number)
brachial
thoracic
e11.5
D
E
F
e12.5
Dmrt3 Lhx1/5
Lbx1 Wt1
G
H
I
J
K
L
M
N
O
Dmrt3
Wt1
P
Q
R
S

3.1.4 Discussion

During embryonic development, the dorsal neural tube generates interneuron populations that contribute to motor circuits or that integrate and relay proprioceptive, sensory or nociceptive information to motor circuits or to higher brain centers. The molecular mechanisms regulating the production of those interneurons have been extensively deciphered (Helms and Johnson, 2003; Lewis, 2006; Zhuang and Sockanathan, 2006), but the developmental determinants controlling their diversification, migration and final distribution (Lai et al., 2016; Lewis, 2006) remain elusive. Here, we provide evidence that the OC transcription factors are present in subsets of differentiating dINs and regulate some aspects of the diversification and of the distribution of these populations, likely impacting on neural circuit formation.

In spinal motor neurons and ventral interneurons, OC transcription factors are present in fractions of homogeneous subpopulations irrelevant to their molecular characteristics, neurotransmitter phenotype, location or contribution to neural circuits (Francius et al., 2013; Roy et al., 2012). Similarly, we detected OC factors in multiple dIN subsets including excitatory (dI2, dI3 and dI5) or inhibitory (dI4 and dI6) populations, generated at various levels along DV axis of the neural tube (from dI2 to dI6), involved in modulating motor control (dI3, dI4, dI5 and dI6) or processing sensory information (dI2), and migrating to ventral (dI3, dI5 and dI6) or deep dorsal (dI2 to dI5) locations in the mature spinal cord (Helms and Johnson, 2003; Lai et al., 2016; Lewis, 2006; Lu et al., 2015; Zhuang and Sockanathan, 2006). As for the other neuronal populations wherein OC factors are detected, this raises the question of the upstream regulators generating such a complex and ill-defined expression pattern in the developing CNS. To date, factors controlling Oc expression in the spinal cord remain unknown. Furthermore, the

cis-acting sequences that stimulate HNF-6 production in the developing liver or pancreas are ineffective in the CNS (Poll et al., 2006), suggesting that Oc expression in the neural tissue is regulated by distant enhancers.

Although OC factors are present in differentiating neurons (Francius and Clotman, 2010; Francius et al., 2013; Roy et al., 2012), their distribution in dINs correlates with the DV morphogen gradients known to determine the production of distinct progenitor domains in the dorsal neural tube. Indeed, OC are present in a larger proportion of cells and for a longer period of time in the more ventral populations of dINs than in their dorsal complement. The fraction of dorsal populations containing OC proteins increases from dI2 to dI6 and the number of cells that maintain Oc expression at e12.5 also rises from dI2 to dI6 (Figures 1–3). This is reminiscent of the gradient of Wnt and BMP morphogens initially produced by the dorsal ectoderm and subsequently maintained by the roof plate, which determines the identity of the three dorsal-most progenitor compartments without affecting the more ventral populations (Timmer et al., 2005; Tozer et al., 2013; Wine-Lee, 2004; Zechner et al., 2007). While expression of receptor Ia to BMP (BMPRIa) is restricted to spinal progenitors, BMPRIb is additionally expressed in the intermediate zone and in differentiating neurons (Yamauchi et al., 2008). Furthermore, Wnt receptors of the Frizzled family are detected at early stages in the whole spinal cord (Hu et al., 2009) and Wnt signaling is active in postmitotic neurons (Avilés and Stoeckli, 2016; Galli et al., 2014). This indicates that, beyond patterning of the neural tube, BMP and Wnt signaling is maintained in differentiating spinal interneurons. Therefore, Oc expression may be inhibited in dIN populations by BMP/Wnt signaling that would remain active in differentiating cells. Consistent with this, exposure of human ES cells to Noggin, a BMP antagonist, combined to retinoic acid and FGF-10 increases Hnf6 expression (Mfopou et al., 2010). In contrast, Wnt1 signaling inhibition by Dkk-1 in ventral

midbrain neural stem cells reduces Hnf6 expression, suggesting that Wnt1 may rather stimulate OC production in neural cells (Yuan et al., 2015). Similar to OC factors, Pax6 is absent from the most dIN populations because its expression is repressed by BMP signaling (Bel-Vialar et al., 2007). In the retina, OC factors act downstream of Pax6 to maintain horizontal cell identity (Klimova et al., 2015). However, regulation of Oc expression by proneural factors or by transcriptional regulators differentially expressed in distinct interneuron populations along the DV axis of the spinal cord has not been reported yet. Hence, identification of the factors upstream of the Oc genes in the neural tube constitutes a prerequisite to understand how their complex distribution pattern is achieved in the developing CNS.

Nevertheless, OC regulation must follow stereotyped mechanisms, as similar spatial and temporal progressions are observed among the different neuronal populations wherein OC are detected. Indeed, the distribution area of the three OC proteins follow a HNF-6 > OC-2 > OC-3 hierarchy and Hnf6 is expressed earlier than Oc2 detected itself before Oc3 in spinal motor neurons (Francius and Clotman, 2010; Roy et al., 2012) and ventral interneurons (Francius et al., 2013). A similar distribution dynamic was generally observed in dINs (Figures 1–3), with the single exception for OC-3 detected in a broader fraction of Phox2a-positive dI5 interneurons than OC-2 at e12.5 (Figure 2P). This suggests that similar mechanisms contributing to control Oc expression are acting in different cell types, raising the possibility that these factors may regulate generic aspects of neuronal development rather than the acquisition of specific characteristics by distinct neuronal subsets.

However, analysis of the few early dIN subpopulations identified to date suggested that OC factors contribute to dIN diversification. Indeed, the Phox2a subset of dI5 interneurons was reduced in the absence of OC proteins whereas

the total number of dI5 cells was maintained. This alteration is not caused by apoptosis, as cell death is not increased in OC mutant embryos (Roy et al., 2012). Lack of markers for other dI5 subsets prevented to investigate whether this resulted from defective production of Phox2a-positive cells or from conversion into other dI5 subtypes. OC factors are known to regulate neuronal diversification in the developing spinal cord. They critically regulate the differentiation ratio between visceral and somatic motor neurons at thoracic levels of the spinal cord and the production of ventral limb innervating motor neurons at brachial and lumbar levels (Francius and Clotman, 2014; Roy et al., 2012). Interestingly, OC control these two developmental events by maintaining significant expression levels of the Lim-homeodomain transcription factors Isl1 in the differentiating motor neurons (Roy et al., 2012). Isl1 maintenance results from direct stimulation of Isl1 expression by the OC factors, as evidenced by direct binding of OC proteins (Kim et al., 2015; Roy et al., 2012) to the CREST-2 enhancer of Isl1 (Uemura et al., 2005) and by the dependence of CREST-2 activity on the OC factors (Kim et al., 2015; Roy et al., 2012). Isl1 is also produced in dI3 interneurons during their differentiation (Bui et al., 2013; Liem et al., 1997), and determines their axonal projections at later developmental stages (Avraham et al., 2010). The CREST-2 enhancer of Isl1 is active in the dI3 interneurons (Kim et al., 2015), suggesting that OC factors may also regulate Isl1 expression in dI3 neurons and possibly later steps of dI3 differentiation. However, Isl1 was detected in dI3 neurons in the absence of OC factors and the number of dI3 cells in Hnf6/Oc2$^{-/-}$ mutant embryos was comparable to that observed in control littermates, indicating that OC are dispensable for dI3 production and for Isl1 expression in dI3. This demonstrates that Isl1 regulation by the OC factors is highly cell-type dependent and suggests that other factors that remain to be identified activate the CREST-2 enhancer in dI3 interneurons independently from OC proteins.

Similarly, OC factors regulate the diversification of spinal ventral interneurons, the production of some ventral interneuron subsets being impaired in the absence of OC proteins (AH, VR and FC, unpublished observations). The characterization of distinct ventral neuronal subsets has been frenetically pursued in the recent years and led to the identification of an extensive, although yet incomplete, collection of dozens of discrete subpopulations with specific molecular, electrophysiological, distribution or functional characteristics (Bikoff et al., 2016; Borowska et al., 2013; Dougherty et al., 2013; Francius et al., 2013; Gosgnach et al., 2006; Panayi et al., 2010; Panayiotou et al., 2013; Talpalar et al., 2013; Zagoraiou et al., 2009). This knowledge provided molecular and genetic tools to specifically identify, record or functionally challenge these different subsets and to characterize their phenotype in mutant embryos. In contrast, only few early dIN subsets have been identified to date, based on molecular markers (Andersson et al., 2012; Ding et al., 2004; Dougherty et al., 2013; Hilde et al., 2016; Rebelo et al., 2007). Thus, a possible involvement of OC proteins in dorsal diversification awaits a more complete characterization of the different subpopulations produced by the known cardinal populations of dINs.

Moreover, our data indicate that the OC factors regulate the distribution of different dIN populations during spinal cord development. Although limited to short-distance cell movements, spinal neuronal migration is a very complex process. On the one hand, each population or subset of motor neurons and of interneurons migrates according to a specific trajectory, in a specific direction, and eventually settles at a specific location. In addition, some populations assume their general migratory trajectory along the ventricular zone as soon as they exit their progenitor domain whereas others migrate first in a radial orientation before turning in ventral or dorsal direction. These combined processes result in an intense intermingling of cells with distinct identities. On the other hand, cells

from a single subset do not migrate as a cohesive compact cluster but rather form a relatively loose population that progresses in a common general direction. Eventually, these cells settle at a more or less focused final location depending on each subset. To analyze this highly dynamic and complex process, we adapted a distribution analysis routine initially developed for motor neurons (Palmesino et al., 2010). This routine enabled to obtain a highly reproducible integrated view of a cell population distribution on the transversal plane of the spinal cord and to precisely compare the migration pathway and the final location adopted by molecularly defined cell populations in wild type or mutant embryos.

Consistent with the presence of OC proteins in small proportions of each dI population, only fractions of dIN subsets were mislocated in Oc mutant embryos. Lack of OC does not affect the capacity of cells to migrate nor their intrinsic motility. Indeed, we did not observe any delay in dIN migration nor any premature arrest of migration at inappropriate settling location in Oc mutant embryos, suggesting that their migration abilities are conserved. In contrast, three types of migration defects were observed in Hnf6/Oc2-/- embryos. First, the migration trajectory of the dI3 interneurons was shifted to a more medial pathway than in control embryos (Figures 4P–Q). Second, the organization of migrating dI3 (Figures 4P–Q) and WT1-positive dI6 interneurons (Figure 6S) was altered, since cells migrated as a more compact cluster with the highest cell density closer to the migration front. Third, Phox2a-positive dI5 interneurons settling position was modified (Figures 5M–P), with a reduced number of cells in the lateral cluster and significant migration in ventro-medial locations where Phox2a-positive dI5 are never found in control embryos. Slight changes in settling location were also observed for dI3 (Figures 4P–Q) and dI6 (Figure 6S) subsets. These observations suggest that the production of environmental cues that determine the migration pathway and the settling location of dIN populations or

their interpretation by migrating cells is altered in the absence of OC factors. They also raise the possibility that factors involved in clustering or in cohesion of these migrating populations may be affected, as previously proposed in the dopaminergic A13 nucleus of Hnf6/Oc2$^{-/-}$ embryos (Espana and Clotman, 2012a), although changes in cell clustering may be secondary to alterations in the migration of individual cells. The molecular mechanisms regulated by OC actors in these processes remain to be identified.

Requirement of proper neuronal migration for adequate formation of neural circuits in the developing spinal cord has been repeatedly questioned (Kania, 2014). Indeed, some mutant lines show mispositioned neuron cell bodies but proper connectivity of the affected cells and organization of the corresponding neural circuits (Coonan et al., 2003; Demireva et al., 2011). However, increasing amount of evidence demonstrate that the location of spinal neurons is critical for proper neuronal connectivity and adequate integration into sensory-motor circuitries (Bikoff et al., 2016; Sürmeli et al., 2011). In dorsal spinal cord, the spatial organization of Lbx1-derived premotor interneurons determines their role, i.e., flexor interneurons born at e10.5 migrate laterally in lamina VI while extensor interneurons born at e12.5 remain closer to the central canal (Tripodi et al., 2011). EphA4 in these cells determines their localization as well as their axonal projections and their contribution to left-right motor alternation (Satoh et al., 2016). Likewise, the sensory cues that trigger motor responses are linked to the ML position of dorsal premotor interneurons in the deep dorsal horn (Hilde et al., 2016). Therefore, identification of the molecular regulators of neuronal migration and distribution in the spinal cord is important to understand circuit formation and neural activity. Interestingly, the interneuron populations altered in absence of OC factors are involved in motor control, either modulating motor neurons (Andersson et al., 2012; Bui et al., 2013; Goetz et al., 2015; Satoh et al., 2016) or

ventral premotor interneuron activity (Hilde et al., 2016; Levine et al., 2014) or mediating presynaptic inhibitory control of proprioceptive sensory neurons (Betley et al., 2009; Fink et al., 2014). Hence, OC factors could have been recruited in different neuronal subsets to coordinate the development of distinct populations eventually involved in motor circuits.

3.1.5 Materials and Methods

Animals

All experiments were strictly performed in accordance with the European Community Council directive of 24 November 1986 (86-609/ECC) and the decree of 20 October 1987 (87-848/EEC). Mice were raised in our animal facilities and treated according to the principles of laboratory animal care, and experiments and mouse housing were approved by the Animal Welfare Committee of Université catholique de Louvain (Permit Number: 2013/UCL/MD/11). CD1 or mutant strain mice were crossed, and the day of the vaginal plug was considered to be embryonic day (e) 0.5. The embryos were collected at e10.5, e11.5 and e12.5, a minimum of 3 embryos of the same genotype were used in each experiment. Hnf6 and Oc2 mutant mice have been described.

Immunofluorescent labeling

Collected embryos were fixed in ice-cold 4% paraformaldehyde (PFA) in phosphate buffered saline (PBS) for 10 to 30 minutes according to their embryonic stage, incubated in PBS/30% sucrose solution overnight at 4°C, embedded and frozen in PBS/15% sucrose/7.5% gelatin. Immunostaining was performed on 12µm cryosections as previously described (Francius and Clotman, 2010). Primary antibodies against the following proteins were used: Arx (rabbit; 1:1000; kindly provided by J. Chelly), Bhlhb5 (goat; 1:700; Santa Cruz #sc-6045),

Brn3 (goat; 1:500; Santa Cruz #sc-6026), Brn3a (guinea pig; 1:2000; kindly provided by J.E. Johnson; or mouse 1:1000; Santa Cruz #sc-8429), Dmrt3 (guinea pig; 1:5000; kindly provided by K. Kullander #170), Foxd3 (guinea pig; 1:5000; or rabbit; 1:2000; kindly provided by T. Müller), Foxp1 (goat; 1:1000; R&D Systems #AF4534), Foxp2 (goat; 1:1000; Abcam #ab1307), β-galactosidase (chicken; 1:2000; Abcam #ab9361), HNF6 (guinea pig; 1:2000; (Espana and Clotman, 2012a); or rabbit; 1:100; Santa Cruz #sc-13050; or sheep; 1:1000 R&D Systems #AF6277), Isl1/2 (goat; 1:3000; Neuromics #GT15051; or mouse; 1:6000; DSHB #39.4D5), Lbx1 (guinea pig; 1:10000; or rabbit; 1:5000; kindly provided by T. Müller), Lhx1/5 (mouse; 1:1000; DSHB #4F2), Lmx1b (guinea pig; 1:10000; or rabbit; 1:2000; kindly provided by T. Müller; or Armenian hamster; 1:2; kindly provided by Y. Ono), MafB (rabbit; 1:5000; kindly provided by H. Wende), cMaf (rabbit; 1:3000; kindly provided by H. Wende), OC2 (rat; 1:400; (Clotman et al., 2005); or sheep; 1:500; R&D Systems #AF6294), OC3 (guinea pig; 1:6000; (Pierreux et al., 2004)), mOct6/Scip/Pou3f1 (rabbit; 1:50; kindly provided by Dies N. Meijer), Nurr1 (rat; 1:2000; kindly provided by Y. Ono), Olig3 (guinea pig; 1:6000; or rabbit; 1:2000; kindly provided by T. Müller), Otp (rabbit; 1:500; kindly provided by F. Vaccarino), Pax2 (rabbit; 1:1000; Covance PRB-276P), Phox2a (rabbit; 1:500; kindly provided by J.-F. Brunet), Prox1 (rabbit; 1:1000; Covance PRB-238C), Tlx3 (guinea pig; 1:10000; or rabbit; 1:2000; kindly provided by T. Müller), Wt1 (rabbit; 1:2000; Santa Cruz #sc-192). Secondary antibodies donkey anti-guinea pig/AlexaFluor 488, 594 or 647, anti-mouse/AlexaFluor 488, 594 or 647, anti-rabbit/AlexaFluor 594 or 647, anti-goat/AlexaFluor 488, anti-rat/AlexaFluor 488 or 647, anti-sheep/AlexaFluor 594, anti-Armenian hamster/AlexaFluor 594, purchased from ThermoFisher Scientific or Jackson Laboratories were used at dilution 1:2000.

Cell quantification

Immunofluorescence images of cryosections were acquired on Zeiss Axio Cell Observer Z1 confocal microscope, EVOS FL or EVOS FL Auto Cell Imaging System. Brightness and contrast were adjusted with Adobe Photoshop CS3 software to match with observations. Cell quantification was performed using Adobe Photoshop CS3 software count analysis tool. Labeled neurons were counted on the two sides of at least three sections in thoracic region from at least 3 different embryos. For mutant analysis, labeled neurons were counted on at least three sections in brachial or thoracic regions from at least 3 pairs of control/mutant embryos. Raw data were exported from Adobe Photoshop CS3 software to SigmaPlot v11.0 software and processed to generate histogram figures and statistical analyses.

Spatial distribution

Pictures for quantification of interneuron spatial distribution were acquired on an EVOS FL Auto Cell Imaging System or a LEICA TCS confocal microscope. Distance and angle were measured using ruler analysis tool in Adobe Photoshop CS5 software. Spinal cord height (H) was defined as the distance from the ventral limit of central canal to the dorsal-most point of spinal cord, and width (W) as the distance from central canal to the most lateral edge (adapted from Palmesino et al., 2010). For each dorsal interneuron, distance (D_{IN}) and angle (α_{IN}) were measured from the ventral limit of the central canal to the interneuron soma. Dorso-ventral (DV) and medio-lateral (ML) position of dorsal interneurons were expressed as percentage of spinal cord height and hemicord width respectively: DV position and ML position were defined as (D_{IN}*sinα_{IN})/H and (D_{IN}*cosα_{IN})/W (Palmesino et al., 2010). (ML; DV) measurements were plotted using Matlab software R2013a (Mathworks, Canada).

3.1.6 Acknowledgments

We thank members of the NEDI lab for material, technical support and discussions. We are grateful to Drs. J. Chelly, J.E. Johnson, K. Kullander, T. Müller, Y. Ono, H. Wende, Dies N. Meijer, F. Vaccarino and J.-F. Brunet for antibodies, and to Dr. D. Castanares Zapatero for expert assistance with the statistical analyses. The antibodies anti-Isl1/2 (39.4D5) and anti-Lhx1/5 (4F2) were obtained from the Developmental Studies Hybridoma Bank, created by the NICHD of the NIH and maintained at The University of Iowa, Department of Biology, Iowa City, IA, USA.

3.2 Pou2f2 regulates the distribution of dorsal interneurons in the mouse developing spinal cord

3.2.1 Foreword

The dIN populations diversify and migrate to precise positions along stereotyped pathways to eventually settle at target locations in the developing spinal cord (Lai et al., 2016). Adequate neuronal positioning is of crucial importance for microcircuit organization. Although our previous study unraveled OC proteins as molecular actors that regulate dI5 diversification and distribution of several dIN populations along the dorso-ventral axis of the spinal cord (Kabayiza et al., 2017), the mechanisms underlying these processes remain poorly understood.

A previous study identified downstream molecular and cellular mechanisms of OC factors by performing a microarray comparison of the transcriptome of 5 control and 5 OC-deficient spinal cords at e11.5 (GEO repository accession number: GSE117871). In the absence of OC factors, Pou2f2 was 1.57-fold upregulated (Harris et al., 2019). In this study, we investigate the role of Pou2f2 transcription factors during dIN differentiation and distribution.

The Pou2f2 transcription factor

As a member of the POU transcription factor family, Pou2f2 contains a bipartite DNA binding domain (POU domain) consisting of a POU-specific and a POU-homeo domains connected by a short flexible linker. Both domains are required to interact with DNA via helix-turn-helix motifs and bind to an octamer motif (ATGCAAAT or ATTTGCAT) with high affinity. The POU domain of Pou2f2 binds as a monomer to the octamer sequence motif (Ingraham et al., 1990; Kristie et al., 1989; Stern et al., 1989; Sturm and Herr, 1988). Of note, Pou2f2 harbors two transactivation domains: a N-terminal glutamine-rich and a C-terminal serine-,

threonine-, and proline-rich transactivation domains. The latter function is essential for the transactivating potential (Annweiler et al., 1992; Annweiler et al., 1994; Pfisterer et al., 1994). Although the mouse genome encodes a single Pou2f2 gene on mouse chromosome 7, multiple isoforms are generated by alternative splicing: B_Pou2f2.1 to B_Pou2f2.6 that differ in their N- and C-terminal transactivation domains (Figure 13) (Wirth et al., 1991). In addition to the 6 described isoforms, 4 spinal isoforms are present in the spinal cord: S_Pou2f2.1 to S_Pou2f2.4 characterized by a distinct E1X, an additional exon E5b and alternative exons E1b and 4 (Harris et al., 2019).

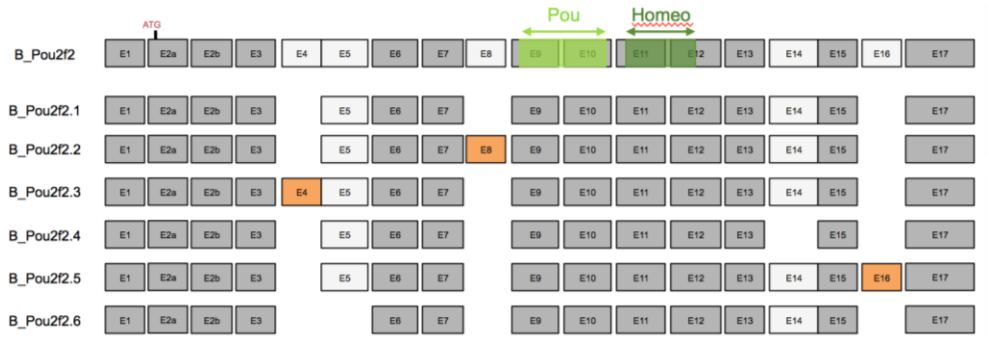

Figure 13: Sequences of the Pou2f2 isoforms resulting from alternative splicing in B cells (Wirth et al., 1991). The 6 Pou2f2 isoforms present in the B cells (B_Pou2f2.1 to B_Pou2f2.6) are characterized by invariant exons (dark grey), alternative exons 4, 5, 8, 14 or 16 (light grey) and isoform-specific exons 4, 8 or 16 (orange). They contain a POU-specific domain (light green) encoded by exons 9 and 10 and a POU-type homeodomain (dark green) encoded by exons 11 and 12.

The Pou2f2 transcriptional activity was assessed by co-transfection of expression vectors encoding different Pou2f2 isoforms and plasmids containing the chloramphenicol acetyltransferase gene downstream of an octamer-containing promoter. Hence, Pou2f2.1, Pou2f2.2 and Pou2f2.3 act as transcriptional activators, while Pou2f2.4 and Pou2f2.5 function as transcriptional repressors.

This difference can be explained by the fact that Pou2f2 isoforms differ from each other in the transactivation domains (Annweiler et al., 1994; Camós et al., 2014; Kaczmarek and Sibbel, 2008; Lillycrop and Latchman, 1992; Wirth et al., 1991). Pou2f2.1 is the predominant isoform in B cells, while Pou2f2.4 and Pou2f2.5 are the main isoforms in neuronal cell lines (Liu et al., 1995). The two latter act as repressors either by direct octamer motif or by preventing the activation mediated by Oct-1, their homolog, by binding to adjacent or overlapping DNA binding sites (Dent and Latchman, 1991).

In addition to B lymphocytes, Pou2f2 has been detected in the developing diencephalon, mesencephalon, metencephalon, myelencephalon, neural tube, and dorsal root ganglia by in situ hybridization and in the mouse adult brain (Hatzopoulos et al., 1990; Schreiber et al., 1990; Lillycrop and Latchman, 1992; Stoykova et al., 1992; Wood et al., 1992; Camós et al., 2014). The Pou2f2$^{-/-}$ mice develop normally but die at birth from undetermined reasons. In B cells, Pou2f2 is required for B-lymphocytes maturation into immunoglobulin-secreting B cells and their ability to respond positively to a B cell receptor signal (Corcoran et al., 1993; Corcoran et al., 2004). In neuronal cells, Pou2f2 acts as a bifunctional regulator of neuronal differentiation with Pou2f2.4 inhibiting the neuronal differentiation of embryonic stem cells, whereas Pou2f2.2 can activate this process (Theodorou et al., 2009).

This work was published in **Frontiers in Molecular Neuroscience** the 7th of November 2019. In this work, I carried out all the experiments.

Pou2f2 regulates the distribution of dorsal interneurons in the mouse developing spinal cord

Gauhar Masgutova[1], Audrey Harris[1], Benvenuto Jacob[2], Lynn M. Corcoran[3] and Frédéric Clotman[1*]

[1] Université catholique de Louvain, Institute of Neuroscience, Laboratory of Neural Differentiation, Brussels, Belgium

[2]Université catholique de Louvain, Institute of Neuroscience, System and Cognition division, Brussels, Belgium

[3]Molecular Immunology Division and Immunology Division, The Walter and Eliza Hall Institute, Parkville, Victoria, Australia.

Corresponding author: Frédéric Clotman, Laboratory of Neural Differentiation, Institute of Neuroscience, Université catholique de Louvain Avenue Hippocrate 55, box B1.55.11, B-1200, Brussels, Belgium Phone: +32.2.764.55.71, Fax: +32.2.764.55.72, Email: frederic.clotman@uclouvain.be

Keywords: embryonic spinal cord, dorsal interneurons, Pou2f2, Onecut, neuronal migration

Abstract

Spinal dorsal interneurons, which are generated during embryonic development, relay and process sensory inputs from the periphery to the central nervous system. Proper integration of these cells into neuronal circuitry depends on their correct positioning within the spinal parenchyma. Molecular cues that control neuronal migration have been extensively characterized but the genetic programs that regulate their production remain poorly investigated. Onecut (OC) transcription factors have been shown to control the migration of the dorsal interneurons (dINs) during spinal cord development. Here, we report that the OC factors moderate the expression of Pou2f2, a transcription factor essential for B-cell differentiation, in spinal dINs. Overexpression or inactivation of Pou2f2 leads to alterations in the differentiation of dI2, dI3 and Phox2a-positive dI5 populations and to defects in the distribution of dI2-dI6 interneurons. Thus, an OC-Pou2f2 genetic cascade regulates adequate diversification and distribution of dINs during embryonic development.

3.2.2 Introduction

The dorsal spinal cord relays and processes somatosensory inputs, nociception, thermosensation, pruriception, mechanosensation and proprioception, from peripheral sensory neurons to central targets. Furthermore, somatosensory perception is crucial for fine regulation and proper execution of motor activities. The complex organization of these neural circuits requires precise spatial position of neuronal cell bodies and integration into proper connectivity routes (Lai et al., 2016; Lu et al., 2015). Neuronal positioning and the cellular and molecular mechanisms involved in this process have been extensively studied in the developing brain (Marín et al., 2010). Although the molecules directing neuronal migration in the developing spinal cord start to be identified (Andrews et al., 2006; Junge et al., 2016; Kim et al., 2015; Leggere et al., 2016), much less is known about the genetic programs that control this essential process.

During embryonic development, eight populations of dorsal interneurons (dINs) are produced from progenitor domains orderly distributed along the dorso-ventral (DV) axis of the ventricular zone in the dorsal spinal cord. A unique combinatorial code of basic helix-loop-helix (bHLH) or homeodomain transcription factors defines, in two neurogenic waves, six early dIN populations (dI1–dI6) generated between embryonic day (e) 10.5 and e12.5, and two late-born dIL^{A} and dIL^{B} INs produced between e11 and e13 (Caspary and Anderson, 2003; Helms and Johnson, 2003). When specified, dINs migrate long distance along the DV axis to their distinctive location and integrate into specific circuits (Hernandez-Miranda et al., 2017). Among the early-born dINs, the dI1 excitatory INs localize in the intermediate spinal cord (Bermingham et al., 2001b) while some dI2 excitatory INs migrate towards the intermediate layers of the spinal cord and others invade the ventral horn (Gross et al., 2002). The intermediate and deep dorsal horn contains

glutamatergic dI3 (Bui et al., 2013). The inhibitory dI4 INs settle laterally in the deep dorsal horn (Gross et al., 2002; Müller et al., 2002; Pillai et al., 2007a) and excitatory dI5 INs invade the deep dorsal and the ventral horns (Ding et al., 2004). Located in the ventromedial region of the spinal cord, dI6 INs give rise to Dmrt3- or WT1-containing subsets (Andersson et al., 2012; Lanuza et al., 2004; Schnerwitzki et al., 2018). The two late-born dIL^A and dIL^B populations occupy the superficial laminae of the dorsal horn (Gross et al., 2000; Müller et al., 2002). During spinal cord development, these heterogeneous dorsal populations continue to diversify into small and discrete subsets (Del Barrio et al., 2013; Ding et al., 2004; Rosenberg et al., 2018) that each follows a stereotyped pattern of migration to reach their final location within the spinal parenchyma.

Spinal neuron distribution along the DV and mediolateral (ML) axes constitute a critical feature of microcircuit organization and functionality (Ladle et al., 2007; Tripodi et al., 2011). Indeed, proper cell body position of dorsal inhibitory INs along the ML axis is crucial for the establishment of their sensorimotor connectivity (Hilde et al., 2016) while the distribution of distinct Lbx1-positive premotor (Goetz et al., 2015) or V1 IN subsets (Bikoff et al., 2016) constrains patterns of input from sensory and motor neurons. In addition, V3 INs segregate into dorsal or ventral sub-populations that differ in their connectivity patterns and are active during distinct motor activities (Borowska et al., 2013; Borowska et al., 2015; Chopek et al., 2018). Furthermore, segmental distinctions exist along therostro-caudal axis of the spinal cord. Columnar organization of motor neurons varies between brachial or lumbar and thoracic regions in register with the part of the body these cells target (Catela et al., 2015; Francius and Clotman, 2014). In parallel, as several INs populations are associated with differential motoroutput, IN integration into local microcircuits is also influenced by their distribution along the antero-posterior axis (Bikoff et al., 2016; Hayashi et al., 2018; Sweeney et al.,

2018). Even if the genetic networks orchestrating the production and the differentiation of spinal INs have been extensively deciphered (Lu et al., 2015), less is known about the transcription factors that dictate their distribution in the developing spinal cord and might consequently influence their connectivity profiles and spinal circuit formation.

The Onecut (OC) transcription factors namely Hepatocyte Nuclear Factor-6 (HNF-6, or OC-1), OC-2 and OC-3, are detected in the digestive tract and in the CNS during embryonic development (Jacquemin et al., 1999; Jacquemin et al., 2003a; Landry et al., 1997; Lemaigre et al., 1996; Vanhorenbeeck et al., 2002). Besides their roles in the production (Espana and Clotman, 2012a), diversification (Francius and Clotman, 2014; Kabayiza et al., 2017; Roy et al., 2012) or maintenance (Espana and Clotman, 2012b; Stam et al., 2012) of specific neuronal populations, they also regulate neuronal distribution of various neuron types. OC regulate proper organization and migration of dopaminergic neurons of the A13 nucleus during their second phase of development (Espana and Clotman, 2012a). Similarly, they contribute to the reorganization of the Purkinje cells during a late phase of cerebellar development (Audouard et al., 2013). More recently, their contribution in the regulation of neuronal distribution was also uncovered in dorsal and in ventral spinal INs (Harris et al., 2019; Kabayiza et al., 2017). However, little is known about the downstream molecular effectors of the OC factors in dIN development, particularly regarding their migration along the DV and the ML axes of the spinal cord.

In the present study, we uncovered that the expression of Pou2f2, a POU family transcription factor (Clerc et al., 1988; Corcoran et al., 1993), is controlled by OC factors in the spinal dINs. We show that Pou2f2 is present in dI2-dI6 populations during the early stages of development. Analysis of OC mutant embryos demonstrated that OC proteins moderate the expression of Pou2f2 in the dorsal

spinal cord. Using gain-of-function experiments, we observed that increased Pou2f2 modulates the distribution of the dI2-dI6 INs. Loss-of-function experiments confirmed that Pou2f2 regulates the localization of the dI2-dI6 and the number of cells in some dIN populations. Thus, Pou2f2 controls the differentiation and the distribution of dINs in the developing spinal cord.

3.2.3 Results

OC factors moderate Pou2f2 expression in dIN populations

The OC transcription factors control the distribution of dIN populations (Kabayiza et al., 2017). In an effort to identify genes downstream of OC involved in this process, we analyzed the results of a transcriptomic comparison between embryonic day (e)11.5 wildtype or OC-deficient spinal cords (GEO repository accession number: GSE117871; Harris et al., 2019). Surprisingly, we could not identify significant changes in expression of genes coding for demonstrated or potential migration cues, except for Draxin. However, expression pattern of Draxin or distribution of the corresponding protein was not changed in OC mutant spinal cords (data not shown). In contrast, we confirmed that the expression level of Pou2f2, a transcription factor containing a POU-specific domain and a POU-type homeodomain, was significantly increased in the spinal cord in the absence of OC proteins. Pou2f2 is expressed in B-lymphocytes, in neuronal cell lines and in neural tissues (Camós et al., 2014; Kaczmarek and Sibbel, 2008; Lillycrop and Latchman, 1992). It is required for differentiation of B lymphocytes and is able to modulate neuronal differentiation of ES cells (Corcoran et al., 1993; Corcoran et al., 2004; Hodson et al., 2016; König et al., 1995; Theodorou et al., 2009). The expression level of Pou2f2 was 2.6-fold upregulated in Hnf6/Oc2$^{-/-}$ spinal cords (Harris et al., 2019). However, a potential contribution of Pou2f2 to dIN development was unknown.

Using in situ hybridization, we first confirmed that Pou2f2 expression was increased in the dorsal part of the spinal cord in Hnf6/Oc2$^{-/-}$ embryos. Consistent with quantifications on the whole spinal cord (Harris et al., 2019), we measure a ~3-fold increase in signal intensity in the absence of OC proteins (Figure 1). To assess the distribution of Pou2f2 in the dIN populations and to determine if the

increase in Pou2f2 expression was due to an expansion of Pou2f2 distribution or to an upregulation in its endogenous expression domain, we quantified the number of Pou2f2-containing dINs between e10.5 and e12.5 in wildtype and in OC-deficient embryos. As previously demonstrated, the OC factors are neither present in dI1 nor in dIL^A and dIL^B INs (Kabayiza et al., 2017). Moreover, due to the lack of antibodies for dI4 and early dI6 specific markers compatible with the Pou2f2 antibody species (see Material and methods), we were unable to study the presence of Pou2f2 in those populations.

Immunofluorescence analyses demonstrated that Pou2f2 is produced in post-mitotic dI2 INs, defined by the presence of Foxd3 at e10.5 and e11.5 and of Foxd3

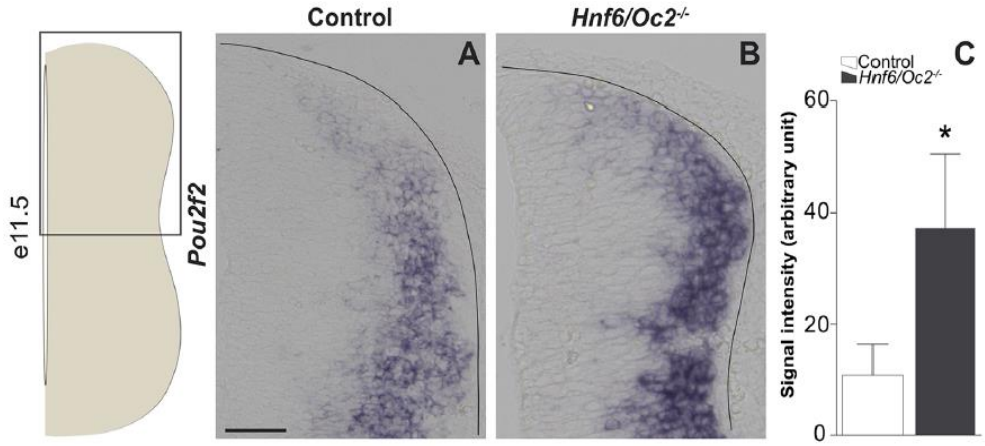

Figure 1. Onecut factors moderate expression of Pou2f2 in the dorsal spinal cord. (A-B) In situ hybridization for Pou2f2 on transverse sections (lumbar level) of control or Hnf6/Oc2$^{-/-}$ spinal cords at e11.5. (A) In control embryos, Pou2f2 is expressed at low levels in the dorsal part of the spinal cord and at higher levels in the intermediate zone. (B) In Hnf6/Oc2$^{-/-}$ mutant embryos, Pou2f2 expression is upregulated and cells displaying high Pou2f2 levels are observed more dorsally than in control littermates. The pictures show part of right hemisections as indicated on the scheme to the left. (C) Measurement of Pou2f2 in situ hybridization signal intensity in control or Hnf6/Oc2$^{-/-}$ at e11.5. Pou2f2 expression is upregulated in the absence of the Onecut factors in the dorsal spinal cord ($p \leq 0.05$). Mean values±SEM, n=3. Solid lines delineate the spinal cord. Scale bar=100 µm.

and Brn3a at e12.5. In control embryos, Pou2f2 was detected in a significant fraction of a ventral dI2 cell contingent at e10.5 (Figure 2A-B) but, as observed for OC factors (Kabayiza et al., 2017), the proportion of dI2 Pou2f2-positive INs decreased at e11.5 (Figure 2C-D) and Pou2f2 was almost completely absent from dI2 cells at e12.5 (Figure 2E-F). In mutant embryos, the number of Pou2f2-positive dI2 tended to increase as compared to control embryos, but this change was not statistically significant. Labeling intensity was stronger in dI2 of OC mutant embryos (Figure 2A-F), consistent with the increased Pou2f2 expression in the dorsal regions of the spinal cord.

In dI3 INs, characterized by the presence of Isl1, Pou2f2 was detected in the ventral part of the population from the early stages of their development (Figure 3A-B). As observed for dI2 INs, the proportion of Pou2f2-positive dI3 cells progressively decreased as development proceeds (Figure 3C-I). Pou2f2 was detected in a similar proportion of dI3 cells in control and in mutant embryos between e10.5 and e12.5 (Figure 3G-I). Nonetheless, the signal intensity was stronger in OC mutant dI3 cells (Figure 3A-F).

Lmx1b early-born dI5 INs were analyzed at e10.5 and e11.5 to distinguish them from late-born dIL^{B} also identified by Lmx1b at later stages. In control embryos, as for the other dIN populations, Pou2f2-positive cells represented a higher proportion of dI5 INs at e10.5, with most of the dI5 containing Pou2f2 (Figure 4A), while this proportion decreased at e11.5 (Figure 4C). In $Hnf6/Oc2^{-/-}$ mutant embryos, the proportion of Pou2f2-positive dI5 cells trended to decrease at e10.5 (Figure 4A-C) and to increase at e11.5 (Figure 4D-F). However, these changes were not statistically significant (Figure 4C, F). Again, stronger intensity of the labeling at e11.5 confirmed increased Pou2f2 production in dI5 INs.

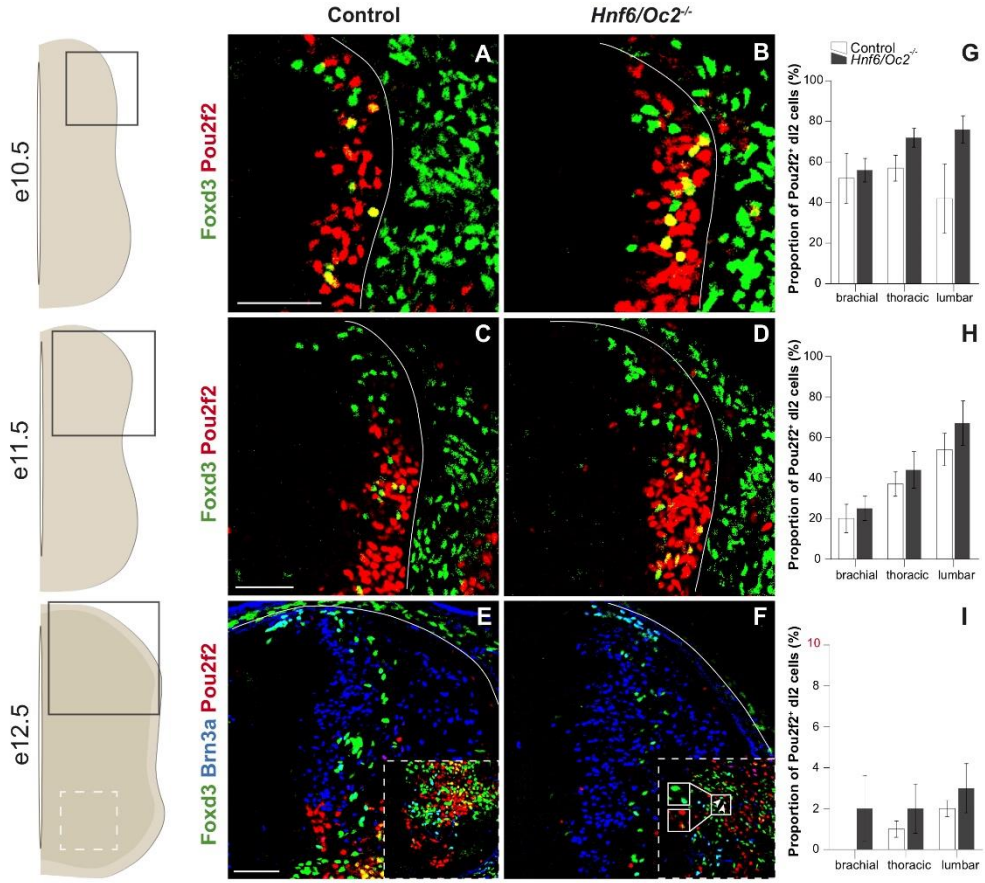

Figure 2. The Onecut factors moderate Pou2f2 expression in dI2 interneurons. (A-F) Immunodetection of Pou2f2 (red) in Foxd3^{+} (green) or Foxd3^{+} (green) Brn3a^{+} (blue) dI2 interneurons on transverse sections of thoracic spinal cord at e10.5 (A-B), e11.5 (C-D) and e12.5 (E-F). Pou2f2 is detected in post-mitotic Foxd3^{+} dI2 interneurons, particularly in the ventral part of the population, at e10.5 and e11.5 but is almost absent at e12.5. Pou2f2 signal is stronger in Foxd3^{+} dI2 interneurons in Hnf6/Oc2$^{-/-}$ spinal cord at all studied developmental stages. (G-I) Relative quantification of Pou2f2 positive dI2 neurons at e10.5 (G), e11.5 (H) and e12.5 (I). The proportion of Pou2f2^{+} dI2 is not significantly different in Hnf6/Oc2$^{-/-}$ spinal cords. The pictures show part of right hemisections as indicated on the schemes to the left. Solid lines delineate the spinal cord. Insets in E-F are magnified views of boxed ventral regions. Arrowheads in F point to triple-labelled cells. Mean values ±SEM, n = 3. Scale bars = 100 µm.

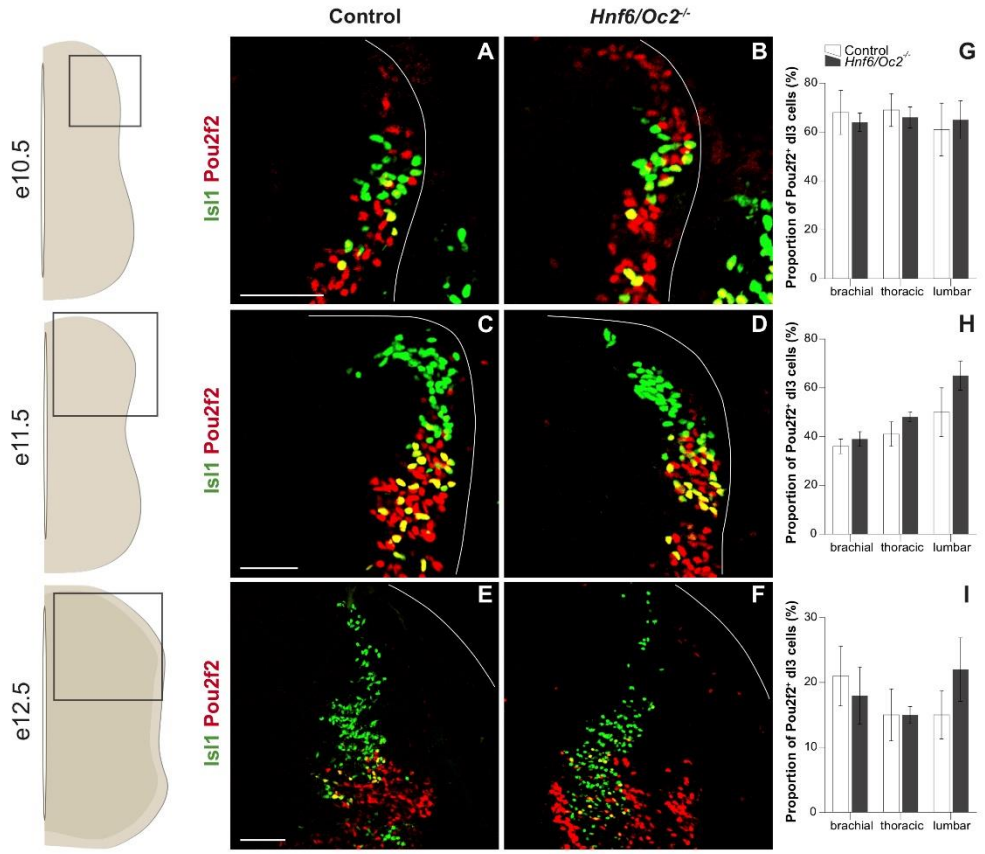

Figure 3. The Onecut factors moderate Pou2f2 expression in dI3 interneurons. (A-F) Immunodetection of Pou2f2 (red) in Isl1^{+} (green) dI3 interneurons on transverse sections of thoracic spinal cord at e10.5 (A-B), at e11.5 (C-D) and e12.5 (E-F). Pou2f2 is detected in the ventral part of the post-mitotic Isl1^{+} dI3 interneuron population from e10.5. Pou2f2 signal is stronger in Isl1^{+} dI3 interneurons in Hnf6/Oc2$^{-/-}$ spinal cord at all studied developmental stages. (G-I) Relative quantification of Pou2f2 positive dI3 neurons at e10.5 (G), e11.5 (H) and e12.5 (I). The proportion of Pou2f2^{+} dI3 is not significantly different in Hnf6/Oc2$^{-/-}$ spinal cords. The pictures show part of right hemisections as indicated on the schemes to the left. Solid lines delineate the spinal cord. Mean values ±SEM, n = 3. Scale bars = 100 µm.

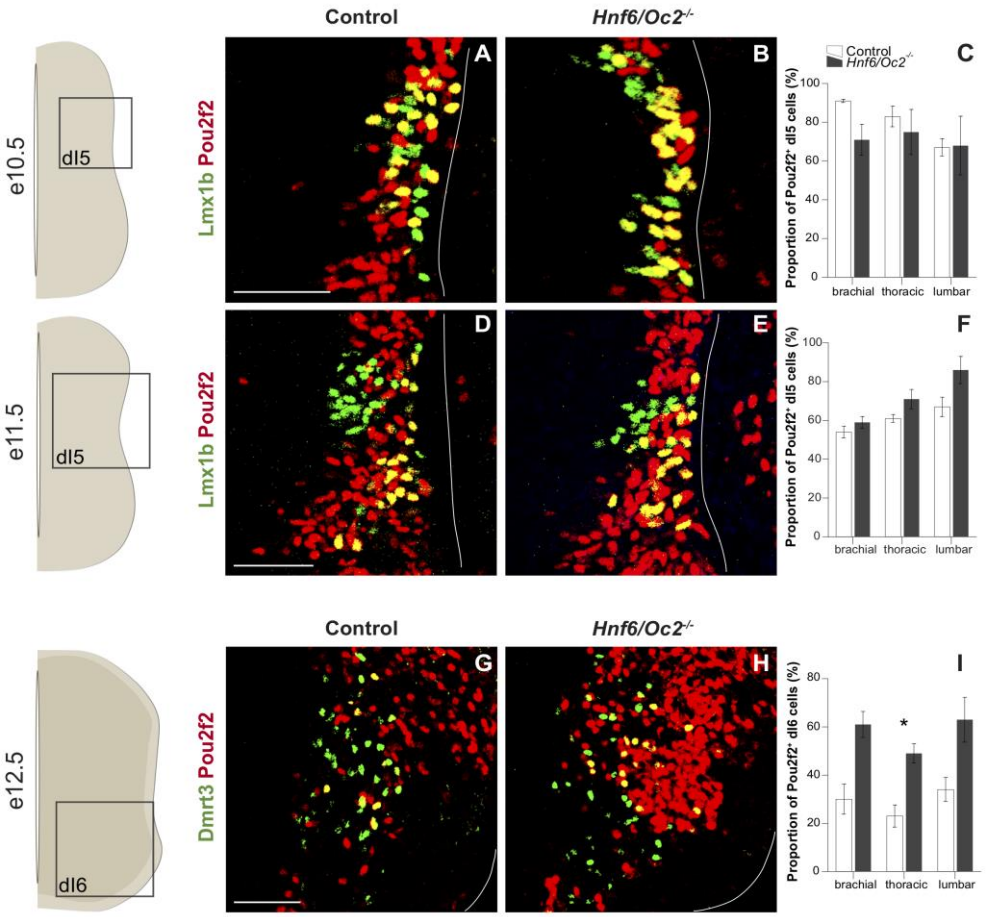

Figure 4. The Onecut factors moderate Pou2f2 expression in dI5 interneurons and Dmrt3$^+$ dI6 interneuron subset. (A-D) Immunodetection of Pou2f2 (red) in Lmx1b$^+$ (green) dI5 neurons on transverse sections of thoracic spinal cord at e10.5 (A-B) and at e11.5 (C-D). Pou2f2 is detected in most of Lmx1b$^+$ dI5 interneurons at e10.5 and is then restricted to the ventral part of the population. Pou2f2 signal is stronger in Lmx1b$^+$ dI5 interneurons in Hnf6/Oc2$^{-/-}$ spinal cord at all studied developmental stages. (E-F) The percentage of Pou2f2 positive dI5 neurons was quantified at e10.5 (E) and e11.5 (F), and is not significantly different in Hnf6/Oc2$^{-/-}$ spinal cords. (G-I) Immunodetection and relative quantification of Pou2f2 in Dmrt3$^+$ (green) dI6 subset at e12.5. The proportion of dI6 Dmrt3$^+$ Pou2f2$^+$ is significantly increased at thoracic level in Hnf6/Oc2$^{-/-}$ mutant embryos ($p \leq 0.05$). Again, Pou2f2 signal is stronger in the absence of OC factors. The pictures show part of right hemisections as indicated on the schemes to the left. Solid lines delineate the spinal cord. Mean values ±SEM, n = 3. Scale bars = 100 µm.

The lack of a unique specific marker for dI6 INs complicates the analysis of Pou2f2 in this population at early stages. Nevertheless, we were able to characterize the presence of Pou2f2 in the dI6 Dmrt3^{+} subset at e12.5 (Figure 4G-I). In control embryos, between 20 to 40% of dI6 cells contained Pou2f2. The proportion of dI6 Dmrt3^{+} producing Pou2f2 trended to increase in mutant compared to control embryos, although the change was statistically significant only at thoracic level (Figure 4I). Moreover, as for the other dorsal populations, Pou2f2 signal was stronger in Hnf6/Oc2$^{-/-}$ mutant embryos. Taken together, these observations suggest that OC factors temper Pou2f2 expression in dINs and restrain its expression to a subset of dI6 INs.

Pou2f2 overexpression alters the distribution of dINs

Our data indicate that Pou2f2 expression is increased in OC-deficient dIN populations. To assess whether Pou2f2 may contribute to the phenotype observed in Hnf6/Oc2$^{-/-}$ embryos (Kabayiza et al., 2017), we mimicked this increase by overexpressing Pou2f2 in chicken embryonic spinal cord. Pou2f2 overexpression did not change the number of dI2 INs, co-labeled for Brn3a and Lhx1/5 (Figure 5A-B). In contrast, it significantly altered their distribution (Figure 5C-E). In HH27-28 control side of the spinal cord (Figure 5C), dI2 cells were distributed in a dorso-medial to ventro-medial manner, with densely packed cells in register with the dI2 progenitor domain. In contrast, in the electroporated side, the dI2 distributed in a dorso-medial to ventro-lateral direction with more cells retained dorsally in the densely packed cluster or located in a more lateral position (Figure 5C-E). As for dI2 INs, overexpression of Pou2f2 in chicken embryonic spinal cord had no effect on the number of dI3 cells (Figure 5F-G). In the control side, dI3 INs distributed in two closely connected clusters in a general dorso-medial to ventro-medial direction (Figure 5H). However, in the

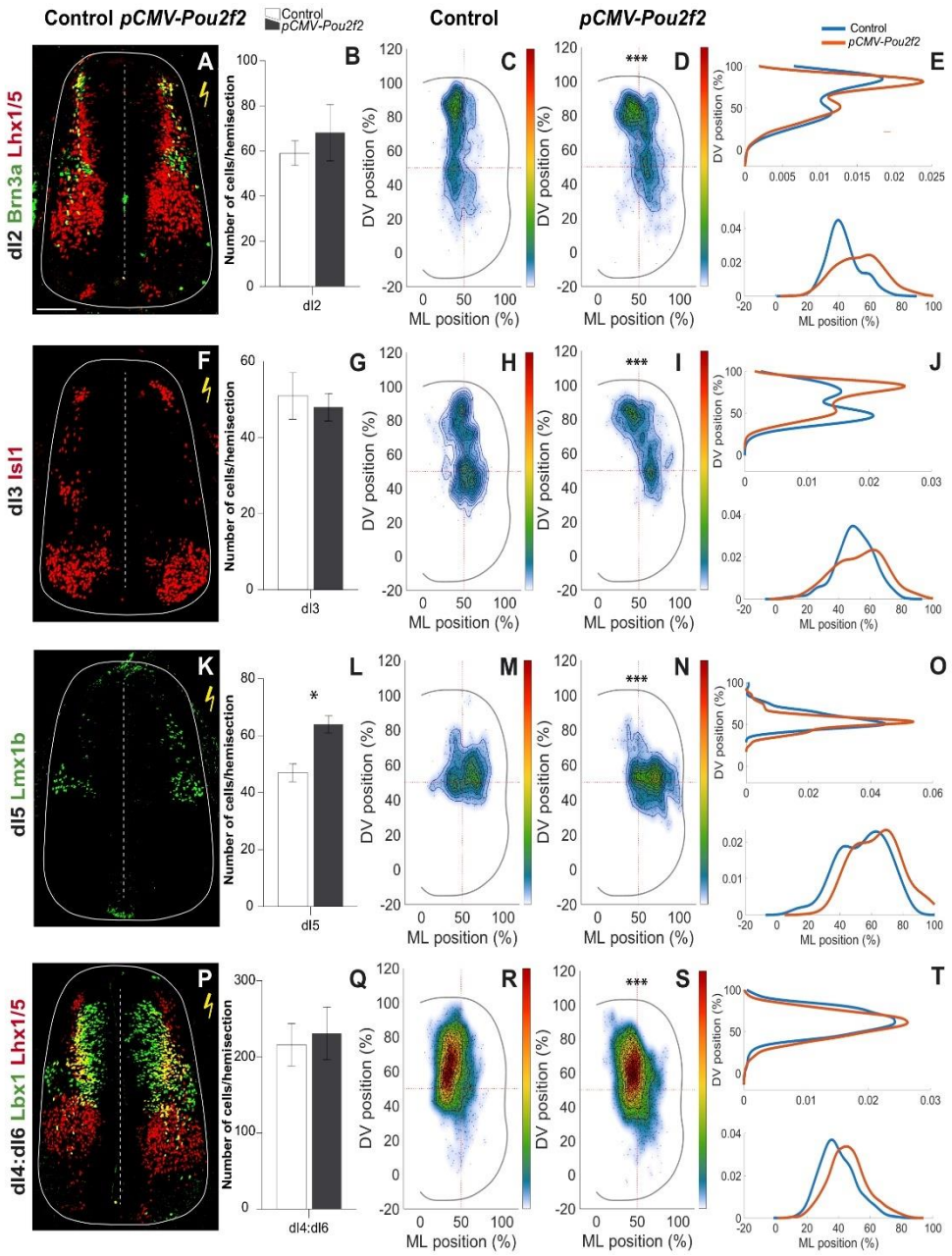
Control pCMV-Pou2f2
Control
pCMV-Pou2f2
dI2 Brn3a Lhx1/5
dI3 Isl1
dI5 Lmx1b
dI4:dI6 Lbx1 Lhx1/5
Number of cells/hemisection
DV position (%)
ML position (%)
***
*

Figure 5. Dorsal interneuron distribution is altered after Pou2f2 overexpression. Overexpression of Pou2f2 in chicken embryonic spinal cord after electroporation at HH14-16 and immunolabelings 72h hours after electroporation. (A-B) Immunodetection and quantification of Brn3a$^+$ (green) Lhx1/5$^+$ (red) dI2 neurons on transverse sections of electroporated spinal cord at HH27-28. Pou2f2 overexpression does not impact the number of dI2 interneurons. (C-E) Distribution analysis of dI2 interneurons in control or electroporated side of the chicken spinal cord. (C-D) Two-dimension distribution graphs (left) show integration of cell distribution from multiple sections of multiple embryos of each genotype. (E) One-dimension graphs compare density distribution in control (blue) and in electroporated spinal cord (red) on the dorso-ventral (upper) or the medio-lateral (lower) axis of the spinal cord (see Materials and methods for details). Overexpression of Pou2f2 alters the distribution of dI2 cells. (C) In control spinal cord, dI2 interneurons are distributed in a dorso-medial to ventro-medial fashion, with densely packed neurons close to the dI2 progenitor domain. (D-E) In electroporated spinal cord, dI2 cells migrate in a dorso-medial to ventro-lateral direction with more cells retained dorsally or located in a more lateral position ($p \leq 0.001$). (F-G) Immunodetection and quantification of Isl1$^+$ (red) dI3 neurons on transverse sections of electroporated spinal cord at HH27-28. All the Isl1$^+$ cells dorsal to the motor columns are considered as dI3 (?). The number of dI3 interneurons is not modified after Pou2f2 overexpression. (H) In control spinal cord, dI3 are distributed in two closely connected clusters in a dorso-medial to ventro-medial direction. (I-J) In electroporated spinal cord, the dI3 interneurons are more dorsal and their lateral migration is increased ($p \leq 0.001$). (K-L) Immunodetection and quantification of Lmx1b$^+$ (green) dI5 neurons on transverse sections of electroporated spinal cord at HH27-28. The number of dI5 interneurons is significantly increased after Pou2f2 overexpression. Moreover, their distribution is altered. (M) In control spinal cord, dI5 are distributed in two connected minor and major clusters both located in the medial tier of the spinal cord. (N-O) In electroporated spinal cord, the dI5 are located more laterally and slightly more ventrally ($p \leq 0.001$). (P-Q) Immunodetection and quantification of Lbx1$^+$ (green) Lhx1/5$^+$ (red) dI4:dI6 neurons on transverse sections of electroporated spinal cord at HH27-28. Pou2f2 overexpression does not alter the number of dI4+dI6 neurons. (R) In control spinal cord, dI4+dI6 are distributed in a dorso-medial to ventro-medial pattern. (S-T) In electroporated spinal cord, the dI4+dI6 neurons organize in a dorso-medial to ventro-lateral fashion with more cells in a lateral position. Analysis was performed on five sections ($n > 710$ cells per condition). Mean values ± SEM, $n = 3$. Scale bar = 100µm.

electroporated side a majority of dI3 INs remained more dorsal and the population extended laterally (Figure 5H-J). These observations indicate that increased Pou2f2 did not change dI2 or dI3 production but altered the migration of these populations in the dorsal spinal cord. In contrast, overexpression of Pou2f2 in chicken embryonic spinal cord resulted in a significant increase in dI5 Lmx1b^{+} INs (Figure 5K-L), suggesting that Pou2f2 may promote dI5 production. Regarding their distribution, dI5 Lmx1b^{+} cells were located in the medial region along the dorso-ventral axis of the spinal cord forming a minor medial cluster connected to a major lateral cluster on the medio-lateral axis in the control side of spinal cord (Figure 5M, O). However, this population was more lateral and slightly more ventral in electroporated spinal cord (Figure 5M-O). Finally, given the lack of a specific marker for dI4 and dI6 INs at this early developmental stage, the consequences of increased Pou2f2 expression in the chick spinal cord were studied using Lbx1 and Lhx1/5 as dI4 and dI6 co-markers. As for dI2 and dI3 INs, Pou2f2 increase did not alter the number of dI4:dI6 cells (Figure 5P-Q). In control spinal cords, these cells were located in a dorso-medial to ventro-medial pattern. In contrast, in electroporated spinal cords, these INs were distributed in a dorso-medial to ventro-lateral direction with more cells in a lateral position (Figure 5R-T). Taken together, these data suggest that Pou2f2 is able to modulate the differentiation of dI5 and the distribution of dI2 to dI6 INs in the developing spinal cord. In particular, increased Pou2f2 resulted in a more dorsal and more lateral distribution of dIN populations.

Pou2f2 is not necessary for proper production of dINs

Our overexpression data suggest that Pou2f2 is sufficient to modulate dI5 differentiation and dIN distribution. To determine whether Pou2f2 is necessary for these developmental processes, we assessed the differentiation and the distribution of each population of dI2-dI6 INs in Pou2f2 mutant embryos (Corcoran et al., 1993). First, we determined whether early IN production was normal at e10.5 in the absence of Pou2f2. The number of dI2 cells, labeled for Foxd3, was similar in control and in Pou2f2 mutants at each level of the spinal cord, as confirmed by cell quantification (Figure 6A-C), although the early distribution of these cells seemed different (Figure 6A-B). Similar analyses were carried out for dI3–dI6 populations. All those populations were produced in normal numbers in Pou2f$^{-/-}$ embryos compared to control littermates (Figure 6D-L). Taken together, these results suggest that Pou2f2 is not necessary for the early steps of dIN differentiation.

Pou2f2 controls the distribution of dI2 INs

However, the early migration of some dIN populations seemed affected at e10.5 (Figure 6). Given that OC factors regulate the distribution of dINs in the embryonic spinal cord (Kabayiza et al., 2017), that OC proteins repress Pou2f2 expression in spinal interneurons (Figure 1-3 and (Harris et al., 2019)) and that Pou2f2 is able to modulate the position of these cells (Figure 5), we assessed whether the loss of Pou2f2 impacts on dIN distribution at e12.5 and e14.5, i.e. in the course of interneuron migration and when migration of these cells in the transverse plan of the spinal cord is completed, respectively.

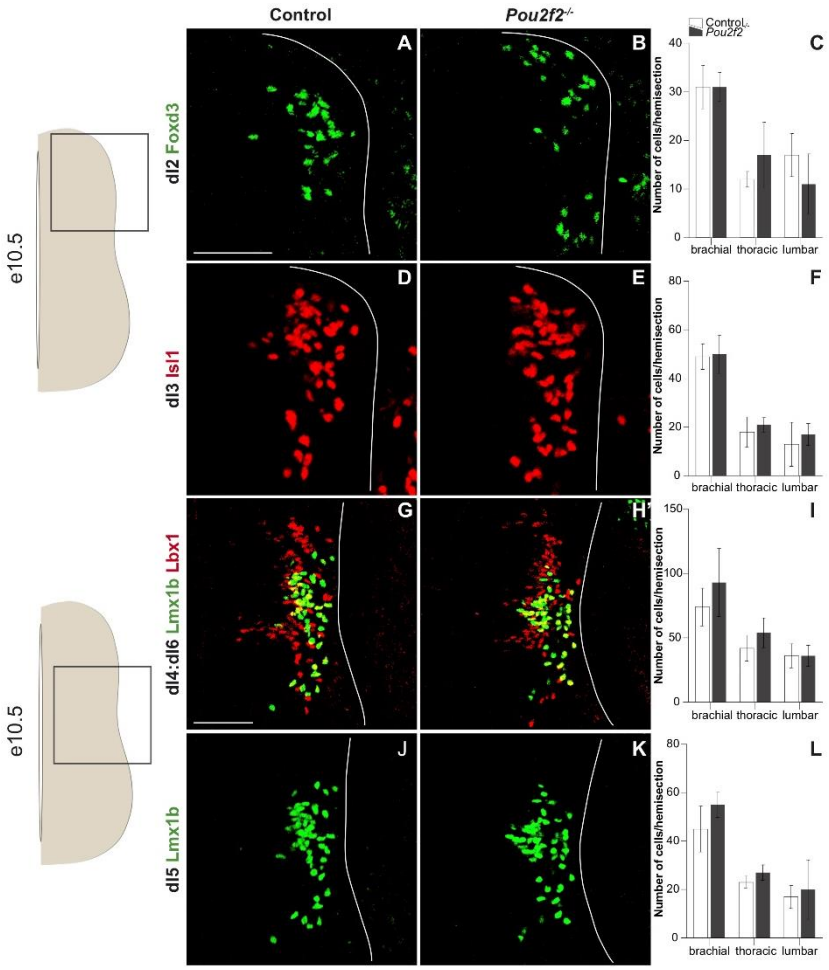

Figure 6. Dorsal interneuron production is normal at e10.5 in Pou2f2 mutant embryos. (A-L) Immunodetection and quantification of Foxd3^{+} (green) dI2 neurons (A-C), Isl1^{+} (red) dI3 neurons (D-F), Lmx1b^{+} (green) Lbx1^{+} (red) dI4:dI6 neurons (G-I) and Lmx1b^{+} (green) dI5 neurons (J-L) on transverse sections of thoracic spinal cord at e10.5. Quantifications show comparable numbers of dI2 (C), dI3 (F), dI4:dI6 (I) and dI5 (L) cells in control or Pou2f2$^{-/-}$ mutant embryos, indicating that the production of these populations is not affected in the absence of Pou2f2. The pictures show part of right hemisections as indicated on the schemes to the left. Solid lines delineate the spinal cord. Mean values ± SEM, n = 3. Scale bar = 100µm.

To discriminate dI2 INs located in ventral regions from V1 cells, which also produce Foxd3, dI2 were additionally labeled for Brn3a. As observed at e10.5, the number of dI2 INs was not altered at e12.5 in the absence of Pou2f2 (Figure 7A-C). In control embryos, a majority of dI2 cells distributed in a medial stream of cells migrating from the dI2 progenitor domain towards the ventral region of the spinal cord and covering 60% of the ventro-dorsal axis. A second cluster of dI2 neurons expressing high amounts of Brn3a (arrow in Figure 7A) was located ventrally in the vicinity of the $Foxd3^{+}$ V1 INs (Figure 7D-F). In $Pou2f2^{-/-}$ mutant embryos, cells producing Foxd3 and Brn3a were detected in similar regions (Figure 7B). However, distribution analysis showed that dI2 INs migrate more ventrally in the absence of Pou2f2, connecting the dorsal and ventral clusters at brachial level and increasing the number of cells in the ventral cluster at thoracic and lumbar levels (Figure 7G-L).

At e14.5, the number of dI2 cells at brachial level was mildly but significantly increased in $Pou2f2^{-/-}$ mutant embryos (Figure 7M-O). In control embryos, a main dI2 cluster settled in the intermediate part of the medial spinal cord (arrow in Figure 7M, P-R) whereas two smaller subsets located in a more ventral or lateral position, respectively (arrowheads in Figure 7M, P-R). In mutant embryos, the cells distributed in a similar pattern to control littermates although, reminiscent of e12.5, dI2 were located more ventrally and the small lateral cluster was depleted at thoracic and lumbar levels (Figure 7N, S-X). Taken together, these observations suggest that Pou2f2 regulates the distribution of dI2 INs.

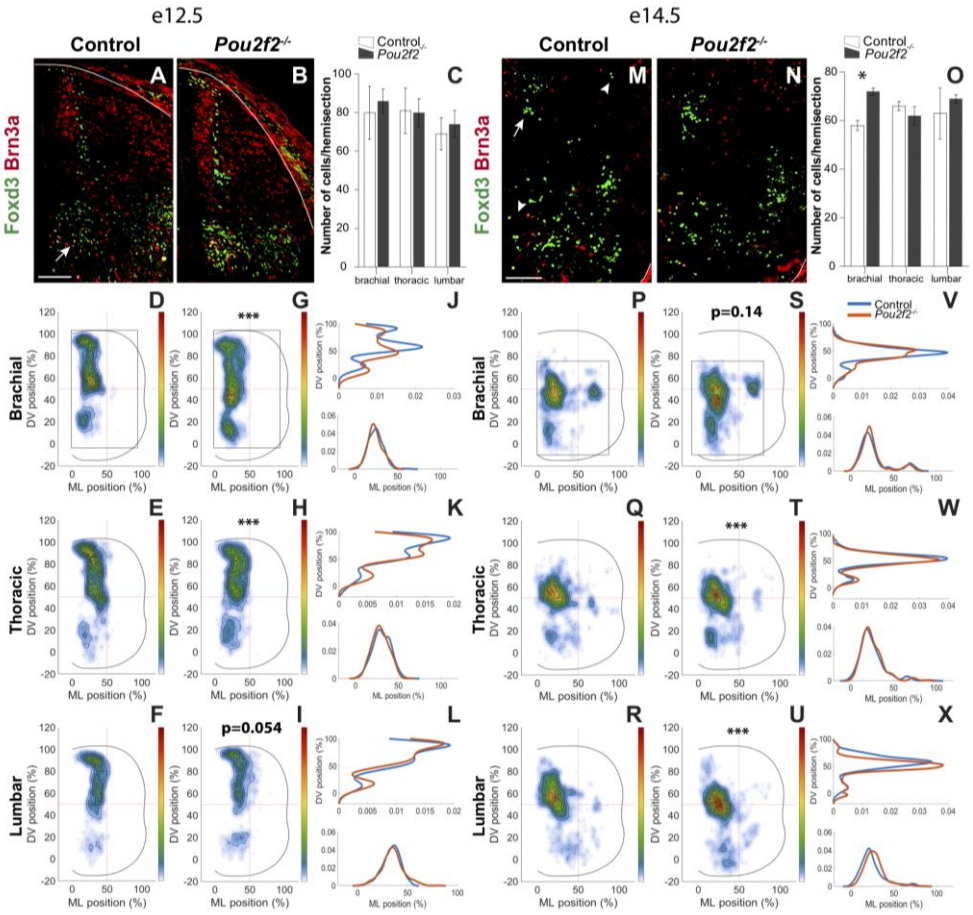

Figure 7. Pou2f2 regulates the distribution of dI2 interneurons. (A-C) Immunodetection and quantification of Foxd3^{+} (green) Brn3a^{+} (red) dI2 interneurons in control or Pou2f2$^{-/-}$ mutant embryos at e12.5. The production of the Foxd3^{+} Brn3a^{+} dI2 interneurons is not altered in the absence of Pou2f2. (D-L) Distribution of dI2 interneurons on the transverse plane of the spinal cord in control or Pou2f2$^{-/-}$ mutant embryos at e12.5. Two-dimension distribution graphs (left) show integration of cell distribution from multiple sections of multiple embryos of each genotype. One-dimension graphs (right) show density distribution in control (blue) or in Pou2f2$^{-/-}$ embryos (red) on the dorso-ventral (upper) or the medio-lateral (lower) axis of the spinal cord. The distribution of dI2 interneurons is affected in Pou2f2$^{-/-}$ mutants, as dI2 cells migrate more ventrally, connecting the dorsal and ventral clusters at brachial level ($p \leq 0.001$) and increasing the number of cells in the ventral cluster at thoracic ($p \leq 0.001$) but not at lumbar levels ($p=0.0536$). (M-O) Immunodetection and quantification of Foxd3^{+} (green) Brn3a^{+} (red) dI2

Pou2f2 controls the distribution of dI3 INs

Except for a mild but significant reduction at e12.5 at brachial level, the number of dI3 INs characterized by the expression of Isl1 was not affected in the absence of Pou2f2 (Figure 8A-C, M-O). At e12.5, the dI3 cells gathered as a single homogeneous cluster in the intermediate region of the spinal cord, resulting in a Gaussian-like distribution along the dorso-ventral and the medio-lateral axes (Figure 8A, D-F). In Pou2f2$^{-/-}$ spinal cords, the population was slightly more ventral at brachial level and more lateral at thoracic and lumbar levels, respectively, with a more diffuse distribution in the center of the cluster (Figure 8B, G-L). Two days later, still gathered in a single cluster, dI3 neurons settled in the intermediate region of the spinal cord. The dI3 INs located more ventral and lateral in the absence of Pou2f2 (Figure 8N, S-X). In addition, a tiny ectopic dI3 cluster was detected at brachial level, whereas a similarly located cluster was missing at lumbar level (arrowheads in Figure 8S, U). These observations suggest, as observed for dI2 cells, that Pou2f2 controls the distribution of dI3 INs in the developing spinal cord.

interneurons in control or Pou2f2$^{-/-}$ mutant embryos at e14.5. The number of Foxd3^{+} Brn3a^{+} dI2 cells is increased at the brachial level, but not at more dorsal levels, in the absence of Pou2f2 ($p \leq 0.05$). (P-X) Distribution of dI2 interneurons on the transverse plane of the spinal cord in control or Pou2f2$^{-/-}$ mutant embryos at e14.5. In the absence of Pou2f2, dI2 neurons settle more ventrally and small lateral clusters are depleted at thoracic and lumbar levels ($p \leq 0.001$). The pictures show part of right hemisections as indicated on the schemes in D,G and in P,S, respectively. Solid lines delineate the spinal cord. Analysis was performed on five sections per level from three control and three mutant embryos ($n > 2803$ cells per condition). Mean values ± SEM, n = 3. Scale bar = 100µm.

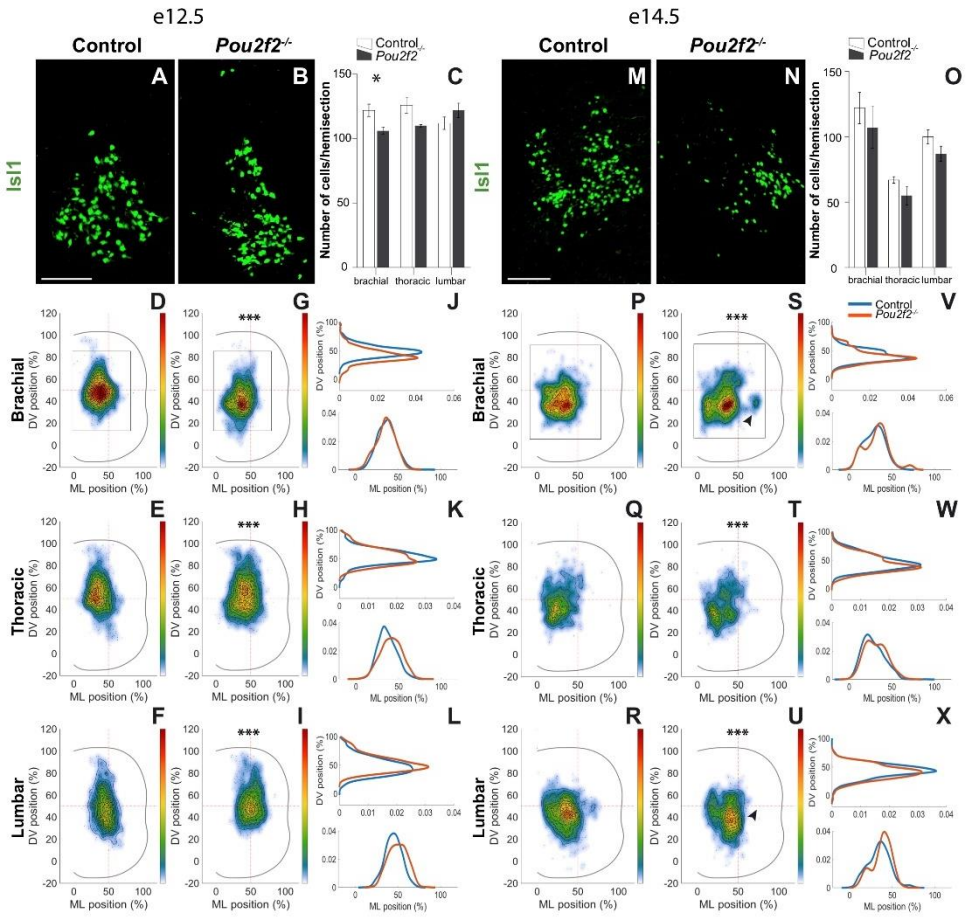

Figure 8. Pou2f2 regulates the distribution of dI3 interneurons. (A-C) Immunodetection and quantification of Isl1^{+} (green) dI3 interneurons in control or Pou2f2$^{-/-}$ mutant embryos at e12.5. The production of the Isl1^{+} dI3 interneurons is not altered in the absence of Pou2f2 except for a slight decrease at brachial level ($p \leq 0.05$). (D-L) Distribution of dI3 interneurons on the transverse plane of the spinal cord in control or Pou2f2$^{-/-}$ mutant embryos. Two-dimension distribution graphs (left) show integration of cell distribution from multiple sections of multiple embryos of each genotype. One-dimension graphs (right) show density distribution in control (blue) or in Pou2f2$^{-/-}$ embryos (red) on the dorso-ventral (upper) or the medio-lateral (lower) axis of the spinal cord. In control spinal cord, dI3 are distributed as a single homogeneous cluster. In Pou2f2$^{-/-}$ mutant embryos, dI3 cells are relatively more ventral at brachial level or lateral at thoracic and lumbar levels ($p \leq 0.001$). (M-O) Immunodetection and quantification of Isl1^{+} (green) dI3 interneurons in control or Pou2f2$^{-/-}$ mutant embryos at e14.5. The number of

Pou2f2 controls the differentiation and the distribution of dI5 INs

In the mouse developing spinal cord, from e11.0 onwards, Lmx1b is present in the dI5 and in the late born dIL^{B} INs. As early- and late-born $Lmx1b^{+}$ cells are difficult to discriminate for reproducible distribution studies, we restricted our analyses to the $Phox2a^{+}$ dI5 subset at e12.5 and e14.5 (Figure 9). Absence of Pou2f2 did not impact the number of dI5 $Phox2a^{+}$ INs except for the lumbar level at e14.5, which showed a significant increase (Figure 9A-C, M-O). In control embryos at e12.5, $Phox2a^{+}$ dI5 distributed in 2 main clusters on the medio-lateral axis of the spinal cord, with a major medial cluster and a minor lateral cluster that trended to coalesce in more caudal sections (Figure 9A, D-F). In $Pou2f2^{-/-}$ embryos, dI5 distribution was dramatically changed with a majority of cells organized in a unique cluster located in a medial position (Figure 9B, G-L). At e14.5, control $Phox2a^{+}$ dI5 gathered in a main medial cluster located more dorsally in more caudal sections (Figure 9M, P-R). In mutant embryos, cells were more compact but occupied a more lateral position at brachial and thoracic levels, and a more dorsal position at lumber level (Figure 9N, S-X). These observations indicate that Pou2f2 regulates the differentiation and the distribution of the $Phox2a^{+}$ dI5 subpopulation.

$Isl1^{+}$ dI3 cells is unaffected in the absence of Pou2f2. (P-X) Distribution of dI3 interneurons on the transverse plane of the spinal cord in control or $Pou2f2^{-/-}$ mutant embryos at e14.5. Still organized in a single cluster, dI3 in control embryos settle in the intermediate to ventral regions of the spinal cord. More ventral and lateral distribution is detected in Pou2f2 depleted embryos ($p \leq 0.001$). A tiny ectopic cluster is present at brachial level or absent at lumbar level. The pictures show part of right hemisections as indicated on the schemes in D,G and in P,S, respectively. Analysis was performed on five sections per level from three control and three mutant embryos (n > 3724 cells per condition). Mean values ± SEM, n = 3. Scale bar = 100µm.

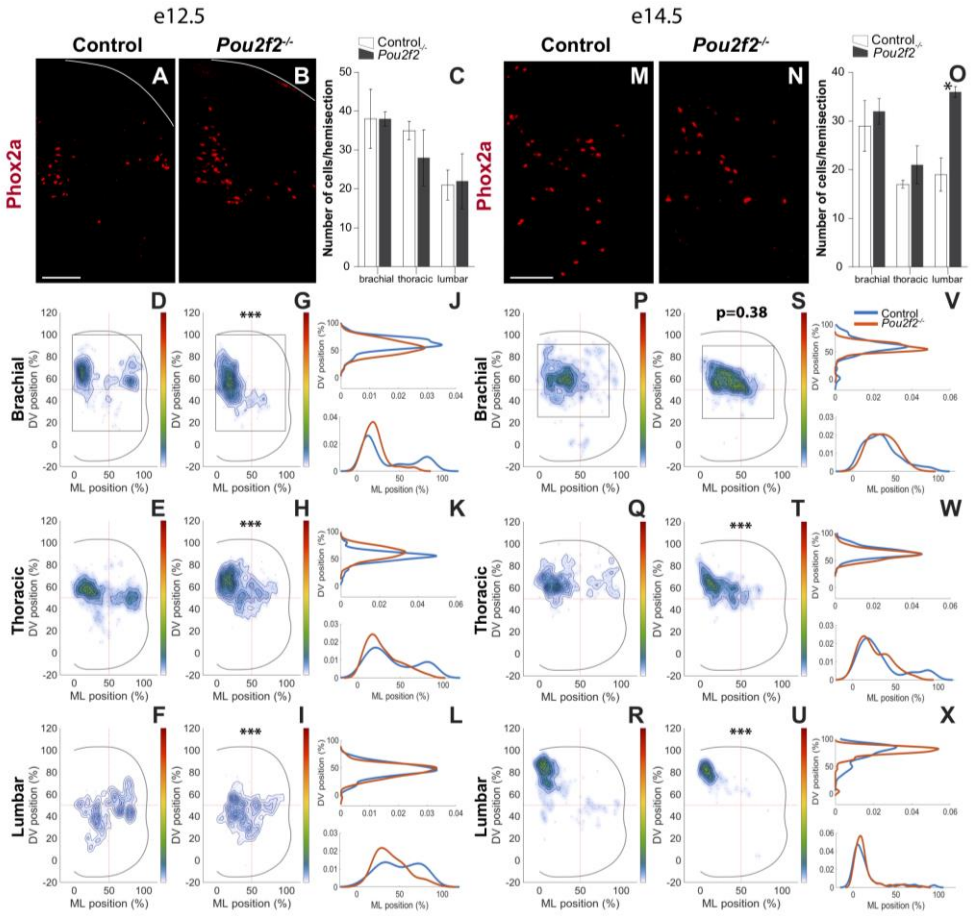

Figure 9. Pou2f2 regulates the distribution of dI5 Phox2a subset. (A-C) Immunodetection and quantification of dI5 Phox2a^{+} (red) subset in control or Pou2f2$^{-/-}$ mutant embryos at e12.5. The production of the Phox2a^{+} dI5 interneurons is not altered in the absence of Pou2f2. (D-L) Distribution of dI5 Phox2a^{+} cells on the transverse plane of the spinal cord in control or Pou2f2$^{-/-}$ mutant embryos. Two-dimension distribution graphs (left) show integration of cell distribution from multiple sections of multiple embryos of each genotype. One-dimension graphs (right) show density distribution in control (blue) or in Pou2f2$^{-/-}$ embryos (red) on the dorso-ventral (upper) or the medio-lateral (lower) axis of the spinal cord. The distribution of dI5 Phox2a^{+} subset is (lower) axis of the spinal cord. The distribution of dI5 Phox2a^{+} subset is dramatically affected in Pou2f2$^{-/-}$ mutants. In control embryos, dI5 Phox2a^{+} cells are organized in a major medial and a minor lateral cluster that progressively coalesce in more caudal regions. In Pou2f2-deficient spinal cords, a unique cluster located in a medial position is observed

Pou2f2 controls the distribution of dI6 INs

At e12.5 and e14.5, two partially overlapping dI6 subpopulations are characterized by the presence of Dmrt3 or WT1, respectively. Absence of Pou2f2 had no impact on dI6 cell number of each subpopulation but resulted in alterations in Dmrt3^{+} (Figure 10A-C) and in WT1^{+} (Figure 11A-C) dI6 distribution. At e12.5, control Dmrt3^{+} dI6 INs were located in the ventro-medial part of the spinal cord (Figure 10A, D-F). In Pou2f2$^{-/-}$ embryos, Dmrt3^{+} INs settled more ventrally at brachial level than in mutant embryos (Figure 10B, G-L). Due to technical restrictions, we limited our distribution analysis of Dmrt3^{+} dI6 subset to e12.5.

In control embryos at e12.5, the WT1^{+} dI6 subset was located, similarly to the Dmrt3^{+} subpopulation, in the ventro-medial part of the spinal cord (Figure 11A, D-F). In Pou2f2$^{-/-}$ embryos, WT1^{+} dI6 INs were more densely packed and were located more ventrally than in control littermates (Figure 11B, G-L). Consistently, at e14.5, WT1^{+} cells remained more densely packed and more ventral than in control littermates (Figure 11M-N, R-X). These observations indicate that Pou2f2 controls some aspects of dI6 distribution in the developing spinal cord.

(p≤0.001). (M-O) Immunodetection and quantification of dI5 Phox2a^{+} (red) subset in control or Pou2f2$^{-/-}$ mutant embryos at e14.5. The number of Phox2a^{+} dI5 cells is significantly increased at lumbar level (p≤0.05). (P-X) Distribution of dI5 Phox2a^{+} neurons on the transverse plane of the spinal cord in control or Pou2f2$^{-/-}$ mutant embryos at e14.5. In control embryos, dI5 Phox2a^{+} gathered in a main medial cluster whereas, in Pou2f2$^{-/-}$ spinal cords, cells were organized in a more compact cluster shifted laterally at brachial and thoracic levels and more dorsally at lumbar level (p≤0.001). The pictures show part of right hemisections as indicated on the schemes in D,G and in P,S, respectively. Solid lines delineate the spinal cord. Analysis was performed on five sections per level from three control and three mutant embryos (n > 930

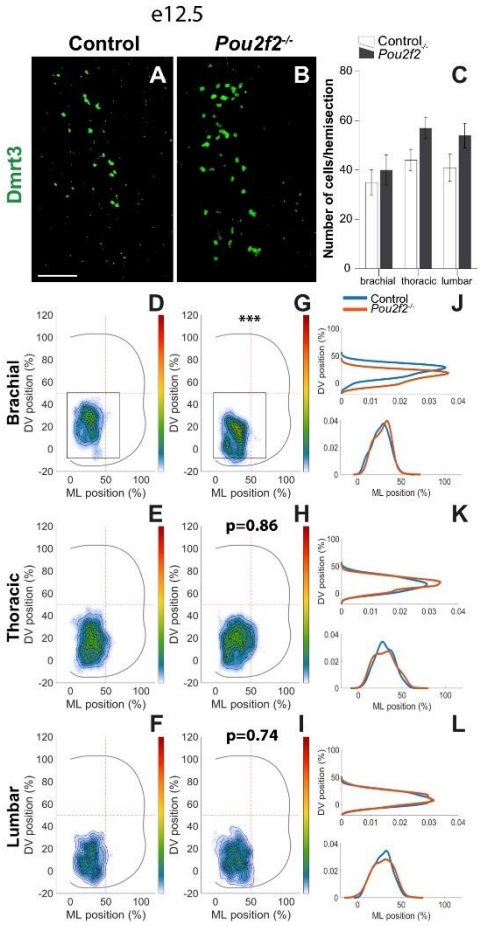

Figure 10. Pou2f2 regulates the distribution of the dI6 Dmrt3 subset. (A-C) Immunodetection and quantification of dI6 interneuron Dmrt3^{+} (green) subset in control or Pou2f2$^{-/-}$ mutant embryos at e12.5. The production of the Dmrt3^{+} dI6 interneurons is not altered in the absence of Pou2f2. (D-L) Distribution of dI6 Dmrt3^{+} cells on the transverse plane of the spinal cord in control or Pou2f2$^{-/-}$ mutant embryos. Two-dimension distribution graphs (left) show integration of cell distribution from multiple sections of multiple embryos of each genotype. One-dimension graphs (right) show density distribution in control (blue) or in Pou2f2$^{-/-}$ embryos (red) on the dorso-ventral (upper) or the medio-lateral (lower) axis of the spinal cord. Dmrt3^{+} dI6 distribution is affected in Pou2f2$^{-/-}$ mutants at brachial level as these cells settle more ventrally relatively to control littermates ($p \leq 0.001$). The pictures show part of right hemisections as indicated on the schemes in D,G. Analysis was performed on five sections per level from three control and three mutant embryos ($n > 1700$ cells per condition). Mean values ± SEM, n = 3. Scale bar = 100µm.

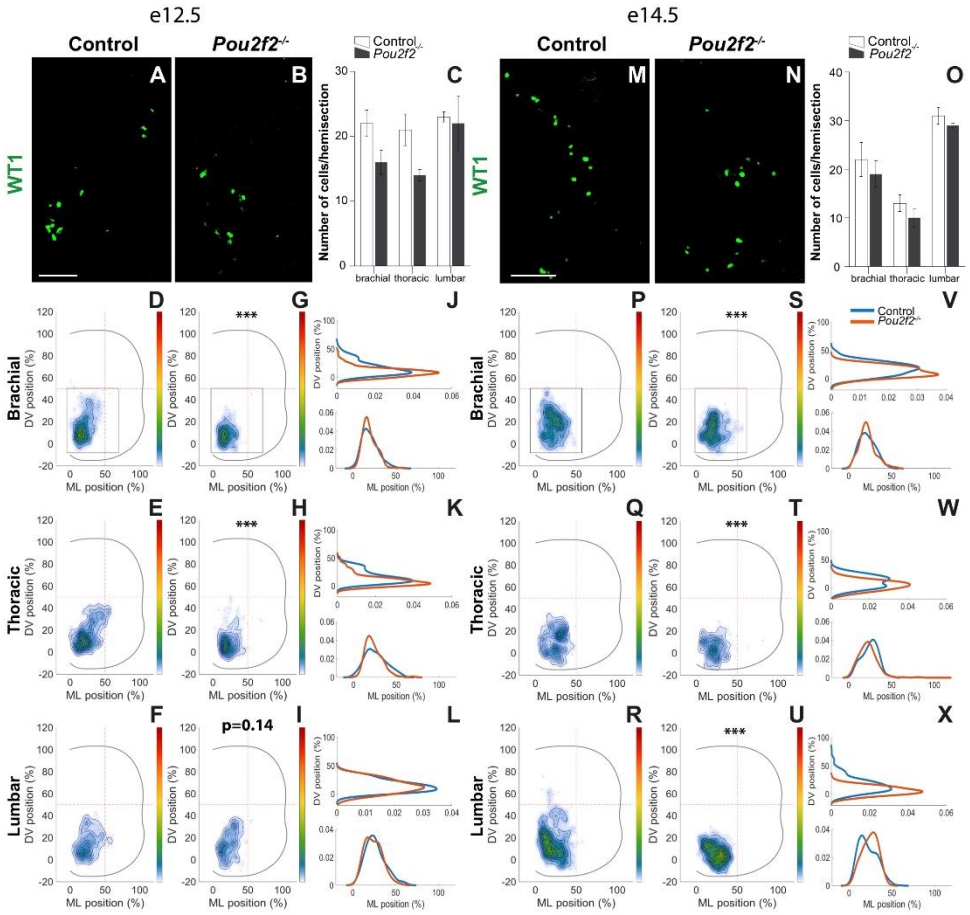

Figure 11. Pou2f2 regulates the distribution of dI6 Wt1 subset. (A-C) Immunodetection and quantification of dI6 Wt1^{+} (green) subset in control or Pou2f2$^{-/-}$ mutant embryos at e12.5. The production of the Wt1^{+} dI6 interneurons is not altered in the absence of Pou2f2. (D-L) Distribution of dI6 Wt1^{+} neurons on the transverse plane of the spinal cord in control or Pou2f2$^{-/-}$ mutant embryos. Two-dimension distribution graphs (left) show integration of cell distribution from multiple sections of multiple embryos of each genotype. One-dimension graphs (right) show density distribution in control (blue) or in Pou2f2$^{-/-}$ embryos (red) on the dorso ventral (upper) or the medio-lateral (lower) axis of the spinal cord. In control spinal cord, the dI6 Wt1^{+} subset is localised in the ventro-medial tier. In Pou2f2$^{-/-}$ mutants, at brachial and thoracic levels, cells were more densely clustered and located more ventrally and medially ($p \leq 0.001$). (M-O) Immunodetection and quantification of dI6 Wt1^{+} (green) subset in control or Pou2f2$^{-/-}$ mutant embryos at e14.5. The size of the Wt1^{+} dI6 subset is not altered in the absence

3.2.4 Discussion

During spinal cord development, proper cell migration is critically required for adequate integration of post-mitotic neurons into specific neural circuits. Recent studies demonstrated the importance of correct population and subpopulation distribution for spinal circuitry formation (Bikoff et al., 2016; Goetz et al., 2015; Hilde et al., 2016; Hinckley et al., 2015; Lu et al., 2015; Sürmeli et al., 2011; Tripodi et al., 2011). Although the involvement of an extensive amount of guidance molecules in the regulation of neuronal migration has been well characterized (Chen, 2019), the genetic programs that control the production of these guidance molecules and the selective responsiveness of distinct neuronal populations to these cues is still poorly understood, particularly in the spinal cord. Here we provide evidence that a genetic cascade composed of OC factors and their downstream target Pou2f2 controls the distribution of dINs in the developing spinal cord.

OC factors repress Pou2f2 expression in the developing spinal cord

The diversification and the distribution of dIN has been recently shown to be regulated by OC transcription factors (Kabayiza et al., 2017). In an effort to identify downstream effectors involved in this process, we uncovered genes regulated by OC factors in the embryonic spinal cord. Only a limited number of genes coding for guidance cues were identified. Moreover, none of the candidate

of Pou2f2. (P-X) Distribution of dI6 $Wt1^{+}$ cells on the transverse plane of the spinal cord in control or $Pou2f2^{-/-}$ mutant embryos at e14.5. Reminiscent of e12.5, dI6 $Wt1^{+}$ subset remained more ventrally and more densely packed in the absence of Pou2f2 ($p \leq 0.001$). The pictures show part of right hemisections as indicated on the schemes in D,G and in P,S, respectively. Analysis was performed on five sections per level from three control and three mutant embryos ($n > 635$ cells per condition). Mean values ± SEM, n = 3. Scale bar = 100µm.

genes known to control neuronal migration were confirmed to be under OC proteins regulation in the spinal cord. The outcome of this analysis suggests that the migration of each spinal neuronal population may be regulated by diverse micro-environmental cues and receptors, instead of a generic mechanism common to all populations. The diversity of migration routes, lengths and endpoints (Chen, 2019; Lai et al., 2016; Lu et al., 2015) is consistent with this hypothesis. However, expression of the Pou2f2 transcription factor appeared to be repressed by the OC factors in the embryonic spinal cord. OC inactivation did not result in a significant increase in the number of dINs containing Pou2f2, unless for the dI6 Dmrt3^{+} subset. In contrast, cells expressing Pou2f2 in control embryos show increased Pou2f2 levels in OC mutant spinal cord. Thus, OC factors seem to moderate Pou2f2 expression in its endogenous domain rather than preventing an ectopic activation in other dINs subpopulations. However, OC factors are supposed to mainly behave as transcriptional activators (Jacquemin et al., 2000; Jacquemin et al., 2003a; Pierreux et al., 2004; Roy et al., 2012). Therefore, our observations suggest an indirect regulation of Pou2f2 expression by the OC factors. Alternatively, we can not exclude that OC factors may exert a dual role as both a transcriptional activator or a repressor depending on the cell type, as previously shown for Gli3, which can act both as an activator or as a repressor during different phases of zebrafish CNS patterning (Tyurina et al., 2005), or Arx known for its bifunctional activity during Xenopus forebrain development (Seufert et al., 2005). Identification of the 5' sequences of the embryonic spinal Pou2f2 transcripts and of the regulating sequence controlling the expression of Pou2f2 in the developing spinal cord would be required to unveil the mechanisms whereby OC regulate Pou2f2 expression. Nevertheless, our analysis uncovered Pou2f2 as a downstream target of OC factors in the dINs.

An OC-Pou2f2 genetic cascade regulates the distribution of dINs

To assess whether Pou2f2 may contribute to the dIN distribution defects observed in OC mutant embryos, we increased Pou2f2 expression in the spinal cord using chicken embryonic electroporation. Pou2f2 overexpression in the chicken spinal cord resulted in dINs mislocalization without any change in their cell number, except for the dI5 Phox2a subset. These alterations are reminiscent of dIN alterations observed in the absence of OC factors (Kabayiza et al., 2017), even if in ovo electroporation constrains the analysis to developmental stages earlier than those studied in the mouse. In Hnf6/Oc2$^{-/-}$ embryos, dI3 interneurons displayed altered migration trajectory (Kabayiza et al., 2017). Similarly, after Pou2f2 overexpression, chicken dI3 migration pathway was altered. Furthermore, the dI5 INs were mislocalized after Pou2f2 overexpression, as observed for the Phox2a-positive dI5 subset in Hnf6/Oc2$^{-/-}$ embryos. However, these changes in distribution were not strictly identical, likely owing to differences in the Pou2f2 overexpression levels between the mouse and the chicken models.

Consistently, Pou2f2 depletion affected dIN distribution with only mild effects on the size of each population. Different types of localization defects were observed in Pou2f2$^{-/-}$ embryos. First, the ventral part of dI2 INs, dI6 Dmrt3 and dI6 Wt1 INs subsets settled to more ventral localizations. These cells seemed to be more advanced in their migration process, reaching faster and even going beyond their targeted localization. Second, dI5 Phox2a subset showed the most dramatic distribution defect, as its organization was altered from two clusters to a unique main cluster. Variations in these localization defects suggest, as proposed above, that different migration cues are affected in each dIN population. Nevertheless, these observations demonstrate that Pou2f2 contributes to regulate dIN migration. Furthermore, a comparison of distribution alterations between Pou2f2

and OC mutant embryos points to a possible contribution of Pou2f2 downstream of OC factors in the control of dIN migration. Indeed, Pou2f2 depletion resulted in a relatively loose dI3 population, whereas dI3 were more compactly distributed in OC mutants. Inversely, Phox2a-positive dI5 were more densely packed along the dorso-ventral axis in Pou2f2 mutants but more spread in OC mutants. However, although depletion or overexpression of Pou2f2 might have opposite effects on the expression of its downstream guidance cue targets, these will not necessarily lead to opposite effects on cellular migration. Nevertheless, we propose that a genetic cascade involving OC and Pou2f2 transcription factors controls the distribution of dI2-dI6 INs.

Pou2f2 acts as a regulator of dIN distribution

Although Pou2f2 has been previously described as a transcription factor regulating the maturation of B cell precursors into immunoglobulin-secreting B cells (Corcoran et al., 1993), it is also expressed in the central nervous system during development and in the adult brain (Camós et al., 2014; Kaczmarek and Sibbel, 2008; Lillycrop and Latchman, 1992; Stoykova et al., 1992). A high-resolution in situ hybridization analysis detected Pou2f2 expression at e13.5 in the midbrain (Thompson et al., 2014), a time point that corresponds to late neurogenesis (Bayer et al., 1995). Consistently, we observed the presence of Pou2f2 in differentiating dI2-dI6 interneurons of the developing spinal cord. In mouse ES cells undergoing neuronal differentiation, Pou2f2 could act as a bifunctional regulator of differentiation depending on the predominant isoform (Theodorou et al., 2009), although the isoforms considered are different from those identified in the developing spinal cord (Harris et al., 2019). However, its role in neuronal CNS development had not been explored yet. Our analysis of several dIN populations suggested that Pou2f2 contributes to dIN migration.

Furthermore, Pou2f2 inactivation is associated with neonatal lethality (Corcoran et al., 1993), suggesting its involvement in the development of vital nervous functions. Potential Pou2f2 targets in the CNS are currently unknown. Recent studies have uncovered the presence of Pou2f2 in several tumors including pancreatic and gastric cancers, the latter having a high frequency of invasiveness and metastasis. Interestingly, Pou2f2 has been identified in a Nf-kB/Pou2f2/Robo1/Slit2 signaling cascade that promotes metastasis in gastric cancer cells (Wang et al., 2016). In this cascade, Pou2f2 directly regulates the Robo1 gene, a member of the ROBO family, and activates its expression. Several studies point out the importance of the Slit/Robo repulsive signals in neuronal migration (Andrews et al., 2006; Causeret et al., 2002; Di Meglio et al., 2008; Wu et al., 1999). In the developing forebrain, through semaphorin-neuropilin/plexin signaling modulation, Robo1 guides interneuron migration through the subpallium and into the cortex (Hernández-Miranda et al., 2011). Oppositely to Robo1 and Robo2 receptors, Robo3 does not bind Slits but instead interacts with Dcc and Netrin-1. This mechanism of action mediates attraction (Zelina et al., 2014) and, probably through Dcc and Robo3, Netrin-1 promotes dINs migration (Junge et al., 2016). Additionally, Slit/Robo repellent signaling, in parallel with Netrin-1/DCC attractive cues, ensures correct positioning of spinal motor neurons in the ventral horn (Kim et al., 2015). Hence, Pou2f2 may regulate Robo1 expression in dIN populations and thereby promote the production of repulsive guidance cues. Interestingly, in Pou2f2 mutants, several dIN populations progress deeper than expected in the ventral spinal cord. Secreted Slits are produced by the ventral spinal cord, which makes it a repulsive territory for neurons expressing Robo1 and Robo2 receptors (Long et al., 2004). In Pou2f2-depleted dINs, Robo1 expression could be downregulated, resulting in altered responsiveness to repellent Slit signals that would authorize a more ventral localization.

Perturbations in neuronal position and/or migration during development result in heavy conditions such as 'type I' lissencephaly related to the mislocalization of cortical neurons (Hirotsune et al., 1998; Vallee and Tsai, 2006) or constitute a risk factor for schizophrenia (Tomita et al., 2011). Interestingly, two other POU domain transcription factors, Pou3f2 and Pou3f3 are suspected to be involved in schizophrenia due to their effect on cortical neuron migration (Dominguez et al., 2013; Potkin et al., 2009). Even if diseases associated with neuronal positioning defects have not been described in the spinal cord yet, it has been recently demonstrated that interneuron localization is critical for proper spinal circuit formation. Indeed, the settlement position of inhibitory V1 IN subsets correlates with their input connectivity (Bikoff et al., 2016). Similarly, stereotypical motor neuron localization is of importance for sensory connection establishment. In fact, proprioceptors target specific dorso-ventral tiers of the spinal cord without regards to the identity of motor neurons present (Sürmeli et al., 2011). Hence, the adequate position of motor neurons is initially of greater importance for sensory-motor connectivity than their identity. Alterations in dIN settling position also cause impairments of sensorimotor signaling, as demonstrated for Satb2^{+} lamina V inhibitory sensory relay neurons. Loss of Satb2 resulted in altered medio-lateral position of these dINs, which subsequently affected the proprioceptive innervation on those cells (Hilde et al., 2016). Soma localization may also influence the ingrowth of sensory afferents to the dorsal horn. Indeed, selective depletion of Bcl11a in dINs alters, besides its role in neuron morphogenesis, the traveling of sensory fibers to their spinal targets (John et al., 2012). Other transcription factors are known to influence dIN migration, including Lmx1b and its downstream targets Drg11 and Rnx, the depletion of which leads to dI5 aberrant localization (Ding et al., 2004). Here we demonstrated that dINs show aberrant soma settling position when Pou2f2 is either overexpressed or depleted.

Interestingly, the dIN populations affected in the absence of Pou2f2 are involved either in the modulation of motor neuron activity (Andersson et al., 2012; Bui et al., 2013; Goetz et al., 2015; Satoh et al., 2016) or of ventral premotor interneuron activity (Hilde et al., 2016; Levine et al., 2014), or in the presynaptic inhibition of proprioceptive sensory neuron terminals that hinder sensory inputs onto motor neurons (Betley et al., 2009; Fink et al., 2014; Zhang et al., 2017). Whether alterations in Pou2f2 mutant embryos affect the activity of the sensory-motor circuits of the spinal cord remains to be determined.

3.2.5 Material and Methods

Ethics statement and mouse lines

All experiments were strictly performed in accordance with the European Community Council directive of 24 November 1986 (86-609/ECC) and the decree of 20 October 1987 (87-848/EEC). Mice were raised in our animal facilities and treated according to the principles of laboratory animal care. Experimental procedures and mouse housing were both approved by the Animal Welfare Committee of Université catholique de Louvain (Permit Numbers: 2013/UCL/MD/11 and 2017/UCL/MD/008). Mutant strain mice were crossed and the day of vaginal plug was considered to be embryonic day (e) 0.5. The embryos were collected at e10.5, e11.5, e12.5 and e14.5. A minimum of three embryos of the same genotype was analyzed in each experiment. The Hnf6;Oc2 and the Pou2f2 mutant mice have been described previously (Clotman et al., 2005; Corcoran et al., 1993; Jacquemin et al., 2000). The Hnf6;Oc2 mutant embryos additionally lack OC-3 in the developing spinal cord (Kabayiza et al., 2017; Roy et al., 2012).

In situ hybridization and immunofluorescence labelings

For in situ hybridization, embryos were fixed in ice-cold 4% paraformaldehyde (PFA) in phosphate buffered-saline (PBS) overnight at 4°C, washed thrice in PBS for 10 minutes, incubated in PBS/30% sucrose solution overnight at 4°C, embedded and frozen in PBS/15% sucrose/7.5% gelatin. Fourteen µm section were prepared and in situ hybridization was performed as previously described (Beguin et al., 2013; Francius et al., 2016; Pelosi et al., 2014) with DIG-conjugated Pou2f2 (NM_011138.1, nucleotides 604-1187) antisense RNA probes. Control or necut mutant sections were placed adjacent on the same histology slides to minimize inter-slide variations of in situ hybridization signals.

For immunofluorescence labelings, embryos were fixed in ice-cold 4% paraformaldehyde (PFA) in phosphate buffered-saline (PBS) for 10 to 35 min according to their embryonic stage, incubated in PBS/30% sucrose solution overnight at 4°C, embedded and frozen in PBS/15% sucrose/7.5% gelatin. Immunostaining was performed on 12 or 14 µm serial cryosections as previously described (Francius and Clotman, 2010). Primary antibodies against the following proteins were used: Brn3a (mouse 1:1000; Santa Cruz #sc-8429), Dmrt3 (guinea pig; 1:1000; kindly provided by K. Kullander #170), Foxd3 (guinea pig; 1:1000; or rabbit; 1:1000; kindly provided by T. Müller), Foxp1 (goat; 1:1000; R&D Systems #AF4534), HNF6 (guinea pig; 1:2000; (Espana and Clotman, 2012b) or rabbit; 1:100; Santa Cruz #sc-13050 or sheep; 1:1000 R&D Systems #AF6277), Isl1/2 (goat; 1:3000; Neuromics #GT15051 or mouse; 1:6000; DSHB #39.4D5), Lbx1 (guinea pig; 1:10,000 or rabbit; 1:5000; kindly provided by T. Müller), Lhx1/5 (mouse; 1:1000; DSHB #4F2), Lmx1b (guinea pig; 1:10,000 or rabbit; 1:2000; kindly provided by T. Müller), OC2 (rat; 1:400; (Clotman et al., 2005) or sheep; 1:500; R&D Systems #AF6294), OC3 (guinea pig; 1:6000; (Pierreux et al., 2004), Phox2a (rabbit; 1:500; kindly provided by J.-F. Brunet), Pou2f2 (rabbit; 1:2000; Abcam

#ab178679), Wt1 (rabbit; 1:2000; Santa Cruz #sc-192). Secondary antibodies were the donkey anti-guinea pig/AlexaFluor 488, 594 or 647, anti-mouse/AlexaFluor 488, 594 or 647, anti-rabbit/AlexaFluor 594 or 647, anti-goat/AlexaFluor 488, anti-rat/AlexaFluor 488 or 647, anti-sheep/AlexaFluor 594, and goat anti-mouse IgG1 specific/AlexaFluor 488 or 594, anti-mouse IgG2A specific/AlexiaFluor 488, anti-mouse IgG2B specific/AlexaFluor 647, purchased from ThermoFisher Scientific or Jackson Laboratories, and were used at dilution 1:1000.

In ovo electroporation

In ovo electroporations were performed at stage HH14-16, as previously described (Roy et al., 2012). The coding sequence of Pou2f2 was amplified by overlapping-PCR, as previously described (Harris et al., 2019) using: forward 5' GCTCTGTCTGCCCAAGAGAAA 3' and reverse 5' GTTGGGACAAGGTGAGCTGT 3' primers for the 5' region, forward 5' CCACCATCACAGCCTACCAG 3' and reverse 5' ATTATCTCGAGCCAGCCTCCTTACCCTCTCT 3' (designed to enable integration at the XhoI restriction site of the pCMV-MCS vector) primers for the 3' region. This sequence was first subcloned in a pCR®II-Topo® vector (Life Technologies, 45-0640) for sequencing then subcloned at the EcoRI (from the pCR®II-Topo® vector) and XhoI restriction sites of a pCMV-MCS vector for the in ovo electroporation. The pCMV-Pou2f2 (0.5 µg/µl) vector was co-electroporated with a pCMV-eGFP plasmid (0.25µg/µl) to visualize electroporated cells. The embryos were collected 72 hours (HH27-28) after electroporation, fixed in PBS/4%PFA for 45 minutes and processed for immunofluorescence labelings as previously described (Francius and Clotman, 2010).

Imaging and quantitative analyses

Immunofluorescence images of cryosections were acquired on a Confocal Laser Scanning microscope FV1000 Fluoview with the FV10-ASW 01.02 software

(Olympus) or an EVOS FL Auto Cell Imaging System (Thermo Fisher Scientific). Brightness and contrast were adjusted uniformly in all replicate panels within an experiment with Adobe Photoshop CS6 software to match with the observation. Quantifications were performed on red or green or blue layer of acquired confocal images and double or triple labeled cells were processed by subtractive method (Francius and Clotman, 2010). For each embryo (n=3), one side of five sections at brachial, at thoracic and at lumbar levels were quantified using the count analysis tool of Adobe Photoshop CS6 software. Raw data were exported from Adobe Photoshop CS6 software to Sigma Plotv12.3 software to perform statistical analyses. The histograms were drawn with Microsoft Excel. Adequate statistical tests were applied based on the number of comparisons and on the variance in each group. For analysis of cell quantifications based on comparison of two groups (control or mutant; control or electroporated side of the spinal cord), standard Student's t-tests or Mann-Whitney U tests were performed. Differences were considered as significant at $p \leq 0.05$ Quantitative analyses of IN spatial distribution were performed as previously described (Kabayiza et al., 2017). Statistical analyses of dorsal IN distribution were performed using a two-sample Hoteling's T2, which is a two-dimensional generalization of the Student's t test. The analysis was implemented using the NCSS software package.

3.2.6 Acknowledgments

We thank members of the NEDI lab for material, technical support and discussions. We are grateful to Dr. K. Kullander for kindly providing the guinea pig anti Dmrt3 antibody, to Dr. T. Müller for the rabbit or guinea pig anti Foxd3 or anti Lbx1 or anti Lmx1b antibodies, and to Dr. J.-F. Brunet for the rabbit anti Phox2a antibody, and to Dr. G. Courtoy for help with image quantifications.

3.3 The Onecut transcription factors regulate early differentiation and axonal projections of sensory neurons

3.3.1 Foreword

In three successive and temporally overlapping neurogenic waves, the NCC generate a variety of sensory subtypes characterized by the expression of Trk receptors (Fariñas et al., 1998; Ma et al., 1999; Maro et al., 2004). Among them, small diameter $TrkA^+$ nociceptors mediate noxious stimuli, while mechanical sensations are perceived by larger diameter $TrkB^+$ and/or $TrkC^+$ mechanoreceptors, and large diameter $TrkC^+$ proprioceptors sense limb and body position. As well as proper type of sensory neuron formation, each neuron must establish accurate central and peripheral connections. Progress has been made in elucidating the establishment of sensory neuron diversity in the DRG with a growing body of TF, including Prdm12, Brn3a, Isl1, Klf7, Shox2, Runx1 and Runx3, demonstrated as key regulators of sensory neuron differentiation and/or axonal projection formation (Bartesaghi et al., 2019; Chen et al., 2006a; Desiderio et al., 2019; Dykes et al., 2011; Inoue et al., 2003; Lei et al., 2005; Lei et al., 2006; Levanon et al., 2002; Marmigère et al., 2006; Sun et al., 2008; Yoshikawa et al., 2007; Zou et al., 2012).

Previous studies demonstrated OC as regulators of neuronal population diversification (Francius and Clotman, 2014; Harris et al., 2019; Kabayiza et al., 2017; Roy et al., 2012), distribution (Audouard et al., 2013; Espana and Clotman, 2012b; Espana and Clotman, 2012a; Harris et al., 2019; Kabayiza et al., 2017), maintenance (Espana and Clotman, 2012b; Espana and Clotman, 2012a; Stam et al., 2012), and connectivity (Hodge et al., 2007). Previously detected in DRG during development (Landry et al., 1997), only OC-1 and OC-2 are present in the sensory neurons (Francius and Clotman, 2010). However, none of these studies

addressed the distribution and the function of OC factors during sensory neuron development.

In the present study, we identified the spatiotemporal distribution pattern of OC-1 and OC-2 in the developing DRG. Then, we determined OC-1 and OC-2 roles in sensory differentiation using *Oc1/Oc2*$^{-/-}$ embryos. In addition, we uncovered a novel role for OC factors as intrinsic cue for sensory neuron central or peripheral axonal projections.

This manuscript is still in preparation for submission in **Journal of Neuroscience**. In this work, I carried out all the experiments.

The Onecut transcription factors regulate early differentiation and axonal projections of sensory neurons

Gauhar Masgutova[1], Youri Adolfs[2], Jeroen Pasterkamp[2] and Frédéric Clotman[1*]

[1]Université Catholique de Louvain, Institute of Neuroscience, Laboratory of Neural Differentiation, Brussels, Belgium

[2]Utrecht University, Brain Center Rudolf Magnus – University Medical Center Utrecht, Department of Translational Neuroscience, Utrecht, The Netherlands

*** Correspondence:**

Corresponding author: Frédéric Clotman, Laboratory of Neural Differentiation, Institute of Neuroscience, Université catholique de Louvain Avenue Hippocrate 55, box B1.55.11, B-1200, Brussels, Belgium Phone: +32.2.764.55.71, Fax: +32.2.764.55.72, Email: frederic.clotman@uclouvain.be

Keywords: Embryonic dorsal root ganglia, sensory neurons, Onecut transcription factors, differentiation, axonal projections

Abstract

The sensory neurons of the peripheral nervous system differentiate into three modalities that convey mechanical, proprioceptive or thermal and nociceptive stimuli from the periphery to the central nervous system where they are processed. Multiple factors controlling the diversification and divergence of distinct sensory populations have been identified but the mechanisms that coordinate different aspects of their development remain partly unknown. Here, we show that the Onecut transcription factors OC-1 and OC-2 regulate early differentiation and segregation of distinct sensory subsets, probably by controlling the initiation or the inhibition of neurotrophin receptor and of *Runx3* expression. Furthermore, Onecut factors are required for proper projections of sensory neurons into the spinal cord or towards their peripheral targets. Thus, Onecut proteins regulate a genetic program that coordinate sensory differentiation and axonal projections during embryonic development.

3.3.2 Introduction

The great variety of perceived sensory modalities primarily relies on the development of various sensory neurons from neural crest cells (NCC) that delaminate from the dorsal neural tube and coalesce into cranial or dorsal root ganglia (DRG). Sensory neuron subtypes are characterized by the differential expression of transmembrane receptor tyrosine kinases (Trk) required for their survival, differentiation, maintenance, and proper target innervation. Small diameter cutaneous $TrkA^+$ nociceptors mediate noxious stimuli, and mechanical sensations are perceived by larger diameter $TrkB^+$ and/or $TrkC^+$ mechanoreceptors while large $TrkC^+$ proprioceptors sense limb and body position. Although progress has been made in elucidating the establishment of sensory neuron diversity in the DRG (Marmigère and Ernfors, 2007; Liu and Ma, 2011; Lallemend and Ernfors, 2012), the mechanisms that regulate early differentiation of each sensory neuron population and those that control their axonal projection are only partly understood.

Three successive and temporally overlapping sensory neurogenic waves take place between embryonic day (e) 9.5 and e13.5 (Ma et al., 1999; Maro et al., 2004). The first wave generates large-diameter $TrkB^+$ and/or $TrkC^+$ mechanoreceptors and proprioceptors but also a minor part of $TrkA^+$ large-diameter nociceptors between e9.5 and e11.5 from NCCs expressing Neurogenin (Neurog) 2 (Ma et al., 1999; Bachy et al., 2011). A second, Neurog1-dependent, wave mainly produces small-diameter $TrkA^+$ nociceptors between e10.5 and e13.5 (Ma et al., 1999). The last neurogenic wave contributes to 5% of $TrkA^+$ nociceptors originating from neural crest derivatives, the boundary cap cells located at the dorsal root entry zone (DREZ) of the spinal cord (Maro et al., 2004). Newly-born sensory neurons often display combined *Trk* expression that eventually

segregates into distinct sensory subsets (Fariñas et al., 1998; Marmigère and Ernfors, 2007; Cheng et al., 2018). Transmission of the different somatosensory modalities from the periphery to the CNS requires bidirectional sensory projections into the pons or the spinal cord on the one hand, and towards peripheral targets on the other hand. Central projections of sensory axons exit the DRG dorsally and enter the spinal cord at the DREZ where they bifurcate rostrally and caudally, forming the dorsal funiculus (DF). Then, axons generate collaterals that penetrate spinal cord gray matter with distinct projection patterns to reach specific spinal laminae (Ozaki and Snider, 1997). $TrkA^+$ nociceptors project to laminae I/II and IV/V, whereas $TrkB^+$ mechanoreceptors mainly target laminae III, IV and V and $TrkC^+$ proprioceptors invade deep layers of the ventral horn (Brown, 1981; Chen et al., 2006a; de Nooij et al., 2013). In contrast, peripheral projections exit the DRG ventrally and, depending on their segmental level, extend either one or several branches along pioneering trajectories of motor efferent axons from e10.0 (Wang et al., 2014). Broadly, nociceptors innervate skin and viscera, mechanoreceptors innervate the skin, whereas proprioceptors contact with muscle spindles and Golgi tendon organs. However, prior studies suggested that two or more distinct peripheral branches protrude from DRG at certain anteroposterior levels (Dykes et al., 2011; Renier et al., 2014).

Genetic programs controlled by transcription factors regulate neuronal development. Previous studies established the presence of Onecut (OC) transcription factors in numerous neuronal populations of the CNS (Francius and Clotman, 2010; Roy et al., 2012; Francius et al., 2013; Kabayiza et al., 2017). The *Oc1, Oc2* and *Oc3* genes encode transcriptional activators known to regulate production (Espana and Clotman, 2012a), diversification (Roy et al., 2012; Francius and Clotman, 2014; Kabayiza et al., 2017; Harris et al., 2019), distribution

(Espana and Clotman, 2012b, 2012a; Audouard et al., 2013; Kabayiza et al., 2017; Harris et al., 2019) and maintenance (Espana and Clotman, 2012b, 2012a; Stam et al., 2012) of specific neuronal populations, and neuromuscular junction formation (Audouard et al., 2012). Previously detected in DRG during development (Landry et al., 1997), only OC-1 and OC-2 are present in the sensory neurons (Francius and Clotman, 2010). However, none of these studies addressed the distribution and the function of OC factors during sensory neuron development.

In the present study, we analyzed the spatio-temporal distribution pattern of OC-1 and OC-2 in the developing sensory neurons. Then we addressed the roles of OC factors in sensory development using *Oc1/Oc2* null mutant embryos. In the absence of OC factors, we observed that the onset of *TrkA* expression was delayed. In addition, $TrkB^+/C^+$ neurons were present in a higher proportion, suggesting a failure in the segregation of the mechanoreceptor and proprioceptor lineages. Consistently, the number of cells containing Runx3, which is necessary to extinguish TrkB production in prospective proprioceptors, was decreased. However, *TrkA* expression eventually normalized and $TrkB^+$ and $TrkC^+$ cells eventually segregated in a normal fashion, indicating a transient requirement for OC factors in the early phases of sensory differentiation. Nevertheless, in the absence of OC proteins, the DRG were located farther from the spinal cord than in control embryos. In addition, $Oc1/Oc2^{-/-}$ individuals demonstrated aberrant invasion by $TrkA^+$ and $TrkC^+$ afferents into the grey matter of the dorsal horn with DF disorganization. Furthermore, peripheral projections of $TrkA^+$ sensory neurons were abnormal and resulted in plexus disorganization. Thus, our findings show that OC factors are essential for timely initiation of *TrkA* expression in prospective nociceptors and of *TrkB* repression in $TrkC^+$ proprioceptors. Moreover, we identified a novel role for OC factors as intrinsic regulators of sensory neuron positioning and central or peripheral axonal projections.

3.3.3 Results

OC transcription factors are present in sensory neurons from the onset of differentiation.

Among *Oc* factors, *Oc1* and *Oc2* were previously shown to be expressed in DRG during embryonic development (Landry et al., 1997; Francius and Clotman, 2010). We first characterized the distribution of OC-1 and OC-2 in the developing DRG sensory neurons by immunofluorescence at different embryonic stages. Given that, in the embryonic spinal cord, OC factors are produced from the onset of neuronal differentiation (Francius and Clotman, 2010; Stam et al., 2012; Francius et al., 2013; Kabayiza et al., 2017), we started our analyses at the onset of DRG formation, namely e9.5. At this stage, solely OC-1 was detected in NCC progenitors coalescing into DRGs identified by Pax3 immunofluorescence (Figure S1). At e10.5, both OC-1 and OC-2 were strongly co-detected throughout the ganglia with the pan-sensory neuron marker Isl1, indicating OC-1 maintenance from progenitors to post-mitotic neurons. The incidence of OC-1^+ Islet1^+ cells decreased from e11.5 onward oppositely to increasing OC-2^+ Islet1^+ co-labeled cells (Figure 1A-D). As previously reported in developing CNS neuronal populations (Francius and Clotman, 2010; Espana and Clotman, 2012b, 2012a; Stam et al., 2012; Francius et al., 2013; Kabayiza et al., 2017; Harris et al., 2019), OC protein distribution significantly overlapped (Figure 1D). Therefore, post-mitotic sensory neurons contained either one or two OC factors

To identify in which sensory neuron subtypes OC-1 and OC-2 are produced, we performed triple immunolabelings to determine their presence within TrkA$^+$, TrkB$^+$ or TrkC$^+$ cells devoted to become nociceptors, mechanoreceptors or proprioceptors, respectively. Both at e10.5 and e11.5, a large proportion of TrkA$^+$ neurons contained OC-1 but the proportion of these cells significantly decreased

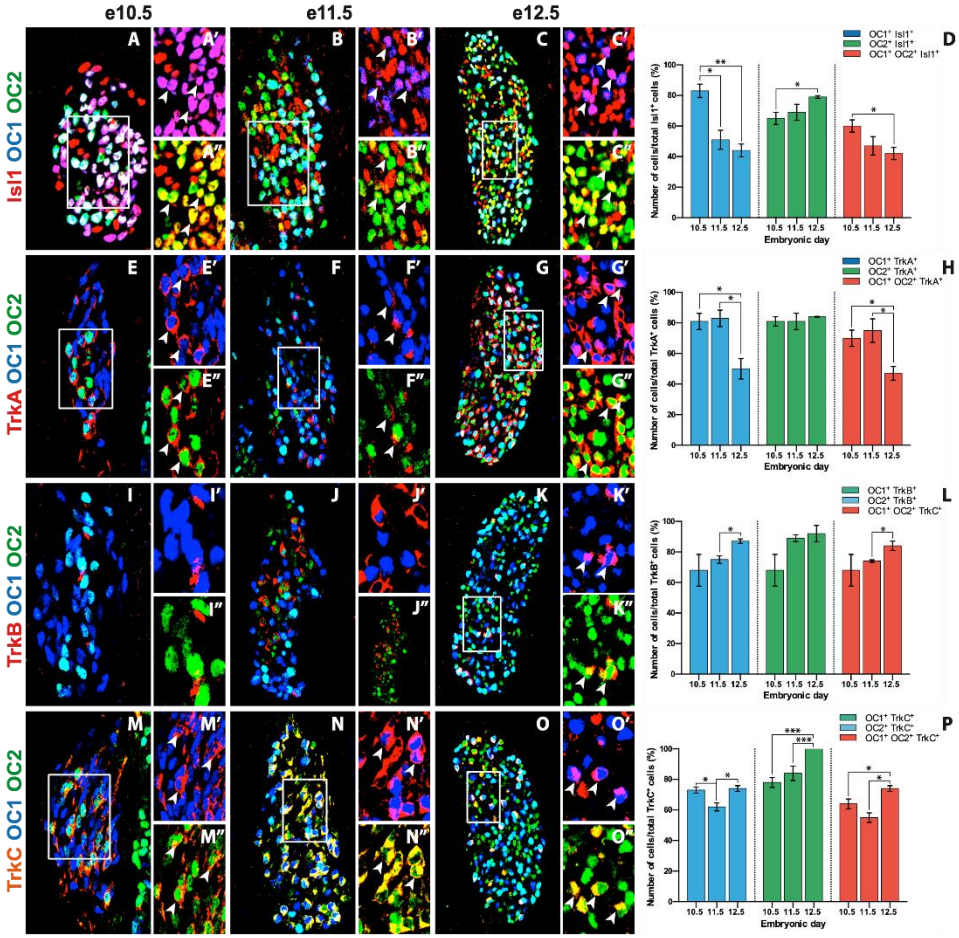

Figure 1. OC transcription factors are present in sensory neurons from the onset of differentiation. (A-C) Immunodetection of OC-1 (blue) and OC-2 (green) in Isl1$^+$ (red) sensory neurons on transverse sections of brachial DRG at e10.5 (A-A"), e11.5 (B-B") or e12.5 (C-C"). (D) The percentage of OC-positive Isl1$^+$ sensory neurons per section was quantified accordingly. OC-1 is visible in a majority of Isl1$^+$ sensory neurons at e10.5 but the percentage decreases at e11.5 and e12.5, while OC-2 proportion increases from e10.5 to e12.5. (E-G) Immunodetection of OC-1 (blue) and OC-2 (green) in TrkA$^+$ (red) nociceptive precursors on transverse sections of brachial DRG at e10.5 (E-E"), e11.5 (F-F") or e12.5 (G-G"). (H) The percentage of OC-positive TrkA$^+$ sensory neurons per section was quantified accordingly. OC-1 is present in a majority of TrkA$^+$ sensory neurons at e10.5 but the percentage decreases at e12.5, while OC-2 is detected in 80% of TrkA$^+$ neurons from e10.5 to e12.5. (I-K) Immunodetection of OC-1 (blue) and OC-2 (green) in

at e12.5 (Figure 1E-H). In contrast, the broad OC-2 presence in TrkA$^+$ cells remained stable at all studied stages (Figure 1E-H). Presence of OC-1 in TrkB$^+$ cells rose from e10.5 to e12.5 (Figure 1I-L), while OC-2 distribution followed an increasing trend to eventually cover almost all TrkB$^+$ neurons (Figure 1I-L). Finally, the proportion of OC-1$^+$ TrkC$^+$ cells among TrkC$^+$ neurons first significantly decreased and then increased between e10.5 and e12.5, while OC-2 production increased to reach almost all TrkC$^+$ neurons (Figure M-P). Thus, OC factors are present in the 3 subdivisions of sensory neurons throughout their differentiation in a dynamic spatio-temporal pattern suggesting a potential involvement in some aspects of sensory neuron development.

Loss of *OC* expression in DRG does not affect sensory neuron production

The early production of OC factors in sensory neuron progenitors led us to hypothesize that OC might be involved in the generation of post-mitotic sensory neurons. To address this question, the production of the pan-sensory marker Isl1 was analyzed in *Oc1/Oc2*$^{-/-}$ double-mutant embryos (Jacquemin et al., 2000; Clotman et al., 2005). However, Isl1$^+$ cells were present in DRG from the early stages of sensory development (Figure 2A-B and data not shown), suggesting that OC factors are not required for sensory neuron generation. To determine if the number of sensory neurons was normal in the absence of OC proteins, we carried

e11.5 (J-J") or e12.5 (K-K"). (L) The percentage of OC-positive TrkB$^+$ sensory neurons per section was quantified accordingly. OC-1 and OC-2 expand progressively from e10.5 to e12.5 in TrkB$^+$ neurons. (M-O) Immunodetection of OC-1 (blue) and OC-2 (green) in TrkC$^+$ (red) proprioceptive neurons on transverse sections of brachial DRG at e10.5 (M-M"), e11.5 (N-N") or e12.5 (O-O"). OC-1 is visible in a majority of TrkC$^+$ sensory neurons at e10.5 but the percentage decreases at e11.5 and increases at e12.5, while OC-2 proportion increases from e10.5 to e12.5. (P) The percentage of OC-positive TrkC$^+$ sensory neurons per section was quantified accordingly. Insets are magnified views of boxed regions. Arrowheads point to double-labeled cells. Mean values ±SEM, $n \geq 3$.

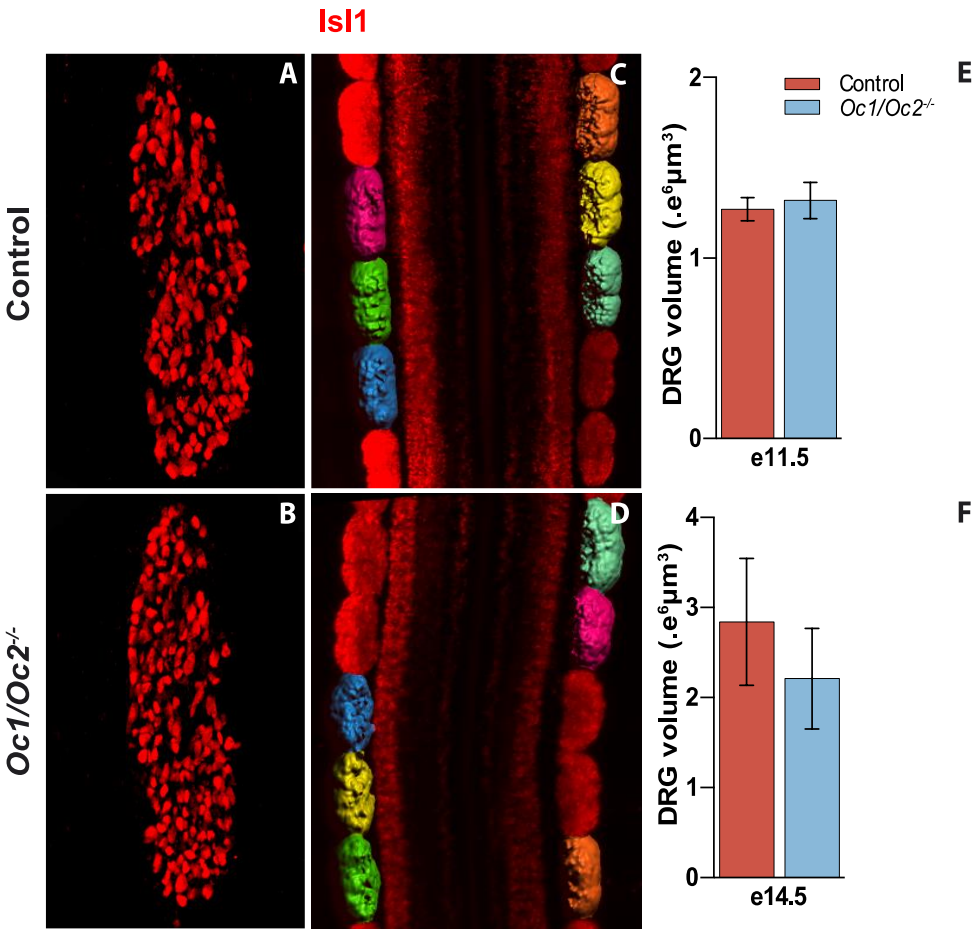

Figure 2. Loss of *OC* expression in DRG does not affect the number of sensory neuron (A-B) Immunodetection of Isl1 in sensory neurons on transverse sections of brachial DRG at e11.5 in control (A) or *Oc1/Oc2*$^{-/-}$ (B) embryos. **(C-D)** Whole-mount immunodetection of Isl1 in brachial sensory neurons and spinal cord in control (C) or *Oc1/Oc2*$^{-/-}$ (D) embryos. Distinct DRG were given a false-color for visualization and for volume measurement. **(E)** Quantification of brachial Isl1^{+} DRG volume at e11.5 or **(F)** at e14.5. Immunodetection and quantification of DRG volumes show no change in mutant embryos at both developmental stages, indicating that the production and the maintenance of sensory neurons is unaffected in the absence of Onecut factors. Mean values ±SEM, $n \geq 3$.

out Isl1 whole-mount immunolabelings and volume quantification of control or *Oc1/Oc2*$^{-/-}$ brachial DRGs (see Material and Methods). At e11.5 and e14.5, the volume of the DRGs was comparable in control and *Oc1/Oc2*$^{-/-}$ embryos (Figure 2A-D). Consistently, the proportion of activated caspase3-positive sensory neuron did not differ between control and *Oc1/Oc2*$^{-/-}$ mutant embryos at e11.5 (Figure S2A-C). Taken together, these observations suggest that OC factors are not required for proper production or survival of sensory neurons.

OC factors regulate the onset of TrkA production and the segregation of *TrkB* and *TrkC* expression during sensory neuron differentiation

OC factors have been shown to regulate the diversification of several spinal neuronal populations into specialized subsets (Roy et al., 2012; Francius and Clotman, 2014; Kabayiza et al., 2017; Harris et al., 2019). Therefore, we assessed whether OC proteins might participate in the divergence of sensory neuron subtypes, namely nociceptors, mechanoreceptors and proprioceptors. To this end, we quantified the proportion of TrkA$^+$, TrkB$^+$ and TrkC$^+$ sensory neurons and their transient combinatorial subtypes in developing DRG in control or *Oc1/Oc2*$^{-/-}$ mutant mice from e10.5 to e12.5 and at e14.5. As previously reported (Ma et al.,

Figure 3. OC factors regulate the onset of TrkA production and the segregation of TrkB$^+$ and TrkC$^+$ sensory neurons during differentiation. Immunodetection of TrkA (blue), TrkB (green) and TrkC (red) in sensory neurons on transverse sections of brachial DRG at a10.5 (A-C), e11.5 (D-F), e12.5 (G-I) or e14.5 (J-L) in control (A,D,G,J) or *Oc1/Oc2*$^{-/-}$ (B,E,H,K) embryos and quantification of the relative number of TrkA$^+$, TrkB$^+$, TrkC$^+$ and their transient combinatorial subtypes (C,F,I,L). Pie charts represent proportions of quantified sensory populations and subtypes. (**A-C**) At e10.5, TrkA was barely detectable in *Oc1/Oc2*$^{-/-}$ DRG. **(D-F)** At e11.5, TrkA distribution is normalized but TrkB$^+$/TrC$^+$ cells are increased at the expanse of TrkC$^+$ proprioceptor precursors. **(G-I)** At e12.5, the number of proprioceptors is mildly decreased. **(J-L)** At e14.5, sensory neuron differentiation is normalized. Mean values, $n \geq 3$. Significance levels $^*p<0.05$, $^{**}p<0.01$.

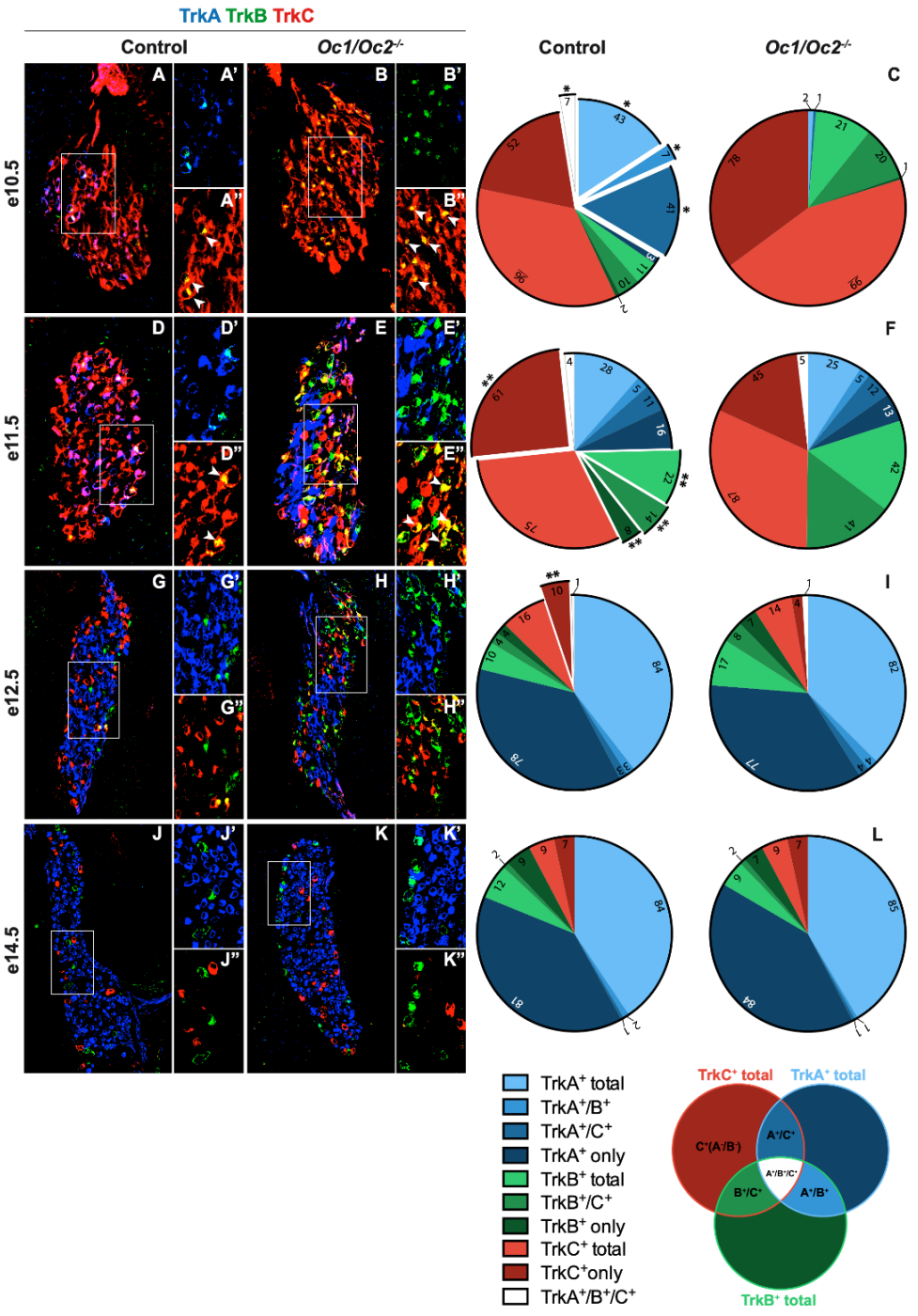
TrkA TrkB TrkC
Control
Oc1/Oc2-/-
e10.5
e11.5
e12.5
e14.5
A
A'
A''
B
B'
B''
C
D
D'
D''
E
E'
E''
F
G
G'
G''
H
H'
H''
I
J
J'
J''
K
K'
K''
L
TrkA+ total
TrkA+/B+
TrkA+/C+
TrkA+ only
TrkB+ total
TrkB+/C+
TrkB+ only
TrkC+ total
TrkC+only
TrkA+/B+/C+
TrkC+ total
TrkA+ total
C+(A-/B-)
A+/C+
A+/B+/C+
B+/C+
A+/B+
TrkB+ total

1999), TrkC was the first receptor to be detected within the developing DRG. At e10.5 in control embryos, almost 100% of the sensory neurons contained TrkC (Figure 3A). No change was observed in $TrkC^+$ neuron proportion in *Oc1/Oc2*$^{-/-}$ mutant embryos (Figure 3A-C). In agreement with previous observations (Fariñas et al., 1998), in control ganglia, hybrid $TrkA^+/B^+$, $TrkA^+/C^+$, $TrkB^+/C^+$ and $TrkA^+/B^+/C^+$ neurons were detected at this early developmental stage (Figure 3A, C). In *Oc1/Oc2*$^{-/-}$ ganglia, $TrkB^+$ and hybrid $TrkB^+/C^+$ neurons were detected in proportions comparable to control ganglia (Figure 3B-C). In contrast, $TrkA^+$ neurons were almost completely absent, which led to a drastic reduction in all the $TrkA^+$ subsets (Figure 3A-C). This observation suggested that OC factors might be necessary either for the generation of nociceptors or for the initiation of *TrkA* expression in sensory neurons. However, at e11.5, *Oc1/Oc2*$^{-/-}$ DRG showed normal percentage of total $TrkA^+$ neurons and $TrkA^+$ subsets (Figure 3D-F), indicating that OC proteins are transiently required for timely production of TrkA in differentiating nociceptors. In contrast, the total number of $TrkB^+$ doubled and the proportion of $TrkB^+/C^+$ cells tripled, whereas a 25% decrease in $TrkC^+$-only neurons was observed (Figure 3D-F). This pointed to a defective segregation of TrkB and TrkC production in the course of mechanoreceptor and proprioceptor differentiation (Fariñas et al., 1998), and abnormal maintenance of TrkB in prospective proprioceptors. Accordingly, an imbalance between $TrkB^+$- and $TrkC^+$-only sensory neurons was still detected in *Oc1/Oc2*$^{-/-}$ mutants at e12.5, but the ratio of hybrid $TrkB^+/C^+$ cells was comparable to control embryos (Figure 3G-I). Finally, at e14.5 in control embryos, transient hybrid subsets were almost absent as main TrkA, TrkB and TrkC lineages segregated into discrete populations. Interestingly, at this stage, the segregation of distinct lineages in *Oc1/Oc2*$^{-/-}$ DRG was indistinguishable from wild-type embryos (Figure 3J-L), demonstrating normalization of the abnormal phenotype observed at earlier developmental

stages. Together, these observations suggest that OC factors regulate the timely initiation of TrkA production in prospective nociceptors and the timely repression of *TrkB* expression in prospective TrkC$^+$ proprioceptors.

Extinction of *TrkB* expression in prospective proprioceptors is dependent on the Runt transcription factor Runx3. In the absence of Runx3, TrkB abnormally persists in TrkC$^+$ neurons, altering subsequent proprioceptor development (Inoue et al., 2003, 2007; Kramer et al., 2006; Nakamura et al., 2008; Lallemend and Ernfors, 2012). Therefore, we assessed whether Runx3 was reduced in the absence of OC factors, which may account for the maintenance of TrkB$^+$/TrkC$^+$ hybrid cells (Figure 3A-F). At e11.5, the relative number of Runx3$^+$ sensory neurons was reduced by 47% in the *Oc1/Oc2*$^{-/-}$ DRG, indicating that OC are required for proper *Runx3* expression in early sensory neurons (Figure 4A-C). In contrast, the

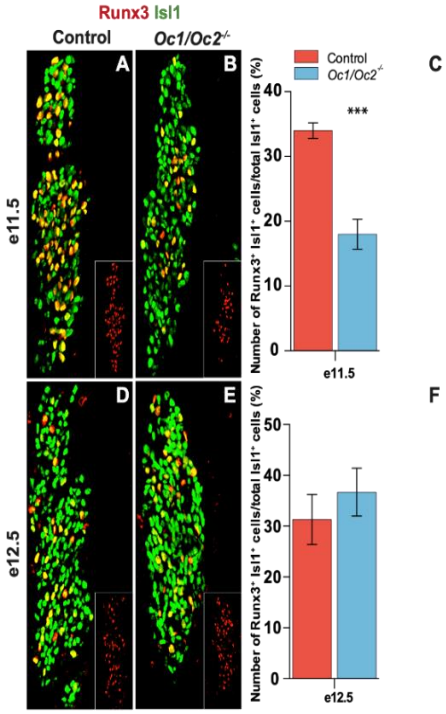

Figure 4. Loss of *OC* expression in DRG affects Runx3 early production. (A-C) Immunodetection of Runx3$^+$ (red) in Isl1$^+$ (green) sensory neurons on transverse sections of brachial DRG at a11.5 in control (A) or *Oc1/Oc2*$^{-/-}$ (B) embryos. (C) The percentage of Runx3$^+$/Isl1$^+$ sensory neurons per section was quantified accordingly. Immunodetection and quantification of Runx3$^+$ Isl1$^+$ sensory neurons reveals a decrease in mutants, indicating that Runx3 production is affected in the absence of OC factors. (D-F) Immunodetection of Runx3$^+$ (red) in Isl1$^+$ (green) sensory neurons on transverse sections of brachial DRG at e12.5 in control (D) or *Oc1/Oc2*$^{-/-}$ (E) embryos. (F) The percentage of Runx3$^+$/Isl1$^+$ sensory neurons per section was quantified accordingly. Mean values ±SEM, $n \geq 3$.

proportion of Runx3^{+} cells in the DRG was normal at e12.5 (Figure 4D-F), consistent with the progressive normalization of the TrkB/TrkC segregation observed from this developmental stage (Fig.3G-L). Thus, OC factors are transiently required for early production of Runx3 in prospective proprioceptors.

OC control the positioning of the DRG

To assess if the early differentiation defects observed in the absence of OC factors resulted in later alterations in the organization of the sensory circuits, whole-mount immunolabeling for TrkA was performed and analyzed using light-sheet microscopy. In *Oc1/Oc2*$^{-/-}$ mutants at e14.5, the overall organization of DRG and sensory projections seemed abnormal. In particular, peripheral projections appeared disorganized, central projections between the DRG and the spinal cord were thinner and the DRG seemed located farther from the spinal cord than in control littermates (Figure 5A-B). To evaluate the positioning of the sensory neuron cell bodies, we measured the length of the proximal afferent bundles between the DRG and the DREZ. This measurement demonstrated that the DRG were more distant from the spinal cord in the *Oc1/Oc2*$^{-/-}$ mutants than in control littermates (Figure 5C), suggesting that OC factors regulate the positioning of the neural crest cells when they aggregate to form the DRG.

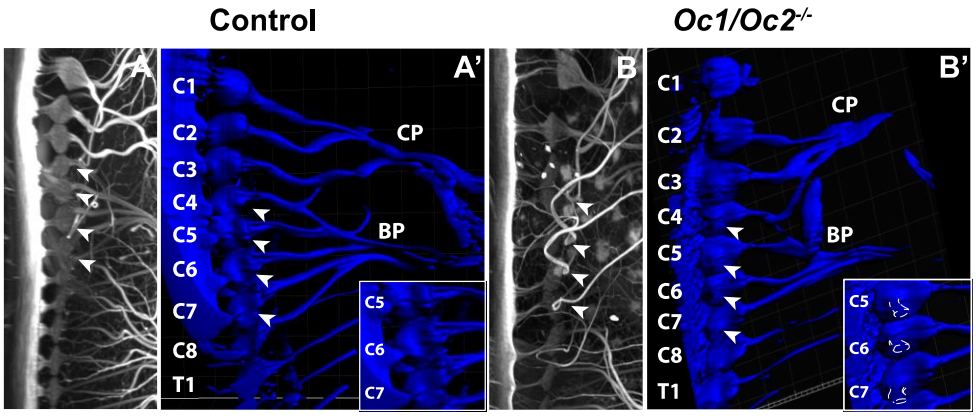

OC regulate central projections of nociceptive and proprioceptive sensory neurons

Previous studies evidenced that several genetic programs that direct sensory subtype specification also regulate the connectivity of sensory neurons to their central and peripheral targets (Chen et al., 2006a, 2006b; Kramer et al., 2006; Dykes et al., 2011). As an example, Runx3 regulates both central projections and peripheral axonal extension of proprioceptors (Inoue et al., 2002; Chen et al., 2006a; Kramer et al., 2006; Lallemend and Ernfors, 2012). From e10.0, DRG neurons are known to send afferences both centrally towards the spinal cord and peripherally towards somatic or visceral targets (Wentworth, 1984). To determine if the OC factors contribute to sensory axon pathfinding and establishment of central projections, we compared the afferences of $TrkA^+$, $TrkB^+$ and $TrkC^+$ neurons towards the dorsal horn of the spinal cord in control or *Oc1/Oc2*$^{-/-}$ embryos during early embryonic stages (e11.5-14.5). At e11.5, numerous control DRG sensory axons reached the DREZ, a compact oval-shaped structure corresponding to the location where axons penetrate the spinal cord (Figure 6A). In *Oc1/Oc2* mutants, $TrkB^+$ and $TrkC^+$ fascicles seemed less compactly organized. $TrkA^+$ axons were absent from the DREZ (Figure 6B) due to the delayed production

Figure 5. OC factors control the positioning of the DRG. (A-B) Whole-mount immunolabeling of e14.5 control (A-A') or *Oc1/Oc2-/-* (B-B') embryos for TrkA visualized using light-sheet microscopy (dorsal view). The overall organization of DRG and sensory projections seemed abnormal in the absence of OC factors, with disorganized peripheral projections, thinner central projections between the DRG and the spinal cord and DRG located farther from the spinal cord than in control littermates. (C) Quantification of the distance between the DRG and the DREZ in control or *Oc1/Oc2-/-* embryos measured using the "Filament tracer" tool of the Imaris software. DREZ-DRG distance tended to increase at all levels and was significantly different at C5 and C6. C1 to T1: anteroposterior position of the DRG. Mean values, n = 3. Significance levels *p<0.05, ***p<0.001. Scale bar = 300µm

of TrkA in sensory neurons. At e12.5, sensory axons entered the spinal cord and progress along the dorsolateral margin. In wild-type embryos, sensory projections formed a crescent-shaped DF with a sharp inner border facing the dorsal mantle layer, and $TrkB^+$, $TrkC^+$ and $TrkA^+$ axons trended to segregate in a medial to a lateral organization, respectively (Figure 6C). By contrast, *Oc1/Oc2*$^{-/-}$ embryos had a thinner and disorganized DF (Figure 6D), and mutant $TrkA^+$, $TrkB^+$ and $TrkC^+$ fibers remained partly intermingled along the mediolateral axis (arrows in Figure 6D). At e13.5 in control embryos, $TrkA^+$ axons formed a thick DF, whereas *Oc1/Oc2* mutant DF appeared thinner and less organized (Figure 5E-F). In controls, proprioceptive $TrkC^+$ axons extended their collaterals ventrally toward the intermediate and ventral regions of the spinal cord (Figure 6E). Oppositely, part of the *Oc1/Oc2* mutant $TrkC^+$ collaterals seemed to enter laterally into the spinal cord and $TrkC^+$ DF appeared thinner (arrowheads in Figure 6F). In control embryos at e14.5, $TrkA^+$ nociceptive collaterals entered the dorsolateral region of the spinal cord and invaded the superficial dorsal layers (Figure 6G). $TrkC^+$ axons located to the most dorsomedial region of the spinal cord wherefrom invading collaterals formed axon bundles growing towards the ventral horn (arrowheads in Figure 6G), whereas TrkB was not detectable. In *Oc1/Oc2* mutant embryos, the DF remained thinner than in controls and fewer $TrkA^+$ axon fascicles entered the dorsal horn (Figure 6H). Surprisingly, the $TrkC^+$ lateral axon bundles observed at e13.5 were not observed anymore, and no $TrkC^+$ collaterals were found to project towards the ventral layers (Figure 6H). Thus, in the absence of OC factors, the DF was disorganized from e11.5 onwards and the sensory projections into the grey matter were strongly altered, suggesting that OC factors are required for the correct pathfinding of $TrkA^+$ and $TrkC^+$ central afferents.

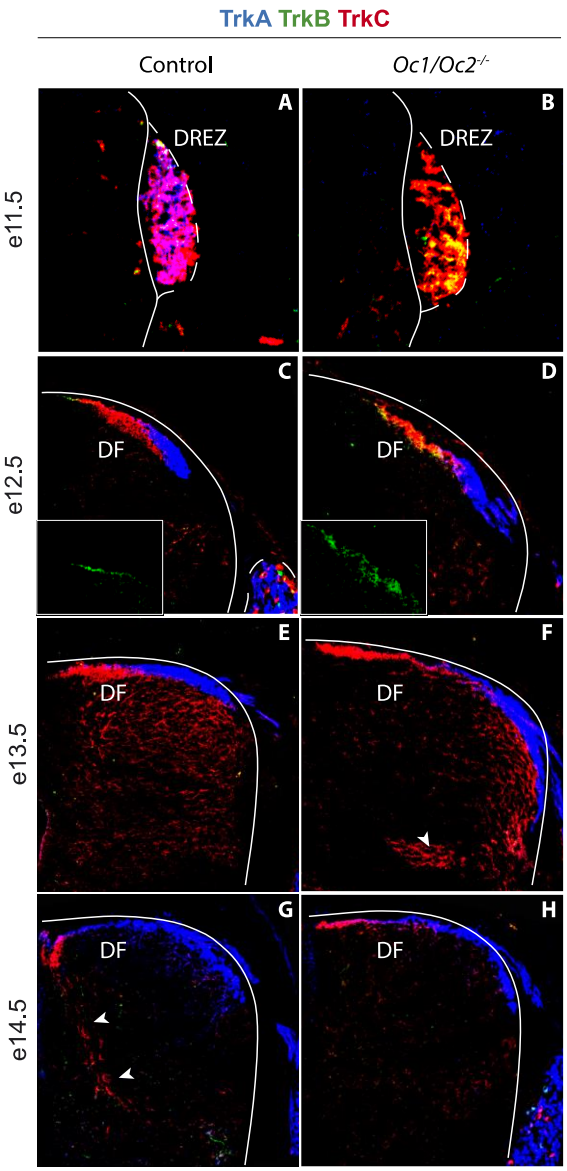

Figure 6. OC regulate central projections of nociceptive and proprioceptive sensory neurons. (A-B) Immunodetection of TrkA (blue), TrkB (green) and TrkC (red) at the DREZ on transverse sections of brachial spinal cord at e11.5 in control (A) or *Oc1/Oc2*$^{-/-}$ (B) embryos. The DREZ of *Oc1/Oc2*$^{-/-}$ embryos is disorganized, with a majority of axons colocalizing TrkB and TrkC, whereas TrkA is absent. (C-D) Immunodetection of TrkA (blue), TrkB (green) and TrkC (red) on transverse sections of brachial spinal cord at e12.5 in control (A) or *Oc1/Oc2*$^{-/-}$ (B) embryos. The DF of *Oc1/Oc2*$^{-/-}$ embryos is disorganized with a majority of axons colocalizing TrkB and TrkC, whereas the boundary between TrkA^{+} and TrkC^{+} axons is fuzzy. (E-F) Immunodetection of TrkA (blue), TrkB (green) and TrkC (red) on transverse sections of brachial spinal cord at e13.5 in control (A) or *Oc1/Oc2*$^{-/-}$ (B) embryos. Arrowhead points to central TrkC^{+} afferences laterally invading the developing dorsal horn in *Oc1/Oc2*$^{-/-}$ embryos, whereas control axons enter the dorsal horn dorsally. (G-H) Immunodetection of TrkA (blue), TrkB (green) and TrkC (red) on transverse sections of brachial spinal cord at a14.5 in control (A) or *Oc1/Oc2*$^{-/-}$ (B) embryos. Arrowheads point to central TrkC^{+} afferences normally invading the developing dorsal horn in control embryos, while TrkC^{+} axon collaterals are absent in *Oc1/Oc2*$^{-/-}$ embryos.

OC regulate peripheral axonal outgrowth of nociceptive sensory axons

As central projections of sensory neurons were altered in *Oc1/Oc2*$^{-/-}$ mutant embryos, we also addressed the organization of peripheral axonal outgrowth in these mice. As at e14.5, TrkA^{+} cells constitute the major population of DRG (Molliver and Snider, 1997), we used TrkA whole-mount immunolabeling and volume imaging of control or *Oc1/Oc2*$^{-/-}$ embryos to assess whether the peripheral sensory processes developed adequately. In the mouse, the first four C1-C4 DRGs send their nerves towards the cervical plexus while the brachial plexus is a network of convergent nerves from C4-T1 DRGs that innervate the upper forelimb region (Hirasawa et al., 2016). By e14.5, control TrkA^{+} axons from C1 to C3 projected ventrally and fasciculated to form the cranial plexus whereas the single projections of C4-T1 DRG reached the brachial plexus region and grew towards the forelimb (Figure 6A). The absence of OC proteins resulted in marked disorganization of peripheral nerves from C1-T1 DRG regions (Figure 6A-D). In *Oc1/Oc2*$^{-/-}$ embryos, the cranial plexus was formed by the abnormal convergence of C2 to C4 projections, whereas the main C4 branch normally projecting to the brachial plexus was missing (Figure 6C). Strikingly, in *Oc1/Oc2* mutant embryos, C5-C7 DRG originated two axon bundles, one directed ventrally while another protruded laterally towards the lateral sides of the embryo (arrowheads in Figure C-D), instead of a single thick nerve projecting ventrally in control littermates (Figure 6A-B, arrows). Thus, the absence of OC is associated with altered peripheral nerve outgrowth and disorganized brachial plexus formation. Taken together, these observations demonstrate that OC factors regulate central and peripheral projections of sensory neurons.

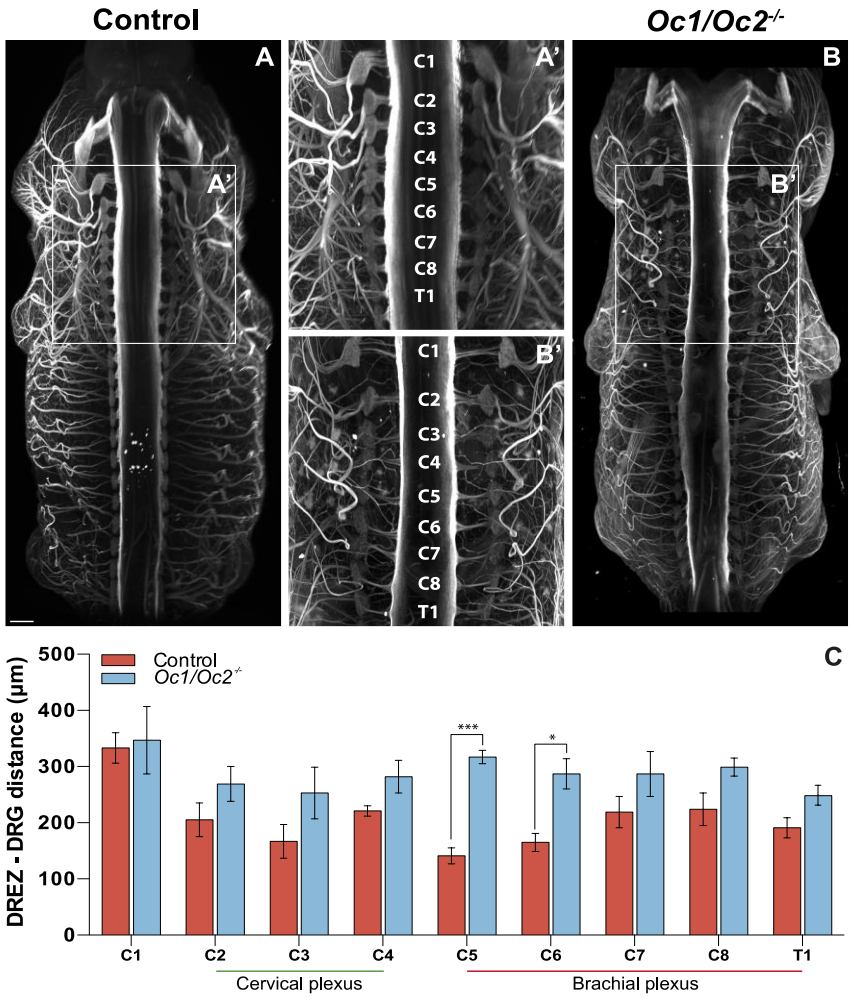

Figure 7. OC regulate peripheral axonal outgrowth of nociceptive sensory axons. (A-B') Whole-mount immunolabeling for TrkA visualized using light-sheet microscopy (lateral view) (A, B) or 3D-reconstructions (A', B') of e14.5 control (A-A') or *Oc1/Oc2*$^{-/-}$ (B-B') embryos in the region of the cervical and brachial plexuses. In *Oc1/Oc2*$^{-/-}$ embryos, the cranial plexus (CP) was formed by the abnormal convergence of C2 to C4 projections, whereas the main C4 branch normally projecting to the brachial plexus (BP) was missing. In addition, C4-C7 DRG originated two axon bundles, one directed ventrally while another protruded laterally towards the lateral sides of the embryo (arrowheads in Figure B, B'; delineated in the inset), instead of a single thick nerve projecting ventrally in control littermates (arrowheads in Figure A, A'). C1 to T1: anteroposterior position of the DRG. n=3. Scale bar = 300µm

3.3.4 Discussion

During neurogenesis, several classes of transcription factors have been identified as regulators of sensory neuron development (Marmigère and Ernfors, 2007). We found that the OC factors are detected in sensory progenitors and in early post-mitotic neurons of the embryonic DRG. We observed that OC proteins transiently regulate timely production of TrkA and extinction of TrkB in differentiating sensory nociceptors or proprioceptors, respectively. In addition, we showed that OC control DRG positioning and central or peripheral projections of sensory neuron subsets. Thus, we identified transcriptional regulators of early differentiation, of positioning and of axonal projections of developing sensory neurons.

The expression of *TrkA* was delayed in the absence of OC factors. It was almost absent at e10.5 but was detected in a normal number of cells from e11.5 onward. OC proteins could be necessary for the production of early nociceptors that would be missing in the *Oc* double-mutant DRG. However, the number of sensory neurons was not altered in these mutants. Alternatively, OC may directly or indirectly regulate the early *TrkA* expression in this population that later develops into thinly myelinated $TrkA^+/NF200^+$ neurons (Bachy et al., 2011). Several transcription factors contribute to the regulation of *TrkA* expression in the nociceptive lineage, including Brn3a, Klf7, and Runx1 (Huang et al., 1999; Lei et al., 2005, 2006; Marmigère et al., 2006). In addition, Prdm12 is necessary for the induction and for the maintenance of *TrkA* expression, and therefore for the production and the function of the nociceptors in embryos or adults, respectively (Bartesaghi et al., 2019; Desiderio et al., 2019). As the percentage of $TrkA^+$ neurons returned to normal at e11.5 in *Oc* mutant embryos, this suggests that OC are transiently required for the initiation of *TrkA* expression at e10.5 but are

dispensary from e11.5. This is reminiscent of the requirement in OC factors for timely initiation of *Pdx1* expression in the developing pancreas wherein OC-1 depletion resulted in delayed *Pdx1* expression (Jacquemin et al., 2003a). How OC factors may integrate or interact with the known regulators of *TrkA* expression remains to be investigated.

In addition, OC-1 and OC-2 contribute to the repression of *TrkB* expression in presumptive TrkC$^+$ proprioceptors, as hybrid TrkB$^+$/TrkC$^+$ cells were present in excess in *Oc* mutant embryos at e11.5. Although known as transcriptional activators (Lemaigre et al., 1996; Jacquemin et al., 1999; Vanhorenbeeck et al., 2002), OC proteins are able to act as indirect transcriptional repressors as previously reported in hepatic cells (Plumb-Rudewiez et al., 2004; Clotman et al., 2005) and recently demonstrated for the regulation of *Pou2f2* expression in the developing spinal cord (Harris et al., 2019; Masgutova et al., 2019). Thus, OC factors may repress *TrkB* expression in prospective proprioceptors, contrary to the positive regulation of *TrkA* proposed above. However, the phenotype described here is reminiscent of that observed in the absence of Runx3. In *Runx3*$^{-/-}$ embryos, the acquisition of solitary TrkC$^+$ cells is altered, as the number of TrkB$^+$/TrkC$^+$ neurons increases, whereas subsequent TrkC$^+$ cell development is impaired (Levanon et al., 2002; Kramer et al., 2006). Runx3 promotes the segregation between TrkB$^+$ and TrkC$^+$ lineages through direct binding to, and repression of the *TrkB* locus in presumptive proprioceptors (Levanon et al., 2002; Kramer et al., 2006; Inoue et al., 2007). The strict specificity of Runx3 for TrkC$^+$ neurons results from a tight spatiotemporal regulation of *Runx3* expression by three regulatory elements (R1-R3) (Appel et al., 2016). Reduction in the number of Runx3$^+$ cells in *Oc1/Oc2*$^{-/-}$ mutant DRG suggests that OC factors act upstream of Runx3 in sensory neurons. Whether OC directly or indirectly regulate *Runx3* expression remains to be investigated. More generally, the identification of genes

bound and regulated by OC factors and of the molecular partners of OC proteins in developing sensory neurons would be a prerequisite to understand the mechanisms and molecular pathways whereby these factors regulate sensory differentiation. As the sensory lineage populations eventually normalizes in the *Oc* mutant embryos at e14.5, other factors and mechanisms must be at play and may compensate for the absence of OC proteins in the mutant embryos.

Beyond early sensory differentiation, our observations indicate that OC regulate the positioning of the DRG, suggesting that the migration of the neural crest cells that will differentiate into sensory neurons is altered in the absence of OC proteins. The migration of neural crest cells that will differentiate into sensory neurons and aggregate to form the DRG is highly dependent on tightly regulated interactions with the extracellular matrix (Delloye-Bourgeois and Castellani, 2019). However, the transcriptional program that determines the response of neural crest cells to these migration cues remains less investigated. OC factors control neuron positioning in different regions of the CNS (Espana and Clotman, 2012b, 2012a; Audouard et al., 2013) and have recently been shown to regulate interneuron migration in the developing spinal cord (Harris et al., 2019; Masgutova et al., 2019). Whether identical mechanisms are controlled by OC for neuronal migration in the CNS and in the PNS remains to be investigated.

Furthermore, central projections of sensory fibers are markedly altered in *Oc* mutant embryos. $TrkA^+$ afferent fibers fail to invade the superficial layers of the spinal cord, whereas $TrkC^+$ collaterals are misrouted and eventually lost by e14.5. Neurotrophin receptors have long been thought to regulate axonal guidance (Patel et al., 2000, 2003b; Tucker et al., 2001). Expression of a rat *TrkC* from the *TrkA* locus in mice resulted in surviving $TrkA^+$ neurons adopting a proprioceptive phenotype with corresponding proprioceptive central projections (Moqrich et al., 2004), suggesting that specific TrkC signaling is sufficient to coherently define

sensory neuron identity and projection pattern. Similarly, NT-3/TrkC signaling is necessary and sufficient to drive expression of the Ets family transcription factors *Er81* in proprioceptors (Arber et al., 2000; Patel et al., 2003b), and ventral projections of proprioceptive axons are mostly absent in *Er81*$^{-/-}$ mice (Arber et al., 2000; de Nooij et al., 2013). However, *Er81*$^{-/-}$ mice exhibit a less severe proprioceptive phenotype than the *NT3*$^{-/-}$ line, suggesting that additional targets of NT-3/TrkC signaling contribute to proprioceptor development (Patel et al., 2003b). Our observations suggest that OC factors contribute to proprioceptive axon pathfinding within the spinal cord. In *Oc1/Oc2*$^{-/-}$ embryos, the central TrkC^{+} axonal projection defects may partly result from the transient aberrant coexpression of *TrkB* and *TrkC* genes in prospective proprioceptors (Inoue et al., 2002; Chen et al., 2006a; Kramer et al., 2006; Lallemend and Ernfors, 2012). Similarly, in addition to early regulation of *TrkA* expression, OC proteins are involved in proper TrkA^{+} axonal projections to the superficial layers of the spinal cord. However, in opposition to NT-3/TrkC signaling, the cognate ligand of TrkA, NGF, is not involved in collateral branching formation (Patel et al., 2000). Interestingly, embryos mutant for Sema3a or for its receptor Nrp1 display abnormal TrkA^{+} axon penetration into the dorsal regions of the spinal cord (Behar et al., 1996; Gu et al., 2003). In the spinal cord, expression of different guidance molecules including ephrin receptors and semaphorins is perturbed in the absence of OC factors (Roy et al., 2012 and unpublished data). Thus, OC factors might regulate the expression of *Nrp1* or other guidance cues in TrkA^{+} neurons to promote adequate central pathfinding. Whatever the nature of the guidance cues that route collateral branching, our results demonstrate that the capacity of the central process of DRG neurons to invade the spinal cord is regulated by OC proteins. OC-1 and OC-2 are present in both peripheral sensory neurons and their central targets (Francius and Clotman, 2010; Kabayiza et al., 2017; Harris et al.,

2019). Therefore, conditional *Oc1/Oc2* mutants would be necessary to clarify the important issue of whether their role in proper sensory connectivity is intrinsic to DRG or may depend on extrinsic interactions with spinal targets.

Interestingly, we also demonstrate a profound defect in peripheral $TrkA^{+}$ nerve outgrowths in *Oc* mutant embryos at e14.5. Briefly, excessive branches sprouted laterally from rostral DRG and the cervical and brachial plexuses were disorganized with converging branches arising from unrelated ganglia. Similar or more severe defects in plexus formation have been described in conditional *Isl1*$^{-/-}$ and *Brn3a/Isl1*$^{-/-}$ embryos (Sun et al., 2008; Dykes et al., 2011). However, Isl1 is normally produced in the DRG of *Oc* mutant embryos. In contrast, additional outgrowth of sensory axons from the DRG has not been reported yet. Thus, our data suggest that, in addition to early sensory differentiation, OC regulate both central and peripheral projections of sensory neurons through mechanisms that remain to be identified.

3.3.5 Material and Methods

Ethics statement and mouse lines

All experiments were strictly performed in accordance with the European Community Council directive of November 24, 1986 (86-609/ECC) and the decree of October 20, 1987 (87-848/EEC). Mice were raised in our animal facilities and treated according to the principles of laboratory animal care. Experimental procedures and mouse housing were both approved by the Animal Welfare Committee of Université Catholique de Louvain (Permit Number: 2017/UCL/MD/008). Mutant strain mice were crossed, and the day of the vaginal plug was the embryonic day (e) 0.5. The embryos were collected at e10.5, e11.5, e12.5 and e14.5. A minimum of three embryos of the same genotype was analysed in each experiment. The *Oc1;Oc2* mutant mice have been described previously (Jacquemin et al., 2000; Clotman et al., 2005). The mice and the embryos were genotyped by PCR (primer information available on request).

Immunofluorescence labelings

For immunofluorescence labelings, embryos were fixed in ice-cold 4% paraformaldehyde (PFA) in phosphate buffered-saline (PBS) for 10 to 35 min according to their embryonic stage, incubated in PBS/30% sucrose solution overnight at 4°C, embedded and frozen in PBS/15% sucrose/7.5% gelatin. Immunostaining was performed on 12 or 14 µm serial cryosections as previously described (Francius and Clotman, 2010). Primary antibodies against the following proteins were used: cleaved Caspase-3 (rabbit; 1/100; Cell Signaling #ASP175), Isl1/2 (goat; 1:3000; Neuromics #GT15051), OC-1 (guinea pig; 1:2000; (Espana and Clotman, 2012a)), OC-2 (rat; 1:400; (Clotman et al., 2005) or sheep; 1:500; R&D Systems #AF6294), OC-3 (guinea pig; 1:6000; (Pierreux et al., 2004)), Runx3

(mouse; 1/500; Abcam #ab135248), TrkA (goat; 1/500; R&D Systems #AF1056 or rabbit; 1/1000; (Clary et al., 1994)), TrkB (chicken; 1/1000; (Von Bartheld et al., 1996)) and TrkC (goat; 1/500; R&D Systems #AF1404). Secondary antibodies used were the donkey anti-chicken/DyLight 488, anti-goat/AlexaFluor 488, 594 or 647, anti-guinea pig/AlexaFluor 647, anti-rabbit/AlexaFluore 488 and anti-rat/AlexaFluor 488 or 594 purchased from ThermoFisher Scientific or Jackson Laboratories, and were used at dilution 1:1000.

In toto immunostainings were performed as described previously (Belle et al., 2017). Briefly, all embryos were dehydrated in methanol, treated overnight at 4°C with a 30% hydrogen peroxide solution in 100% methanol, and rehydrated in methanol to suppress blood autofluorescence and hematomas. Embryos were conditioned and blocked for 3h or 24 h according to their embryonic stage in PBS containing 0.2% gelatin (VWR-2460.233), and 0.5% Triton X-100 (Sigma-Aldrich) (PBSGT) under agitation at room temperature. They were then transferred in PBSGT solution containing 0.1% saponin (Sigma-Aldrich S-7900; 10 mg/mL) and primary antibodies and incubated at 37°C with rotation at 70 rpm, for 3 to 7 days depending on tissue size. Primary antibodies used were Isl1/2 (goat; 1:1000; Neuromics #GT1505) and TrkA (goat; 1/400; R&D Systems #AF1056). Samples were washed over one day at room temperature under agitation in multiple PBSGT baths. Then, tissues were incubated in PBSGT solution containing 0.1% saponin and secondary antibodies and incubated at 37°C with rotation at 70 rpm for 3 days. The secondary antibody used was the donkey anti-sheep AlexaFluor 647 purchased from Jackson Laboratories and was used at 1: 1000 dilution. Samples were finally washed over one day at room temperature with agitation with multiple PBSGT baths. Samples were then cleared using the protocol detailed below.

Tissue clearing

All tissue was cleared using adapted iDISCO clearing protocol as previously described (Renier et al., 2016; Belle et al., 2017). Briefly, all incubation steps were performed in dark conditions at RT in a fume hood, on a tube rotator (SB3, Stuart) at 14 rpm, using a 5 mL amber TPP Eppendorf tube (Eppendorf, VWR # 75874-634). Samples were first dehydrated in ascending concentrations (50%, 80%, 100% and 100%) of tetrahydrofuran (THF; anhydrous, containing 250 ppm butylated hydroxytoluene inhibitor, Sigma-Aldrich #186562) diluted in H_2O. The initial 50% THF bath was done overnight while the 80% and 100% THF incubations were left for 30 min or 1hr each for e11.5 and e14.5 embryos, respectively. Samples next underwent a delipidation step of either 10 (e11.5) or 20 min (e14.5) in dichloromethane (DCM; Sigma-Aldrich #270997) followed by a 20 min (e11.5) or an overnight (e14.5) clearing step in dibenzyl ether (DBE; Sigma-Aldrich #108014). The next day, samples were stored in individual light-protected glass vials (Rotilabo, Roth #XC40.1 and #XC44.1) at RT. In these conditions, samples could be stored and imaged for up to 9 months without any significant fluorescence loss.

Imaging and quantitative analyses

Immunofluorescence images of cryosections were acquired on a Confocal Laser Scanning microscope FV1000 Fluoview with the FV10-ASW 01.02 software (Olympus). Brightness and contrast were adjusted uniformly in all replicate panels within an experiment with Adobe Photoshop CS6 software. Quantifications were performed on red or green or blue layer of acquired confocal images and double or triple labeled cells were processed by the subtractive method (Francius and Clotman, 2010).

For each embryo (n≥3), five serial sections from brachial DRG were quantified using the count analysis tool of Adobe Photoshop CS6 software. To compare the number of neurons labeled with each marker, Isl1 or pan-Trk staining was used to determine the total number of DRG neurons. Raw data were exported from Adobe Photoshop CS6 software to Sigma Plotv12.3 software to perform statistical analyses. The histograms were drawn with GraphPad Prism v6.0. Adequate statistical tests were applied based on the number of comparisons and on the variance in each group. For analysis of cell quantifications based on comparison of two groups (control or mutant), standard Student's *t*-tests or Mann-Whitney U tests were performed. Differences were considered significant at $p \leq 0.05$.

Three-dimension (3D) imaging was performed with an ultramicroscope I (LaVision BioTec) using ImspectorPro software (LaVision BioTec). The light sheet was generated by a laser (wavelength 640 nm, Coherent OBIS 640-100LX laser, LaVision BioTec). A binocular stereomicroscope (MXV10, Olympus) with a 2X objective (MVPLAPO, Olympus) was used at different magnifications (0.8x, 1x, 1.25x, 1.6x, 2x, 2.5x, 3.2x, 4x, 5x and 6.3x). Samples were placed in an imaging reservoir made of 100% quartz (LaVision BioTec) filled with DBE and illuminated from the side by the laser light. Images were acquired with a PCO Edge SCMOS CCD camera (LaVision BioTec). The stepsize between each image was fixed to 3 µm. Image processing was performed as previously described (Belle et al., 2017) using Imaris x64 software version 9.2.1, Bitplane. The distance between the DRG and the DREZ was measured using the "Filament tracer" tool of the Imaris software, following the central projection from the exit of the DRG to the contact with the DREZ.

3.3.6 Supplementary figures

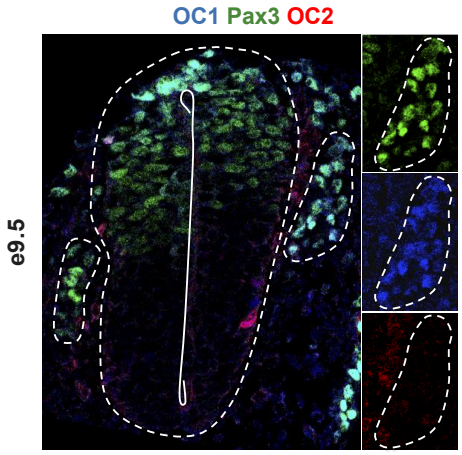

Figure S1. OC-1 and OC-2 detection in sensory neuron progenitors. (A-C) Immunodetection of OC-1 (blue) and OC-2 (red) in Pax3^{+} (green) sensory neuron progenitors on transverse sections of brachial DRG at e9.5 in wild-type embryos. OC-1, but not OC-2, is detected in sensory progenitors

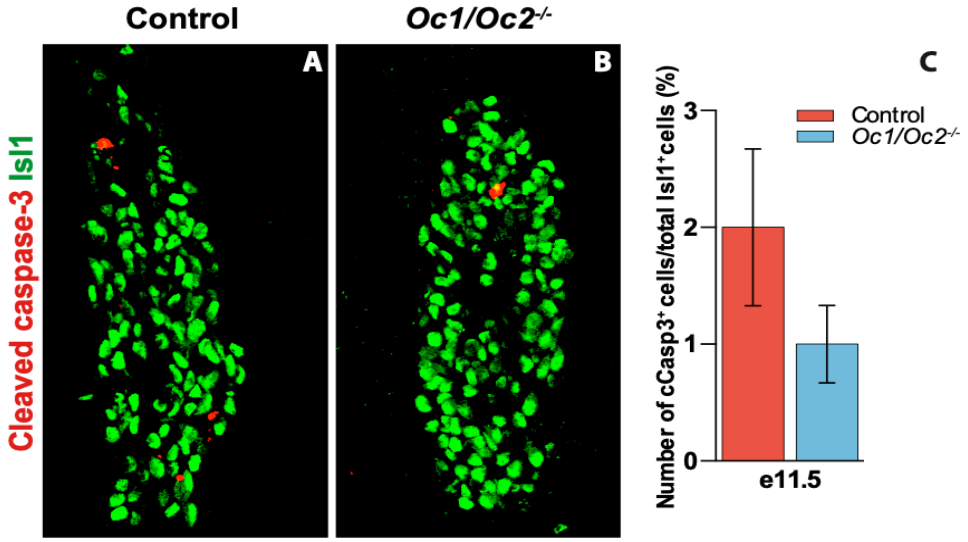

Figure S2. Loss of *OC* expression in DRG does not affect sensory neuron survival. (A-B) Immunodetection of cleaved caspase-3 (red) in Isl1^{+} (green) sensory neurons on transverse sections of brachial DRG at e11.5 in control (A) or *Oc1/Oc2*$^{-/-}$ (B) embryos. **(C)** The percentage of cCasp3^{+}/Isl1^{+} sensory neurons per section was quantified accordingly. Immunodetection and quantification of apoptotic Isl1^{+} sensory neurons did not reveal any change between control and mutant embryos, indicating that the survival of sensory neurons is unaffected in the absence of Onecut factors. Mean values ±SEM, $n \geq 3$.

3.3.7 Acknowledgments

We thank members of the NEDI lab for material, technical support and discussions. We are grateful to Dr. L. Reichardtfor his generous gift of the rabbit anti TrkA, the chicken anti TrkB and the goat anti TrkC antibodies. We would like to acknowledge Pr. Dr. J-M. Vanderwinden and M. A. Martens of the Light Microscopy Facility (LiMiF), Université Libre de Bruxelles, Brussels, Belgium, for their support with the lightsheet imaging presented herein, and to M. S. Henrotte for help with figure design.

4 General discussion

Peripheral sensory inputs are relayed by primary sensory neuron axons synapsing mainly in the dorsal spinal cord on projection neurons, local circuit interneurons, or even directly onto MN in the ventral spinal cord. A variety of specialized neurons are produced during the development of the dorsal spinal cord and the DRG. Each neuron types have been extensively characterized and differ from each other in their molecular identity, migration, function, or connectivity (Lai et al., 2016).

In this work, we demonstrated that OC factors regulate the diversification of dI5 and the distribution of dI3, dI5 and dI6 populations. Then, we discovered a genetic cascade involving OC factors and their downstream target Pou2f2, which control dIN distribution during development. In addition, we provided evidence that OC factors regulate the expression of *TrkA* and *TrkB* in early sensory neuron development. Also, we identified a novel role for OC factors as intrinsic regulators of sensory neuron positioning and central or peripheral axonal projections.

4.1 OC factors control dI5 diversification

The mature nervous system is characterized by the astonishing diversity of neurons critical for the elaboration of functional circuits. In the spinal cord, diverse networks of interneurons and MN organize into circuits to ensure somatosensory relay and complex locomotor schemes (Goulding, 2009; Kiehn, 2016). Importantly, mature and functional neurons are characterized by proper cell body position, the expression of specific ion channels and neurotransmitter receptors, the production of adequate neurotransmitter, and the elaboration of

dendritic and axonal connectivity. Combinatorial TF programs often drive the acquisition of functional properties. Many of these transcriptional networks are active transiently at specific time point during mammalian nervous system development (Lu et al., 2015). Although the specification of cardinal neuronal populations has been extensively deciphered within the spinal cord, the genetic networks that contribute to subset diversification remain elusive (Briscoe and Small, 2015; Lu et al., 2015). Incomplete characterization of molecular or genetic markers that define neuron subsets is a major barrier to progress in the field. It is now well established that just as the hundreds of distinct motor pools generated from the single pMN, a similar principle applies for interneurons (Bikoff, 2019). Recent studies have applied transcriptional profiling to examine the heterogeneity among ventral spinal interneuron populations (Bikoff et al., 2016; Hayashi et al., 2018; Sweeney et al., 2018; Delile et al., 2019). Based on 19 TF combinatorial expression in V1 and their electrophysiological properties, this cardinal population can be divided into about 50 distinct subsets (Bikoff et al., 2016). Among V2 interneurons, V2a subpopulations are further divided into type I and type II populations with functional divergence, as the type I is involved in left-right alternation control, while the type II regulates target reaching phase of forelimbs. At birth, the diversification goes further with fractioning of these two groups into 11 subsets (Hayashi et al., 2018). Interestingly, OC factors have been demonstrated to promote the LMCm and the somatic MN identities by controlling *Isl1* expression (Roy et al., 2012; Francius and Clotman, 2014). In addition to MN diversification, OC factors contribute to the diversification of V2a $MafA^{+}$ and $cMaf^{+}$ subpopulations (Harris et al., 2019). Furthermore, emerging studies have uncovered dIN subpopulations that integrate and mediate specific sensory afferents or coordinate locomotion pattern formation to shape motor output (Andersson et al., 2012; Bui et al., 2013, 2016; Bourane et al., 2015c; Hilde et al.,

2016; Griener et al., 2017; Koch et al., 2017). However, the subdivision of cardinal dIN into more discrete subsets and genetic mechanisms behind are only sparsely elucidated (Ding et al., 2004; Andersson et al., 2012; Schnerwitzki et al., 2018; Perry et al., 2019). Within the dIN populations, dI5 Lmx1b^{+} interneurons were normally produced in *Oc1/Oc2*$^{-/-}$ mutant embryos (Qian et al., 2002; Ding et al., 2004). It suggests that OC factors do not contribute to the production of dI5 cells. Nevertheless, our observations demonstrate that OC proteins control the diversification of the dI5 Phox2a^{+} subset, as evidenced by the subset decrease. Incomplete knowledge of the whole collection of dI5 subpopulations prevented to assess whether this reduction was compensated by the expansion of neighbouring subsets. Interestingly, these observations exhibit some traits reminiscent of *Lmx1b*$^{-/-}$ dI5 interneuron phenotype. Indeed, the number of dI5 Phox2a^{+} neurons was reduced in those mutants. Also, similar to *Oc1/Oc2*$^{-/-}$ embryos, dI5 Phox2a^{+} subset distributed abnormally in *Lmx1b* mutants (Ding et al., 2004). These observations combined to the apparent normal *Lmx1b* expression in dI5 neurons of *Oc1/Oc2*$^{-/-}$ mutants raises several possibilities. OC factors may act downstream of *Lmx1b* to specify the fate of dI5 Phox2a^{+} neurons, even if we do not know whether the OC factors directly control the expression of *Phox2a*. Alternatively, OC proteins might act synergistically with Lmx1b to determine the dI5 Phox2a^{+} identity. Previous studies using chromatin immunoprecipitation/sequencing (ChIP-seq) analysis brought some insights into synergistic interactions between transcription factors that contribute to MN diversification (Mazzoni et al., 2013; Rhee et al., 2016). Depending on the developmental stage, Isl1 is known to bind with Lhx3 to nascent MN specific enhancers. Then, Isl1 is recruited to maturing MN enhancers already bound by OC-1 from nascent MN-stage (Rhee et al., 2016). We cannot rule out the possibility of a similar mechanism in dI5 nascent neurons, with OC factors acting as Lmx1b recruiters on maturing dI5 enhancers. Taken

together, these observations suggest that cardinal IN populations only constitute the first organization level of functionally distinct neuronal subsets. The latter contribute to the diversity and flexibility within spinal sensorimotor circuits. Identification of genetic programs involved in spinal interneuron diversification combined to the dissection of circuit connectivity will continue to play an important role in understanding neuronal diversity at higher resolution.

4.2 OC factors control dIN distribution

The great variety of neuronal populations produced during spinal cord development has to undergo neuronal migration and axonal pathfinding to integrate appropriately into neuronal circuits. In the spinal cord, progenitors undergo radial migration within the ventricular zone before cell cycle exit. Then, differentiated neurons continue to migrate either radially along the ML axis or tangentially along the DV axis (Caspary and Anderson, 2003; Helms and Johnson, 2003; Lu et al., 2015). In addition, neuronal populations migrate along the antero-posterior axis to form proper local CPG and MN connections with target muscles (Chen, 2019). Although several elegant studies demonstrated the involvement of reelin signaling in MN radial migration and cadherins in proper organization of motor pools (Yip et al., 2000; Phelps et al., 2002; Palmesino et al., 2010; Chen, 2019), regulators of dIN migration are still unknown.

We uncovered that OC factors regulate proper settling position of dI3, dI5 populations and dI6 Dmrt3^{+} and Wt1^{+} subsets while their population size remains stable in *Oc1/Oc2*$^{-/-}$ embryos, with exception for dI5 Phox2a^{+} cells. We hypothesize that even slight alterations of neuronal distribution might have an impact on microcircuit organization. Indeed, Satb2^{+} inhibitory dIN population that relay sensory information to ventral IN and MN diversify into two subpopulations,

wherein Satb2 regulates their proper localization on the ML axis of the spinal cord. Mislocated Satb2^{+} neurons lead to input and output connectivity impairments, showing that a specific localization is critical for proper integration of Satb2^{+} neurons in motor circuitry (Hilde et al., 2016). In addition, a ML segregation of Lbx1-derived dIN biases their premotor functions. Indeed, cell bodies located laterally in lamina VI are flexor premotor IN, whereas extensor premotor IN are positioned closer to the central canal (Tripodi et al., 2011). In addition to neuronal connectivity, mislocated dIN populations could impact locomotor coordination. Interestingly, *Oc1*$^{-/-}$ mice exhibit muscular weakness, abnormal hindlimb positioning, balance and coordination defects (Audouard et al., 2012, 2013). Although locomotor phenotype would likely be severely impaired, behavioural analysis is impossible due to lethality of *Oc1/Oc2*$^{-/-}$ animals at birth. As dI3 localization is impaired in *Oc1/Oc2*$^{-/-}$ embryos, this could lead to defects in adaptive changes of grasping behaviour (Bui et al., 2013). Also, dI6 Dmrt3^{+} subset displacement might account for flexor-extensor, left-right coordination and locomotion speed defects (Andersson et al., 2012; Vallstedt and Kullander, 2013; Perry et al., 2019). In *Oc1/Oc2*$^{-/-}$ embryos, a great number of spinal populations are affected. A conditional OC mutant could elucidate their specific role in the development of dI3 neurons or dI6 Dmrt3^{+} and Wt1^{+} subsets, but also enable to evaluate their impact on locomotion.

4.3 OC factors repress the expression of Pou2f2

In an effort to delineate the molecular mechanisms of OC factors, and consequently identify downstream genes that may contribute with OC to the regulation of dIN diversification and distribution, we performed a microarray comparison of control and of *Oc1/Oc2*$^{-/-}$ spinal cord transcriptomes (Harris et al.,

2019). Relatively few genes were differentially expressed in the absence of OC factors. To improve the sensitivity of the transcriptome comparison, we should have dissected separately the dorsal and the ventral regions of the spinal cord. Nevertheless, among these genes, *Pou2f2* expression showed a trend to increase (1.57-fold increase). We characterized its expression profile in the spinal cord and confirmed the observed upregulation by *in situ* hybridization on sections of control or *Oc1/Oc2*$^{-/-}$ embryos. Interestingly, several neuron-specific Pou2f2 isoforms produced in the developing spinal cord are more efficiently regulated by OC factors than the 6 B-cell Pou2f2 isoforms (Harris et al., 2019). The OC factors being characterized as transcriptional activators, this suggests that they indirectly repress *Pou2f2* expression (Jacquemin et al., 2000, 2003a; Lannoy et al., 2000; Pierreux et al., 2004; Roy et al., 2012). Nevertheless, ChIP-seq experiments would allow us to assess the direct or indirect OC factor interaction on the neuronal *Pou2f2* promoter. Phenotypically, besides from thoracic dI6 Dmrt3^{+} cells, the proportion of Pou2f2^{+} dI2-dI6 interneurons was similar to control littermates in *Oc1/Oc2*$^{-/-}$ embryos. These observations suggest that in the absence of OC factors, *Pou2f2* expression is upregulated in its endogenous territory but only modestly expanded in dIN populations. Pou2f2 upregulation could be involved in the dI5 diversification and the dIN distribution defects discussed above.

4.4 OC-Pou2f2 genetic cascade controls the dI2-dI6 distribution

Our gain- and loss-of-function experiments demonstrated that Pou2f2 is involved in a genetic cascade that regulates the distribution of dI2-dI6 populations. Although reminiscent of distribution defects in the Pou2f2-upregulated *Oc1/Oc2*$^{-/-}$ embryos, the changes in distribution are not fully identical after *Pou2f2* overexpression in developing chick spinal cords. First, as we use different

embryonic stages in two experimental models, the phenotype might correlate at later developmental stages. Second, higher expression levels often observed after *in ovo* electroporation could trigger phenotype discrepancies between chicken and mouse models. Third, Pou2f2 is absent from the chicken genome, which could result in non-physiological interactions. Finally, gain- and loss-of-function experiments do not give systematically opposite effects, but rather complementary data. However, through these experiments, we showed a contribution of Pou2f2 to the control of dI2-dI6 population distribution. Even if Pou2f2 CNS targets are currently unknown, it was reported that Pou2f2 positively regulates *Robo1* expression in gastric cancer metastasis (Wang et al., 2016). Also, preliminary data in the laboratory indicate that the expression of Sema6A and its Plxn4 receptor is reduced in ventral regions of the spinal cord in *Oc1/Oc2*$^{-/-}$ embryos. Both signaling pathways are best known for mediating repulsion.

The reduction of repellent cues, produced by cells that express *Pou2f2* or *Oc* factors, could result in distribution defects in the majority of dIN populations. These observations lead us hypothesize that downstream effectors of the newly characterized OC-Pou2f2 genetic cascade are guidance molecules for growth cones. In the spinal cord, several signaling pathways, i.e. SLIT ligands and their ROBO receptors, netrins and their DCC/UNC5 receptors, semaphorins and their neuropilin/plexin receptors, ephrins and their Eph receptors, are important repellent or attractive cues for commissural axon guidance of spinal interneuron populations but also for MN axon guidance and soma positioning (Chen, 2019). Thus, characterization of *Robo1* expression in both *Oc1/Oc2*$^{-/-}$ and *Pou2f2*$^{-/-}$ embryos or *Sema6A* and *Plxn4* expression in *Pou2f2*$^{-/-}$ embryos would be necessary to assess a possible role of these molecules downstream of OC/Pou2f2 in the control of dIN migration.

As dI3 and dI6, two dorsal populations involved in motor coordination, are also mislocated in the absence of *Pou2f2*, we could expect the emergence of locomotor defects (Dyck et al., 2012; Bui et al., 2013, 2016). As *Pou2f2*$^{-/-}$ mice die at birth, locomotor behaviour analyses are impossible to perform at adult stage. Nevertheless, fictive locomotion in the isolated developing spinal cord could unveil locomotor coordination defects in *Pou2f2*$^{-/-}$ embryos. Fictive locomotion experiments allow generation and evaluation of locomotor-like activity, namely rhythmicity and speed, left-right alternation, and flexor-extensor alternation. However, an impact from mislocation of vIN population on these motor functions in *Pou2f2*$^{-/-}$ embryos is highly probable (Harris et al., 2019). Thus, discriminating the putative impact of mislocated dIN on the locomotor function would require a conditional Pou2f2 ablation in motor-related dI3 and dI6 populations for which conditional mouse lines are available (Wessels et al., 2012; Hodson et al., 2016; Perry et al., 2019).

4.5 OC factors control early expression of *TrkA* and *TrkB* in sensory neurons

During embryonic development, a hierarchy of genetic programs leads to the generation of a great variety of specialized nociceptors, mechanoreceptors and proprioceptors from a multipotent progenitor pool (Marmigère and Ernfors, 2007; Lallemend and Ernfors, 2012). In spite of considerable molecular advances, our understanding of the transcriptional mediators that regulate differentiation of NCC into distinct sensory types in the DRG remains sparse. Time course analysis of TrkA^{+} sensory neuron development showed that these cells first arise at e11.5 in *Oc1/Oc2*$^{-/-}$ mutants, while TrkA^{+} neurons are detected as early as e10.5 in control embryos. Although TrkA^{+} sensory neurons are mostly produced as a result of *Neurog1*-dependent neurogenesis, with a majority being born between e12.0 and

e13.0, an early TrkA$^+$ subpopulation arises during a *Neurog2*-dependent period of differentiation (Bachy et al., 2011). Yet, OC role in the control of NCC differentiation remains unclear, but we cannot exclude that the phenotype observed in the nociceptive lineage of the *Oc1/Oc2*$^{-/-}$ mutant results from the absence of the first neurogenic wave, which produces a part of TrkA$^+$ neurons (Ma et al., 1999; Bachy et al., 2011). Nevertheless, early TrkA$^+$ neurons appear simultaneously with TrkC$^+$ cells from the same neurogenic wave. At e10.5, TrkC$^+$ neurons are present at normal proportions in control or *Oc1/Oc2*$^{-/-}$ mutant embryos. Interestingly, for the microarray comparison of control or *Oc1/Oc2*$^{-/-}$ spinal cord transcriptomes, the spinal cord was dissected out with the DRG. Only few genes were differentially expressed in the absence of OC proteins. Nevertheless, *TrkA* expression was downregulated (0,58-fold change) in mutant embryos. This likely results from reduced expression in *Oc1/Oc2*$^{-/-}$ sensory neurons of the DRG as there is no *TrkA* expression in the developing spinal cord (Mu et al., 1993). This raises the possibility that OC factors control the initiation of *TrkA* expression in developing sensory neurons at e10.5 as observed at protein levels by immunofluorescence. The OC factors being characterized as transcriptional activators (Lemaigre et al., 1996; Samadani and Costa, 1996a; Jacquemin et al., 1999; Vanhorenbeeck et al., 2002), this suggests that they might directly activate *TrkA* expression by binding one of the 15 identified *cis*-elements within its minimal enhancer (Ma et al., 2000). ChIP-seq experiments should allow determining if OC factors interact directly or indirectly on the *TrkA* promoter or regulatory regions. Nevertheless, our phenotypical analysis of *Oc1/Oc2*$^{-/-}$ embryos suggests that OC function is restricted to the regulation of *TrkA* onset but not its maintenance. Indeed, TrkA$^+$ neuron proportion returned to normal in *Oc1/Oc2*$^{-/-}$ mutant embryos at e11.5. The *Oc1/Oc2*$^{-/-}$ mutant ganglia were of comparable size to control littermates both at e11.5 and e14.5, thereby demonstrating that the

TrkA expression delay does not impact on the later NGF-dependent survival of the TrkA$^+$ population. In addition to *TrkA* expression phenotype, our data have shown an involvement of OC in *TrkB* repression within TrkC$^+$ sensory neurons. We do not know whether the OC factors directly control the expression of *TrkB*. Further experiments will be necessary to elucidate whether OC factors directly bind to the *TrkB* promoter or regulatory regions. However, coding regions of *TrkB* extend over 300kb, which complicates dissection of spatiotemporal regulation of *TrkB* expression. Complementary to our loss-of-function study, it is interesting to perform *in ovo* electroporation of *Oc1* or *Oc2* in chicken embryo to elucidate if *TrkA* and *TrkB* levels would be different (Roy et al., 2012). Interestingly, transient reduction of Runx3$^+$ neurons in *Oc1/Oc2*$^{-/-}$ mutants suggests a direct or indirect regulation of *Runx3* expression. As previously demonstrated, Runx3 functions as a *TrkB* repressor in hybrid TrkB$^+$/C$^+$ neurons to induce TrkC$^+$ specification at critical TrkB and TrkC lineage divergence period, around e11.0-12.0 (Inoue et al., 2002, 2007; Levanon et al., 2002; Kramer et al., 2006). Also around this developmental stage, Runx3 is known to directly repress *Shox2* in presumptive TrkC$^+$ proprioceptors (Abdo et al., 2011; Scott et al., 2011). Interestingly, conditional *Oc1/Oc2*$^{-/-}$ mutation in MN unveiled by RNA-seq Shox2 upregulation by a 4,98-fold change ($p<0.0026$) (Toch et al., submitted). As Shox2 is unable to repress *Runx3*, it raises the possibility of OC factors stimulating *Runx3* expression that then inhibits *Shox2* to promote TrkC fate. Nevertheless, Shox2 remains unaffected in V2a IN when OC factors are depleted (Francius et al., 2013; Harris et al., 2019). To determine if *Oc1/Oc2* deletion affects *Shox2* expression, quantification of Shox2$^+$ among DRG neurons should bring insight on the OC factor contribution. Complementary, from a regulation point of view, the miR-183 cluster acts as a timer of *Shox2* extinction through direct mRNA targeting. Reminiscently of *Oc1/Oc2*$^{-/-}$ mutants, conditional miR-183 mutation, leads to fate-switch from TrkC$^+$

to TrkB$^+$ neurons in the DRG without changes in absolute numbers of cells (Peng et al., 2018). In the liver, OC factors have been shown to stimulate *miR-122* expression (Laudadio et al., 2012). As miR-183 directly targets Shox2, we cannot exclude a direct or indirect regulation of *miR-183* expression by the OC factors in the developing DRG. Combining *in situ* hybridization for the miR-183 cluster with quantitative RT-PCR in *Oc1/Oc2*$^{-/-}$ should allow a better comprehension of regulatory mechanisms involving OC factors in TrkB$^+$ and TrkC$^+$ fate specification.

Beyond early sensory differentiation, OC regulate the positioning of the DRG. This suggests that the migration of the neural crest cells that will differentiate into sensory neurons is altered in the absence of OC proteins. However, the transcriptional program that determines the response of neural crest cells to migration cues remains less investigated. OC factors control neuron positioning in different regions of the CNS (Espana and Clotman, 2012b, 2012a; Audouard et al., 2013) and have recently been shown to regulate interneuron migration in the developing spinal cord (Harris et al., 2019). Whether identical mechanisms are controlled by OC for neuronal migration in the CNS and in the PNS remains to be investigated.

4.6 OC factors regulate axonal projection ingrowth of TrkA and TrkC sensory neurons into the dorsal horn

In *Oc1/Oc2*$^{-/-}$ mutants, the blocking of cutaneous afferent ingrowth into the spinal cord demonstrates that OC may regulate the projection of TrkA$^+$ afferents. Altered ingrowth of TrkA$^+$ projections is also observed in *Lbx1*, *Lmx1b* or *Tlx1/3* mutants. Although *Lbx1* and *Tlx3* are expressed in the DRG, *Lmx1b* is limited to the spinal cord. Therefore, the TrkA projection defects detected in *Lmx1b* mutants indicate a dorsal horn origin (Gross et al., 2002; Müller et al., 2002; Qian et al., 2002; Ding et

al., 2004). Previous studies and our observations show that OC factors, widely present in the spinal cord, regulate certain aspects of interneuron distribution (Roy et al., 2012; Harris et al., 2019). Sensory neuron projections synapse on inhibitory interneurons in the dorsal horn, with differential innervation depending on the distribution of GABAergic and glycinergic cells (Alvarez et al., 1992; Todd, 2017). Broadly, the superficial layers I – III of the spinal cord are enriched with GABAergic interneurons, while glycinergic neurons were found throughout the spinal cord with higher concentration in the layer III and deeper (Todd and Sullivan, 1990; Tamamaki et al., 2003; Todd, 2017). In the superficial dorsal horn, GABAergic and glycinergic inhibitory neurons consist of dIL^A and dIL^B interneurons, respectively (Glasgow et al., 2005). Aberrant distribution of interneurons targeted by the sensory afferents might lead to central innervation defects. Although we were unable to directly assess the fate of the superficial layer interneurons in *Oc1/Oc2*$^{-/-}$ mutant, OC factors are not detected in the late-born populations, suggesting normal distribution of these cells. However, non-cell autonomous effects cannot be excluded, one prediction being that dorsal late-born interneurons might still encounter settlement alteration in response to the overall dorsal horn neuronal disorganization observed in *Oc1/Oc2*$^{-/-}$ mutants.

Differences in TrkC$^+$ axon pathfinding were also noted in *Oc1/Oc2*$^{-/-}$ mutants. While ventrally projecting TrkC$^+$ fibers were present in e13.5 mutant spinal cord, these axons were completely lost a day later. Several studies have shown that NT-3 is involved in proprioceptive axonal projections (Patel et al., 2003a), but the mechanism by which NT-3/TrkC signaling controls this process is not well understood. At the DREZ and DF in the *Oc1/Oc2*$^{-/-}$ mutant, TrkC and TrkB distributions extensively overlapped probably due to the failed *TrkB* repression in TrkC$^+$ sensory neurons. It is likely that the altered central projection of TrkC$^+$ axons in *Oc1/Oc2*$^{-/-}$ spinal cords may partly result from the aberrant coexpression of

TrkB and *TrkC* in certain subsets of DRG sensory neurons, which in turn, alters the NT-3/TrkC signaling. Mice lacking proprioceptive sensory neurons show defects in muscle activation (Akay et al., 2014). Although we cannot exclude a compensation by OC-2, certain motor phenotypes of *Oc1* mutant mice, i.e posture defects and hindlimb mispositioning, might result from a mild loss of proprioceptive innervation into the ventral horn of the spinal cord (Audouard et al., 2013). Future studies should seek to fully characterize the sensory neuron development in single *Oc1* and *Oc2* conditional mutants, especially as OC-1 is detected from progenitor stages. Also, to clarify if OC contribution to the $TrkA^{+}$ and $TrkC^{+}$ axonal ingrowth into the spinal cord is direct or a result of spinal neuronal defects, we should use a transgenic mouse model in which we inactivate the expression of $Oc1/Oc2^{-/-}$ in all post-mitotic sensory neurons using the $Advillin\text{-}CreER^{T2}$ mice crossed with our $Oc1^{flox/flox}$; $Oc2^{flox/flox}$ mouse line (Lau et al., 2011). Furthermore, the use of a tamoxifen-inducible mouse line would provide the advantage to separate the early and late potential roles of OC factors in the DRG.

4.7 OC factors regulate TrkA sensory neuron peripheral trajectories

During the development, numerous molecular cues and corresponding receptors guide axons to navigate through the environment to reach their final targets (O'Donnell et al., 2009). Although sensory neurons are growing towards their peripheral targets early in embryos, the formation of specialized sensory endings, as well as the assembly of sensory circuits, stretches over a long period of time, even after birth (Hasegawa et al., 2007). MN develop axons with high degree of autonomous targeting specificity (Landmesser, 2001), whereas sensory neuron peripheral fibers appear to be under the influence of their interaction with earlier motor projections (Wang et al., 2011). To what degree sensory axons depend on

motor projections during peripheral innervation has been controversial. A partial MN elimination indicates that a minimal scaffold suffice to allow the formation of sensory projections (Huettl et al., 2011). Previously, it has been shown that LMC axons, a motor column innervating the limbs, are redirected towards the dorsal part of the limbs, with complete absence of the ventral branch in *Oc1/Oc2*$^{-/-}$ embryos (Roy et al., 2012). The nociceptive projection defects observed in cervical and brachial plexus regions might be partly explained by the lack of scaffolding MN. The guidance receptor Npn-1 is present both in LMC neurons at brachial and lumbar levels as well as in sensory neurons of the DRG (Huettl et al., 2011). It makes it a plausible candidate to mediate these inter-axonal interactions. Given that multiple axonal guidance cues are expressed in the spinal cord and their expression is altered in *Oc1/Oc2*$^{-/-}$ mutants (unpublished data), it is tempting to hypothesize that multiple axonal guidance molecules, working synergistically to coordinate the projections of sensory afferents, could be also altered in sensory neurons.

4.8 General conclusion

During spinal cord development, a diversity of populations and their subsets integrate into specific neuronal circuits. In the spinal cord, this research work provides evidence that a genetic cascade composed of OC factors and their downstream target Pou2f2 controls the diversification of dI5 interneurons and the distribution of dIN. In the DRG, OC factors play different roles as they contribute to the timely *TrkA* initiation and to the proper segregation of *TrkB* from the TrkC^{+} lineage. In addition to early sensory differentiation, OC regulate both central and peripheral projections of sensory neurons through mechanisms that remain to be identified.

5 Bibliography

Abdo, H., Li, L., Lallemend, F., Bachy, I., Xu, X. J., Rice, F. L., et al. (2011). Dependence on the transcription factor Shox2 for specification of sensory neurons conveying discriminative touch. *Eur. J. Neurosci.* doi:10.1111/j.1460-9568.2011.07883.x.

Abraira, V. E., and Ginty, D. D. (2013). The sensory neurons of touch. *Neuron*. doi:10.1016/j.neuron.2013.07.051.

Akay, T., Tourtellotte, W. G., Arber, S., and Jessell, T. M. (2014). Degradation of mouse locomotor pattern in the absence of proprioceptive sensory feedback. *Proc. Natl. Acad. Sci. U. S. A.* 111, 16877–16882. doi:10.1073/pnas.1419045111.

Alaynick, W. A., Jessell, T. M., and Pfaff, S. L. (2011). SnapShot: Spinal Cord Development. *Cell* 146, 178-178.e1. doi:10.1016/j.cell.2011.06.038.

Alvarez, F. J., Kavookjian, A. M., and Light, A. R. (1992). Synaptic interactions between GABA-immunoreactive profiles and the terminals of functionally defined myelinated nociceptors in the monkey and cat spinal cord. *J. Neurosci.*

Andersson, L. S., Larhammar, M., Memic, F., Wootz, H., Schwochow, D., Rubin, C. J., et al. (2012). Mutations in DMRT3 affect locomotion in horses and spinal circuit function in mice. *Nature* 488, 642–646. doi:10.1038/nature11399.

Andrews, M. G., Kong, J., Novitch, B. G., and Butler, S. J. (2019). "New perspectives on the mechanisms establishing the dorsal-ventral axis of the spinal cord," in *Current Topics in Developmental Biology*, 417–450. doi:10.1016/bs.ctdb.2018.12.010.

Appel, E., Weissmann, S., Salzberg, Y., Orlovsky, K., Negreanu, V., Tsoory, M., et al. (2016). An ensemble of regulatory elements controls Runx3 spatiotemporal expression in subsets of dorsal root ganglia proprioceptive neurons. *Genes Dev.* 30, 2607–2622. doi:10.1101/gad.291484.116.

Arber, S., Ladle, D. R., Lin, J. H., Frank, E., and Jessell, T. M. (2000). ETS gene Er81 controls the formation of functional connections between group Ia sensory afferents and motor neurons. *Cell* 101, 485–98. doi:10.1016/s0092-8674(00)80859-4.

Audouard, E., Schakman, O., Ginion, A., Bertrand, L., Gailly, P., and Clotman, F. (2013). The Onecut transcription factor HNF-6 contributes to proper reorganization of Purkinje cells during postnatal cerebellum development. *Mol. Cell. Neurosci.* 56, 159–168. doi:10.1016/j.mcn.2013.05.001.

Audouard, E., Schakman, O., René, F., Huettl, R. E., Huber, A. B., Loeffler, J. P., et al. (2012). The Onecut Transcription Factor HNF-6 Regulates in Motor Neurons the Formation of the Neuromuscular Junctions. *PLoS One* 7. doi:10.1371/journal.pone.0050509.

Avraham, O., Hadas, Y., Vald, L., Hong, S., Song, M. R., and Klar, A. (2010). Motor and dorsal root ganglion axons serve as choice points for the ipsilateral turning of dI3 axons. *J. Neurosci.* doi:10.1523/JNEUROSCI.2380-10.2010.

Bachy, I., Franck, M. C. M., Li, L., Abdo, H., Pattyn, A., and Ernfors, P. (2011). The transcription factor Cux2 marks development of an A-delta sublineage of TrkA sensory neurons. *Dev. Biol.* 360, 77–86. doi:10.1016/j.ydbio.2011.09.007.

Barber, M., and Pierani, A. (2016). Tangential migration of glutamatergic neurons and cortical patterning during development: Lessons from Cajal-Retzius cells. *Dev. Neurobiol.* doi:10.1002/dneu.22363.

Bartesaghi, L., Wang, Y., Fontanet, P., Lallemend, F., Hadjab, S., and Correspondence, R. C. (2019). PRDM12 Is Required for Initiation of the Nociceptive Neuron Lineage during Neurogenesis. *CellReports* 26, 3484-3492.e4. doi:10.1016/j.celrep.2019.02.098.

Behar, O., Golden, J. A., Mashimo, H., Schoen, F. J., and Fishman, M. C. (1996). Semaphorin III is needed for normal patterning and growth of nerves, bones and heart. *Nature*. doi:10.1038/383525a0.

Bermingham, N. A., Hassan, B. A., Wang, V. Y., Fernandez, M., Banfi, S., Bellen, H. J., et al. (2001). Proprioceptor pathway development is dependent on MATH1. *Neuron* 30, 411–422. doi:10.1016/S0896-6273(01)00305-1.

Bikoff, J. B. (2019). Interneuron diversity and function in the spinal motor system. *Curr. Opin. Physiol.* 8, 36–43. doi:10.1016/j.cophys.2018.12.013.

Bikoff, J. B., Gabitto, M. I., Rivard, A. F., Drobac, E., MacHado, T. A., Miri, A., et al. (2016). Spinal Inhibitory Interneuron Diversity Delineates Variant Motor Microcircuits. *Cell* 165, 207–219. doi:10.1016/j.cell.2016.01.027.

Block, G. D., Locker, J., Bowen, W. C., Petersen, B. E., Katyal, S., Strom, S. C., et al. (1996). Population expansion, clonal growth, and specific differentiation patterns in primary cultures of hepatocytes induced by HGF/SF, EGF and TGFα in a chemically defined (HGM) medium. *J. Cell Biol.* 132, 1133–1149. doi:10.1083/jcb.132.6.1133.

Borowska, J., Jones, C. T., Deska-Gauthier, D., and Zhang, Y. (2015). V3 interneuron subpopulations in the mouse spinal cord undergo distinctive postnatal maturation processes. *Neuroscience* 295, 221–228. doi:10.1016/J.NEUROSCIENCE.2015.03.024.

Borowska, J., Jones, C. T., Zhang, H., Blacklaws, J., Goulding, M., and Zhang, Y. (2013). Functional subpopulations of V3 interneurons in the mature mouse spinal cord. *J. Neurosci.* 33, 18553–18565. doi:10.1523/JNEUROSCI.2005-13.2013.

Borromeo, M. D., Castro, D. S., Meredith, D. M., Guillemot, F., Tung, K.-C., Chang, J. C., et al. (2014a). A transcription factor network specifying inhibitory versus excitatory neurons in the dorsal spinal cord. *Development*. doi:10.1242/dev.114728.

Borromeo, M. D., Castro, D. S., Meredith, D. M., Guillemot, F., Tung, K.-C. K. C., Chang, J. C., et al. (2014b). Erratum to A transcription factor network specifying inhibitory versus excitatory neurons in the dorsal spinal cord (Development (Cambridge) (2014), 141, (2803-2812)). *Dev.* 141, 3102. doi:10.1242/dev.114728.

Bourane, S., Duan, B., Koch, S. C., Dalet, A., Britz, O., Garcia-Campmany, L., et al. (2015a). Gate control of mechanical itch by a subpopulation of spinal cord interneurons. *Science (80-.).* 350, 550–4. doi:10.1126/science.aac8653.

Bourane, S., Garces, A., Venteo, S., Pattyn, A., Hubert, T., Fichard, A., et al. (2009). Low-Threshold Mechanoreceptor Subtypes Selectively Express MafA and Are Specified by Ret Signaling. *Neuron* 64, 857–870. doi:10.1016/j.neuron.2009.12.004.

Bourane, S., Grossmann, K. S., Britz, O., Dalet, A., Del Barrio, M. G., Stam, F. J., et al. (2015b). Identification of a spinal circuit for light touch and fine motor control. *Cell*. doi:10.1016/j.cell.2015.01.011.

Bourane, S., Grossmann, K. S. S., Britz, O., Dalet, A., Del Barrio, M. G., Stam, F. J. J., et al. (2015c). Identification of a spinal circuit for light touch and fine motor control. *Cell* 160, 503–515. doi:10.1016/j.cell.2015.01.011.

Briscoe, J., Pierani, A., Jessell, T. M., and Ericson, J. (2000). A homeodomain protein code specifies progenitor cell identity and neuronal fate in the ventral neural tube. *Cell* 101, 435–445. doi:10.1016/S0092-8674(00)80853-3.

Briscoe, J., and Small, S. (2015). Morphogen rules: design principles of gradient-mediated embryo patterning. *Development* 142, 3996–4009. doi:10.1242/dev.129452.

Brown, A. G. (1981). *Organization in the Spinal Cord*. doi:10.1007/978-1-4471-1305-8.

Bui, T. V., Stifani, N., Panek, I., and Farah, C. (2015). Genetically identified spinal interneurons integrating tactile afferents for motor control. *J. Neurophysiol.* 114, 3050–3063. doi:10.1152/jn.00522.2015.

Bui, T. V. V., Akay, T., Loubani, O., Hnasko, T. S. S., Jessell, T. M. M., and Brownstone, R. M. M. (2013). Circuits for Grasping: Spinal dI3 Interneurons Mediate Cutaneous Control of Motor Behavior. *Neuron* 78, 191–204. doi:10.1016/j.neuron.2013.02.007.

Bui, T. V, Stifani, N., Akay, T., and Brownstone, R. M. (2016). Spinal microcircuits comprising dI3 interneurons are necessary for motor functional recovery following spinal cord transection. *Elife* 5. doi:10.7554/eLife.21715.

Caspary, T., and Anderson, K. V. (2003). Patterning cell types in the dorsal spinal cord: What the mouse mutants say. *Nat. Rev. Neurosci.* 4, 289–297. doi:10.1038/nrn1073.

Chakrabarty, K., Von Oerthel, L., Hellemons, A., Clotman, F., Espana, A., Groot Koerkamp, M., et al. (2012). Genome wide expression profiling of the mesodiencephalic region identifies novel factors involved in early and late dopaminergic development. *Biol. Open*. doi:10.1242/bio.20121230.

Chang, J. C., Meredith, D. M., Mayer, P. R., Borromeo, M. D., Lai, H. C., Ou, Y. H., et al. (2013). Prdm13 Mediates the Balance of Inhibitory and Excitatory Neurons in Somatosensory Circuits. *Dev. Cell*. doi:10.1016/j.devcel.2013.02.015.

Chen, A. I., De Nooij, J. C., and Jessell, T. M. (2006a). Graded activity of transcription factor Runx3 specifies the laminar termination pattern of sensory axons in the developing spinal cord. *Neuron* 49, 395–408. doi:10.1016/j.neuron.2005.12.028.

Chen, C. L., Broom, D. C., Liu, Y., De Nooij, J. C., Li, Z., Cen, C., et al. (2006b). Runx1 determines nociceptive sensory neuron phenotype and is required for thermal and neuropathic pain. *Neuron* 49, 365–377. doi:10.1016/j.neuron.2005.10.036.

Chen, Z. (2019). Common cues wire the spinal cord: Axon guidance molecules in spinal neuron migration. *Semin. Cell Dev. Biol.* 85, 71–77. doi:10.1016/j.semcdb.2017.12.012.

Chen, Z. F., Rebelo, S., White, F., Malmberg, A. B., Baba, H., Lima, D., et al. (2001). The paired homeodomain protein DRG11 is required for the projection of cutaneous sensory afferent fibers to the dorsal spinal cord. *Neuron* 31, 59–73. doi:10.1016/S0896-6273(01)00341-5.

Cheng, L., Arata, A., Mizuguchi, R., Qian, Y., Karunaratne, A., Gray, P. A., et al. (2004). Tlx3 and Tlx1 are post-mitotic selector genes determining glutamatergic over GABAergic cell fates. *Nat. Neurosci.* doi:10.1038/nn1221.

Cheng, L., Samad, O. A., Xu, Y., Mizuguchi, R., Luo, P., Shirasawa, S., et al. (2005). Lbx1 and Tlx3 are opposing switches in determining GABAergic versus glutamatergic transmitter phenotypes. *Nat. Neurosci.* doi:10.1038/nn1569.

Clary, D. O., Weskamp, G., Austin, L. A. R., and Reichardt, L. F. (1994). TrkA cross-linking mimics neuronal responses to nerve growth factor. *Mol. Biol. Cell*. doi:10.1091/mbc.5.5.549.

Clotman, F., Jacquemin, P., Plumb-Rudewiez, N., Pierreux, C. E., Van Der Smissen, P., Dietz, H. C., et al. (2005). Control of liver cell fate decision by a gradient of TGFβ signaling modulated by Onecut transcription factors. *Genes Dev.* 19, 1849–1854. doi:10.1101/gad.340305.

Clotman, F., Lannoy, V. J., Reber, M., Cereghini, S., Cassiman, D., Jacquemin, P., et al. (2002). The onecut transcription factor HNF6 is required for normal development of the biliary tract. *Development*.

Corcoran, L. M., Karvelas, M., Nossal, G. J. V., Ye, Z. S., Jacks, T., and Baltimore, D. (1993). Oct-2, although not required for early B-cell development, is critical for later B-cell maturation and for postnatal survival. *Genes Dev.* 7, 570–582. doi:10.1101/gad.7.4.570.

Crowley, C., Spencer, S. D., Nishimura, M. C., Chen, K. S., Pitts-Meek, S., Armaninl, M. P., et al. (1994). Mice lacking nerve growth factor display perinatal loss of sensory and sympathetic neurons yet develop basal forebrain cholinergic neurons. *Cell*. doi:10.1016/0092-8674(94)90378-6.

de Nooij, J. C., Doobar, S., and Jessell, T. M. (2013). Etv1 Inactivation Reveals Proprioceptor Subclasses that Reflect the Level of NT3 Expression in Muscle Targets. *Neuron* 77, 1055–1068. doi:10.1016/j.neuron.2013.01.015.

Delile, J., Rayon, T., Melchionda, M., Edwards, A., Briscoe, J., and Sagner, A. (2019). Single cell transcriptomics reveals spatial and temporal dynamics of gene expression in the developing mouse spinal cord. *Dev.* 146. doi:10.1242/dev.173807.

Delloye-Bourgeois, C., and Castellani, V. (2019). Hijacking of embryonic programs by neural crest-derived neuroblastoma: From physiological migration to metastatic dissemination. *Front. Mol. Neurosci.* 12. doi:10.3389/fnmol.2019.00052.

Dennis, D. J., Han, S., and Schuurmans, C. (2019). bHLH transcription factors in neural development, disease, and reprogramming. *Brain Res.* 1705, 48–65. doi:10.1016/j.brainres.2018.03.013.

Desiderio, S., Vermeiren, S., Van Campenhout, C., Kricha, S., Malki, E., Richts, S., et al. (2019). Prdm12 Directs Nociceptive Sensory Neuron Development by Regulating the Expression of the NGF Receptor TrkA. *Cell Rep.* 26, 3522-3536.e5. doi:10.1016/j.celrep.2019.02.097.

Ding, Q., Joshi, P. S., Xie, Z. H., Xiang, M., and Gan, L. (2012). BARHL2 transcription factor regulates the ipsilateral/contralateral subtype divergence in postmitotic dI1 neurons of the developing spinal cord. *Proc. Natl. Acad. Sci. U. S. A.* 109, 1566–1571. doi:10.1073/pnas.1112392109.

Ding, Y. Q., Yin, J., Kania, A., Zhao, Z. Q., Johnson, R. L., and Chen, Z. F. (2004). Lmx1b controls the differentiation and migration of the superficial dorsal horn neurons of the spinal cord. *Development* 131, 3693–3703. doi:10.1242/dev.01250.

Dougherty, K. J., Zagoraiou, L., Satoh, D., Rozani, I., Doobar, S., Arber, S., et al. (2013). Locomotor Rhythm Generation Linked to the Output of Spinal Shox2 Excitatory Interneurons. *Neuron*. doi:10.1016/j.neuron.2013.08.015.

Dubreuil, V., Hirsch, M.-R., Jouve, C., Brunet, J.-F., and Goridis, C. (2002). The role of Phox2b in synchronizing pan-neuronal and type-specific aspects of neurogenesis. *Development* 129, 5241–53. Available at: http://www.ncbi.nlm.nih.gov/pubmed/12399315.

Dumoulin, A., Ter-Avetisyan, G., Schmidt, H., and Rathjen, F. (2018). Molecular Analysis of Sensory Axon Branching Unraveled a cGMP-Dependent Signaling Cascade. *Int. J. Mol. Sci.* 19, 1266. doi:10.3390/ijms19051266.

Dyck, J., Lanuza, G. M., and Gosgnach, S. (2012). Functional characterization of dI6 interneurons in the neonatal mouse spinal cord. *J. Neurophysiol.* 107, 3256–66. doi:10.1152/jn.01132.2011.

Dykes, I. M., Tempest, L., Lee, S. I., and Turner, E. E. (2011). Brn3a and Islet1 act epistatically to regulate the gene expression program of sensory differentiation. *J. Neurosci.* 31, 9789–9799. doi:10.1523/JNEUROSCI.0901-11.2011.

Eng, S. R., Lanier, J., Fedtsova, N., and Turner, E. E. (2004). Coordinated regulation of gene expression by Brn3a in developing sensory ganglia. *Development*. doi:10.1242/dev.01260.

Ernfors, P., Lee, K. F., Kucera, J., and Jaenisch, R. (1994). Lack of neurotrophin-3 leads to deficiencies in the peripheral nervous system and loss of limb proprioceptive afferents. *Cell*. doi:10.1016/0092-8674(94)90213-5.

Ernfors, P., Merlio, J. -P, and Persson, H. (1992). Cells Expressing mRNA for Neurotrophins and their Receptors During Embryonic Rat Development. *Eur. J. Neurosci.* doi:10.1111/j.1460-9568.1992.tb00141.x.

Espana, A., and Clotman, F. (2012a). Onecut factors control development of the Locus Coeruleus and of the mesencephalic trigeminal nucleus. *Mol. Cell. Neurosci.* 50, 93–102. doi:10.1016/j.mcn.2012.04.002.

Espana, A., and Clotman, F. (2012b). Onecut transcription factors are required for the second phase of development of the A13 dopaminergic nucleus in the mouse. *J. Comp. Neurol.* 520, 1424–1441. doi:10.1002/cne.22803.

Fariñas, I., Wilkinson, G. A., Backus, C., Reichardt, L. F., and Patapoutian, A. (1998). Characterization of neurotrophin and Trk receptor functions in developing sensory ganglia: direct NT-3 activation of TrkB neurons in vivo. *Neuron* 21, 325–34. Available at: http://www.ncbi.nlm.nih.gov/pubmed/9728914 [Accessed August 19, 2019].

Fedtsova, N. G., and Turner, E. E. (1995). Brn-3.0 expression identifies early post-mitotic CNS neurons and sensory neural precursors. *Mech. Dev.* 53, 291–304. doi:10.1016/0925-4773(95)00435-1.

Francius, C., and Clotman, F. (2010). Dynamic expression of the Onecut transcription factors HNF-6, OC-2 and OC-3 during spinal motor neuron development. *Neuroscience* 165, 116–129. doi:10.1016/j.neuroscience.2009.09.076.

Francius, C., and Clotman, F. (2014). Generating spinal motor neuron diversity: A long quest for neuronal identity. *Cell. Mol. Life Sci.* 71, 813–829. doi:10.1007/s00018-013-1398-x.

Francius, C., Harris, A., Rucchin, V., Hendricks, T. J., Stam, F. J., Barber, M., et al. (2013). Identification of Multiple Subsets of Ventral Interneurons and Differential Distribution along the Rostrocaudal Axis of the Developing Spinal Cord. *PLoS One*. doi:10.1371/journal.pone.0070325.

Frank, E., and Sanes, J. R. (1991). Lineage of neurons and glia in chick dorsal root ganglia: Analysis in vivo with a recombinant retrovirus. *Development* 111, 895–908.

Gannon, M., Ray, M. K., Van Zee, K., Rausa, F., Costa, R. H., and Wright, C. V. E. (2000). Persistent expression of HNF6 in islet endocrine cells causes disrupted islet architecture and loss of beta cell function. *Development*.

Glasgow, S. M., Henke, M. R., MacDonald, R. J., Wright, C. V. E., and Johnson, J. E. (2005). Ptf1a determines GABAergic over glutamatergic neuronal cell fate in the spinal cord dorsal horn. *Development* 132, 5461–5469. doi:10.1242/dev.02167.

Goetz, C., Pivetta, C., and Arber, S. (2015). Distinct Limb and Trunk Premotor Circuits Establish Laterality in the Spinal Cord. *Neuron* 85, 131–144. doi:10.1016/j.neuron.2014.11.024.

Gosgnach, S., Lanuza, G. M., Butt, S. J. B., Saueressig, H., Zhang, Y., Velasquez, T., et al. (2006). V1 spinal neurons regulate the speed of vertebrate locomotor outputs. *Nature*. doi:10.1038/nature04545.

Goulding, M. (2009). Circuits controlling vertebrate locomotion: Moving in a new direction. *Nat. Rev. Neurosci.* doi:10.1038/nrn2608.

Goulding, M. D., Chalepakis, G., Deutsch, U., Erselius, J. R., and Gruss, P. (1991). Pax-3, a novel murine DNA binding protein expressed during early neurogenesis. *EMBO J.* doi:10.1002/j.1460-2075.1991.tb08054.x.

Gowan, K., Helms, A. W., Hunsaker, T. L., Collisson, T., Ebert, P. J., Odom, R., et al. (2001). Crossinhibitory activities of Ngn1 and Math1 allow specification of distinct dorsal interneurons. *Neuron* 31, 219–232. doi:10.1016/S0896-6273(01)00367-1.

Griener, A., Zhang, W., Kao, H., Haque, F., and Gosgnach, S. (2017). Anatomical and electrophysiological characterization of a population of dI6 interneurons in the neonatal mouse spinal cord. *Neuroscience*. doi:10.1016/j.neuroscience.2017.08.031.

Gross, M. K., Dottori, M., and Goulding, M. (2002). Lbx1 specifies somatosensory association interneurons in the dorsal spinal cord. *Neuron* 34, 535–549. doi:10.1016/S0896-6273(02)00690-6.

Gross, M. K., Moran-Rivard, L., Velasquez, T., Nakatsu, M. N., Jagla, K., and Goulding, M. (2000). Lbx1 is required for muscle precursor migration along a lateral pathway into the limb. *Development* 127, 413–24. Available at: http://www.ncbi.nlm.nih.gov/pubmed/10603357 [Accessed March 8, 2019].

Grossmann, K. S., Giraudin, A., Britz, O., Zhang, J., and Goulding, M. (2010). "Genetic dissection of rhythmic motor networks in mice," in *Progress in Brain Research* doi:10.1016/B978-0-444-53613-6.00002-2.

Gu, C., Rodriguez, E. R., Reimert, D. V., Shu, T., Fritzsch, B., Richards, L. J., et al. (2003). Neuropilin-1 conveys semaphorin and VEGF signaling during neural and cardiovascular development. *Dev. Cell*. doi:10.1016/S1534-5807(03)00169-2.

Guo, J., and Anton, E. S. (2014). Decision making during interneuron migration in the developing cerebral cortex. *Trends Cell Biol.* doi:10.1016/j.tcb.2013.12.001.

Hanotel, J., Bessodes, N., Thélie, A., Hedderich, M., Parain, K., Driessche, B. Van, et al. (2014). The Prdm13 histone methyltransferase encoding gene is a Ptf1a-Rbpj downstream target that suppresses glutamatergic and promotes GABAergic neuronal fate in the dorsal neural tube. *Dev. Biol.* doi:10.1016/j.ydbio.2013.12.024.

Harris, A., Masgutova, G., Collin, A., Toch, M., Hidalgo-Figueroa, M., Jacob, B., et al. (2019). Onecut factors and Pou2f2 regulate the distribution of V2 interneurons in the mouse developing spinal cord. *Front. Cell. Neurosci.* 13, 184. doi:10.3389/fncel.2019.00184.

Hasegawa, H., Abbott, S., Han, B. X., Qi, Y., and Wang, F. (2007). Analyzing somatosensory axon projections with the sensory neuron-specific Advillin gene. *J. Neurosci.* doi:10.1523/JNEUROSCI.4908-07.2007.

Hayashi, M., Hinckley, C. A., Driscoll, S. P., Moore, N. J., Levine, A. J., Hilde, K. L., et al. (2018). Graded Arrays of Spinal and Supraspinal V2a Interneuron Subtypes Underlie Forelimb and Hindlimb Motor Control. *Neuron* 97, 869-884.e5. doi:10.1016/j.neuron.2018.01.023.

Helms, A. W. (2005). Sequential roles for Mash1 and Ngn2 in the generation of dorsal spinal cord interneurons. *Development* 132, 2709–2719. doi:10.1242/dev.01859.

Helms, A. W., and Johnson, J. E. (1998). Progenitors of dorsal commissural interneurons are defined by MATH1 expression. *Development* 125, 919–928. Available at: https://dev.biologists.org/content/develop/125/5/919.full.pdf [Accessed July 16, 2019].

Helms, A. W., and Johnson, J. E. (2003). Specification of dorsal spinal cord interneurons. *Curr. Opin. Neurobiol.* 13, 42–49. doi:10.1016/S0959-4388(03)00010-2.

Henke, R. M., Savage, T. K., Meredith, D. M., Glasgow, S. M., Hori, K., Dumas, J., et al. (2009). Neurog2 is a direct downstream target of the Ptf1a-Rbpj transcription complex in dorsal spinal cord. *Development* 136, 2945–2954. doi:10.1242/dev.035352.

Hernandez-Miranda, L. R., Müller, T., and Birchmeier, C. (2017). The dorsal spinal cord and hindbrain: From developmental mechanisms to functional circuits. *Dev. Biol.* 432, 34–42. doi:10.1016/j.ydbio.2016.10.008.

Hilde, K. L., Levine, A. J., Hinckley, C. A., Hayashi, M., Montgomery, J. M., Gullo, M., et al. (2016). Satb2 Is Required for the Development of a Spinal Exteroceptive Microcircuit that Modulates Limb Position. *Neuron* 91, 763–776. doi:10.1016/j.neuron.2016.07.014.

Hirasawa, T., Fujimoto, S., and Kuratani, S. (2016). Expansion of the neck reconstituted the shoulder-diaphragm in amniote evolution. *Dev. Growth Differ.* 58, 143–153. doi:10.1111/dgd.12243.

Hjerling-Leffler, J., Marmigère, F., Heglind, M., Cederberg, A., Koltzenburg, M., Enerbäck, S., et al. (2005). The boundary cap: A source of neural crest stem cells that generate multipe sensory neuron subtypes. *Development* 132, 2623–2632. doi:10.1242/dev.01852.

Hodge, L. K., Klassen, M. P., Han, B. X., Yiu, G., Hurrell, J., Howell, A., et al. (2007). Retrograde BMP Signaling Regulates Trigeminal Sensory Neuron Identities and the Formation of Precise Face Maps. *Neuron* 55, 572–586. doi:10.1016/j.neuron.2007.07.010.

Hodson, D. J., Shaffer, A. L., Xiao, W., Wright, G. W., Schmitz, R., Phelan, J. D., et al. (2016). Regulation of normal B-cell differentiation and malignant B-cell survival by OCT2. *Proc. Natl. Acad. Sci. U. S. A.* 113, E2039–E2046. doi:10.1073/pnas.1600557113.

Huang, E. J., Zang, K., Schmidt, A., Saulys, A., Xiang, M., and Reichardt, L. F. (1999). POU domain factor Brn-3a controls the differentiation and survival of trigeminal neurons by regulating Trk receptor expression. *Development* 126, 2869–2882.

Huettl, R. E., Soellner, H., Bianchi, E., Novitch, B. G., and Huber, A. B. (2011). Npn-1 contributes to axon-axon interactions that differentially control sensory and motor innervation of the limb. *PLoS Biol.* 9. doi:10.1371/journal.pbio.1001020.

Inoue, K. I., Ito, K., Osato, M., Lee, B., Bae, S.-C. C., and Ito, Y. (2007). The transcription factor Runx3 represses the neurotrophin receptor TrkB during lineage commitment of dorsal root ganglion neurons. *J. Biol. Chem.* 282, 24175–24184. doi:10.1074/jbc.M703746200.

Inoue, K. I., Ozaki, S., Ito, K., Iseda, T., Kawaguchi, S., Ogawa, M., et al. (2003). Runx3 is essential for the target-specific axon pathfinding of trkC-expressing dorsal root ganglion neurons. *Blood Cells, Mol. Dis.* 30, 157–160. doi:10.1016/S1079-9796(03)00032-9.

Inoue, K. ichi, Ozaki, S., Shiga, T., Ito, K., Masuda, T., Okado, N., et al. (2002). Runx3 controls the axonal projection of proprioceptive dorsal root ganglion neurons. *Nat. Neurosci.* 5, 946–954. doi:10.1038/nn925.

Iyaguchi, D., Yao, M., Watanabe, N., Nishihira, J., and Tanaka, I. (2007). DNA Recognition Mechanism of the ONECUT Homeodomain of Transcription Factor HNF-6. *Structure* 15, 75–83. doi:10.1016/j.str.2006.11.004.

Jacquemin, P., Durviaux, S. M., Jensen, J., Godfraind, C., Gradwohl, G., Guillemot, F., et al. (2000). Transcription Factor Hepatocyte Nuclear Factor 6 Regulates Pancreatic Endocrine Cell Differentiation and Controls Expression of the Proendocrine Gene ngn3. *Mol. Cell. Biol.* 20, 4445–4454. doi:10.1128/mcb.20.12.4445-4454.2000.

Jacquemin, P., Lannoy, V. J., O'Sullivan, J., Read, A., Lemaigre, F. P., and Rousseau, G. G. (2001). The transcription factor Onecut-2 controls the microphthalmia-associated transcription factor gene. *Biochem. Biophys. Res. Commun.* doi:10.1006/bbrc.2001.5294.

Jacquemin, P., Lannoy, V. J., Rousseau, G. G., and Lemaigre, F. P. (1999). OC-2, a novel mammalian member of the ONECUT class of homeodomain transcription factors whose function in liver partially overlaps with that of hepatocyte nuclear factor-6. *J. Biol. Chem.* 274, 2665–2671. doi:10.1074/jbc.274.5.2665.

Jacquemin, P., Lemaigre, F. P., and Rousseau, G. G. (2003a). The Onecut transcription factor HNF-6 (OC-1) is required for timely specification of the pancreas and acts upstream of Pdx-1 in the specification cascade. *Dev. Biol.* 258, 105–116. doi:10.1016/S0012-1606(03)00115-5.

Jacquemin, P., Pierreux, C. E., Fierens, S., van Eyll, J. M., Lemaigre, F. P., and Rousseau, G. G. (2003b). Cloning and embryonic expression pattern of the mouse Onecut transcription factor OC-2. *Gene Expr. Patterns* 3, 639–644. doi:10.1016/S1567-133X(03)00110-8.

Jessell, T. M. (2000). Neuronal specification in the spinal cord: Inductive signals and transcriptional codes. 20, 20–29. doi:10.1038/35049541.

Kabayiza, K. U., Masgutova, G., Harris, A., Rucchin, V., Jacob, B., and Clotman, F. (2017). The onecut transcription factors regulate differentiation and distribution of dorsal interneurons during spinal cord development. *Front. Mol. Neurosci.* 10, 157. doi:10.3389/fnmol.2017.00157.

Kiehn, O. (2016). Decoding the organization of spinal circuits that control locomotion. doi:10.1038/nrn.2016.9.

Kim, J., Lo, L., Dormand, E., and Anderson, D. J. (2003). SOX10 maintains multipotency and inhibits neuronal differentiation of neural crest stem cells. *Neuron* 38, 17–31. doi:10.1016/S0896-6273(03)00163-6.

Koch, S. C., Del Barrio, M. G., Dalet, A., Gatto, G., Günther, T., Zhang, J., et al. (2017). RORβ Spinal Interneurons Gate Sensory Transmission during Locomotion to Secure a Fluid Walking Gait. *Neuron*. doi:10.1016/j.neuron.2017.11.011.

Kramer, I., Sigrist, M., De Nooij, J. C., Taniuchi, I., Jessell, T. M., and Arber, S. (2006). A role for Runx transcription factor signaling in dorsal root ganglion sensory neuron diversification. *Neuron* 49, 379–393. doi:10.1016/j.neuron.2006.01.008.

Kriks, S. (2005). Gsh2 is required for the repression of Ngn1 and specification of dorsal interneuron fate in the spinal cord. *Development* 132, 2991–3002. doi:10.1242/dev.01878.

Ladle, D. R., Pecho-Vrieseling, E., and Arber, S. (2007). Assembly of motor circuits in the spinal cord: driven to function by genetic and experience-dependent mechanisms. *Neuron* 56, 270–283. doi:10.1016/j.neuron.2007.09.026.

Lai, H. C., Seal, R. P., and Johnson, J. E. (2016). Making sense out of spinal cord somatosensory development. *Development* 143, 3434–3448. doi:10.1242/dev.139592.

Lallemend, F., and Ernfors, P. (2012). Molecular interactions underlying the specification of sensory neurons. *Trends Neurosci.* 35, 373–381. doi:10.1016/j.tins.2012.03.006.

Landmesser, L., and Honig, M. G. (1986). Altered sensory projections in the chick hind limb following the early removal of motoneurons. *Dev. Biol.* doi:10.1016/0012-1606(86)90023-0.

Landmesser, L. T. (2001). The acquisition of motoneuron subtype identity and motor circuit formation. *Int. J. Dev. Neurosci.* doi:10.1016/S0736-5748(00)00090-3.

Landry, C., Clotman, F., Hioki, T., Oda, H., Picard, J. J., Lemaigre, F. P., et al. (1997). HNF-6 is expressed in endoderm derivatives and nervous system of the mouse embryo and participates to the cross-regulatory network of liver- enriched transcription factors. *Dev. Biol.* 192, 247–257. doi:10.1006/dbio.1997.8757.

Lanier, J., Quina, L. A., Eng, S. R., Cox, E., and Turner, E. E. (2007). Brn3a target gene recognition in embryonic sensory neurons. *Dev. Biol.* doi:10.1016/j.ydbio.2006.10.050.

Lannoy, V. J., Bürglin, T. R., Rousseau, G. G., and Lemaigre, F. P. (1998). Isoforms of hepatocyte nuclear factor-6 differ in DNA-binding properties, contain a bifunctional homeodomain, and define the new ONECUT class of homeodomain proteins. *J. Biol. Chem.* 273, 13552–62. doi:10.1074/jbc.273.22.13552.

Lannoy, V. J., Rodolosse, A., Pierreux, C. E., Rousseau, G. G., and Lemaigre, F. P. (2000). Transcriptional stimulation by hepatocyte nuclear factor-6: Target-specific recruitment of either CREB-binding protein (CBP) or p300/CBP-associated factor (p/CAF). *J. Biol. Chem.* 275, 22098–22103. doi:10.1074/jbc.M000855200.

Lau, J., Minett, M. S., Zhao, J., Dennehy, U., Wang, F., Wood, J. N., et al. (2011). Temporal control of gene deletion in sensory ganglia using a tamoxifen-inducible Advillin-Cre-ERT2 recombinase mouse. *Mol. Pain*. doi:10.1186/1744-8069-7-100.

Laudadio, I., Manfroid, I., Achouri, Y., Schmidt, D., Wilson, M. D., Cordi, S., et al. (2012). A feedback loop between the liver-enriched transcription factor network and miR-122 controls hepatocyte differentiation. *Gastroenterology*. doi:10.1053/j.gastro.2011.09.001.

Le Dréau, G., and Martí, E. (2012). Dorsal-ventral patterning of the neural tube: A tale of three signals. *Dev. Neurobiol.* doi:10.1002/dneu.22015.

Lee, K. J., Mendelsohn, M., and Jessell, T. M. (1998). Neuronal patterning by BMPs: A requirement for GDF7 in the generation of a discrete class of commissural interneurons in the mouse spinal cord. *Genes Dev.* doi:10.1101/gad.12.21.3394.

Lei, L., Laub, F., Lush, M., Romero, M., Zhou, J., Luikart, B., et al. (2005). The zinc finger transcription factor Klf7 is required for TrkA gene expression and development of nociceptive sensory neurons. *Genes Dev.* doi:10.1101/gad.1227705.

Lei, L., Zhou, J., Lin, L., and Parada, L. F. (2006). Brn3a and Klf7 cooperate to control TrkA expression in sensory neurons. *Dev. Biol.* 300, 758–769. doi:10.1016/J.YDBIO.2006.08.062.

Lemaigre, F. P., Durviaux, S. M., Truong, O., Lannoy, V. J., Hsuan, J. J., and Rousseau, G. G. (1996). Hepatocyte nuclear factor 6, a transcription factor that contains a novel type of homeodomain and a single cut domain. *Proc. Natl. Acad. Sci. U. S. A.* 93, 9460–9464. doi:10.1073/pnas.93.18.9460.

Levanon, D., Bettoun, D., Harris-Cerruti, C., Woolf, E., Negreanu, V., Eilam, R., et al. (2002). The Runx3 transcription factor regulates development and survival of TrkC dorsal root ganglia neurons. *EMBO J.* 21, 3454–3463. doi:10.1093/emboj/cdf370.

Levanon, D., Brenner, O., Negreanu, V., Bettoun, D., Woolf, E., Eilam, R., et al. (2001). Spatial and temporal expression pattern of Runx3 (Aml2) and Runx1 (Aml1) indicates non-redundant functions during mouse embryogenesis. *Mech. Dev.* doi:10.1016/S0925-4773(01)00537-8.

Lewis, K. E. (2006). How do genes regulate simple behaviours? Understanding how different neurons in the vertebrate spinal cord are genetically specified. *Philos. Trans. R. Soc. B Biol. Sci.* 361, 45–66. doi:10.1098/rstb.2005.1778.

Liu, B., Liu, Z., Chen, T., Li, H., Qiang, B., Yuan, J., et al. (2007). Selective expression of Bhlhb5 in subsets of early-born interneurons and late-born association neurons in the spinal cord. *Dev. Dyn.* doi:10.1002/dvdy.21061.

Lopes, C., Liu, Z., Xu, Y., and Ma, Q. (2012). Tlx3 and Runx1 act in combination to coordinate the development of a cohort of nociceptors, thermoceptors, and pruriceptors. *J. Neurosci.* 32, 9706–15. doi:10.1523/JNEUROSCI.1109-12.2012.

Lu, D. C., Niu, T., and Alaynick, W. A. (2015). Molecular and cellular development of spinal cord locomotor circuitry. *Front. Mol. Neurosci.* 8, 25. doi:10.3389/fnmol.2015.00025.

Luo, W., Enomoto, H., Rice, F. L., Milbrandt, J., and Ginty, D. D. (2009). Molecular Identification of Rapidly Adapting Mechanoreceptors and Their Developmental Dependence on Ret Signaling. *Neuron*. doi:10.1016/j.neuron.2009.11.003.

Ma, L., Merenmies, J., and Parada, L. F. (2000). Molecular characterization of the TrkA/NGF receptor minimal enhancer reveals regulation by multiple cis elements to drive embryonic neuron expression. *Development* 127, 3777–3788.

Ma, Q., Fode, C., Guillemot, F., and Anderson, D. J. (1999). NEUROGENIN1 and NEUROGENIN2 control two distinct waves of neurogenesis in developing dorsal root ganglia. *Genes Dev.* 13, 1717–1728. doi:10.1101/gad.13.13.1717.

Margagliotti, S., Clotman, F., Pierreux, C. E., Beaudry, J. B., Jacquemin, P., Rousseau, G. G., et al. (2007). The Onecut transcription factors HNF-6/OC-1 and OC-2 regulate early liver expansion by controlling hepatoblast migration. *Dev. Biol.* 311, 579–589. doi:10.1016/j.ydbio.2007.09.013.

Marmigère, F., and Ernfors, P. (2007). Specification and connectivity of neuronal subtypes in the sensory lineage. *Nat. Rev. Neurosci.* 8, 114. doi:10.1038/nrn2057.

Marmigère, F., Montelius, A., Wegner, M., Groner, Y., Reichardt, L. F., and Ernfors, P. (2006). The Runx1/AML1 transcription factor selectively regulates development and survival of TrkA nociceptive sensory neurons. *Nat. Neurosci.* 9, 180–187. doi:10.1038/nn1631.

Maro, G. S., Vermeren, M., Voiculescu, O., Melton, L., Cohen, J., Charnay, P., et al. (2004). Neural crest boundary cap cells constitute a source of neuronal and glial cells of the PNS. *Nat. Neurosci.* 7, 930–938. doi:10.1038/nn1299.

Masgutova, G., Harris, A., Jacob, B., Corcoran, L. M., and Clotman, F. (2019). Pou2f2 Regulates the Distribution of Dorsal Interneurons in the Mouse Developing Spinal Cord . *Front. Mol. Neurosci.* 12, 263. Available at: https://www.frontiersin.org/article/10.3389/fnmol.2019.00263.

Matsuda, S., Kobayashi, N., Wakisaka, H., Saito, S., Saito, K., Miyawaki, K., et al. (2000). MORPHOLOGICAL TRANSFORMATION OF SENSORY GANGLION NEURONS AND SATELLITE CELLS. Available at: http://www.bgscb.org/blog/wp-content/uploads/2012/02/Vol11-2000-06.pdf [Accessed August 27, 2019].

Mazzoni, E. O., Mahony, S., Closser, M., Morrison, C. A., Nedelec, S., Williams, D. J., et al. (2013). Synergistic binding of transcription factors to cell-specific enhancers programs motor neuron identity. *Nat. Neurosci.* 16, 1219–1227. doi:10.1038/nn.3467.

McEvilly, R. J., Erkman, L., Luo, L., Sawchenko, P. E., Ryan, A. F., and Rosenfeld, M. G. (1996). Requirement for Brn-3.0 in differentiation and survival of sensory and motor neurons. *Nature* 384, 574–577. doi:10.1038/384574a0.

Mizuguchi, R., Kriks, S., Cordes, R., Gossler, A., Ma, Q., and Goulding, M. (2006). Ascl1 and Gsh1/2 control inhibitory and excitatory cell fate in spinal sensory interneurons. *Nat. Neurosci.* 9, 770–778. doi:10.1038/nn1706.

Molliver, D. C., and Snider, W. D. (1997). Nerve growth factor receptor TrkA is down-regulated during postnatal development by a subset of dorsal root ganglion neurons. *J. Comp. Neurol.* 381, 428–438. doi:10.1002/(SICI)1096-9861(19970519)381:4<428::AID-CNE3>3.0.CO;2-4.

Molliver, D. C., Wright, D. E., Leitner, M. L., Parsadanian, A. S., Doster, K., Wen, D., et al. (1997). IB4-binding DRG neurons switch from NGF to GDNF dependence in early postnatal life. *Neuron*. doi:10.1016/S0896-6273(00)80966-6.

Montelius, A., Marmigère, F., Baudet, C., Aquino, J. B., Enerbäck, S., and Ernfors, P. (2007). Emergence of the sensory nervous system as defined by Foxs1 marking neuronally and sensory committed cells. *Differentiation* 75, 404–417. doi:10.1111/j.1432-0436.2006.00154.x.

Moqrich, A., Earley, T. J., Watson, J., Andahazy, M., Backus, C., Martin-Zanca, D., et al. (2004). Expressing TrkC from the TrkA locus causes a subset of dorsal root ganglia neurons to switch fate. *Nat. Neurosci.* doi:10.1038/nn1283.

Mu, X., Inmaculada Silos-Santiago, Iva, Carroll, S. L., and Snider, W. D. (1993). Neurotrophin Receptor Genes Are Expressed in Distinct Patterns in Developing Dorsal Root Ganglia. Available at: https://www.jneurosci.org/content/jneuro/13/9/4029.full.pdf [Accessed September 3, 2019].

Müller, T., Anlag, K., Wildner, H., Britsch, S., Treier, M., and Birchmeier, C. (2005). The bHLH factor Olig3 coordinates the specification of dorsal neurons in the spinal cord. *Genes Dev.* 19, 733–743. doi:10.1101/gad.326105.

Müller, T., Brohmann, H., Pierani, A., Heppenstall, P. A., Lewin, G. R., Jessell, T. M., et al. (2002). The homeodomain factor lbx1 distinguishes two major programs of neuronal differentiation in the dorsal spinal cord. *Neuron* 34, 551–62. doi:10.1016/S0896-6273(02)00689-X.

Nakada, Y., Hunsaker, T. L., Henke, M. R., and Johnson, J. E. (2004). Distinct domains within Mash1 and Math1 are required for function in neuronal differentiation versus neuronal cell-type specification. *Development* 131, 1319–1330. doi:10.1242/dev.01008.

Nakamura, S., Senzaki, K., Yoshikawa, M., Nishimura, M., Inoue, K.-I., Ito, Y., et al. (2008). Dynamic regulation of the expression of neurotrophin receptors by Runx3. *Development* 135, 1703–11. doi:10.1242/dev.015248.

Nakazaki, H., Reddy, A. C., Mania-Farnell, B. L., Shen, Y. W., Ichi, S., McCabe, C., et al. (2008). Key basic helix-loop-helix transcription factor genes Hes1 and Ngn2 are regulated by Pax3 during mouse embryonic development. *Dev. Biol.* doi:10.1016/j.ydbio.2008.01.008.

O'Donnell, M., Chance, R. K., and Bashaw, G. J. (2009). Axon Growth and Guidance: Receptor Regulation and Signal Transduction. *Annu. Rev. Neurosci.* doi:10.1146/annurev.neuro.051508.135614.

Ozaki, S., and Snider, W. D. (1997). Initial trajectories of sensory axons toward laminar targets in the developing mouse spinal cord. *J. Comp. Neurol.* 380, 215–229. doi:10.1002/(SICI)1096-9861(19970407)380:2<215::AID-CNE5>3.0.CO;2-6.

Palmesino, E., Rousso, D. L., Kao, T. J., Klar, A., Laufer, E., Uemura, O., et al. (2010). Foxp1 and Lhx1 coordinate motor neuron migration with axon trajectory choice by gating reelin signalling. *PLoS Biol.* 8, 41–42. doi:10.1371/journal.pbio.1000446.

Patel, T. D., Jackman, A., Rice, F. L., Kucera, J., and Snider, W. D. (2000). Development of sensory neurons in the absence of NGF/TrkA signaling in vivo. *Neuron*. doi:10.1016/S0896-6273(00)80899-5.

Patel, T. D., Kramer, I., Kucera, J., Niederkofler, V., Jessell, T. M., Arber, S., et al. (2003a). Peripheral NT3 signaling is required for ETS protein expression and central patterning of proprioceptive sensory afferents. *Neuron* 38, 403–16. doi:10.1016/s0896-6273(03)00261-7.

Patel, T. D., Kramer, I., Kucera, J., Niederkofler, V., Jessell, T. M., Arber, S., et al. (2003b). Peripheral NT3 signaling is required for ETS protein expression and central patterning of proprioceptive sensory afferents. *Neuron* 38, 403–416. doi:10.1016/S0896-6273(03)00261-7.

Peng, C., Furlan, A., Zhang, M. D., Su, J., Lübke, M., Lönnerberg, P., et al. (2018). Termination of cell-type specification gene programs by the mir-183 cluster determines the population sizes of low-threshold mechanosensitive neurons. *Dev*. 145. doi:10.1242/dev.165613.

Perry, S., Larhammar, M., Vieillard, J., Nagaraja, C., Hilscher, M. M., Tafreshiha, A., et al. (2019). Characterization of Dmrt3-Derived Neurons Suggest a Role within Locomotor Circuits. *J. Neurosci.* 39, 1771–1782. doi:10.1523/JNEUROSCI.0326-18.2018.

Phelps, P. E., Rich, R., Dupuy-Davies, S., Ríos, Y., and Wong, T. (2002). Evidence for a cell-specific action of Reelin in the spinal cord. *Dev. Biol.* 244, 180–198. doi:10.1006/dbio.2002.0580.

Pierreux, C. E., Poll, A. V., Kemp, C. R., Clotman, F., Maestro, M. A., Cordi, S., et al. (2006). The Transcription Factor Hepatocyte Nuclear Factor-6 Controls the Development of Pancreatic Ducts in the Mouse. *Gastroenterology*. doi:10.1053/j.gastro.2005.12.005.

Pierreux, C. E., Vanhorenbeeck, V., Jacquemin, P., Lemaigre, F. P., and Rousseau, G. G. (2004). The transcription factor hepatocyte nuclear factor-6/Onecut-1 controls the expression of its paralog Onecut-3 in developing mouse endoderm. *J. Biol. Chem.* 279, 51298–51304. doi:10.1074/jbc.M409038200.

Pillai, A., Mansouri, A., Behringer, R., Westphal, H., and Goulding, M. (2007). Lhx1 and Lhx5 maintain the inhibitory-neurotransmitter status of interneurons in the dorsal spinal cord. *Development* 134, 357–366. doi:10.1242/dev.02717.

Plumb-Rudewiez, N., Clotman, F., Strick-Marchand, H., Pierreux, C. E., Weiss, M. C., Rousseau, G. G., et al. (2004). Transcription factor HNF-6/OC-1 inhibits the stimulation of theHNF-3?/Foxa1 gene by TGF-? in mouse liver. *Hepatology* 40, 1266–1274. doi:10.1002/hep.20459.

Poirier, K., Van Esch, H., Friocourt, G., Saillour, Y., Bahi, N., Backer, S., et al. (2004). Neuroanatomical distribution of ARX in brain and its localisation in GABAergic neurons. *Mol. Brain Res.* doi:10.1016/j.molbrainres.2003.11.021.

Qian, Y., Shirasawa, S., Chen, C. L., Cheng, L., and Qiufu, M. (2002). Proper development of relay somatic sensory neurons and D2/D4 interneurons requires homeobox genes Rnx/Tlx-3 and Tlx-1. *Genes Dev.* doi:10.1101/gad.982802.

Raisa Eng, S., Dykes, I. M., Lanier, J., Fedtsova, N., and Turner, E. E. (2007). POU-domain factor Brn3a regulates both distinct and common programs of gene expression in the spinal and trigeminal sensory ganglia. *Neural Dev.* doi:10.1186/1749-8104-2-3.

Raisa Eng, S., Gratwick, K., Rhee, J. M., Fedtsova, N., Gan, L., and Turner, E. E. (2001). Defects in sensory axon growth precede neuronal death in Brn3a-deficient mice. *J. Neurosci.*

Rausa, F., Samadani, U., Ye, H., Lim, L., Fletcher, C. F., Jenkins, N. A., et al. (1997). The cut-homeodomain transcriptional activator HNF-6 is coexpressed with its target gene HNF-3β in the developing murine liver and pancreas. *Dev. Biol.* doi:10.1006/dbio.1997.8744.

Renier, N., Wu, Z., Simon, D. J., Yang, J., Ariel, P., and Tessier-Lavigne, M. (2014). IDISCO: A simple, rapid method to immunolabel large tissue samples for volume imaging. *Cell* 159, 896–910. doi:10.1016/j.cell.2014.10.010.

Rhee, H. S., Closser, M., Guo, Y., Bashkirova, E. V., Tan, G. C., Gifford, D. K., et al. (2016). Expression of Terminal Effector Genes in Mammalian Neurons Is Maintained by a Dynamic Relay of Transient Enhancers. *Neuron* 92, 1252–1265. doi:10.1016/j.neuron.2016.11.037.

Rousso, D. L., Gaber, Z. B., Wellik, D., Morrisey, E. E., and Novitch, B. G. (2008). Coordinated Actions of the Forkhead Protein Foxp1 and Hox Proteins in the Columnar Organization of Spinal Motor Neurons. *Neuron* 59, 226–240. doi:10.1016/j.neuron.2008.06.025.

Roy, A., Francius, C., Rousso, D. L., Seuntjens, E., Debruyn, J., Luxenhofer, G., et al. (2012). Onecut transcription factors act upstream of isl1 to regulate spinal motoneuron diversification. *Dev.* 139, 3109–3119. doi:10.1242/dev.078501.

Sagner, A., and Briscoe, J. (2019). Establishing neuronal diversity in the spinal cord: a time and a place. *Development* 146. doi:10.1242/dev.182154.

Samadani, U., and Costa, R. H. (1996a). The transcriptional activator hepatocyte nuclear factor 6 regulates liver gene expression. *Mol. Cell. Biol.* doi:10.1128/mcb.16.11.6273.

Samadani, U., and Costa, R. H. (1996b). The Transcriptional Activator Hepatocyte Nuclear Factor 6 Regulates Liver Gene Expression. Available at: https://www.ncbi.nlm.nih.gov/pmc/articles/PMC231630/pdf/166273.pdf [Accessed August 15, 2019].

Sapkota, D., Chintala, H., Wu, F., Fliesler, S. J., Hu, Z., and Mu, X. (2014). Onecut1 and Onecut2 redundantly regulate early retinal cell fates during development. *Proc. Natl. Acad. Sci. U. S. A.* 111, E4086-95. doi:10.1073/pnas.1405354111.

Schnerwitzki, D., Perry, S., Ivanova, A., Caixeta, F. V, Cramer, P., Günther, S., et al. (2018). Neuron-specific inactivation of Wt1 alters locomotion in mice and changes interneuron composition in the spinal cord. *Life Sci. Alliance* 1. doi:10.26508/lsa.201800106.

Scott, A., Hasegawa, H., Sakurai, K., Yaron, A., Cobb, J., and Wang, F. (2011). Transcription factor short stature homeobox 2 is required for proper development of tropomyosin-related kinase B-expressing mechanosensory neurons. *J. Neurosci.* 31, 6741–6749. doi:10.1523/JNEUROSCI.5883-10.2011.

Smeyne, R. J., Klein, R., Schnapp, A., Long, L. K., Bryant, S., Lewin, A., et al. (1994). Severe sensory and sympathetic neuropathies in mice carrying a disrupted Trk/NGF receptor gene. *Nature* 368, 246–249. doi:10.1038/368246a0.

Snider, W. D., and Wright, D. E. (1996). Neurotrophins cause a new sensation. *Neuron* 16, 229–232. doi:10.1016/S0896-6273(00)80039-2.

Southard-Smith, E. M., Kos, L., and Pavan, W. J. (1998). Sox10 mutation disrupts neural crest development in Dom hirschsprung mouse model. *Nat. Genet.* 18, 60–64. doi:10.1038/ng0198-60.

Stam, F. J., Hendricks, T. J., Zhang, J., Geiman, E. J., Francius, C., Labosky, P. A., et al. (2012). Renshaw cell interneuron specialization is controlled by a temporally restricted transcription factor program. *Development* 139, 179–190. doi:10.1242/dev.071134.

Stepien, A. E., Tripodi, M., and Arber, S. (2010). Monosynaptic Rabies Virus Reveals Premotor Network Organization and Synaptic Specificity of Cholinergic Partition Cells. *Neuron* 68, 456–472. doi:10.1016/j.neuron.2010.10.019.

Sun, Y., Dykes, I. M., Liang, X., Eng, S. R., Evans, S. M., and Turner, E. E. (2008). A central role for Islet1 in sensory neuron development linking sensory and spinal gene regulatory programs. *Nat. Neurosci.* 11, 1283–1293. doi:10.1038/nn.2209.

Sürmeli, G., Akay, T., Ippolito, G. C., Tucker, P. W., and Jessell, T. M. (2011). Patterns of spinal sensory-motor connectivity prescribed by a dorsoventral positional template. *Cell* 147, 653–665. doi:10.1016/j.cell.2011.10.012.

Sweeney, L. B., Bikoff, J. B., Gabitto, M. I., Brenner-Morton, S., Baek, M., Yang, J. H., et al. (2018). Origin and Segmental Diversity of Spinal Inhibitory Interneurons. *Neuron* 97, 341–355. doi:10.1016/j.neuron.2017.12.029.

Szabo, N. E., Da Silva, R. V., Sotocinal, S. G., Zeilhofer, H. U., Mogil, J. S., and Kania, A. (2015). Hoxb8 intersection defines a role for Lmx1b in excitatory dorsal horn neuron development, spinofugal connectivity, and nociception. *J. Neurosci.* 35, 5233–5246. doi:10.1523/JNEUROSCI.4690-14.2015.

Takebayashi, H., Ohtsuki, T., Uchida, T., Kawamoto, S., Okubo, K., Ikenaka, K., et al. (2002). Non-overlapping expression of Olig3 and Olig2 in the embryonic neural tube. *Mech. Dev.* 113, 169–174. doi:10.1016/S0925-4773(02)00021-7.

Talpalar, A. E., Bouvier, J., Borgius, L., Fortin, G., Pierani, A., and Kiehn, O. (2013). Dual-mode operation of neuronal networks involved in left-right alternation. *Nature*. doi:10.1038/nature12286.

Tamamaki, N., Yanagawa, Y., Tomioka, R., Miyazaki, J. I., Obata, K., and Kaneko, T. (2003). Green Fluorescent Protein Expression and Colocalization with Calretinin, Parvalbumin, and Somatostatin in the GAD67-GFP Knock-In Mouse. *J. Comp. Neurol.* 467, 60–79. doi:10.1002/cne.10905.

Thaler, J. P., Koo, S. J., Kania, A., Lettieri, K., Andrews, S., Cox, C., et al. (2004). A Postmitotic Role for Isl-Class LIM Homeodomain Proteins in the Assignment of Visceral Spinal Motor Neuron Identity. *Neuron* 41, 337–350. doi:10.1016/S0896-6273(04)00011-X.

Timmer, J., Chesnutt, C., and Niswander, L. (2005). The Activin signaling pathway promotes differentiation of dI3 interneurons in the spinal neural tube. *Dev. Biol.* 285, 1–10. doi:10.1016/j.ydbio.2005.05.039.

Toch, M., and Clotman, F. (2019). CBP and p300 coactivators contribute to the maintenance of Isl1 expression by the Onecut transcription factors in embryonic spinal motor neurons. *Mol. Cell. Neurosci.* 101. doi:10.1016/j.mcn.2019.103411.

Todd, A. J. (2010). Neuronal circuitry for pain processing in the dorsal horn. *Nat. Rev. Neurosci.* 11, 823–836. doi:10.1038/nrn2947.

Todd, A. J. (2017). Identifying functional populations among the interneurons in laminae I-III of the spinal dorsal horn. *Mol. Pain* 13, 1–19. doi:10.1177/1744806917693003.

Todd, A. J., and Sullivan, A. C. (1990). Light microscope study of the coexistence of GABA-like and glycine-like immunoreactivities in the spinal cord of the rat. *J. Comp. Neurol.* 296, 496–505. doi:10.1002/cne.902960312.

Tozer, S., Le Dreau, G., Marti, E., and Briscoe, J. (2013). Temporal control of BMP signalling determines neuronal subtype identity in the dorsal neural tube. *Development* 140, 1467–1474. doi:10.1242/dev.090118.

Tripodi, M., Stepien, A. E., and Arber, S. (2011). Motor antagonism exposed by spatial segregation and timing of neurogenesis. *Nature* 479, 61–66. doi:10.1038/nature10538.

Tucker, K. L., Meyer, M., and Barde, Y. A. (2001). Neurotrophins are required for nerve growth during development. *Nat. Neurosci.* doi:10.1038/82868.

Uemura, O., Okada, Y., Ando, H., Guedj, M., Higashijima, S. I., Shimazaki, T., et al. (2005). Comparative functional genomics revealed conservation and diversification of three enhancers of the isl1 gene for motor and sensory neuron-specific expression. *Dev. Biol.* doi:10.1016/j.ydbio.2004.11.031.

Vallstedt, A., and Kullander, K. (2013). Dorsally derived spinal interneurons in locomotor circuits. *Ann. N. Y. Acad. Sci.* 1279, 32–42. doi:10.1111/j.1749-6632.2012.06801.x.

Vanhorenbeeck, V., Jacquemin, P., Lemaigre, F. P., and Rousseau, G. G. (2002). OC-3, a novel mammalian member of the ONECUT class of transcription factors. *Biochem. Biophys. Res. Commun.* 292, 848–854. doi:10.1006/bbrc.2002.6760.

Vanhorenbeeck, V., Jenny, M., Cornut, J. F., Gradwohl, G., Lemaigre, F. P., Rousseau, G. G., et al. (2007). Role of the Onecut transcription factors in pancreas morphogenesis and in pancreatic and enteric endocrine differentiation. *Dev. Biol.* 305, 685–694. doi:10.1016/j.ydbio.2007.02.027.

Von Bartheld, C. S., Williams, R., Lefcort, F., Clary, D. O., Reichardt, L. F., and Bothwell, M. (1996). Retrograde transport of neurotrophins from the eye to the brain in chick embryos: Roles of the p75NTR and trkB receptors. *J. Neurosci.*

Wang, G., and Scott, S. A. (1999). Independent development of sensory and motor innervation patterns in embryonic chick hindlimbs. *Dev. Biol.* 208, 324–336. doi:10.1006/dbio.1999.9212.

Wang, L., Klein, R., Zheng, B., and Marquardt, T. (2011). Anatomical Coupling of Sensory and Motor Nerve Trajectory via Axon Tracking. *Neuron* 71, 263–277. doi:10.1016/J.NEURON.2011.06.021.

Wang, S. M., Tie, J., Wang, W. L., Hu, S. J., Yin, J. P., Yi, X. F., et al. (2016). POU2F2-oriented network promotes human gastric cancer metastasis. *Gut* 65, 1427–1438. doi:10.1136/gutjnl-2014-308932.

Watanabe, M., Dymecki, S. M., Chirila, A. M., Springel, M. W., Toliver, A. A., Zimmerman, A. L., et al. (2017). The Cellular and Synaptic Architecture of the Mechanosensory Dorsal Horn. *Cell* 168, 295-310.e19. doi:10.1016/j.cell.2016.12.010.

Wentworth, L. E. (1984). The development of the cervical spinal cord of the mouse embryo. II. A Golgi analysis of sensory, commissural, and association cell differentiation. *J. Comp. Neurol.* 222, 96–115. doi:10.1002/cne.902220109.

Wessels, A., van den Hoff, M. J. B., Adamo, R. F., Phelps, A. L., Lockhart, M. M., Sauls, K., et al. (2012). Epicardially derived fibroblasts preferentially contribute to the parietal leaflets of the atrioventricular valves in the murine heart. *Dev. Biol.* doi:10.1016/j.ydbio.2012.04.020.

West, S. J., Bannister, K., Dickenson, A. H., and Bennett, D. L. (2015). Circuitry and plasticity of the dorsal horn - Toward a better understanding of neuropathic pain. *Neuroscience*. doi:10.1016/j.neuroscience.2015.05.020.

Wildner, H., Müller, T., Cho, S. H., Bröhl, D., Cepko, C. L., Guillemot, F., et al. (2006). dILA neurons in the dorsal spinal cord are the product of terminal and non-terminal asymmetric progenitor cell divisions, and require Mash1 for their development. *Development* 133, 2105–2113. doi:10.1242/dev.02345.

Windhorst, U. (2007). Muscle proprioceptive feedback and spinal networks. *Brain Res. Bull.* doi:10.1016/j.brainresbull.2007.03.010.

Wine-Lee, L. (2004). Signaling through BMP type 1 receptors is required for development of interneuron cell types in the dorsal spinal cord. *Development*. doi:10.1242/dev.01379.

Wu, F., Sapkota, D., Li, R., and Mu, X. (2012). Onecut 1 and Onecut 2 are potential regulators of mouse retinal development. *J. Comp. Neurol.* 520, 952–969. doi:10.1002/cne.22741.

Xu, Y., Lopes, C., Wende, H., Guo, Z., Cheng, L., Birchmeier, C., et al. (2013). Ontogeny of excitatory spinal neurons processing distinct somatic sensory modalities. *J. Neurosci.* 33, 14738–14748. doi:10.1523/JNEUROSCI.5512-12.2013.

Yip, J. W., Yip, Y. P. L., Nakajima, K., and Capriotti, C. (2000). Reelin controls position of autonomic neurons in the spinal cord. *Proc. Natl. Acad. Sci. U. S. A.* doi:10.1073/pnas.150040497.

Yoshida, Y., Han, B., Mendelsohn, M., and Jessell, T. M. (2006). PlexinA1 Signaling Directs the Segregation of Proprioceptive Sensory Axons in the Developing Spinal Cord. *Neuron* 52, 775–788. doi:10.1016/j.neuron.2006.10.032.

Yoshikawa, M., Senzaki, K., Yokomizo, T., Takahashi, S., Ozaki, S., and Shiga, T. (2007). Runx1 selectively regulates cell fate specification and axonal projections of dorsal root ganglion neurons. *Dev. Biol.* 303, 663–674. doi:10.1016/j.ydbio.2006.12.007.

Yuengert, R., Hori, K., Kibodeaux, E. E., McClellan, J. X., Morales, J. E., Huang, T. W. P., et al. (2015). Origin of a Non-Clarke's Column Division of the Dorsal Spinocerebellar Tract and the Role of Caudal Proprioceptive Neurons in Motor Function. *Cell Rep*. doi:10.1016/j.celrep.2015.09.064.

Zagoraiou, L., Akay, T., Martin, J. F., Brownstone, R. M., Jessell, T. M., and Miles, G. B. (2009). A Cluster of Cholinergic Premotor Interneurons Modulates Mouse Locomotor Activity. *Neuron* 64, 645–662. doi:10.1016/j.neuron.2009.10.017.

Zechner, D., Müller, T., Wende, H., Walther, I., Taketo, M. M., Crenshaw, E. B., et al. (2007). Bmp and Wnt/β-catenin signals control expression of the transcription factor Olig3 and the specification of spinal cord neurons. *Dev. Biol.* 303, 181–190. doi:10.1016/j.ydbio.2006.10.045.

Zhang, H., Ables, E. T., Pope, C. F., Washington, M. K., Hipkens, S., Means, A. L., et al. (2009). Multiple, temporal-specific roles for HNF6 in pancreatic endocrine and ductal differentiation. *Mech. Dev.* doi:10.1016/j.mod.2009.09.006.

Zhong, J., Pevny, L., and Snider, W. D. (2006). "Runx"ing towards sensory differentiation. *Neuron* 49, 325–327. doi:10.1016/j.neuron.2006.01.013.

Zhuang, B., and Sockanathan, S. (2006). Dorsal-ventral patterning: A view from the top. *Curr. Opin. Neurobiol.* 16, 20–24. doi:10.1016/j.conb.2005.11.001.

Zirlinger, M., Lo, L., McMahon, J., McMahon, A. P., and Anderson, D. J. (2002). Transient expression of the bHLH factor neurogenin-2 marks a subpopulation of neural crest cells biased for a sensory but not a neuronal fate. *Proc. Natl. Acad. Sci. U. S. A.* 99, 8084–8089. doi:10.1073/pnas.122231199.

Zou, M., Li, S., Klein, W. H., and Xiang, M. (2012). Brn3a/Pou4f1 regulates dorsal root ganglion sensory neuron specification and axonal projection into the spinal cord. *Dev. Biol.* 364, 114–127. doi:10.1016/j.ydbio.2012.01.021.